



University of Pennsylvania
ScholarlyCommons


Publicly Accessible Penn Dissertations

2020

Role Of Soluble Fibrin And Fibrin Degradation Products On Platelet Signaling During Trauma

Christopher Verni
University of Pennsylvania

Follow this and additional works at: <https://repository.upenn.edu/edissertations>

 Part of the [Biomedical Commons](#), and the [Chemical Engineering Commons](#)

Recommended Citation

Verni, Christopher, "Role Of Soluble Fibrin And Fibrin Degradation Products On Platelet Signaling During Trauma" (2020). *Publicly Accessible Penn Dissertations*. 4176.
<https://repository.upenn.edu/edissertations/4176>

This paper is posted at ScholarlyCommons. <https://repository.upenn.edu/edissertations/4176>
For more information, please contact repository@pobox.upenn.edu.

Role Of Soluble Fibrin And Fibrin Degradation Products On Platelet Signaling During Trauma

Abstract

Platelets and coagulation proteins work in concert to maintain proper blood flow through the vasculature. When an injury occurs, this hemostatic system must respond efficiently by sealing the wound to prevent excessive bleeding. Deviations from normal hemostasis arise in the clinic frequently; one such condition that is characterized by uncontrolled bleeding is known as trauma-induced coagulopathy (TIC). Severe platelet dysfunction is one key contributing factor to TIC, though its mechanistic causes are still yet to be fully understood. In order to investigate biological explanations for platelet dysfunction during trauma, various cell-based assays were designed and conducted in both healthy and patient populations. Specifically, intracellular calcium mobilization and other fluorescently tracked biomarkers were used as dynamic indicators of platelet activation in response to common agonists. Microtiter well plates prepared with liquid handling systems enabled high-throughput data collection and minimal manual pipetting. Significant platelet dysfunction in response to 31 unique stimulation conditions spanning several signaling pathways was observed in a cohort of trauma patients and tracked at multiple timepoints after initial hospital admission. In experiments designed to interrogate plasma effects on healthy platelet function, patient-derived plasma imparted significant inhibition which implied the presence of a unique soluble plasma species with downregulatory effects on endogenous and transfused platelets. With established knowledge of coinciding coagulant and lytic states during trauma, strategic addition of agonists to healthy platelet suspensions led to generation of soluble fibrin species and desensitization to agonist stimulation through glycoprotein VI (GPVI). Downstream platelet dysfunction was only observed when thrombin was added to the system to polymerize fibrin, whereas stimulation with other agonists or inhibition of various stages of coagulation had no effect on subsequent GPVI function. Maximal inhibition (~95%) was attained when tissue plasminogen activator (tPA) was also incorporated to lyse fibrin polymers into fibrin degradation products (FDP). Concentrations of a small FDP called D-dimer were elevated in trauma patient samples and inversely correlated with a quantitative measure of platelet function. Finally, preliminary results indicate potential binding affinity between platelet receptors and D-dimer. These results shed light on specific biological entities that may be responsible for platelet dysfunction in trauma patients.

Degree Type

Dissertation

Degree Name

Doctor of Philosophy (PhD)

Graduate Group

Chemical and Biomolecular Engineering

First Advisor

Scott L. Diamond

Keywords

coagulopathy, D-dimer, fibrin, platelet, trauma

Subject Categories

Biomedical | Chemical Engineering

This dissertation is available at ScholarlyCommons: <https://repository.upenn.edu/edissertations/4176>

ROLE OF SOLUBLE FIBRIN AND FIBRIN DEGRADATION PRODUCTS ON PLATELET SIGNALING DURING TRAUMA

Christopher C. Verni

A DISSERTATION

in

Chemical and Biomolecular Engineering

Presented to the Faculties of the University of Pennsylvania

in

Partial Fulfillment of the Requirements for the

Degree of Doctor of Philosophy

2020

Supervisor of Dissertation

Scott L. Diamond

Professor, Department of Chemical and Biomolecular Engineering

Graduate Group Chairperson

John C. Crocker

Professor, Department of Chemical and Biomolecular Engineering

Dissertation Committee

Talid R. Sinno, Professor, Department of Chemical and Biomolecular Engineering

Ravi Radhakrishnan, Professor, Department of Chemical and Biomolecular Engineering

Lawrence F. Brass, Professor, Department of Medicine

ROLE OF SOLUBLE FIBRIN AND FIBRIN DEGRADATION PRODUCTS ON PLATELET SIGNALING DURING TRAUMA

COPYRIGHT

2020

Christopher C. Verni

ACKNOWLEDGMENTS

My journey through graduate school has certainly been influenced by many people, several of whom deserve recognition. Firstly, I'd like to send thanks and appreciation to my thesis advisor, Dr. Scott L. Diamond. I can't imagine working under anyone else over the past five years, and I attribute the success of my research largely to his guidance and support. Dr. Diamond's advising method, a balance between guided suggestions and permission of individual exploration, perfectly fit my learning style and facilitated my growth as an independent researcher. In the same light, the rest of my committee—Dr. Talid R. Sinno, Dr. Ravi Radhakrishnan, and Dr. Lawrence F. Brass—provided helpful advice and encouragement throughout the course of my project.

Next, I would like to thank the other members of the Diamond Lab who will remain lifelong friends. During my first months in the lab, I grew close with Mei Yan Lee, Shu Zhu, and Brad Herbig who trained me on various pieces of lab equipment and helped establish the foundation of my work. The core years were shared with Jason Rossi, Xinren Yu, Jason Chen, and Evan Tsiklidis, each of whom has aided me in some capacity, both in and out of the lab. More recently, I have had the pleasure of working with Mike DeCortin, Kevin Trigani, Daniel Zhang, Jen Crossen, Yue Liu, and Kaushik Shankar. Lastly, I'd like to thank our phlebotomist and lab manager, Huiyan Jing. Without Jing, experiments with fresh blood from our donors (who also merit a shout-out) would not be possible.

Since the bulk of my PhD work has relied on a relationship with the Penn Acute Research Collaboration, I would like to acknowledge a few people who have proven to be especially important. Dr. Carrie A. Sims served as the main PI of the project, while Antonio Davila Jr. and Steve Balian more closely facilitated my work through granting access to lab space and coordination of patient sample collection, respectively. It has been a pleasure learning from them and having the opportunity to work directly with patient blood.

The friendships I have developed outside the classroom and the lab have also been crucial, especially during inevitable struggles and frustration. Despite being one of the smallest incoming cohorts over the past several years, we were able to become close during our course-heavy first year and “gather” every so often during the later years. To Jason, Paul, Sean, Giuseppe, and Emily: thanks for all the laughs and distractions from everyday PhD life. I wish you all nothing but the best in your future endeavors.

I also feel responsible to extend gratitude to everyone that shaped my early academic career. From my early days at Medway High School where I was originally introduced to the wonders of science and mathematics, especially by Mrs. Pereira and Mr. Ryan, I look back on those four years with appreciation and satisfaction. Choosing Lafayette for my undergrad studies will always be one of the best decisions of my life, as I was able to obtain a strong engineering education while still focusing on other interests like foreign language and extracurricular activities. I still enjoy coming back to visit and knocking on professors’ doors, specifically Dr. Lindsay Soh, my Honors Thesis advisor, and Dr. Michael Senra, who really steered me towards pursuing a PhD in the first place. To all my teachers and professors over the past few decades, thank you for everything.

Finally, my acknowledgment would be remiss without thanking my Mom and sister Erin for being my primary support system from day one. I greatly appreciate your active interest in the status of my work, reminders to take time for myself and have fun, and encouragement to work hard and think outside the box. I must also thank my Dad, who I know has been watching over me from above and whose battle with lung cancer is my primary inspiration to pursue a career in biomedical research. My last, but certainly not least, thank you goes to my incredibly special and amazing girlfriend, Alicia. The support and motivation you’ve given me can’t be overstated, and you push me to be the best version of myself every day. The past five years with you have been absolutely perfect, and I can’t wait to see what countless more years have in store.

ABSTRACT

ROLE OF SOLUBLE FIBRIN AND FIBRIN DEGRADATION PRODUCTS ON PLATELET SIGNALING DURING TRAUMA

Christopher C. Verni

Scott L. Diamond

Platelets and coagulation proteins work in concert to maintain proper blood flow through the vasculature. When an injury occurs, this hemostatic system must respond efficiently by sealing the wound to prevent excessive bleeding. Deviations from normal hemostasis arise in the clinic frequently; one such condition that is characterized by uncontrolled bleeding is known as trauma-induced coagulopathy (TIC). Severe platelet dysfunction is one key contributing factor to TIC, though its mechanistic causes are still yet to be fully understood. In order to investigate biological explanations for platelet dysfunction during trauma, various cell-based assays were designed and conducted in both healthy and patient populations. Specifically, intracellular calcium mobilization and other fluorescently tracked biomarkers were used as dynamic indicators of platelet activation in response to common agonists. Microtiter well plates prepared with liquid handling systems enabled high-throughput data collection and minimal manual pipetting. Significant platelet dysfunction in response to 31 unique stimulation conditions spanning several signaling pathways was observed in a cohort of trauma patients and tracked at multiple timepoints after initial hospital admission. In experiments designed to interrogate plasma effects on healthy platelet function, patient-derived plasma imparted significant inhibition which implied the presence of a unique soluble plasma species with downregulatory effects on endogenous and transfused platelets. With established knowledge of coinciding coagulant and lytic states during trauma, strategic addition of

agonists to healthy platelet suspensions led to generation of soluble fibrin species and desensitization to agonist stimulation through glycoprotein VI (GPVI). Downstream platelet dysfunction was only observed when thrombin was added to the system to polymerize fibrin, whereas stimulation with other agonists or inhibition of various stages of coagulation had no effect on subsequent GPVI function. Maximal inhibition (~95%) was attained when tissue plasminogen activator (tPA) was also incorporated to lyse fibrin polymers into fibrin degradation products (FDP). Concentrations of a small FDP called D-dimer were elevated in trauma patient samples and inversely correlated with a quantitative measure of platelet function. Finally, preliminary results indicate potential binding affinity between platelet receptors and D-dimer. These results shed light on specific biological entities that may be responsible for platelet dysfunction in trauma patients.

TABLE OF CONTENTS

ACKNOWLEDGMENTS	iii
ABSTRACT	v
TABLE OF CONTENTS	vii
LIST OF FIGURES AND TABLES	x
CHAPTER 1: INTRODUCTION	1
1.1 Hemostasis, Thrombosis, and Bleeding	1
1.2 Platelet Activation	3
1.2.1 Platelets	3
1.2.2 Surface Receptors.....	3
1.2.3 Common Signaling Pathways and Markers of Platelet Activation	6
1.3 Trauma-Induced Coagulopathy (TIC)	9
1.3.1 Platelet Dysfunction in Trauma Patients	9
1.3.2 Coagulation Abnormalities and Hyperfibrinolysis	11
1.3.3 Efficacy of Transfusion Strategies	14
CHAPTER 2: PLATELET FUNCTION PHENOTYPING METHODS	17
2.1 Intracellular Calcium Mobilization	17
2.2 Flow Cytometry	20
2.3 Platelet Aggregometry	22
2.4 Thromboelastography (TEG)	24
CHAPTER 3: SOLUBLE FIBRIN CAUSES AN ACQUIRED PLATELET GPVI SIGNALING DEFECT: IMPLICATIONS FOR COAGULOPATHY	28
3.1 Introduction	28
3.2 Materials and Methods	30
3.2.1 Platelet calcium assays	30
3.2.2 Microfluidic assays	31
3.3 Results	32
3.3.1 Thrombin stimulation, but not ADP or U46619, attenuated subsequent platelet GPVI signaling	32
3.3.2 Thrombin-induced GPVI signaling defect was time dependent.....	36
3.3.3 Activating PAR-1 and PAR-4 does not attenuate GPVI signaling	36
3.3.4 Soluble fibrin caused convulxin insensitivity independent of receptor shedding or fibrin binding to $\alpha_{IIb}\beta_3$	39
3.3.5 Thrombin treatment of washed platelets in purified fibrinogen displays convulxin insensitivity	43
3.3.6 Soluble fibrin reduces platelet deposition to collagen under flow	43
3.4 Discussion	46
CHAPTER 4: PLATELET DYSFUNCTION DURING TRAUMA INVOLVES DIVERSE SIGNALING PATHWAYS AND AN INHIBITORY ACTIVITY IN PATIENT-DERIVED PLASMA	50
4.1 Introduction	50
4.2 Materials and Methods	52

4.2.1	Reagents.....	52
4.2.2	Study design	52
4.2.3	Intracellular calcium mobilization assays	54
4.2.4	Flow cytometry assays	56
4.2.5	Washed platelet preparation for plasma reconstitution experiments	56
4.2.6	Thromboelastography	57
4.2.7	Statistical analysis.....	57
4.3	Results.....	58
4.3.1	Calcium mobilization measurements indicate global platelet dysfunction in trauma patients.....	58
4.3.2	Trauma patient platelets exhibit decreased $\alpha_{2b}\beta_3$ activation, P-selectin expression, and phosphatidylserine exposure upon stimulation in flow cytometry ..	59
4.3.3	Thromboelastography (TEG) data reveal patient platelet defects in whole blood samples.....	60
4.3.4	Healthy human platelets exhibit impaired function in plasma from trauma patients.....	63
4.3.5	Healthy plasma imparts a detectable inhibition of washed platelet activation but patient plasma samples result in more potent effect	63
4.3.6	Plasma concentration is correlated with decreased platelet function	65
4.4	Discussion	67

CHAPTER 5: D-DIMER AND FIBRIN DEGRADATION PRODUCTS IMPAIR PLATELET SIGNALING: PLASMA D-DIMER IS A PREDICTOR AND MEDIATOR OF PLATELET DYSFUNCTION DURING TRAUMA..... 70

5.1	Introduction	70
5.2	Materials and Methods.....	72
5.2.1	Reagents.....	72
5.2.2	Phlebotomy and patient enrollment	73
5.2.3	Intracellular calcium mobilization	74
5.2.4	Platelet aggregometry	75
5.2.5	ELISA.....	75
5.2.6	Flow cytometry	76
5.2.7	Statistical analysis.....	76
5.3	Results	77
5.3.1	Factor XIIIa and fibrinolysis contribute to platelet signaling defect.....	77
5.3.2	D-dimer impairs platelet aggregation in response to various agonists	80
5.3.3	Plasma D-dimer is a predictor of trauma-induced platelet dysfunction.....	82
5.3.4	Healthy washed platelets bind D-dimer over time and trauma platelets feature D-dimer on cell surface.....	84
5.4	Discussion	87

CHAPTER 6: OTHER STUDIES..... 90

6.1	Dual antiplatelet and anticoagulant (APAC) heparin proteoglycan mimetic with shear-dependent effects on platelet-collagen binding and thrombin generation	90
6.1.1	Introduction	90
6.1.2	Methods	91
6.1.3	Results and Discussion	94
6.2	Testing efficacy, potency, and specificity of platelet inhibitors.....	100
6.2.1	Effect of PAR-4 specific antagonist	100

6.2.2	Effect of custom GPVI inhibitor.....	103
6.2.3	Effect of N-acetylcysteine on platelet activation.....	105
6.3	Computational modeling of the coagulation response during trauma....	107
6.3.1	Introduction.....	107
6.3.2	Coagulation during bleeding.....	108
6.3.3	Data-driven development of subject-specific platelet function profiles	109
6.3.4	Conclusions.....	113
CHAPTER 7: FUTURE WORK		115
7.1	Further characterization and study of physiological significance of fibrin species distribution in trauma patient blood	115
7.1.1	Using gel electrophoresis and western blot to analyze size and composition of fibrin-related species.....	115
7.1.2	Observing interactions between D-dimer and platelets under flow conditions in microfluidic device.....	117
7.1.3	Studying mechanisms of D-dimer binding in mouse knockout cell lines..	119
7.2	Comparison of PAR signaling via activation with thrombin or synthetic peptide combination	120
7.2.1	Investigating trends in different measures of platelet function.....	120
7.2.2	Training machine learning model to generalize PAR signaling events	123
7.3	Extension of PAS to studying toll-like receptors	124
7.3.1	Toll-like receptors (TLR).....	124
7.3.2	TLR activation involvement in platelet activation and signaling.....	127
7.3.3	Application of PAS to study TLR-mediated platelet function	128
CHAPTER 8: APPENDIX I (SUPPLEMENTAL FIGURES)		131
CHAPTER 9: APPENDIX II (DATA ANALYSIS SCRIPTS).....		154
CHAPTER 10: BIBLIOGRAPHY.....		155

LIST OF FIGURES AND TABLES

Figure 1-1. Schematic of common platelet signaling pathways.....	7
Figure 1-2. Classes of fibrin-related species.....	12
Figure 2-1. Mechanisms of calcium mobilization in platelets.....	19
Figure 2-2. Platelet aggregometry experimental basis.....	23
Figure 2-3. Generalized TEG output.....	25
Figure 3-1. Thrombin but not ADP or U46619 blocks subsequent platelet GPVI activation by convulxin.....	34
Figure 3-2. Thrombin treatment of platelets blocks subsequent activation via fibrillar collagen when measuring calcium mobilization.....	35
Figure 3-3. Effect of thrombin dose and exposure time to drive convulxin-insensitivity ..	37
Figure 3-4. Attenuation of convulxin sensitivity was not observed by pretreatment with PAR-1 and PAR-4 agonist peptides.....	38
Figure 3-5. Inhibition of fibrin polymerization with GPRP prevents thrombin-induced convulxin-insensitivity.....	41
Figure 3-6. Inhibition of cross-linking enzyme FXIIIa with T101 results in significant restoration of platelet GPVI activity and inhibition of ADAM10 shows no effect of GPVI shedding.....	42
Figure 3-7. Thrombin activation of washed platelets in purified fibrinogen reduced subsequent activation by convulxin, an effect blocked by GPRP.....	44
Figure 3-8. Under thrombin-free conditions, presence of soluble fibrin in whole blood reduces platelet adhesion on collagen under flow.....	45
Figure 4-1. Trauma patients exhibit a severely impaired calcium mobilization phenotype in response to platelet agonists.....	59

Figure 4-2. Trauma patient samples show impaired integrin $\alpha_{2b}\beta_3$ activation, P-selectin expression, and phosphatidylserine exposure in flow cytometry	61
Figure 4-3. Thromboelastography results for patient samples over time	62
Figure 4-4. Healthy donor platelets lose function when reconstituted in trauma patient-derived plasma	64
Figure 4-5. Screening several plasma samples reveals a more potent inhibitory effect in trauma samples than healthy samples.....	65
Figure 4-6. Increasing plasma concentrations reduces the calcium fluorescent signal in both healthy and patient plasma settings.....	66
Figure 5-1. Effect of cross-linked fibrinolytic products on healthy platelet function	79
Figure 5-2. Effect of presence of D-dimer on healthy platelet aggregation following agonist stimulation	81
Figure 5-3. Correlation between D-dimer level and total platelet calcium mobilization ...	83
Figure 5-4. Binding of D-dimer by platelets over time	85
Figure 5-5. Overall summary schematic showing proposed understanding of interactions between platelets and fibrin-related species	89
Figure 6-1. Thrombin- and collagen-dependent calcium mobilization is specifically reduced in the presence of APAC.....	96
Figure 6-2. Platelet aggregation in PRP is inhibited by APAC.....	97
Figure 6-3. Effects of PAR-4 antagonist BMS-986141 on array of platelet agonists.....	102
Figure 6-4. Inhibitory effects of custom scFv against GPVI.....	104
Figure 6-5. Global antiplatelet effects of cysteine derivatives.....	106
Figure 6-6. Connecting experimental measurements and numerical predictions of platelet activation state	111
Figure 7-1. Proposed experimental setup for microfluidic investigation of platelet-FDP interactions.....	118

Figure 7-2. Matching of various platelet activation markers for PAR agonists	122
Figure 7-3. Proposed structure of machine learning model for PAR-specific signaling.	123
Figure 7-4. Proposed set of experiments for investigating TLR activation in platelets ..	129
Table 2-1. TEG parameters	26
Table 4-1. Summary of patient demographics and clinical presentations	53
Table 5-1. Summary of subject characteristics for complete study cohort.....	74
Table 7-1. Expression of toll-like receptors in platelets	126
Table 7-2. Platelet biochemical signaling mediated by TLR activation	128

CHAPTER 1: INTRODUCTION

1.1 Hemostasis, Thrombosis, and Bleeding

Following blood vessel injury, the body's normal response to prevent excessive blood loss and restore fluid flow throughout the vasculature is known as hemostasis [1]. Though it is an incredibly complex process involving cells, proteins, and other biological entities, the hematology community generally classifies two main mechanisms: primary and secondary hemostasis [2]. Primary hemostasis relies on the functionality and activity of platelets to report to the injury site and aggregate into a "platelet plug" [2]. Initial platelet adhesion to the vessel wall takes place as a result of binding affinity between platelets and subendothelial collagen and von Willebrand Factor (vWF), both of which become exposed post-injury [2]. Several biophysical and biochemical events, notably the change of platelet cytoskeletal configuration from discoid to pseudopodia-rich shapes [3] and the release of intracellular granule contents [4], further potentiate the recruitment and activation of other circulating platelets. Located within platelet dense granules, adenosine diphosphate (ADP) and thromboxane A₂ (TXA₂) act as autocrine activators upon release and are among the most important contributors to positive feedback signaling and secondary platelet aggregation [4].

Concurrent with the initial platelet response to a wound, oncoming blood flow is exposed to tissue factor (TF), which serves as a cofactor for the serine protease Factor VIIa (FVIIa) and subsequently triggers a series of reactions known as the coagulation cascade [5]. Coagulation can be TF-mediated, known as the extrinsic pathway, or activated through surface contact, referred to as the intrinsic pathway, but both routes lead to the generation of thrombin [2]. Thrombin is the most critical enzyme in secondary hemostasis, as it cleaves and polymerizes the plasma protein fibrinogen to an insoluble polymer aptly called fibrin [2]. Once sufficiently polymerized and cross-linked, fibrin acts

as a stabilizing mesh for the platelet aggregate and strengthens the clot to completely seal the damaged vasculature [6].

In order to prevent excessive clot buildup, down-regulatory mechanisms exist to control the generation and activity of thrombin. Serine protease inhibitors (SERPINs), such as antithrombin and heparin cofactor II, and other circulating species like protein C, which elicits anticoagulant properties when activated by thrombin, are examples of naturally occurring inhibitors of the coagulation process [7]. Fibrinolysis is another reactive process which targets already existing fibrin networks. The plasma protein plasminogen circulates as an inactive zymogen until encountering endothelial-released tissue plasminogen activator (tPA), upon which it becomes activated to plasmin and is capable of dissolving polymerized fibrin [7,8].

These antithrombotic mechanisms sometimes progress defectively, which has the potential to lead to bleeding in the case of insufficient clotting, or thrombosis, a condition characterized by excessive clot development and blockage of blood flow upon vessel occlusion [2]. Thrombi produced in arteries and veins typically exhibit different compositions, which are associated with different risk factors. Venous clots are comprised mostly of fibrin and red blood cells, whereas arterial clots are usually platelet-rich due to higher shear rates and ruptured atherosclerotic plaque [9]. Without proper identification and treatment, pathologic thrombi can lead to several life-threatening clinical presentations, including myocardial infarction (MI), stroke, venous thromboembolism (VTE) or pulmonary embolism (PE) [9]. On the other hand, bleeding presents its own set of concerns, though it is often more easily diagnosed than thrombosis. Despite the fact that most bleeding disorders are genetically inherited (e.g. hemophilia and Von Willebrand disease) [2], others can be developed as a result of coagulopathic behavior. One such example is trauma-induced coagulopathy (TIC), which commonly presents in patients who have experienced major injuries. This condition is known to be extremely complex, but is

broadly identified by impaired clotting activity, hyperfibrinolysis, and platelet dysfunction [10]. Understanding mechanisms of TIC has been a grand challenge over the years, and any significant progress has the potential to alter the treatment strategies currently employed in the clinic.

1.2 Platelet Activation

1.2.1 Platelets

The three main types of blood cells are red blood cells, white blood cells, and platelets. While the others feature nuclei and are larger in size, platelets are anucleate cells that typically range between 2-4 μm in diameter [11]. Also known as thrombocytes, platelets are generated through a process called thrombopoiesis which takes place in the bone marrow. After hematopoietic stem cells differentiate into megakaryocytes (among several other subclasses of blood progenitor cells) and with the aiding action of thrombopoietin, long protruding fragments called proplatelets are released from the cytoplasm and further divided into platelets [11]. Once introduced to the circulation, platelets have an average lifespan of about 7-10 days before being cleared by the spleen and liver. Younger platelets tend to exhibit higher responsiveness to stimuli than older platelets, primarily due to higher RNA content, but platelets of all ages can still participate in hemostasis and become activated by a plethora of signals and mechanisms [11].

1.2.2 Surface Receptors

Platelets are decorated with numerous surface receptors, each of which is engaged by one or more specific ligands. Some receptors are involved in the initial adhesion process to a prothrombotic surface (e.g. damaged vessel wall), while others are called into action to bind soluble agonists or interact with other platelets. The variety of functions also pertains to subclasses of receptors that lead to either inhibitory or activating

processes, which work in concert to keep the level of platelet activation under control [12,13].

For the studies in this work, receptors that trigger activating networks will be the primary focus. Receptors that initiate the platelet activation process are often classified into two main groups: immunoreceptor tyrosine-based activation motif (ITAM)-coupled receptors and G-protein coupled receptors (GPCR) [13]. Examples of ITAMs include FcR γ , which complexes with glycoprotein VI (GPVI) and GPIb-IX-V, and Fc γ RIIa, which is associated with the integrin $\alpha_{IIb}\beta_3$ and GPIb-IX-V, as well as C-type lectin-like receptor 2 (CLEC-2) [13]. GPVI and GPIb-IX-V are each responsible for initial platelet recruitment and binding to endothelial-exposed collagen and vWF, respectively. Integrin $\alpha_{IIb}\beta_3$, also termed GPIIb/IIIa, attracts the plasma protein fibrinogen to link individual platelets together and strengthen the developing platelet mass. CLEC-2 is stimulated by the transmembrane protein podoplanin, which is commonly expressed on the surface of lymphatic endothelial cells (LEC), and is important for maintaining natural barriers between blood flow and the lymphatic system [13,14]. In addition to these naturally occurring receptor activators, lab-based ligands have been discovered and developed, including convulxin for GPVI [15] and rhodocytin for CLEC-2 [16]. Different from GPCRs, which are discussed next, ITAM receptors are essential for maintaining vascular integrity at sites of inflammation in addition to promoting platelet function [14].

The majority of platelet receptors that are activated by binding of soluble agonists to the cell surface belong to the GPCR family. Though GPCRs come in a variety of flavors, they are all composed of seven transmembrane domains that transmit intracellular signals upon activation by the appropriate ligand [13]. Most platelet agonists activate G α_q receptors—thrombin, the essential protease for coagulation described previously, also has platelet activation capability through its affinity for the two protease activated receptors 1 and 4 (PAR-1,4) in human blood, and ADP and TXA $_2$, important for secondary platelet

activation, bind the P_2Y_1 and TP receptors, respectively. Often, lab analogs with higher specificity and stability are substituted for these natural ligands. For example, the PAR-specific peptide chains Ser-Phe-Leu-Leu-Arg-Asn (SFLLRN) and Ala-Tyr-Pro-Gly-Lys-Phe (AYPGKF) are used to study PAR-1 and PAR-4, respectively [17,18], while U46619 is a synthetic agonist for the TP receptor [19]. $G\alpha_i$ -coupled receptors, which include another ADP receptor called P_2Y_{12} , and the $G\alpha_s$ -coupled receptors, such as the inhibitory prostaglandin I_2 (IP) receptor, round out the most well-studied platelet surface receptors and will be discussed at length throughout this work [13]. Recently, GPCRs and associated intracellular signaling pathways have gained interest as targets for drug development due to their involvement in the amplification of the platelet activation process [20]. This strategy enables initial platelet function to adequately seal a wound, but prevents excessive platelet activity which could lead to restriction of blood flow and other complications of thrombosis.

As discussed previously, regulating mechanisms for controlling the extent of platelet activation exist in both damaged and healthy vasculatures. In order to maintain the normal quiescent state of circulating platelets, intact endothelium releases nitric oxide (NO) and prostacyclin (PGI_2) as inhibitory signals [12]. Unlike prostacyclin which binds to the IP receptor and leads to the production of cyclic adenosine monophosphate (cAMP), nitric oxide does not physically bind to platelets. Rather, it suppresses platelet activity through the conversion of soluble guanyl cyclase to cyclic guanosine monophosphate (cGMP) [12]. Both cAMP and cGMP activate protein kinases (PKA and PKG, respectively), which contribute to the phosphorylation of numerous substrates. These phosphorylated entities carry inhibitory properties against platelet adhesion, aggregation, and other markers of platelet activation [21].

1.2.3 Common Signaling Pathways and Markers of Platelet Activation

Binding or cleavage of platelet surface receptors by physiologic or mimetic ligands acts as the initiation step for several intracellular signaling pathways, many of which are depicted in **Figure 1-1**, that eventually lead to platelet activation events. Several receptors described in the previous section signal primarily through regulators of G-protein signaling (RGS), and each unique G protein can be activated by a multitude of different receptors. The vast majority of GPCRs, those that are $G\alpha_q$ -coupled, activate the β isoform of phospholipase C ($PLC\beta$) which in turn catalyzes the hydrolysis of phosphatidylinositol 4,5-bisphosphate (PIP_2) into the secondary messenger inositol triphosphate (IP_3) [13]. The $G\alpha_q$ -coupled class of receptors tend to signal both through $PLC\beta$ as well as against adenylyl cyclase (AC), which prevents inhibitory signals from being transmitted. Signaling through AC and guanylyl cyclase (GC) for that matter, through either $G\alpha_s$ -coupled receptors or nitric oxide donation through the plasma membrane, respectively, trigger inhibitory pathways via cAMP and cGMP synthesis as discussed above. Non-GPCRs, such as the ITAM receptors, are often associated with tyrosine phosphorylation by Src family kinases (SFK) and subsequent binding of spleen tyrosine kinase (Syk) to the intracellular domain of the receptor. This event then triggers activation of $PLC\gamma$ and convergence to IP_3 generation as is observed through $G\alpha_q$ signaling [13].

The example of ITAM signaling via $GPVI$ activation and $G\alpha_q$ signaling both converging on IP_3 synthesis exhibits the high degree of crosstalk between individual platelet activation pathways. Other examples include ADP signaling through two independent GPCR-dependent pathways, $PAR4$ - $P2Y_{12}$ dimerization, and inside-out integrin activation amplifying platelet responses to GPCR agonists [13,22]. This synergy and positive feedback is essential for ensuring proper platelet activation during hemostasis, as the cooperative effects of multiple pathways can overcome certain scenarios in which low levels of specific agonists are present. It is important to note that

the pathways outlined here and in **Figure 1-1** are only a selection of the countless mechanisms of platelet activation. However, for the purposes of this work, analysis of these primary pathways will provide a holistic and sufficiently broad understanding of how platelets respond to various stimuli throughout the course of the hemostatic response.

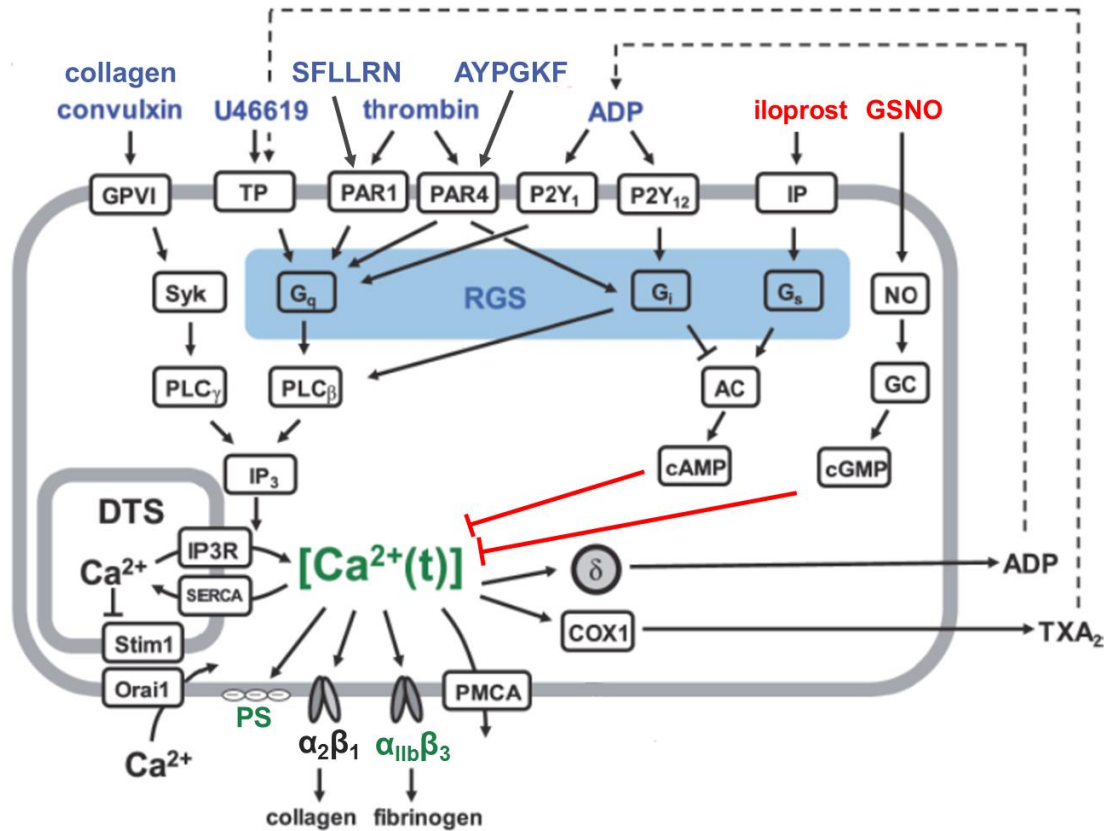


Figure 1-1. Schematic of common platelet signaling pathways

The platelet surface (grey box) features several receptors that become activated by specific ligands. Certain ligand-receptor pairs lead to activating events (denoted by agonists in blue), while others trigger inhibitory signals to prevent excessive platelet activation (denoted by agonists in red). The intracellular signaling pathways are rather complex, which is often attributed to crosstalk between multiple events. Several markers of platelet activation, including dynamic calcium mobilization, phosphatidylserine (PS) exposure, and $\alpha_{IIb}\beta_3$ activation, are also indicated (shown in green).

In a normal response to injury, there is typically a step-by-step sequence of events that leads to clot formation and restoration of blood flow: (1) initial adhesion and activation of platelets; (2) amplification of the platelet activation response and recruitment of

additional cells; (3) aggregation of activated platelets and stabilization through coagulation proteins. Even in this “healthy” process, there are several important players that contribute to addressing the issues presented by vessel damage, and understanding the individual significance of each signaling event as well as the importance of evidenced interactions gives rise to high-dimensional problems. The level of complication only increases when hemostasis fails in one way or another, an example being the case of a patient with pre-existing medical conditions. Identification of specific markers of platelet function that are affected by multiple activation mechanisms (e.g. output-input systems) becomes crucial in the effort to simplify the study of platelet activation while still maintaining access to the inner workings of the aforementioned biochemical signaling processes. The experimental setups that are utilized in this work enable the collection of data representative of complex signaling situations, whether multiple platelet agonists are present simultaneously or sequentially.

After the successful activation of a platelet through one or more signaling pathways, a number of events serve as indicators of the dynamics and extent of the activation state. Contained within quiescent platelets, content of intracellular granules becomes released as a result of platelet activation. There exist at least three different types of granules— α -granules, dense granules, and lysosomes—and each class is known to be composed of unique substances. For example, α -granules hold proteins like P-selectin, vWF, fibrinogen, and other coagulation factors, while dense granules release secondary platelet agonists like ADP and serotonin among other non-protein molecules [23]. Intracellular granule release can be measured through luminescent assays in conjunction with platelet shape change and aggregation [24], and expression of specific granule content, notably P-selectin (CD62P), can be detected with monoclonal antibodies in a flow cytometry setting [25]. In a similar fashion as P-selectin, other markers on the platelet surface can be identified, including CD40L, CD63, activated integrin $\alpha_{IIb}\beta_3$, and

phosphatidylserine, as well as other entities like platelet-leukocyte aggregates, cross-linking agent Factor XIII, and platelet-derived microparticles (PMPs) [25]. Finally, a marker of platelet activation that remains within the cell and must be probed by dyes that penetrate through the plasma membrane is the concentration of intracellular calcium, which is known to depend on two distinct but related mechanisms [26,27]. Each of these classical biomarkers, along with the specific principles of each assay, will be discussed in more detail in Chapter 2.

1.3 Trauma-Induced Coagulopathy (TIC)

1.3.1 Platelet Dysfunction in Trauma Patients

Trauma-induced coagulopathy (TIC) is a complex clinical state that is characterized largely by a bleeding phenotype. Statistically, about 25% of patients admitted to a trauma unit due to severe physical injury will develop TIC, and about 10% of all worldwide deaths are linked to trauma [10]. These metrics increase when considering military subjects, and about half of trauma-related deaths are caused by immediate, rapid, and uncontrollable exsanguination. Though clinicians and emergency response teams have developed various treatment regimens for these patients, the mortality rate still remains high which presents significant room for improvement. Over the years, several groups have set out to understand the underlying biology of TIC in an effort to identify potential ways to design new therapies or preventative methodologies. However, one of the key obstacles in learning about mechanisms is that each trauma patient typically presents with unique conditions; in other words, no single trauma patient is identical to another. Previous medical history or medication use, as well as the relative severity of the injury, may complicate the analysis. Nevertheless, a great deal of work has identified a few key pillars of TIC, each with several contributing factors, that the majority of patients will experience due to drastic changes to their blood biochemistry. These contributing

factors include platelet dysfunction, decreased clotting factor activity, and hyperfibrinolysis, each of which will be discussed in more detail [10].

To start with platelet dysfunction, several previous studies have utilized a variety of laboratory assays to characterize the inability of platelets to respond to activating stimuli. For example, one group employed thromboelastography with a platelet mapping feature to observe sensitivity to ADP stimulation and found about 80% reduction on average compared to a control response [28]. A separate study reported impaired aggregation potential in response to at least one stimulating agonist in almost half of the 100 analyzed trauma patients upon admission and upwards of 90% of the patients at some point during their stay in the hospital [29]. Previous work from our lab using microfluidic technology also showed platelet function defects in terms of impaired deposition onto a prothrombotic surface in a majority of the patients studied [30]. Despite all this observational work, the community's identification of specific physiologic events that carry direct implications in relation to platelet dysfunction is still lacking.

Multiple pieces of literature, including those cited above, have confirmed this dysfunctional platelet phenotype and some have gone as far to identify it as a potential biomarker for TIC or the related traumatic brain injury (TBI) [31,32]. Traditionally, the first hypothesized cause of platelet dysfunction has been thrombocytopenia, or decreased platelet counts, as correlations between platelet number and survival have been drawn previously in various disease states. However, trauma patients largely present with normal platelet counts and acceptable levels of P-selectin, an important protein in the platelet activation process [33]. This observation sheds light on a few possible explanations: (1) a significant fraction of the circulating platelets are simply not functional [31]; (2) platelet pre-activation upon initial shock results in "exhausted" cells that are unable to respond to stimuli upon arrival to the injury site [28]; (3) shedding or internalization of crucial surface receptors renders platelets from sequential activation [34,35]. Unfortunately, it has been

difficult to confirm or reject any of these hypotheses, though the likelihood of a combination of multiple contributing factors is high. In this work, we strive to improve the understanding of platelet dysfunction in trauma patients, while taking into consideration the progress already established.

1.3.2 *Coagulation Abnormalities and Hyperfibrinolysis*

Following the initial stages of hemostasis in which platelet activation and aggregation dominate, the effects of coagulation start to take effect. A sequence of serine protease-mediated cleavage events eventually concludes with the conversion of the inactive zymogen prothrombin into thrombin. In turn, thrombin generation leads to the enzymatic cleavage and polymerization of monomeric fibrinogen into its polymeric form called fibrin. Fibrinogen is a soluble plasma protein that circulates at ~3 mg/mL and is structurally composed of three unique disulfide-linked polypeptide chains, which are represented by E- and D-domains. Thrombin activity causes the release of two peptides from the central E-domain, called fibrinopeptides A and B (FPA/B), and enables interaction between the E-domain of one monomer with a D-domain of a second molecule [8]. This interaction begins to form a staggered, overlapping pattern of individual fibrinogen molecules. An additional coagulation factor, factor XIII, is also converted to its active form through the action of thrombin. Factor XIIIa acts on resulting fibrin polymers by cross-linking multiple chains together via adjacent lysine residues in D-domains, which ultimately stabilizes the clot structure [8]. A simplified visual representation of the fibrin polymerization process with depictions of the changing protein structure from monomeric fibrinogen to cross-linked fibrin is shown in **Figure 1-2**.

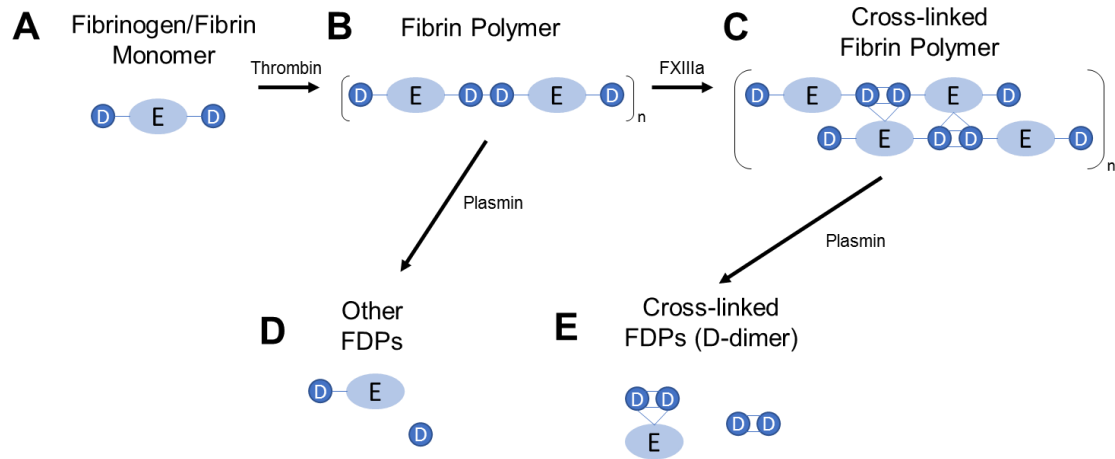


Figure 1-2. Classes of fibrin-related species

Coagulation begins with the monomeric plasma protein fibrinogen (A), then proceeds to become polymerized into soluble fibrin (B) through the enzymatic action of thrombin. Soluble fibrin chains are cross-linked into an insoluble polymer mesh (C) via factor XIIIa, which is converted to its active form in the presence of thrombin. Fibrin polymers are degraded by plasmin into fibrin degradation products of various sizes and compositions (D, E).

Once a stable fibrin aggregate is formed, it has the potential to serve as its own cofactor substrate for lysis. Another inactive zymogen, plasminogen, is known to be activated by two distinct proteases—tissue plasminogen activator (tPA) and urokinase plasminogen activator (uPA)—via different mechanisms [2,8]. Released from activated endothelium and understood to exhibit higher affinity for plasminogen, tPA physically binds to the fibrin surface with plasminogen to generate active plasmin. In the alternative case, uPA is produced by immune cells like monocytes and macrophages and imparts its ability to convert plasminogen to plasmin via the uPA receptor on various cell types [2,8]. Regardless of the mechanism, plasmin then proceeds to lyse fibrin at different sites and results in the release and circulatory uptake of fibrin degradation products (FDP) from the clot. Some examples of FDP generated from either soluble or cross-linked fibrin constructs, including D-dimer (the smallest known FDP) are shown in **Figure 1-2**. Similar to the naturally occurring anticoagulant mechanisms in the hemostatic system, there also exist regulatory systems to control the level of fibrinolysis and prevent excessive clot

degradation. Some key players that inhibit the fibrinolytic system are α 2-antiplasmin and plasminogen activator inhibitors 1 and 2 (PAI-1, PAI-2), which downregulate the activity of plasmin, tPA, and uPA, respectively [2,8]. However, when these serine protease inhibitors (SERPINs) fail to function properly or cannot keep up with the rate of plasmin generation, a hyperfibrinolytic state may ensue.

Along with platelet dysfunction, hyperfibrinolysis is another reported contributing factor to the clinical bleeding phenotype commonly observed in TIC patients [10]. This observation has been made primarily on the basis of biological understanding as well as laboratory measurements of common markers of fibrinolysis. Upon severe tissue injury, a multitude of biochemical changes in the blood take place in response to extreme blood loss and associated shock. Firstly, several procoagulant mechanisms are upregulated which leads to increased potential of thrombin generation [36]. However, many more anticoagulant systems are triggered during trauma which contributes heavily to the observed coagulopathy in a significant portion of these patients. The existence of thrombin in the presence of thrombomodulin results in the activation of protein C (APC), a key anticoagulant. The endothelium also becomes highly activated, which leads to the shedding of the protective endothelial glycocalyx layer (EGL) and release of a number of anticoagulant components like chondroitin sulfate and heparin sulfate [10]. In addition, elevated fibrinolytic agents like tPA, and to a lesser degree decreases in PAI-1 levels, are crucial to the state of hyperfibrinolysis in several trauma patients [37]. This co-existence of procoagulant, anticoagulant, and fibrinolytic states is a perfect recipe for abnormally high production of FDP, which has been characterized by several studies, both in trauma patients and other related conditions like disseminated intravascular coagulation (DIC), and is commonly quantified by measuring the concentration of soluble fibrin or D-dimer in whole blood or plasma samples [38–41]. Though this is certainly not an exhaustive

discussion of fibrinolysis during trauma, further elaboration will be presented in the following chapters of this work.

With knowledge of elevated FDP in the blood of trauma patients, consideration of the time scales of circulation before clearance becomes important. Unless otherwise activated, platelets are known to survive in the bloodstream for 7-10 days before the bone marrow produces a new generation of cells [11]. On the contrary, the clearance rate of fibrin and FDP is likely faster, though different sources have reported different quantifications. One of the first reports studying uptake of coagulation products was performed using a rat liver, in which the authors concluded that the clearance half-life for FDP was at least 12 hours [42]. Another group set up an investigation in mice and considered several variations of FDP through different preparation schemes, as confirmed by gel electrophoresis characterization. Using a radio-labeled isotope tag, the authors concluded that the fragments ranged from 200-250 minutes in clearance half-life [43]. A third study calculated a half-life time of approximately 5 hours in acute myocardial infarction (AMI) patients after receiving thrombolytic therapy [44]. Though previous findings of FDP clearance have differed, there is relative agreement that the general time scale for clearance half-life is several hours, which would correspond to a few days before full clearance. It is unclear whether this lingering ability of FDP bears any physiological significance, especially in the context of trauma patients.

1.3.3 Efficacy of Transfusion Strategies

Trauma-induced coagulopathy is one of several conditions associated with major bleeding complications, though it may be at the top of the list as far as urgency to treat patients. The universally accepted and utilized immediate form of therapy for trauma patients is transfusion of a range of blood products depending on the specific components that may be most deficient for a given patient. Red blood cells are administered to treat

hemorrhaging patients and to aid in oxygen delivery to tissues, which are often common conditions in patients with anemia or sickle cell disease. Fresh frozen plasma (FFP) is delivered in an effort to promote coagulation and reduce the activity of natural anticoagulant mechanisms that may be upregulated. FFP can be further processed by centrifugation to yield fibrinogen-rich cryoprecipitate to be given to subjects with fibrinogenemia. Finally, fresh platelets from healthy pools are commonly transfused to patients with thrombocytopenia or platelet function defects [45]. Blood tests are performed upon arrival to the hospital to evaluate the state of the patient at hand and determine the best course of action to maximize the probability of survival. However, due to the non-native sources of these blood products, there are risks associated with transfusions that may lead to both infectious and noninfectious complications. For example, allergic reactions, lung injury, or circulatory overload are among the most common setbacks that may occur as a result of transfusion [45]. Therefore, guidelines for the most effective use of blood products as treatment are constantly being amended to prevent these unintended life-threatening effects.

With more respect to platelets and functional defects that are well-understood as a key pillar of the coagulopathic phenotype in trauma patients, analyses of the efficacy of platelet transfusions in an attempt to help restore hemostasis have been conducted. In a systematic review of several independent studies, Thorn et al. focused on traumatic brain injury (TBI) patients that were treated with platelet transfusions, and ended up including 10 articles in the analysis which amounted to >1000 patients from 14 hospitals [46]. The authors tracked several variables across the reports but the key result was comparing mortality rates between transfused and non-transfused patient populations. Surprisingly, most of the studies showed increased mortality in patients receiving platelet transfusions, indicating both lack of efficacy and potential harm with this method of treatment. Though it is possible that the higher death rates observed in transfused patients may also be a

result of more severe injury conditions, there is clearly a lack of evidence that platelet transfusions were effective. In a separate paper, Vulliamy et al. conducted a much smaller study inclusive of ~150 trauma patients and investigated the effects of platelet transfusion on restoring native platelet function [47]. To summarize the results, there was found to be no detectable improvement in the ability of platelets to aggregate or overall platelet count in patients receiving transfusions. However, there was a reduction in the level of fibrinolytic products in these patients, which may be attributed to corresponding increases in plasminogen activator inhibitor-1 (PAI-1).

With knowledge of platelet activation defects, hyperfibrinolysis, and potential lack of efficacy in restoring cell function through transfusion in trauma patients, we strive to further understand the underlying mechanisms that contribute to these clinical observations. In this work, we will apply several common lab techniques to characterize various aspects of platelet function and simulate different scenarios with strategic experimental design. A key aspect of the work will rely on a collaborative effort with Penn Presbyterian Medical Center's Acute Research Collaboration (PARC), through which acquisition of blood samples from admitted trauma patients will be possible.

CHAPTER 2: PLATELET FUNCTION PHENOTYPING METHODS

2.1 Intracellular Calcium Mobilization

Following initial platelet activation, increases in the level of cytosolic calcium (Ca^{2+}) become incredibly important for the amplification of the hemostatic response, as it serves as a communicative measure for recruiting additional platelets to the developing thrombus [26]. As briefly discussed in Chapter 1, several distinct signaling pathways converge upon the intracellular mobilization of calcium ions, which then gives rise to “inside-out” activation of other important biological processes. Calcium mobilization is known to occur through two primary mechanisms which proceed in a sequential fashion and are depicted visually in **Figure 2-1** [27]. First, internal stores which contain high concentrations of calcium ions in resting platelets release their contents upon agonist-induced activation. The stores typically mimic endoplasmic reticulum in other cells and are generally referred to as the dense tubular system (DTS). Activation via the binding of GPCR or ITAM ligands leads to phospholipase C (PLC)-mediated production of inositol triphosphate (IP_3), which facilitates transport of Ca^{2+} through IP_3 receptor (IP_3R) channels and into the cytosolic space. As long as the Ca^{2+} concentration in the DTS does not become too low, this mechanism is prioritized and proceeds without significant interruption. Recirculation of Ca^{2+} back into the DTS to replenish the supply or escape into the extracellular space also occurs; these events are largely dependent on the action of sarcoplasmic/endoplasmic reticulum Ca^{2+} ATPases (SERCA) or plasma membrane Ca^{2+} ATPases (PMCA), respectively [27].

The second mechanism of calcium mobilization is initiated upon depletion of the internal stores and is termed store-operated calcium entry (SOCE). On the surface of the endoplasmic reticulum, stromal interaction molecule 1 (STIM1) acts as a sensor for the Ca^{2+} levels present in the stores. Upon failed binding to Ca^{2+} due to decreased concentrations, STIM1 opens SOC channels in the plasma membrane, which have been

discovered to be transmembrane proteins called calcium-release activated calcium modulator 1 (CRACM1, or the more conventionally used Orai1) [27]. The regulation of Orai1 permits additional extracellular calcium to be transported into the cell as a backup source for the internal stores. A few other mechanisms of calcium transport within platelets exist, but the aforementioned systems are predominantly responsible and are heavily studied in the platelet biology community. Since there are multiple entities with distinct roles in promoting and regulating calcium mobilization, potential for therapeutic target has been proposed and analyzed by several groups, primarily using mouse models. Calcium entry has been determined to be critical for thrombus development without direct implications on hemostasis [27].

Calcium mobilization can be thought of as a dynamic flux of ions across physical barriers, and has been identified as a process that can be tracked in real time as platelets are activated by various stimuli. Harnessing fluorescent technology, several chemical calcium indicators have been designed for specific applications [48]. Most commonly used for cytosolic detection are high affinity dyes, which include Calcium Green-1, Fluo-3, Fluo-4, Fura-2, Indo-1, and Oregon Green 488 BAPTA, among others. Each of these indicators carries benefits and drawbacks; some are single wavelength dyes for easier excitation, some are more suitable for microscopy, some are ratiometric for feasible quantification of ion concentrations. However, they all generally function by permeating into the cell of interest and binding to free calcium ions to produce fluorescent signals. Literature in the platelet biology field tends to highlight the use of Fluo-3, Fluo-4, and Fura-2 in studies of platelet function. Fluo-3 is one of the most popular single wavelength dyes and has sufficient affinity without risk of cytosolic buffering. Fura-2 is a widely used ratiometric dye, but requires dual wavelength excitation. However, in this work we will utilize Fluo-4 due to its overall similarity to Fluo-3 with brighter and more photostable properties [48]. Lower

dye concentrations are required which results in shorter incubation times during experimentation.

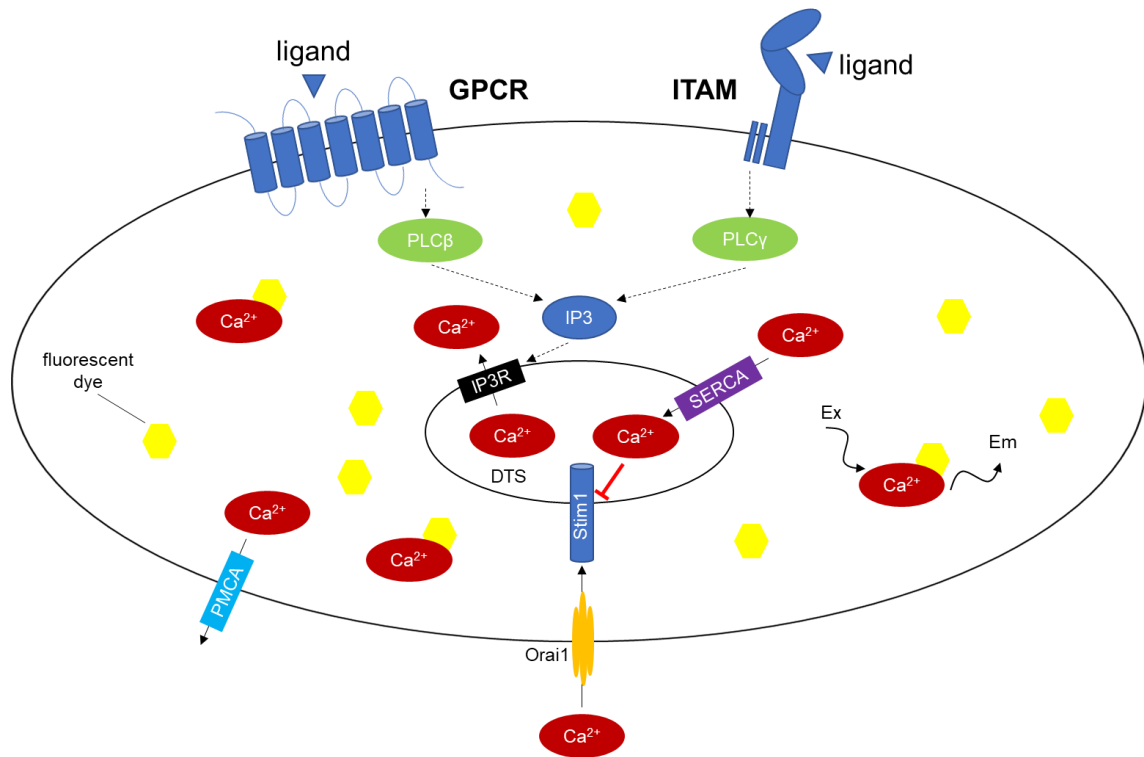


Figure 2-1. Mechanisms of calcium mobilization in platelets

Calcium ions are stored in the dense tubular system (DTS) and can transport into the cytosolic space upon platelet activation. The generation of IP₃ via diverse signaling pathways causes outward calcium flux from the internal stores after binding to the IP₃ receptor (IP₃R). Calcium ions can also be transported back into the stores through sarcoplasmic/endoplasmic reticulum Ca²⁺ ATPases (SERCA) or out of the cell via plasma membrane Ca²⁺ ATPases (PMCA). As the calcium concentration in the DTS depletes, a second mechanism called store-operated calcium entry (SOCE) is initiated by stromal interaction molecule 1 (Stim1) activation of Orai1 channels on the platelet surface. Permeable calcium dyes can be incubated with platelet suspensions to track the mobilization of ions over time following stimulation.

Studying calcium signaling in platelets is of interest to several research groups, and has been documented in previous reports as well as in our lab over the years. Since multiple independent activation events converge upon calcium mobilization, it can be used as a single output in high-throughput experiments, and present a great opportunity to apply automated technologies in well-plate setups to collect large sets of data. The first evidence

of being able to use fluorescent imaging plate readers (FLIPR) with microplate formats to study calcium mobilization in platelet samples was provided by Liu et al. [49]. The authors employed the Fluo-4 dye and characterized the activation or inhibition potential of a few physiologic agents as a proof of principle. A few years later in 2010, our lab presented a similar approach but took advantage of the increased capacity of a 384-well plate to unlock the ability to observe combinatorial stimulation events [50]. The method is known as Pairwise Agonist Scanning and has been used extensively to characterize subject-specific platelet function phenotypes, predict increasingly complex stimulation conditions, and compare donors or patients based on demographics or clinical states to identify potentially hidden trends in hemostatic performance. Though calcium mobilization is certainly a reliable metric for measuring the dynamic processes of platelet activation, other methods are also traditionally used and should ideally be combined together to generate as concrete an understanding of platelet function as possible.

2.2 Flow Cytometry

Experimentalists are often interested in studying multiple characteristics of cells (e.g. size, granularity, receptor expression) simultaneously on a single-cell basis, which has led to the development of a technique called flow cytometry. This method is comprised of two main components: (1) a fluidic system, which handles dilute cell suspensions and orients cells individually through the use of a sheath fluid on either side of the primary sample flow path, called hydrodynamic focusing; (2) an optical system, which measures light scattering and fluorescence emission as the cells pass through the detection zone in a single file fashion [51]. The scattering of light is characterized by both forward and side scatter, and provides a representation of the relative size, shape, and other physical features of the cell. Fluorescent dyes or biomarkers specific for intracellular or extracellular targets of interest are also included in the sample, and are excited by an appropriate laser

beam during the data collection process. Many commonly used flow cytometry systems, such as the BD Accuri C6, are equipped with as many as four laser configurations to scan different wavelengths of transmitted light. A subclass of flow cytometry takes data processing a step further by sorting cells based on fluorescent properties, typically referred to as fluorescent activated cell sorting (FACS) [51]. Overall, flow cytometry and FACS have been used as a high-throughput technique for a variety of applications including characterization of cellular processes like apoptosis, expression of soluble regulators like cytokines, and phenotyping of blood cell populations.

Flow cytometry has been used extensively in the hematology community, ranging from studies of immune cell markers to blood-related cancers to platelet biology [52]. In relation to this work, platelet analysis tends to include both structural and functional property assessment. For study of structural features, surface receptor expression and overall platelet count can be identified with platelet-bound antibodies to suggest potential thrombocytopathies or thrombocytopenias, respectively. Glanzmann thrombasthenia and Bernard-Soulier disease are examples of syndromes related to abnormal expression of surface glycoproteins important for platelet activation and aggregation, and can be detected in this assay by low levels of GPIIb/IIIa or GPIb, respectively [52].

Markers of platelet activation, as discussed previously, can also be probed in flow cytometry [25]. Though GPIIb/IIIa (or integrin $\alpha_{IIb}\beta_3$) expression is often identified to diagnose or rule out Glanzmann thrombasthenia, the activated form of the molecule is a key indicator of outside-in platelet signaling. This active configuration is recognized by the PAC-1 monoclonal antibody, originally developed by Shattil et al [53]. P-selectin (CD62P), which is expressed on the platelet surface upon activation, is detected with fluorescent anti-CD62P antibodies. Phosphatidylserine (PS) exposure to the extracellular surface is measured by Annexin V binding to platelets in the presence of calcium, however this metric is also indicative of cellular apoptosis. As a result, PS measurements should be

conducted in conjunction with other markers to distinguish platelet-specific events. Other less common platelet activation markers studied in flow cytometry include platelet-derived microparticles (PMPs), platelet-leukocyte aggregates, and the transglutaminase factor XIII [25]. Sometimes individual markers are analyzed in simple studies, but the functionality of the flow cytometry design permits more complex experiments with multiple activation events to be conducted. For example, Jaeger et al. designed an assay with three different platelet activation markers in the setting of combinatorial stimulation with an array of platelet agonists [54].

2.3 Platelet Aggregometry

Perhaps a more simplified determination of platelet function is attained through a technique known as aggregometry, which was first introduced in the 1960s [55]. The basic principles rely on light transmission through a stirred cell suspension, which increases as a result of agonist addition [56,57]. Typically, fresh whole blood is split into two aliquots; one aliquot is centrifuged at a modest speed to generate platelet-rich plasma (PRP), while the other is centrifuged more aggressively to isolate platelet-poor plasma (PPP). The PPP sample serves as a reference standard and resembles pure 100% aggregation due to its relatively transparent appearance. As the cells in the PRP sample are activated exogenously, the transmission increases and approaches that of the PPP control, usually quantified on a percent basis [56]. A schematic of the underlying theory for light transmission aggregometry (LTA) is shown in **Figure 2-2**.

Agonists commonly used for optical aggregometry include collagen, ADP, arachidonic acid (AA), epinephrine, and ristocetin. The assay is also often utilized to study inhibitory effects of antiplatelet drugs, and to identify dysfunction in surface receptors that lead to conditions like von Willebrand disease or Bernard-Soulier syndrome [57]. Certain aggregometry-measuring devices, such as Chronolog's Model 700 aggregometer, are

also equipped with luminescence detection. This mode of operation is capable of detecting granule release via ATP monitoring with a luminescent tracker [24]. Understanding granule performance in conjunction with simultaneous platelet aggregation is important because these two concepts are related to each other in the hemostatic process.

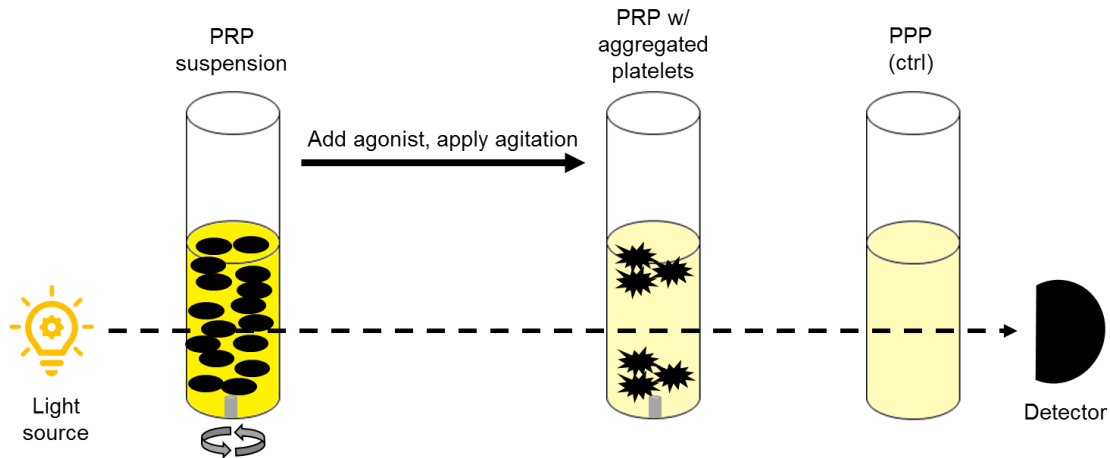


Figure 2-2. Platelet aggregometry experimental basis

Whole blood is centrifuged at various speeds to isolate PRP and PPP. The cuvette loaded with PRP is also given a magnetic stir bar to agitate the cell suspension before and after agonist dispense. The PRP tube is initially cloudy due to dispersity of cells, but after stimulation the clarity of the sample increases due to platelet aggregation, allowing more light to pass through the sample. The amount of light transmission is compared to the theoretical maximum produced by the control PPP cuvette.

Overall, platelet aggregometry has been used as the “gold standard” in studying platelet function, but more recently developed techniques are increasing in usage to assess activation profiles with more complexity. Additionally, aggregometry lacks in the high-throughput category, since only two experimental runs can be performed at the same time, and each sample must include hundreds of microliters of pure PRP, which impacts the amount of blood initially to be drawn. The calcium mobilization and flow cytometry assays described in the previous sections require significantly less whole blood, are usually conducted in dilute conditions, and can be run in microtiter well plates, all of which increase the quantity of data that can be collected per experiment. In this dissertation,

data attained from aggregometry experiments will be reported, but usually in a supplemental fashion to provide support to observations made in other assays.

2.4 Thromboelastography (TEG)

In clinical settings, rapid testing of hemostatic state is required in order to inform decisions regarding treatment options. First developed in the 1940s, thromboelastography (TEG) is a method used to evaluate several aspects of hemostasis and effects of different blood components on platelet function and coagulation. TEG utilizes principles of viscoelasticity to extract information about the strength and stability of thrombi throughout the stages of the hemostatic response [58]. The original assay design included a single reaction chamber – a whole blood sample would be inserted into a cup and a stationary pin capable of tracking movement would be immersed into the sample. The sample oscillates back and forth as an activator of the coagulation cascade is added, and the pin's oscillations change over time as influenced by the dynamic clot strength. The resulting signal increases as a function of stronger clots and then decreases as the clot begins to break down due to shear forces [58]. A depiction of the visual output from a TEG experiment is shown in **Figure 2-3**.

The graphic below is annotated with various parameters, details for each of which along with physiological significance and typical reference ranges are listed in **Table 2-1**. At the beginning of the experiment, a time delay between reagent addition and initial fibrin formation will occur, which is termed the reaction time (R). As the clot begins to develop, the signal read by the TEG device will increase exponentially and eventually reach an inflection point as the clot slows its growth. At this inflection point, the angle between the baseline and the generated curve (α -angle), sheds light on the kinetics of clot growth. An intermediate time, from the end of the reaction time to a pre-determined level of clot growth (e.g. 20 mm), is also recorded as the amplification time (K). The curve then asymptotically

approaches an upper limit, signifying the completion of thrombus development, and referred to as the maximum amplitude (MA) of the data. While the reaction and propagation times are typically indicative of coagulation-related processes, the point of maximum clot strength is highly dependent on platelet function and concentration. The rotational speed of the reaction chamber persists and imparts shear forces on the clot, which causes varying levels of degradation depending on the inherent strength of the clot. After 30 minutes have passed since attaining maximum development, the amplitude is again recorded and compared to MA to yield the LY30 parameter as a measure of clot breakdown via fibrinolysis [58]. The normal values for each parameter shown in **Table 2-1** and the general shape of the curve in **Figure 2-3** are often used as reference to identify potential disorders in specific aspects of the clotting process or to confirm adequate hemostatic performance in an individual.

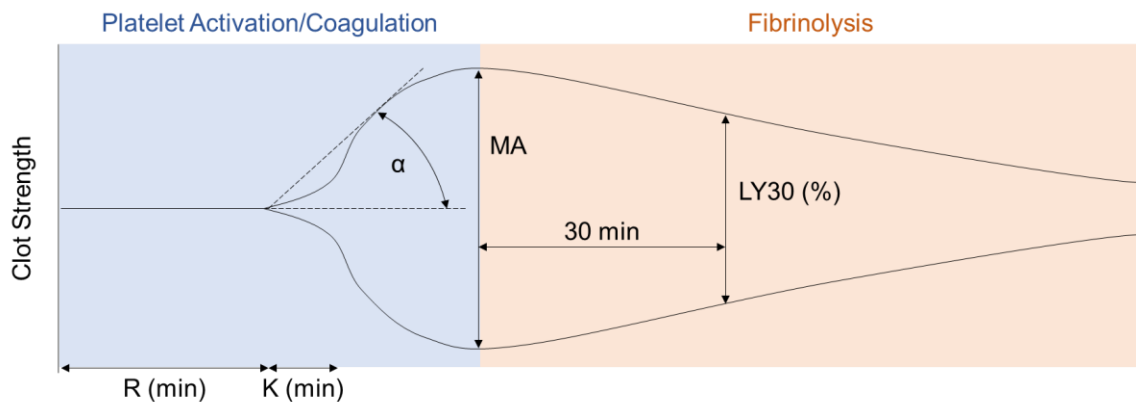


Figure 2-3. Generalized TEG output

Clot strength as a function of time is plotted during acquisition of TEG data, which generates a number of parameters to quantify various stages of hemostasis. The R and K parameters respectively represent the time to achieve initial coagulation and time to another stage of coagulation, dictated by the alpha angle as the maximum rate of clot formation. The maximum amplitude (MA) indicates the point at which the clot is strongest immediately prior to the beginning of lysis. After 30 min of lysis, LY30 indicates the degradation of the clot as a fraction of the maximum strength, and conveys information about clot stability.

Though the overall principles of the assay have remained constant over the years, new designs to increase throughput and decrease required sample volume have been developed. Microfluidic technology-based, one-time use cartridges are now commonly employed as a plug-and-play method of generating TEG data with a custom analyzer. Additionally, different aspects of the coagulation cascade and platelet function can be studied using specifically designed cartridges. For example, certain cartridges are pre-loaded with tissue factor and/or kaolin to simulate the extrinsic and intrinsic pathways, respectively, or a platelet mapping alternative (TEG-PM) enables analysis of platelet response to ADP stimulation. Unfortunately, the reliability and accuracy of TEG in general has become a topic of debate in the medical community [59].

TEG Parameter	Significance	Normal Values
R (reaction time)	Time from start to initial fibrin formation	4-8 min
K (amplification time)	Time to achieve certain level of clot strength (dictated by α)	1-4 min
α angle (propagation rate)	Kinetic rate of clot formation	47-74°
MA (maximum amplitude)	Strongest point of fibrin clot	55-73 mm
LY30 (clot stability)	Percentage decrease in amp. 30 min after MA	0-8%

Table 2-1. TEG parameters

Common TEG parameters that are extracted from data depicted in Figure 2-3 each contribute specific information towards understanding the full scope of hemostasis. Reference ranges of normal values are often used to determine presence or absence of hemostatic disorders.

TEG is often used by trauma units to guide surgeons and other physicians in the attempts to resuscitate injured patients with hemorrhage and other bleeding complications [60]. Different from other conventional tests like prothrombin time (PT) or partial thromboplastin time (PTT), TEG provides information about the evolution of clot development and highlights specific stages of hemostasis that may be under- or over-performing. Since trauma patients often present with coagulopathic conditions, the best course of action is often to initiate massive transfusion protocols (MTP). The ratios of blood

products—platelets, plasma, red blood cells, etc—are often fixed and equivalent, but using TEG data can improve the recommendations for addressing a given patient [60]. For example, a patient may have a long R-time or K-time, indicating a potential coagulation factor deficiency that can be treated with additional plasma delivery. Therefore, application of TEG can allow for more strategic blood product transfusion that may improve mortality in severely injured patients.

CHAPTER 3: SOLUBLE FIBRIN CAUSES AN ACQUIRED PLATELET GPVI SIGNALING DEFECT: IMPLICATIONS FOR COAGULOPATHY

3.1 Introduction

Thrombin generation within the systemic circulation can drive complex changes in blood associated with coagulopathy. During trauma, for example, major changes in blood biochemistry occur due to hemorrhagic shock, release of tissue factor (TF) into the vasculature, endothelial release of tPA, endothelial glycocalyx shedding, and systemic inflammatory events [61–63]. Following trauma, thrombin and plasmin are generated in the systemic circulation as indicated by elevated plasma levels of thrombin-antithrombin, fibrin degradation products, and activated protein C [33,64–66].

Soluble fibrin monomer or soluble fibrin in various states of multimerization can circulate for several hours [67] and reach levels of 100 nM in trauma-induced coagulopathy (TIC) patients [38], 40 nM in Day 0 trauma patients (estimated from fibrinopeptide A levels) [68], 90 nM in neck fracture patients [69], 54 nM in sepsis patients [70], 42 nM in coronary artery disease patients [71], 30-300 nM in ECMO patients [72], and up to 67 nM in post-operative AAA patients [73], all relative to a healthy human baseline of ~7.5 nM soluble fibrin monomer [71]. Also, soluble fibrin exceeds 600 nM (50X baseline) in the rat model of Noble-Collip drum trauma [74].

Platelets obtained from trauma patients can display a hypofunctional phenotype, potentially contributing to TIC [28,32]. Platelet dysfunction after trauma has been detected by aggregometry [29,33], by thromboelastography [28], and by microfluidic assay of platelet deposition on collagen [30]. Interestingly, trauma patients often display no significant differences in baseline platelet count or platelet P-selectin levels compared to healthy individuals [33].

Platelet GPVI is an immunoglobulin superfamily receptor [75] present at about 4000 copies/platelet [76], corresponding to about 1 nM concentration in platelet-rich plasma (PRP). Known GPVI-activating ligands include collagen, collagen-related peptide (CRP), and convulxin [77,78], as well as fibronectin [77], vitronectin [78], and laminins [79]. Within a forming clot and on fibrin-coated surfaces, insoluble fibrin has recently been described as a ligand and agonist of platelet GPVI signaling [75,80]. Platelet GPVI binding to fibrin surfaces increases platelet procoagulant activity [75], amplifies collagen-independent thrombin generation and platelet recruitment at the clot surface [80], and contributes to thrombus growth and stabilization [75,81].

However, the function of soluble fibrin species on platelets in suspension is less well understood, since circulating platelets may eventually encounter a wound site presenting various adhesive matrix stimuli such as collagen, vitronectin, and laminin. Fibrinogen can be activated to desA and desB soluble fibrin monomer which will immediately bind fibrinogen (an assembly also considered, confusingly, as soluble fibrin monomer). Additionally, thrombin activity results in assemblies of sub-micron soluble fibrin multimers (<50 monomer units) which are easily detectable by light scattering. In diluted apixaban-treated PRP where added thrombin is consumed without further thrombin generation, these dilute, soluble multimeric fibrin species are stable in suspension and never reach a concentration to form long fibrin strands, laterally aggregated bundles, or fibrin gels (insoluble fibrin). We use the term “soluble fibrin” to refer to sub-micron desA/B fibrin multimeric assemblies that may also contain bound fibrinogen. The fibrin polymerization inhibitor Gly-Pro-Arg-Pro (GPRP) keeps soluble fibrin monomer from binding fibrinogen or assembling into longer multimer units.

We hypothesized that platelet hypofunction can result from exposure to low levels of thrombin and/or thrombin-generated plasma species such as soluble fibrin. Since elevated soluble fibrin levels have been implicated in trauma and disseminated

intravascular coagulation (DIC) [39,74,82,83], understanding GPVI signaling after soluble fibrin exposure has clinical implications. We developed approaches using apixaban-treated, diluted PRP that allows addition of low-dose thrombin ($t_{1/2} \sim 1$ minute via inhibition by antithrombin) to trigger limited fibrin monomer generation without formation of an insoluble fibrin gel for studies of platelet GPVI signaling in the presence of soluble fibrin species.

3.2 Materials and Methods

3.2.1 Platelet calcium assays

Apixaban and GM6001 (SelleckChem), Fluo-4 NW dye and probenecid (Invitrogen), ADP, GPRP, PGE₁, apyrase, and Factor Xa (Sigma-Aldrich), convulxin (Cayman Chemical), thrombin and human fibrinogen (Haematologic Technologies Inc.), PAR-1/4 agonist peptides (Bachem), U46619 (Tocris Bioscience), T101 (Zedira), vorapaxar (Ryan Scientific), and GR144053 (R&D Systems) were stored and used according to manufacturers' instructions. Whole blood was drawn by venipuncture from healthy donors with University of Pennsylvania Institutional Review Board approval into a syringe containing apixaban (final concentration, 250 nM) to prevent Factor Xa-driven generation of thrombin. Donors self-reported to be free of any medications or alcohol use for three days prior to the blood draw. Female donors self-reported not using oral contraceptives.

Platelet calcium measurements were conducted in 384-well plate assay as previously described [84]. Briefly, 2 mL PRP was obtained from whole blood (120g centrifugation, 10 min) and incubated with a vial of Fluo-4 NW dye mixture reconstituted with 7.8 mL of sterile 20 mM HEPES (N-2-hydroxyethylpiperazine-N'-2-ethanesulfonic acid) buffered saline (HBS, pH 7.4) and 200 μ L of 77 mg/mL probenecid for 30 minutes. In some experiments, GPRP and/or vorapaxar were added with the calcium dye to give

final concentrations of 500 μM and/or 100 nM, respectively. Additionally, a 384-well plate containing platelet agonists was assembled, including thrombin, ADP, U46619 (a stable thromboxane analog), SFLLRN and AYPGKF (PAR-1 and PAR-4 receptor agonists), as well as convulxin (a potent and specific GPVI activator). Dye-loaded PRP was then dispensed into a 384-well plate. Both plates were loaded into a FlexStation 3 (Molecular Devices, Inc.) fluorescence reader. Agonists were dispensed column-wise to PRP, where dynamic fluorescence intensity $F(t)$ was read and normalized by the pre-dispense baseline (F_0). For all experiments, 10 μL of agonist was added to 30 μL of PRP in each well, followed by a subsequent addition of 10 μL of convulxin at a later specified time. In each well, the final concentration of PRP after agonist addition was 12% PRP by volume. The fluorescence was read for 20 seconds before first dispense, and readings were taken every 2.5 seconds (Ex: 485 nm; Em: 525 nm). In previous tests, there was no evidence for autocrine signaling in the dilute PRP conditions of the experiment [84]. In calcium experiments using washed platelets instead of PRP, 500 nM human fibrinogen was added. In this case, the platelet pellet from 2 mL PRP was resuspended in 1.1 mL of HBS to obtain a washed platelet suspension. For calcium assay using type 1 fibrillar collagen (Chronolog), PRP was prepared as described, however the small FlexStation automation pipettes resulted in variable delivery, thus requiring manual pipetting and assay using a FluoroSkan Ascent 384-well plate reader.

3.2.2 *Microfluidic assays*

Fluorescent human fibrinogen (Thermo Fisher Scientific, Alexa Fluor® 647 conjugate) was reacted with thrombin (2.5 nM final concentration) for 5 minutes after a 15-minute incubation with either 5 mM GPRP or HBS (to prevent or allow fibrin polymerization, respectively), after which D-Phenylalanyl-prolyl-arginyl Chloromethyl Ketone (PPACK; Haematologic Technologies Inc.) was added (100 μM final

concentration) to inhibit thrombin. The mixture was then diluted 10-fold into whole blood that had been drawn into PPACK (100 μM) and apixaban (1 μM). Platelets were labeled using PE fluorescent anti-CD61 (BD Biosciences). The 8-channel microfluidic device was fabricated out of polydimethyl-siloxane (PDMS) (Ellsworth Adhesives) as previously described [85]. The device was blocked with 0.5% bovine serum albumin (BSA; Sigma-Aldrich) for 30 minutes before sample perfusion (each channel: 60 μm high, 250 μm wide). Apixaban/PPACK-treated whole blood was perfused through the device using a syringe pump (Harvard Apparatus) at a wall shear rate of 200 s^{-1} over a patterned 250- μm long strip of 1 mg/mL fibrillar collagen type 1 (Chronolog). The deposited platelet and fibrin fluorescence intensities were recorded every minute for 6 minutes.

3.3 Results

3.3.1 *Thrombin stimulation, but not ADP or U46619, attenuated subsequent platelet GPVI signaling*

Addition of thrombin (1-10 nM) to diluted apixaban-treated PRP caused a dose-dependent calcium mobilization (**Figure 3-1,A**). Pretreatment with thrombin, however, resulted in a marked inhibition of calcium mobilization when 20 nM convulxin was added 480 seconds after thrombin (**Figure 3-1,A**). In the absence of thrombin pretreatment, convulxin drives a massive and sustained calcium mobilization lasting over 700 seconds in the measurement. Dasatinib, a Syk inhibitor, blocked convulxin-induced GPVI signaling with minimal effect on $\text{G}\alpha_q$ agonists of calcium mobilization (via thrombin, U46619, and ADP), thus confirming that convulxin is activating GPVI with concomitant calcium mobilization dependent on Syk signaling (**Supplemental Figure 1**). Even the lowest dose of thrombin (1 nM), which caused minimal calcium mobilization, had significant inhibitory effect on GPVI activation by convulxin. However, convulxin-insensitivity was not observed when ADP or U46619 were added instead of thrombin (**Figure 3-1,B-C**) even though both

agonists caused dose-dependent calcium mobilizations similar to that evoked by thrombin treatment.

When ADP was added instead of thrombin, a very low dose of ADP (10 nM) did not affect subsequent calcium response to convulxin compared to the control condition (**Figure 3-1,B**). Low to medium doses of ADP (100 nM-1 μ M) slightly increased subsequent calcium response to convulxin. A high dose of ADP (10 μ M) resulted in a detectable reduction in subsequent final platelet calcium response to convulxin, but not nearly to the extent seen in the case of thrombin. When U46619 was used as the first stimulus, very low to medium doses of U46619 (10 nM-1 μ M) did not affect subsequent calcium response to convulxin compared to the control condition (**Figure 3-1,C**). Similarly, as seen in the case of ADP, a high dose of U46619 (10 μ M) resulted in a detectable reduction in subsequent final platelet calcium response to convulxin, but not nearly to the extent caused by any dose of thrombin. In a related experiment, thrombin treatment of apixaban-treated PRP caused a marked loss in platelet sensitivity to CRP (**Supplemental Figure 2**), although 25 μ g/mL CRP was not as potent as 20 nM convulxin in activating platelet GPVI. Type I fibrillar collagen (20 μ g/mL) was tested as a platelet agonist instead of convulxin. In this unstirred reaction, the platelet calcium response to collagen alone was slower than that observed with convulxin alone. As seen with convulxin and CRP, pretreatment of the PRP with thrombin (2-10 nM) resulted in a complete insensitivity to subsequent exposure to fibrillar collagen (**Figure 3-2,A-C**).

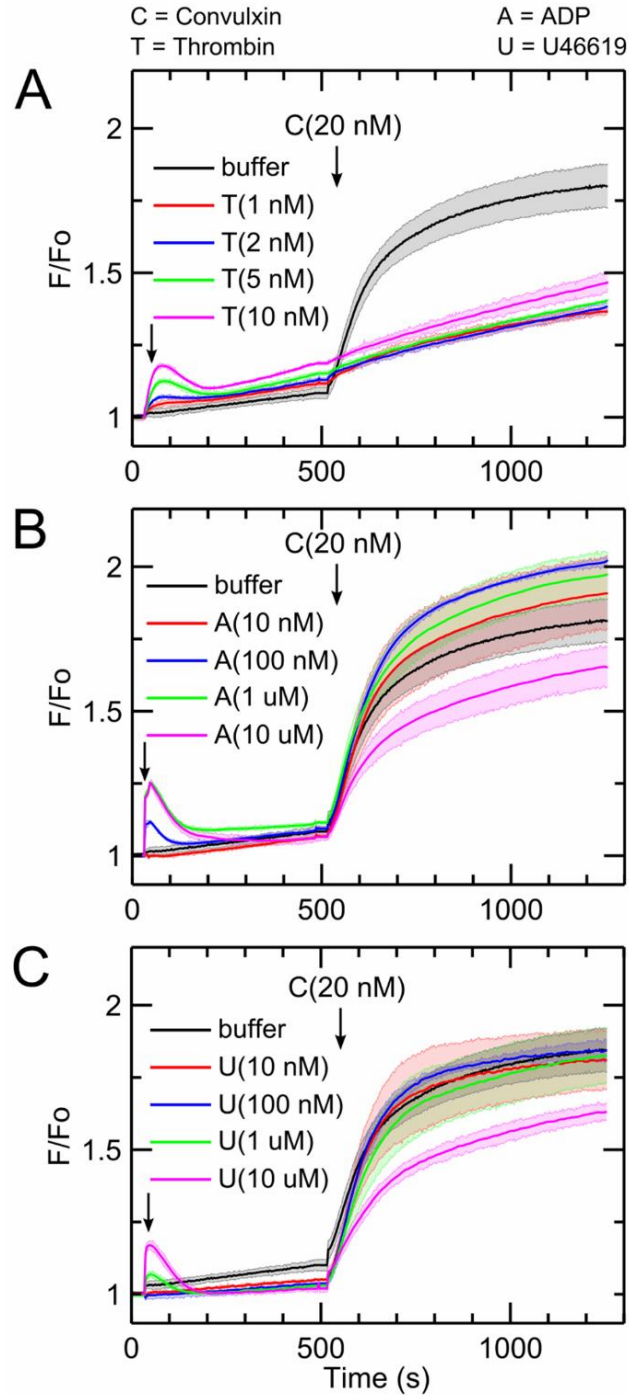


Figure 3-1. Thrombin but not ADP or U46619 blocks subsequent platelet GPVI activation by convulxin

(A) Platelet activation by thrombin for 480 seconds causes a significant reduction in subsequent convulxin-induced calcium response. This effect was apparent for doses of thrombin (1 – 10 nM) treatment of diluted (12%), apixaban-treated PRP. (B) Platelet activation by ADP does not significantly attenuate subsequent convulxin-induced calcium response. (C) Platelet activation by the thromboxane analog, U46619, did not significantly attenuate subsequent convulxin-induced calcium response. (C, convulxin; T, thrombin; A, ADP; U, U46619).

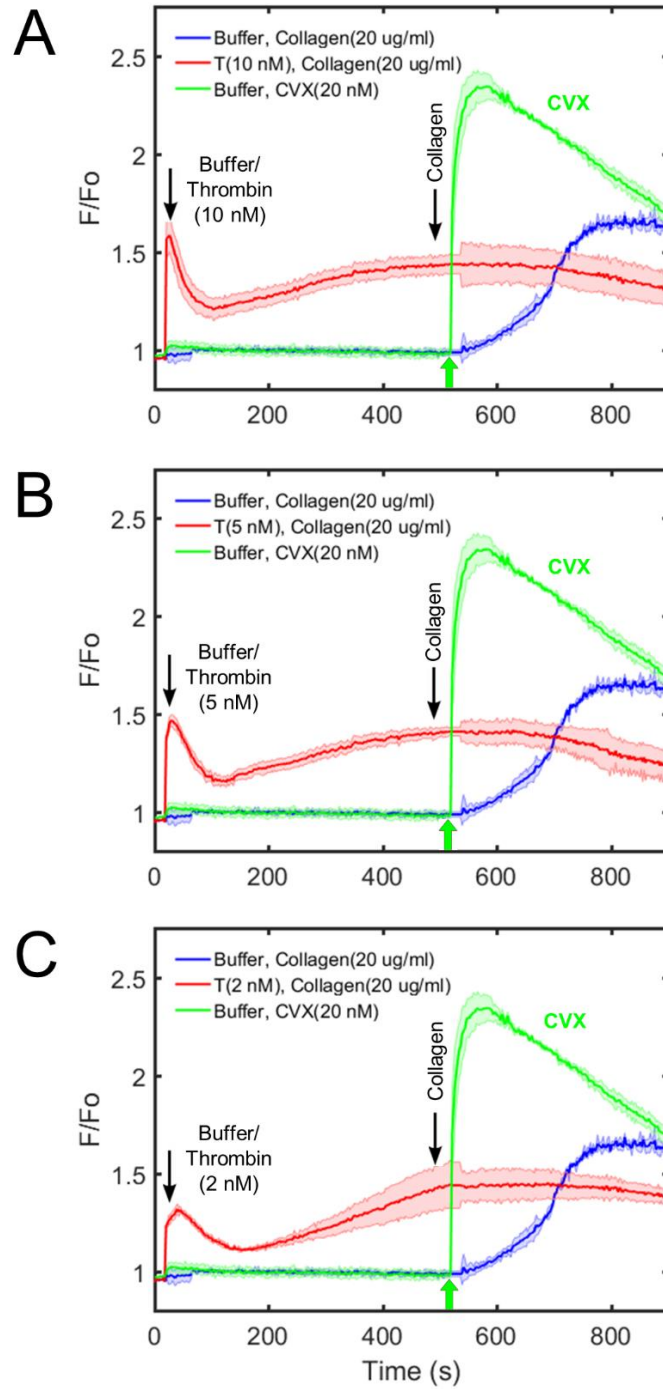


Figure 3-2. Thrombin treatment of platelets blocks subsequent activation via fibrillar collagen when measuring calcium mobilization

Various doses of thrombin (A: 10 nM; B: 5 nM; C: 2 nM) prevent further downstream platelet activation via collagen (Chrono-log; 10 $\mu\text{g}/\text{mL}$), fully consistent with the previous findings using convulxin. Additionally, collagen and convulxin show significantly different kinetic profiles of GPVI signaling which can be attributed to the molecular composition of each species. Collagen, a larger and more fibrillar molecule, activates GPVI in a slower but more sustained manner, while convulxin elicits a rapid and transient response.

3.3.2 *Thrombin-induced GPVI signaling defect was time dependent*

Convulxin (20 nM) was added to PRP at varying times after thrombin addition (1-2 nM). When convulxin was added after low-dose thrombin (1 nM) incubation times of 150, 210, and 335 seconds, the calcium signal in response to convulxin was comparable to the control condition in which PRP was not first activated by thrombin (**Figure 3-3,A**). However, when the incubation time with 1 nM thrombin increased to 480 seconds, subsequent calcium responses to convulxin decreased significantly. When a slightly higher dose of thrombin (2 nM) was first added to PRP, subsequent calcium responses to convulxin were not attenuated until incubation times increased to 210 seconds or higher (**Figure 3-3,B**). The onset time of convulxin-insensitivity depended on thrombin dose (**Figure 3-3,C**). In comparing peak calcium response to convulxin (no thrombin pretreatment) with that obtained with prior thrombin treatment, an incubation with 2 nM thrombin for 220 seconds or incubation with 1 nM thrombin for 500 seconds led to a marked 80% reduction in convulxin-triggered GPVI signaling.

3.3.3 *Activating PAR-1 and PAR-4 does not attenuate GPVI signaling*

Thrombin signals through G_{α_q} -linked PAR-1 and PAR-4 receptors in human platelets, but when PAR-1 and PAR-4 agonists (SFLLRN and AYPGKF) were added to PRP (instead of active thrombin), the subsequent platelet calcium response to convulxin was unaffected compared to the control condition (**Figure 3-4,A**). In combination with the observations with ADP and U46619, this result indicated that thrombin activity played a unique role other than through G_{α_q} -dependent signaling through PAR-1/4. When vorapaxar, a PAR-1 specific inhibitor was added, calcium signaling in response to 10 nM thrombin was fully blocked (**Figure 3-4,B**). However, when thrombin was added to PRP incubated with vorapaxar, the lack of thrombin-induced calcium mobilization had no effect

on the subsequent thrombin-dependent GPVI-signaling defect when convulxin was added (Figure 3-4,C). In separate calcium mobilization experiments using PAR-1 and PAR-4 activating peptides, vorapaxar was found to be a PAR-1 selective inhibitor (Supplemental Figure 3), as expected.

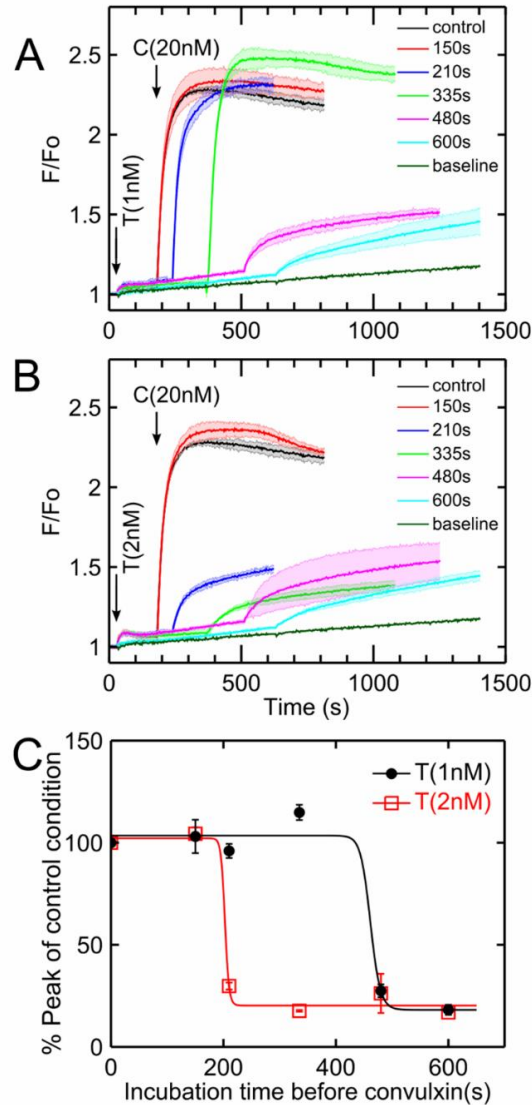


Figure 3-3. Effect of thrombin dose and exposure time to drive convulxin-insensitivity

(A) When platelets were treated with low dose thrombin (1 nM), the reduction of convulxin-sensitivity was time-dependent with strong onset detected between 335 and 480 sec of thrombin incubation. (B) When platelets were activated by a slightly higher thrombin dose (2 nM), thrombin-induced convulxin-insensitivity was detected after 200 sec of thrombin incubation. (C) Sensitivity to convulxin decreased with thrombin incubation time (data fitted with a Hill function) with more rapid onset observed at higher thrombin dose. (C, convulxin; T, thrombin).

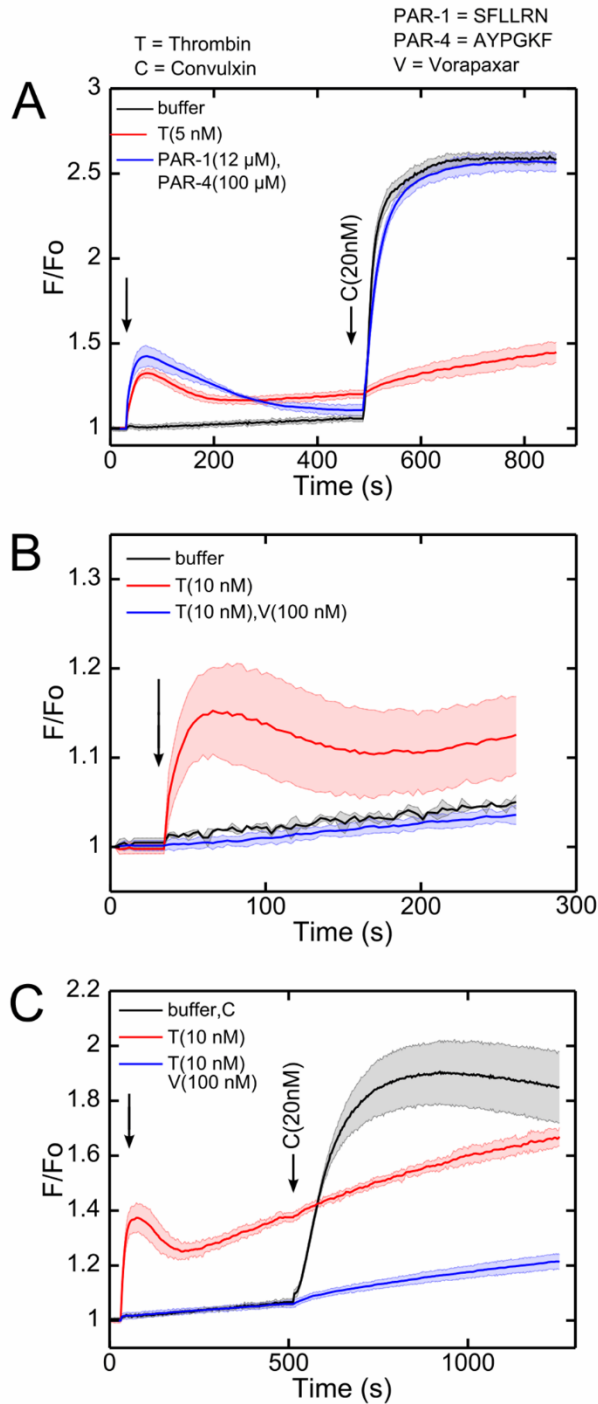


Figure 3-4. Attenuation of convulxin sensitivity was not observed by pretreatment with PAR-1 and PAR-4 agonist peptides

(A) Despite calcium mobilization through PAR-1 and PAR-4, platelet activation by PAR-1 and PAR-4 specific agonist peptides (SFLLRN and AYPGKF) did not reduce subsequent convulxin-insensitivity, as was observed with thrombin. (B) Vorapaxar, a PAR-1 antagonist, blocked thrombin-induced calcium signaling. (C) The convulxin-insensitivity after thrombin treatment was still apparent in the presence of vorapaxar. (PAR-1=SFLLRN activation peptide; PAR-4=AYPGKF activation peptide; V, vorapaxar; T, thrombin; C, convulxin).

3.3.4 Soluble fibrin caused convulxin insensitivity independent of receptor shedding or fibrin binding to $\alpha_{IIb}\beta_3$

The results shown in the previous figures are fully consistent with thrombin acting on a plasma element to attenuate platelet sensitivity to GPVI agonists. This was confirmed in an assay comparing the effect of thrombin pretreatment of washed platelets versus PRP. Thrombin pretreatment of washed platelets caused substantial calcium mobilization, but had little effect on the GPVI response to convulxin (**Supplemental Figure 4**), confirming the role of thrombin on a plasma component. We next tested the ability of GPRP to block soluble fibrin multimerization and rescue GPVI function in the presence of active thrombin. When thrombin was first added to PRP incubated with GPRP, subsequent calcium response to convulxin was completely normal when compared to the control condition where no thrombin was first added (**Figure 3-5,A**). This demonstrated that soluble fibrin assembly was essential for the thrombin-induced ablation of platelet sensitivity to convulxin. GPRP rescued GPVI sensitivity to convulxin for thrombin pretreatment concentrations ranging from 2-20 nM (**Supplemental Figure 5**). Unlike thrombin, the P2Y₁/P2Y₁₂ agonist ADP does not induce polymerization of fibrinogen into fibrin. Therefore, as expected, when the experiment in **Figure 3-5,A** was repeated with ADP instead of thrombin, GPRP had no effect on the subsequent calcium response to convulxin (**Figure 3-5,B**). Notably, in the calcium responses to thrombin alone, the calcium signal displayed an upward trend, consistent with soluble fibrin acting as a weak GPVI activator [75]. However, in cases with GPRP present, the thrombin-induced calcium mobilization was transient and eventually returned to baseline (**Figure 3-5,C**).

Since fibrin assembly was required for convulxin insensitivity, we tested if FXIIIa activity played a role in thrombin-induced GPVI attenuation. Interestingly, the FXIIIa inhibitor T101 had little effect on platelet response to thrombin, but caused a marked reduction in the thrombin-induced convulxin insensitivity (**Figure 3-6,A-B**). Additionally,

T101 alone had little effect on the convulxin response of platelets without thrombin pretreatment. T101 was unable to overcome the attenuation of GPVI at the highest thrombin concentration tested (20 nM).

Since GPVI activators like CRP (as well as thrombin) can cause GPVI dimerization [86,87] and shedding by metalloproteases such as α -disintegrin-and-metalloproteinase 10 (ADAM10), we tested the role of shedding in thrombin-induced GPVI-signaling deficiency. Treatment of PRP with the metalloprotease inhibitor GM6001 had little effect on the ability of thrombin to attenuate platelet response to convulxin (**Figure 3-6,C**). GPRP maintained its ability to prevent thrombin-induced convulxin-insensitivity in the presence of GM6001.

Use of the $\alpha_{IIb}\beta_3$ inhibitor, GR144053, inhibited fibrinogen-dependent platelet aggregation (via aggregometry) as expected, however GR144053 did not alter the thrombin-mediated attenuation of convulxin-induced signaling (**Supplemental Figure 6**). This finding eliminates the potential role of fibrin(ogen)-driven integrin $\alpha_{IIb}\beta_3$ outside-in signaling in the observed deficiency in response to GPVI agonists. These results indicate that GPVI shedding and $\alpha_{IIb}\beta_3$ -mediated fibrin binding were not the cause of convulxin-insensitivity in the presence of soluble fibrin, even when soluble fibrin served as a relatively weak agonist for platelet GPVI. When soluble fibrin is formed in the presence of vorapaxar (to prevent thrombin activation), there is little change in calcium signal (**Figure 3-4,C**), indicating that the generation of soluble fibrin is not strongly activating in this system. Still, in this experiment with vorapaxar present, a marked convulxin insensitivity was observed (an effect fully reversed by GPRP and indicative of soluble fibrin driving the GPVI-signaling deficiency).

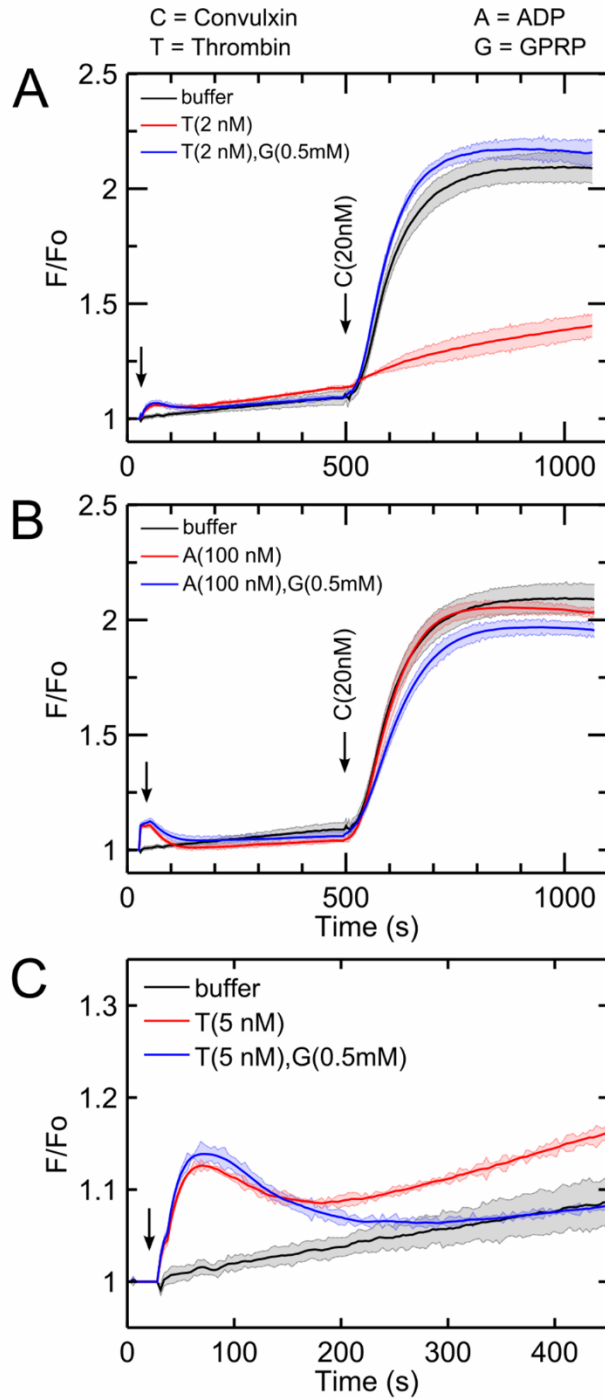


Figure 3-5. Inhibition of fibrin polymerization with GPRP prevents thrombin-induced convulxin-insensitivity

(A) The thrombin-induced attenuation of platelet calcium GPVI signaling was not observed when GPRP was present. (B) Because platelet activation by ADP does not cause fibrinogen to polymerize into fibrin, GPRP has no effect on subsequent convulxin response. (C) Following thrombin stimulation of platelets, fibrin results in a sustained calcium mobilization that returned to unstimulated levels in the presence of GPRP.

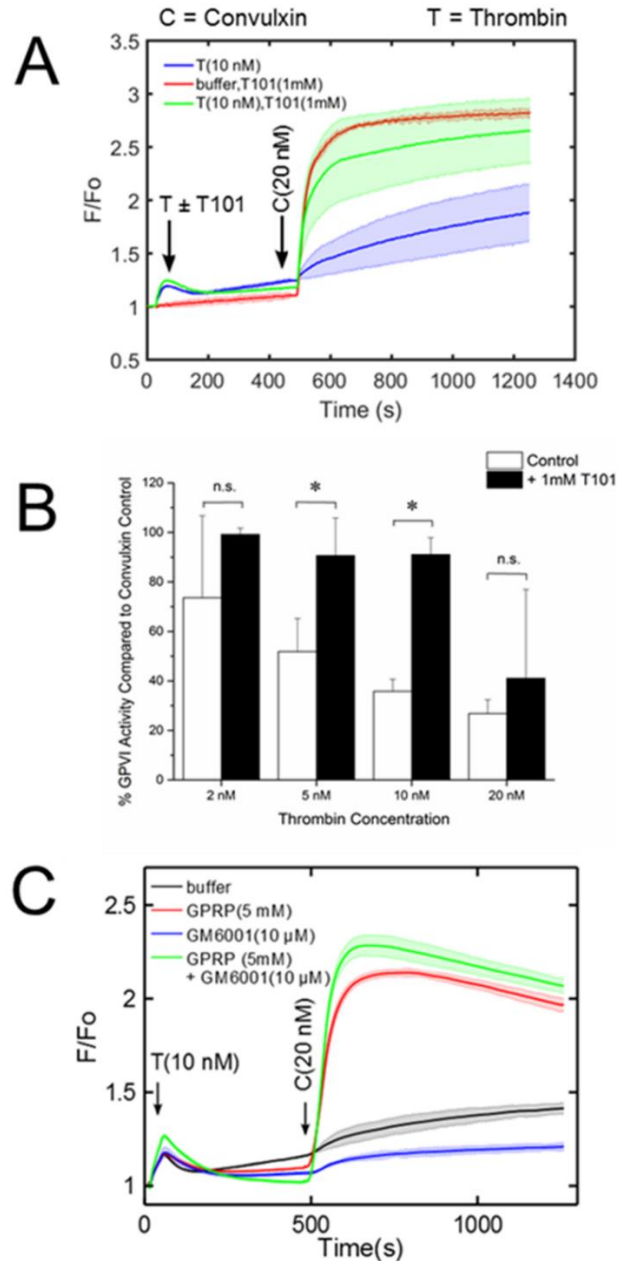


Figure 3-6. Inhibition of cross-linking enzyme FXIIIa with T101 results in significant restoration of platelet GPVI activity and inhibition of ADAM10 shows no effect of GPVI shedding

(A) Calcium dye-loaded platelets were incubated with 1 mM T101 for 10 minutes prior to activation with thrombin (2-20 nM). In the presence of the FXIIIa inhibitor, fibrin still polymerizes but cannot cross-link to form the traditional mesh network which is crucial for clot stabilization. The plot shows the effect of T101 towards greatly restoring convulxin-induced platelet activation. (B) Platelet GPVI exhibits a marked increase in sensitivity, especially at intermediate concentrations of thrombin (n=4 donors, * p<0.05). (C) Thrombin-induced convulxin-insensitivity does not require GPVI shedding. Activation of platelets by thrombin resulted in attenuation of subsequent convulxin-induced calcium mobilization even in the presence of GM6001, which blocks GPVI shedding. When GPRP was present to block fibrin polymerization, thrombin treatment had no effect convulxin sensitivity, even in the presence of GM6001 which blocks GPVI shedding.

3.3.5 *Thrombin treatment of washed platelets in purified fibrinogen displays convulxin insensitivity*

Since thrombin can act on numerous proteins in plasma, washed platelets were placed in a buffer containing purified fibrinogen to explore the role of soluble fibrin generation. Distinct from PRP, this buffer does not contain plasma antithrombin or FXIII. The washed platelets were incubated with human fibrinogen (500 nM) with and without GPRP for 10 minutes before the assay (**Figure 3-7,A**). Exposure for 480 seconds of the washed platelets in purified fibrinogen to a low dose of thrombin (1 nM) caused a marked attenuation of the subsequent convulxin response (**Figure 3-7,B**). Similar to the PRP experiments, GPRP prevented the thrombin-dependent signaling defect in response to convulxin. Soluble fibrin assemblies reached a size of $1.095 \pm 0.347 \mu\text{m}$ after 10 min of thrombin-fibrinogen reaction, as detected by light scattering (**Supplemental Figure 7**).

3.3.6 *Soluble fibrin reduces platelet deposition to collagen under flow*

Fluorescent fibrinogen (0.788 mg/mL) was incubated in either 5 mM GPRP or HBS (control condition) for 10 min. Following incubation, 2.5 nM thrombin was added to generate either soluble fibrin monomer (GPRP present) or soluble fibrin polymer (HBS control). After 300 seconds, thrombin activity was inhibited with 100 μM PPACK. The resulting solutions were diluted by a factor of 10 in PPACK/apixaban-treated whole blood (treated to prevent endogenous thrombin production or thrombin activity). Platelet deposition from whole blood with 230 nM soluble fibrin monomer (GPRP condition) or 230 nM soluble fibrin polymer (HBS control condition), nominal concentrations assuming 100% fibrinopeptide release by thrombin, was then tested on collagen at a wall shear rate of 200 s^{-1} (**Figure 3-8,A**).

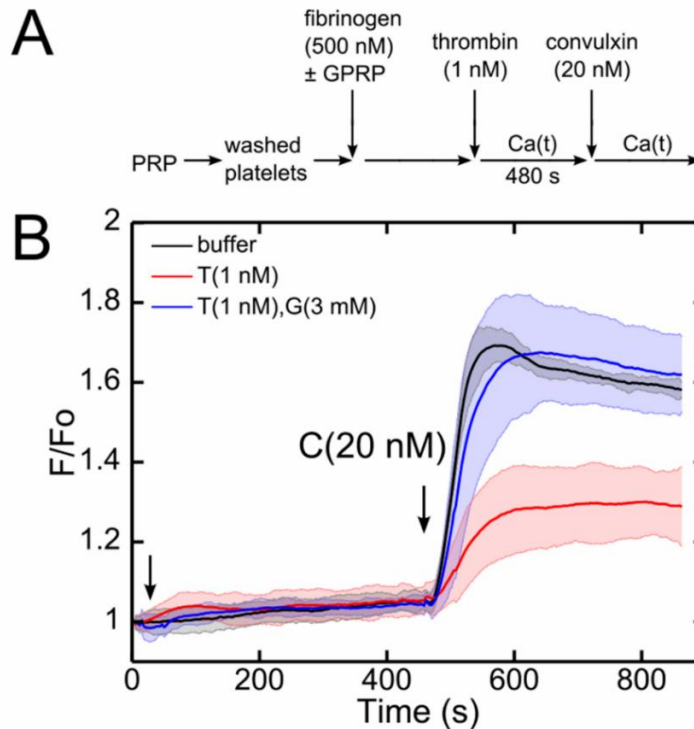


Figure 3-7. Thrombin activation of washed platelets in purified fibrinogen reduced subsequent activation by convulxin, an effect blocked by GPRP
 (A) Schematic of experimental protocol. (B) In a washed platelet and fibrinogen (500 nM) mixture, low dose of thrombin (1 nM) at 480 seconds incubation time significantly attenuated subsequent convulxin response.

As expected, 5 mM GPRP substantially blocked the amount of fibrin that co-deposited with the platelets (**Figure 3-8,C-E**). This indicated that ~8000 nM fibrinogen in whole blood outcompeted 230 nM fibrin monomer for platelet binding. In contrast, 230 nM soluble fibrin polymer added to whole blood co-deposited with platelets, even in the presence of normal levels of fibrinogen. When GPRP is present, there still appears to be a small amount of fibrin detected by fluorescence, which can be attributed to platelet-bound fibrinogen or soluble fibrin monomer. Consistent with a defect in collagen-induced platelet activation via GPVI, the presence of soluble fibrin polymer (HBS control condition) caused a substantial reduction of platelet deposition on collagen (**Figure 3-8,B-E**), especially after ~100 seconds when ADP and thromboxane release are especially important for platelet buildup [88].

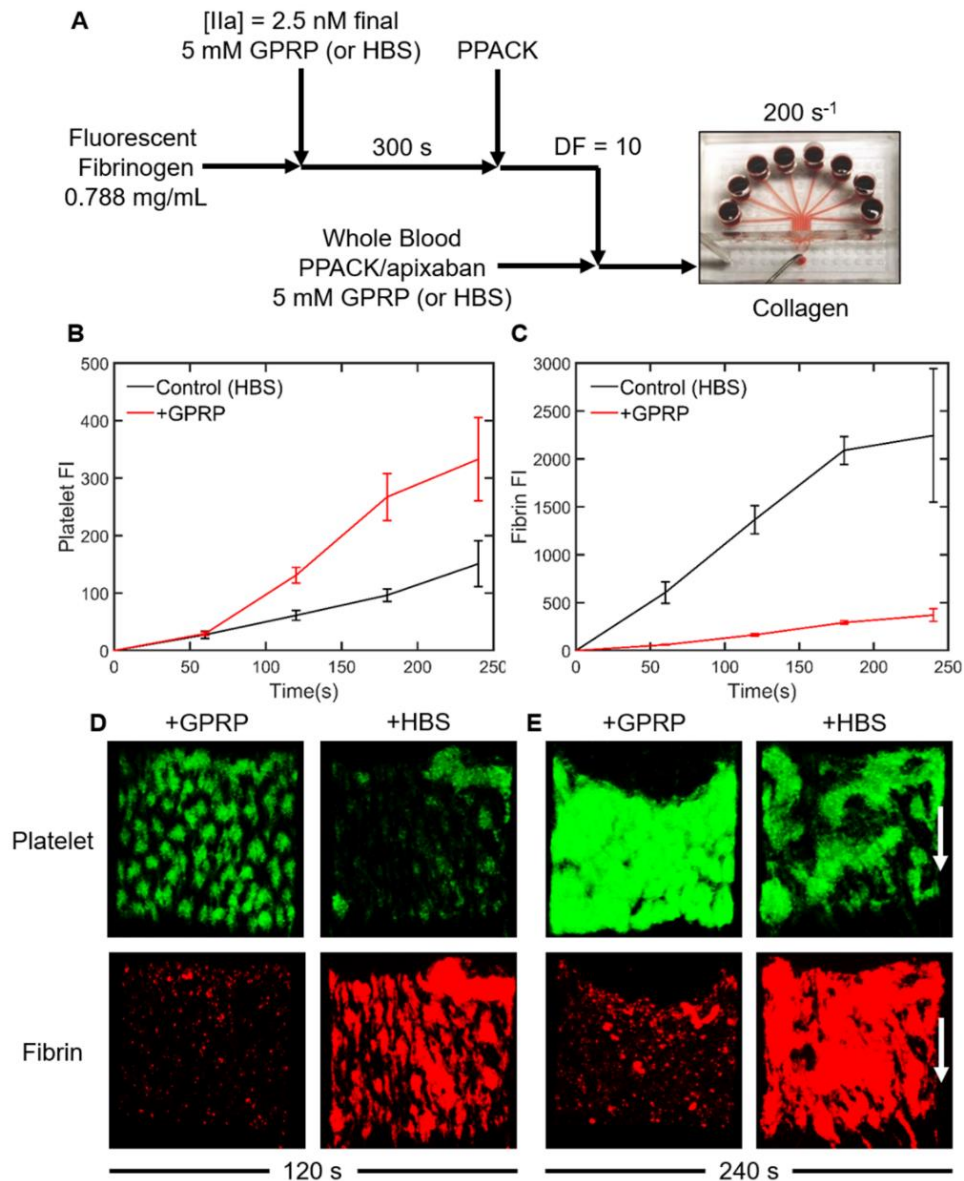


Figure 3-8. Under thrombin-free conditions, presence of soluble fibrin in whole blood reduces platelet adhesion on collagen under flow

(A) Schematic of experimental protocol. Fluorescent fibrinogen was exposed to 2.5 nM thrombin with either 5 mM GPRP (inhibit fibrin formation) or HBS (control). After 300 s, the thrombin was quenched with 100 μ M PPACK. This reacted fibrinogen/fibrin solution was diluted by a factor of 10 into PPACK/apixaban-inhibited whole blood with either 5 mM GPRP or HBS and then perfused through an 8-channel microfluidic device at 200 s⁻¹ over a collagen surface. (B) GPRP increased platelet deposition on the collagen surface after 60 s. (C) Fibrin co-deposition with platelets was significantly decreased with 5 mM GPRP. (D) At 120 s, soluble fibrin monomer (GPRP present) resulted in more platelet deposition to collagen, while soluble fibrin polymer (no GPRP) resulted in less platelet adhesion to collagen. (E) At 240 s, platelet deposition and aggregation on collagen was quite pronounced in the presence of GPRP which blocked fibrin co-deposition, as expected.

3.4 Discussion

In coagulopathic blood, low levels of thrombin in the systemic circulation may generate soluble fibrin monomers and small submicron-scale soluble protofibrils (<10-50 monomers) that never reach the point of gelation. Several lines of evidence are presented that soluble fibrin, not thrombin cleavage of PARs, was the cause of GPVI-signaling deficiency in response to convulxin, CRP, and collagen. PAR-1 and PAR-4 activating peptides that trigger calcium mobilization had no effect on convulxin response. Vorapaxar, which blocked thrombin-induced calcium signaling, had no effect on thrombin-mediated convulxin-insensitivity. Agonists such as ADP and U46619, which similarly trigger signaling through G_{α_q} -coupled receptors, were not able to alter subsequent convulxin sensitivity. Importantly, GPRP blocked the ability of thrombin to attenuate platelet sensitivity to convulxin. Also, the time of thrombin exposure and kinetics of onset were consistent with fibrin monomer generation and soluble fibrin multimerization. Thrombin treatment of washed platelets did not induce convulxin-insensitivity, unless platelets were supplemented with purified fibrinogen. Both the calcium mobilization assay with fibrillar collagen (**Figure 3-2**) and microfluidic platelet deposition from flowing whole blood on collagen-coated surfaces (**Figure 3-8**) indicated that exposure of plasma to thrombin drives an attenuation of platelet GPVI signaling in response to collagen.

To test the findings under non-dilute PRP conditions, we used aggregometry to generate soluble fibrin under non-static conditions and challenge GPVI through addition of convulxin. The results were consistent with those observed in the calcium mobilization experiments: a low dose of thrombin with stirring (1200 rpm) permitted fibrin polymerization and subsequent addition of GPVI agonists shows a significant (~35%) reduction in aggregation compared to the control, a result which is completely reversed with GPRP (**Supplemental Figure 8**). Platelet aggregation in PRP and platelet deposition from whole blood in a microfluidic device were reduced by a similar amount when fibrin

was allowed to polymerize, an effect reversed by GPRP. Given the multimeric nature of most GPVI activators, it was not unexpected that fibrin monomer which exists in the presence of GPRP was insufficient to block GPVI activation.

GPVI-deficiency is extremely rare and not linked to a strong bleeding phenotype in healthy individuals. However, GPVI-deficient patients can display spontaneous bleeds [89]. The potential risk of genotypic GPVI-deficiency in combination with trauma is unknown. Importantly, a combined deficiency in mouse platelet PAR-4 and GPVI causes a severe bleeding phenotype in the tail bleed assay [90]. A level of only 1% conversion of fibrinogen (90 nM soluble fibrin) would be sufficient to overwhelm platelet GPVI which exists at ~1 nM in PRP, as the avidity of binding between polyvalent soluble fibrin and clustering receptors on platelets may be much stronger relative to the K_d of the monovalent affinity involving soluble forms of ligand and receptor. Since soluble fibrin can circulate without rapid clearance and GPVI signaling through fibrin is fairly weak compared to that driven by collagen, platelet hypofunction of endogenous or transfused platelets may be a cofactor in certain coagulopathies.

We are much obliged to highlight recent work demonstrating platelet GPVI as a receptor for fibrin, which was also found to bind to a distinct configuration of GPVI [91]. In that study, sonicated crosslinked fibrin (but not D-dimer) caused <10% washed platelet aggregation over 6 min, while 30 $\mu\text{g}/\text{mL}$ D-dimer substantially inhibited platelet aggregation by subsequent challenge by 0.1-0.3 $\mu\text{g}/\text{mL}$ collagen (but interestingly not higher doses of collagen). As noted in [91], an agent that selectively blocks the interaction of fibrin but not collagen with GPVI has the potential as antithrombotic therapy with reduced bleeding risk. Such an agent might hypothetically also protect circulating platelet function in trauma patients with circulating levels of soluble fibrin polymer and lytic assemblies of D-dimer.

Our results and prior studies of fibrin activation of GPVI during thrombosis [75,80] are not particularly discordant on close examination. To mimic systemic blood changes and subsequent local hemostatic response, we challenge GPVI with a subsequent agonist after pre-exposure to soluble fibrin. In studies of thrombus generation at a wound site, there is no additional GPVI ligand added to the assay other than the original fibrin generated in the clot [75,80]. Also, there is no reason to expect sub-micron soluble fibrin multimers bound to a platelet in suspension to induce the same signaling as a spread platelet experiencing large expanses of solid-phase fibrin gel. Since platelets (and many other cell types) can sense the rigidity of their adhesive-mechanical environment [92], we suggest that platelet signaling on solid fibrin presented on glass/plastic or in a clot may be different from platelets in suspension interacting with soluble fibrin. We also observed that soluble fibrin multimers induce a weak signal in our assay that was blocked by GPRP (**Figure 3-5,C**).

We found GPVI attenuation occurred acutely at ~200 seconds with 2 nM thrombin treatment (**Figure 3-3,B-C**) and was not blocked by a metalloprotease inhibitor (**Figure 3-6,C**). This timescale of GPVI attenuation and the potency of GPRP to block convulxin-insensitivity was fully consistent with the known dynamics of fibrin polymerization, which typically requires <5-10 minutes. Several prior studies have demonstrated minimal soluble GPVI release over 60 min exposure of PRP to tissue factor (200 nM peak thrombin) or to thrombin (1 U/ml), both of which generate fibrin in PRP [93,94]. Thrombin alone does not release soluble GPVI from washed platelets [95], fully consistent with an absence of convulxin-insensitivity following strong thrombin stimulation of washed platelets (**Supplemental Figure 4**). Even strong agonists like collagen, convulxin, or Factor Xa typically require 60 min for full release of soluble GPVI. The exposure of washed platelets to one of the most potent inducers of shedding, Factor Xa, did not phenocopy the kinetics or severity of GPVI-signaling defects (**Supplemental Figure 9**) that we observed with

soluble fibrin generation. Thus, the observed rapid and acute attenuation of convulxin-sensitivity is highly unlikely to be caused by fibrin-induced GPVI shedding, which is also fully consistent with the lack of effect of GM6001 (**Figure 3-6,C**). GM6001 is a known inhibitor of ADAM-mediated GPVI shedding [93–96]. Platelet GPVI shedding is regulated primarily by ADAM10 [97], and may also be facilitated by other members of the a-disintegrin-and-metalloproteinase family (such as ADAM17) [34]. The GM6001 result supports the conclusion that soluble fibrin polymer blocks other more potent ligands from binding GPVI, an effect not requiring GPVI shedding. Since fibrin in clots is known to bind GPVI, soluble fibrin is likely serving as a receptor antagonist to sterically block other ligands from binding. The observed data do not prove mechanism, but are most consistent with (1) steric hindrance of GPVI by soluble fibrin species bound to the receptor and/or (2) soluble fibrin-triggered GPVI signaling that desensitizes the receptor. The observations were not consistent with GPVI shedding, $G\alpha_q$ -dependent GPVI attenuation, or $\alpha_{IIb}\beta_3$ -mediated GPVI attenuation as mechanisms of the observed phenotype.

Distinct from the role of intrathrombus generation of fibrin, low levels of non-gelling, soluble fibrin may function differently in the context of trauma to cause an acquired GPVI-signaling defect in the systemic circulation. Generation of low and transient levels of thrombin in coagulopathic blood may generate circulating soluble fibrin able to bind platelet GPVI to cause platelet insensitivity to stronger GPVI agonists such as collagen. Soluble fibrin is a long-lived species once it is generated, so platelet transfusion therapies for high-risk trauma patients may become affected by these pre-existing species in the systemic circulation. If transfused platelets display an acquired deficiency in GPVI-signaling in trauma patients with elevated soluble fibrin, the extraordinary hemostatic demands essential for survival may not be fully achieved.

CHAPTER 4: PLATELET DYSFUNCTION DURING TRAUMA INVOLVES DIVERSE SIGNALING PATHWAYS AND AN INHIBITORY ACTIVITY IN PATIENT-DERIVED PLASMA

4.1 Introduction

Traumatic injuries are one of the most common causes of death in the United States and abroad, accounting for about 10% of fatalities worldwide [10]. Trauma is well recognized as the leading cause of death for younger populations (persons aged 30-40) [10,61]. Upon admission to trauma centers for a wide range of mechanisms of injury (MOI), approximately 25% of patients will present with a condition known as trauma-induced coagulopathy (TIC) [10,31], a complex clinical state highlighted by impaired activity of important blood clotting proteins, excessive fibrinolysis, and significant platelet dysfunction [10]. The intersection of these phenomena tends to lead to a coagulopathic bleeding phenotype which becomes difficult to treat and increases the chance of mortality by more than 4-fold [64].

Several events may combine to drive TIC. For example, perturbation of the endothelium during a response to a traumatic episode can lead to generation of activated protein C (APC) and glycocalyx shedding, both of which serve anticoagulant and profibrinolytic roles [10]. Other biochemical changes also occur in concert with hemorrhagic shock, including release of tissue factor (TF) and tissue plasminogen activator (tPA), which lead to thrombin and plasmin generation in the circulation [36,61,98]. The coinciding coagulant and lytic processes are responsible for elevated levels of soluble fibrin species, which have traditionally been quantified by plasma levels of fibrin degradation products such as D-dimer [38–40,68]. However, the full extent and mechanisms of acquired platelet dysfunction remain poorly understood.

Platelet dysfunction in trauma patients has been reported in several studies through the use of traditional assays like aggregometry, thromboelastography (TEG), and

microfluidics [28–30,33]. Key findings include decreased aggregation responses to an array of platelet agonists in about half of the tested subjects [29], 80% inhibition of ADP-induced platelet function [28], and defects in deposition to collagen under flow in two-thirds of the patient cohort [30]. The concept of an “exhausted” platelet arises from initial hyperstimulation in response to tissue damage and eventual tiring of the cell as it continues in circulation [28]. Proteolysis or internalization of platelet receptors, including glycoproteins VI (GPVI) or Ib (GP1b), might also play a role in downregulation of platelet function [34]. Soluble fibrin has been shown to cause a signaling defect in GPVI [99], possibly contributing to impaired initial platelet adhesion to exposed collagen at the site of vascular injury if platelets interact with circulating fibrin species prior to encountering a wound site in need of hemostatic response.

Studies of platelets from trauma patients have typically only used one or two major agonists. With technologies for high dimensional phenotyping of calcium signaling pathways [50,84,100], building patient-specific phenotypic profiles of blood cell function may provide more information for treatment decisions. This work focuses on assessing platelet function in trauma patients using a high-throughput technique to interrogate up to six platelet signaling pathways via combinatorial stimulation of surface receptors and using intracellular calcium mobilization as a dynamic readout. Additionally, we investigated platelet dysfunction during trauma by examining the effects of trauma patient plasma on healthy platelets. By all metrics, platelets from trauma patients frequently display a defect in agonist response and the plasma from trauma patients may influence this dysfunctional platelet phenotype.

4.2 Materials and Methods

4.2.1 Reagents

Apixaban (SelleckChem, Houston, TX, USA), D-phenylalanyl-prolyl-arginyl chloromethylketone (PPACK; Essex Junction, VT, USA), adenosine 5'-diphosphate sodium salt (ADP), prostaglandin E₁ (PGE₁), citrate concentrated solution, and apyrase (Sigma-Aldrich, St. Louis, MO, USA), the GPVI agonist convulxin (Cayman Chemical, Ann Arbor, MI, USA), the TP agonist U46619, the IP agonist iloprost (Tocris Bioscience, Bristol, UK), the PAR4 agonist peptide H-Ala-Tyr-Pro-Gly-Lys-Phe-NH₂ trifluoroacetate salt (AYPGKF) and the PAR1 agonist peptide H-Ser-Phe-Leu-Leu-Arg-Asn-OH trifluoroacetate salt (SFLLRN) (Bachem, Torrance, CA, USA), Fluo-4 NW calcium dye and probenecid (Invitrogen, Carlsbad, CA, USA), and FITC mouse anti-human PAC-1, PE mouse anti-human CD62P, and Cy5 Annexin V fluorescent antibodies (BD Biosciences, San Jose, CA, USA) were used and stored according to manufacturers' instructions. HEPES-buffered saline (HBS, pH 7.4) was prepared with 20 mM N-2-hydroxyethylpiperazine-N'-2-ethanesulfonic acid (HEPES, Fisher Scientific, Fair Lawn, NJ, USA) and 150 mM NaCl (Fisher); Tyrode's buffer (pH 7.4) was prepared with 10 mM HEPES, 127.2 mM NaCl, 11.9 mM NaHCO₃ (Fisher), 5 mM KCl (Fisher), 0.4 mM NaH₂PO₄ (Fisher), 1 mM MgCl₂ · 6 H₂O (Sigma), and 5 mM D-glucose (Sigma). Where specified, Ca²⁺ HBS was prepared by dissolving CaCl₂ · 2 H₂O in HBS to achieve a calcium concentration of 2 mM.

4.2.2 Study design

Under Institutional Review Board approval, blood was obtained from trauma patients (n=16) who had been admitted to the Penn Presbyterian Medical Center Level 1 Trauma Center following a severe injury. Patients who are 18-years-old or older, present as a trauma alert, and are admitted to the Trauma and Surgical Intensive Care Unit

(TSICU) were eligible for the study. Upon arrival to the trauma bay, a research blood sample (15 mL) and clinical data were collected by Penn Acute Research Collaboration (PARC) research staff. The legal authorized representative and/or patient is consented once available and after being debriefed by the clinical care team. Descriptions of patient demographics and clinical presentations are outlined in **Table 4-1**.

Patient No.	Age (y)	Gender	Mechanism of Injury (MOI)*	Injury Severity Score (ISS)**	Units of Blood Products Given	Patient Presentation Synopsis	
1	014	45	M	GSW	9	43	N/A
2	019	19	M	GSW	17	2	Multiple penetrating wounds over scapula; received thoracotomy
3	020	60	M	MVC	59	13	N/A
4	025	18	M	GSW	24	11	N/A
5	027	21	M	GSW	38	28	N/A
6	028	33	M	GSW	17	7	N/A
7	036	26	M	SW	17	96	Exsanguination, hemorrhagic shock, cardiac arrest; massive transfusion
8	038	87	F	Fall	13	0	N/A
9	044	67	M	Fall	14	0	N/A
10	055	54	M	MVC	43	4	N/A
11	068	22	M	GSW	26	19	Wounds to thigh, posterior axillary, stomach; sent to OR for thoracotomy
12	075	24	M	GSW	34	3	Wounds to right upper quadrant, liver laceration, adrenal hemorrhage
13	078	30	F	MVC	26	4	Fractures (ankle, femoral, rib) due to extrication
14	086	24	M	GSW	25	2	Wounds to left lower quadrant, sent to OR on two occasions
15	096	34	M	GSW	29	6	Wound to abdomen, sent to OR, initiated exsanguination protocol
16	102	76	M	MVC	43	13	Rib fractures, pneumothorax, liver laceration; fast taken to OR

*GSW: gun shot wound; SW: stab wound; MVC: motor vehicle crash; MCC: motorcycle crash

**ISS>15 corresponds to major trauma

Table 4-1. Summary of patient demographics and clinical presentations

Data were collected for 16 enrolled trauma patients to Penn Presbyterian Medical Center's Trauma-Induced Coagulopathy and Inflammation (TrICI) study. Patient ages were distributed over a wide range (median=31.5, IQR=32.0), and gender distribution was 14 males (87.5%) and 2 females (12.5%). Patients presented with a variety of injuries, though the mechanisms were limited to gun shot wounds, stab wounds, motor vehicle crashes, and falls. Injury severity scores (ISS) were calculated as a measure of the extent of trauma (median=24.5, IQR=15.0), where ISS>15 represents a major traumatic episode.

For each enrolled patient, blood samples were taken at specific time points (0, 3, 6, 12, 24, 48, and 120 h) after initial admission. Several aliquots with specific anticoagulants were prepared for various clinical tests according to the previously established protocol; one such tube pre-loaded with apixaban (1.25 μ M, final concentration) and PPACK (100 μ M, final concentration) was prepared for the studies in this paper. Collecting blood (2 mL) into two anticoagulants ensured inhibition of factor Xa-mediated thrombin generation and thrombin activity, respectively. The sample was split into two microcentrifuge tubes to isolate platelet-rich plasma (PRP) for immediate platelet function studies and platelet-poor plasma (PPP) to be frozen for future analysis. In addition to the patient cohort, a set of healthy donors (n=11) was recruited to donate blood according to University of Pennsylvania Institutional Review Board approval. Donors self-reported to being free of any medication or alcohol use for 3 days leading up to the blood draw. Additionally, female donors self-reported to not using oral contraceptives.

4.2.3 *Intracellular calcium mobilization assays*

Platelet calcium measurements were conducted using a 384-well plate format as previously described [99]. Briefly, PRP was prepared via centrifugation of whole blood (120g, 10 min) and incubated with Fluo-4 NW calcium dye for 30 min. The dye was reconstituted with 5 mL HBS and 200 μ L probenecid (77 mg/mL) to prevent dye leakage from cells during incubation. One 384-well plate was filled with dilute, dye-loaded PRP (12% final concentration after agonist dispense), while a second plate was prepared with platelet agonists at specified concentrations. Using the pairwise agonist scanning (PAS) method as motivation [50,84], an array of combinatorial stimuli (platelet agonists/antagonists) was used to develop subject-specific phenotypic profiles of platelet activity. As reported previously, PAS involves exposing dilute PRP to all single and pairwise combinations of up to six stimuli at low, medium, and high concentrations,

resulting in 154 unique conditions. In order to complete two replicates/condition, ~15-20 mL of whole blood is required to isolate the necessary amount of PRP. However, due to volume constraints in the protocol (2 mL whole blood per patient sample), the combinatorial space was restricted to 31 unique conditions – single combinations of five agonists (ADP, EC₅₀=1µM; U46619, EC₅₀=1µM; convulxin, EC₅₀=2nM; SFLLRN, EC₅₀=10µM; and AYPGKF, EC₅₀=300µM) at three dosage levels each (0.1x, 1x, 10xEC₅₀), and pairwise combinations of the same five agonists as well as one antagonist (iloprost, EC₅₀=0.2µM) with each component present at a medium dose (1xEC₅₀) (**Supplemental Figure 10**). Validation of this restricted combinatorial space was performed by training neural networks on data acquired from the smaller set of conditions and using the models to predict the responses for the full 154 conditions. A relatively reliable correlation (R=0.8125) was observed between the measured and predicted data sets after 10 neural networks per donor (80 total) were averaged together (**Supplemental Figure 11**). The two well plates were then inserted into a FlexStation 3 automated plate reader (Molecular Devices, Sunnyvale, CA, USA) and liquid handling functions were used to dispense 20 µL of agonist(s) directly into each well of 30 µL PRP. The fluorescence of the plate was read column-wise (Ex: 485 nm; Em: 525 nm) for 20 s prior to dispense and then for an additional 4 min; the dynamic signal F(t) was also normalized to the pre-dispense baseline F₀. As a metric of each platelet sample, the amount of calcium mobilized for all stimuli can be calculated as the Total Platelet Calcium Mobilization (TPCM) by **Equation (1)**:

$$\text{Total Platelet Calcium Mobilization} = \sum_{i=\text{PAS condition}} (\text{Ca}^{2+} \text{ AUC}(i) - \text{Ca}^{2+} \text{ AUC}(\text{buffer})) \quad (1)$$

where *AUC* is area-under-the-curve for calcium trace obtained for the *i*th-condition.

4.2.4 Flow cytometry assays

Monitoring platelet activation via flow cytometry was conducted as documented previously [54]. In short, PRP was isolated as described above and diluted to 10% v/v with Ca^{2+} HBS. In each test tube, 10 μL dilute PRP was added to 74 μL Ca^{2+} HBS and 2 μL each of three fluorescently-labeled antibodies (FITC anti-PAC-1 for $\alpha_{2b}\beta_3$ activation, PE anti-CD62P for P-selectin expression, and Cy5 Annexin V for PS exposure). Prior to analysis, 10 μL of platelet agonists were added to the tubes and allowed to incubate in the dark for 10 min. Each sample was analyzed using an Accuri C6 Plus flow cytometer (BD Biosciences, San Jose, CA, USA), setting the flow rate to low (14 $\mu\text{L}/\text{min}$, 10 μm core) and reading for 60 s. Data were collected and reported as mean fluorescence intensity (MFI) for activated $\alpha_{2b}\beta_3$ and P-selectin, or % PS-positive cells as determined by pre-set gating techniques.

4.2.5 Washed platelet preparation for plasma reconstitution experiments

Plasma samples were collected from healthy/patient whole blood and stored at -80°C for future analysis. Healthy washed platelets (WP) were prepared fresh following standard procedures. Specifically, whole blood was drawn into syringes containing citrate concentrated solution (4% w/v) in a 1:9 citrate:whole blood ratio and apixaban (1.25 μM). PRP was isolated as described above, incubated in calcium dye for 30 min, and recalcified with 2 mM CaCl_2 . The PRP mixture was diluted into Tyrode's buffer supplemented with 1 μM PGE_1 and 1 U/mL apyrase prior to further centrifugation (1200g, 14 min). The supernatant was removed and the resulting platelet pellet was resuspended in Ca^{2+} HBS. Washed platelets were combined with plasma samples at specified volume fractions and incubated for approximately 30 min prior to platelet function challenge with various agonists (**Supplemental Figure 12**). For example, a final plasma concentration of 12% is achieved by addition of 6 μL PPP to 24 μL WP and 20 μL agonist. Calcium mobilization

measurements were recorded following the same procedure detailed in the previous section.

4.2.6 *Thromboelastography*

Blood samples were collected on arrival to the trauma bay (T0), and at 3h, 6h, 12h, 24h, 48h, and 120h and immediately aliquoted into tubes containing distinct anticoagulants for assessment of platelet function or hemostasis state using the TEG 6s Hemostasis system (Haemonetics Corp., Braintree, MA, USA) as per the manufacturer's instructions. To monitor the kinetics of patient blood clotting, one mL of blood was mixed with 15.87 units of heparin (Sagent Pharmaceuticals, Schaumburg, IL, USA) and was pipetted into the PlateletMapping ADP cartridge (Haemonetics, 07-615-US). Separately, whole blood was anticoagulated in 3.2% buffered sodium citrate (BD Vacutainer, Becton, Dickson & Co., Franklin Lakes, NJ, USA) and pipetted into the Citrated Multichannel Cartridge (Haemonetics, 07-601-US) which provides clotting characteristics data simultaneously from four independent assays. The de-identified data was stored in a secure server.

4.2.7 *Statistical analysis*

Analysis of raw calcium fluorescence data was performed by MATLAB version R2016a (MathWorks, Natick, MA). Statistical significance tests of results based on experimental condition were conducted using a two-tailed unpaired Student's t-test in Prism version 5.03 (GraphPad Software, San Diego, CA).

4.3 Results

4.3.1 Calcium mobilization measurements indicate global platelet dysfunction in trauma patients

A total of 31 blank, single, and pairwise mixtures of platelet agonists were prepared as shown in the color-coded concentration map (**Figure 4-1,A**) where each row corresponds to a specific input agonist mixture (dark blue = no agonist; light blue = low concentration; yellow = medium concentration; red = high concentration). Each stimulation condition yields a normalized calcium trace $[F(t)/F_0]$ and all 31 traces are shown as 31 rows in a heatmap (**Figure 4-1,B-C**). Comparison of the platelets from healthy donors (**Figure 4-1,B**) and trauma patients (**Figure 4-1,C**) demonstrate a markedly dysfunctional phenotype in the trauma patient platelets across all types of agonist stimuli. While trauma platelets responded best to the highest dose of convulxin, this response was greatly attenuated compared to healthy platelets. Overall, the healthy donor pool exhibited a significantly greater extent of TPCM than the trauma patient cohort (**Figure 4-1,D-E**). The average TPCM for healthy platelets was 220 ± 62 a.u. (**Figure 4-1,D**), greater than that found for every trauma patient at the initial time point of the test 0-hr TPCM (**Figure 4-1,E**). TPCM was depressed for every patient in blood samples tested between 0 and 12 hr. In general, TPCM displayed an increasing trend with time in several patients, but only 4 patients (Patients 014, 019, 020, 038) had a single reading in the healthy range at times between 12 and 120 hr, potentially due to platelet transfusion.

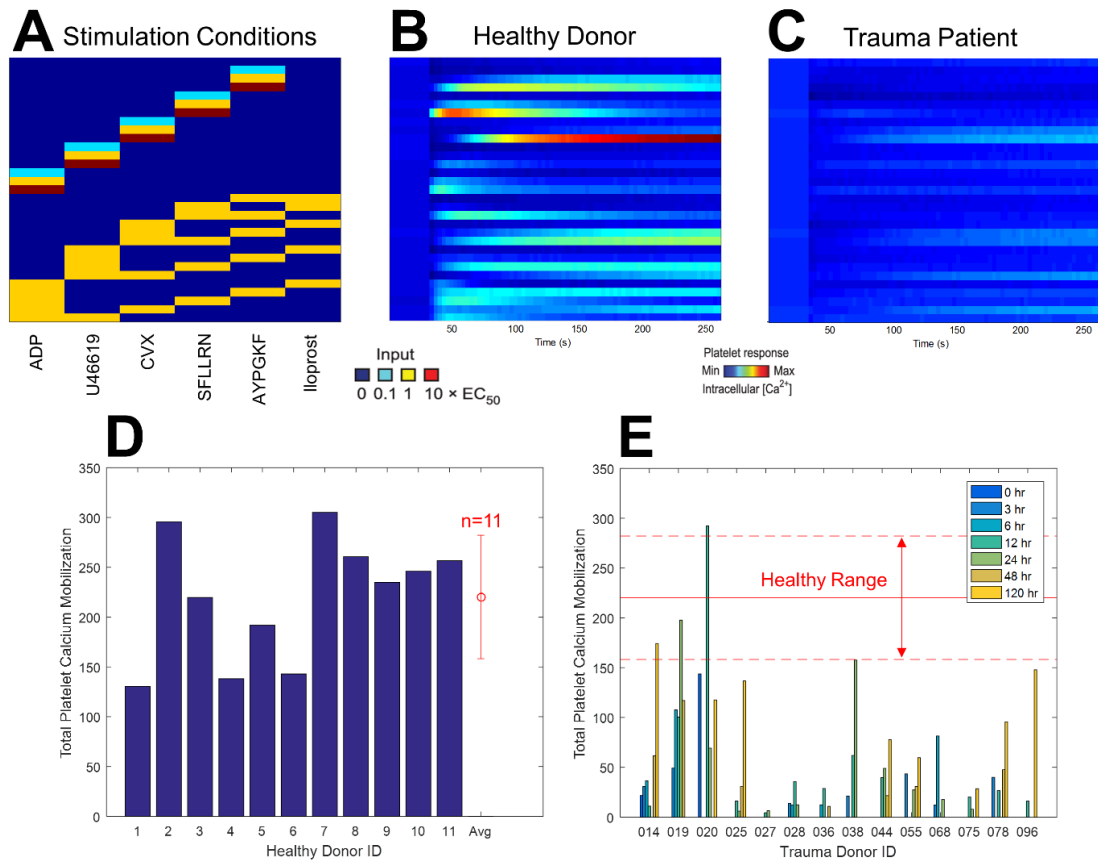


Figure 4-1. Trauma patients exhibit a severely impaired calcium mobilization phenotype in response to platelet agonists

(A) Five platelet agonists (ADP, U46619, convulxin, SFLLRN, and AYPGKF) and one platelet antagonist (iloprost) were prepared according to the concentration map shown. Low, medium, and high doses (0.1x, 1x, and 10x EC₅₀) of the five platelet agonists as well as pairwise combinations of the full six compounds at medium doses (1x EC₅₀) resulted in 31 total conditions including a null buffer control. Representative calcium responses to the array of agonists are shown for a healthy donor (B) and a trauma patient (C). Observations are quantified on the basis of total area under the curve for all conditions (Eq. 1) and results for 11 healthy donors (D) and 15 trauma patients (E) are shown. The mean and standard deviation of the healthy donor responses are overlaid on the plot of patient data to provide context as to the extent of coagulopathy observed in trauma patients and the ability of certain patients to show recovery in platelet function over 120 hr.

4.3.2 Trauma patient platelets exhibit decreased $\alpha_{2b}\beta_3$ activation, P-selectin expression, and phosphatidylserine exposure upon stimulation in flow cytometry

Beyond calcium mobilization, platelet activation also can drive integrin activation, granule release and phosphatidylserine exposure (especially with collagen/thrombin stimulation). Fluorescently activated $\alpha_{2b}\beta_3$ antibody (PAC1), P-selectin antibody, and annexin V were used in a flow cytometry assay to measure platelet activation in the healthy

and patient cohorts. Dilute (1%) PRP was stimulated with calcium-containing HBS, ADP (2 μ M), or convulxin (4 nM). Unstimulated trauma platelets displayed low levels of activated $\alpha_{2b}\beta_3$, P-selectin, and PS indicating that they were not in a classically “activated” state at the start of the assay. The trauma platelets, however, were able to display stimulated levels of $\alpha_{2b}\beta_3$, P-selectin, and PS, but to an extent much lower than that seen with healthy platelets (**Figure 4-2,A-C**). As was observed in the calcium mobilization assay, addition of convulxin caused the greatest response in both healthy subjects and trauma patients. Significant PS exposure was only observed in healthy donors when subjected to convulxin; the other data showed no detectable difference above the buffer control response (**Figure 4-2,C**). A representative set of results for a healthy donor is shown in **Supplemental Figure 13**.

4.3.3 *Thromboelastography (TEG) data reveal patient platelet defects in whole blood samples*

Whole blood samples from trauma patients were anticoagulated with sodium citrate or heparin and dispensed into TEG cartridges to measure platelet function and/or hemostatic state. For each test using citrated blood, the machine generates an output of five parameters describing different aspects of the clot formation process: the time to initial fibrin formation (R), the time to achieve a certain level of clot strength (K), the rate of clot generation (angle), the strongest point of fibrin clot (MA), and the extent of fibrinolysis 30 min after achieving MA (LY30). Using the RapidTEG reagent to interrogate both the intrinsic and extrinsic coagulation pathways with kaolin and tissue factor, respectively, patient blood samples exhibit relatively accelerated coagulation characteristics, namely clotting times and rates, with little to no observed lysis (**Figure 4-3,A-D**). However, platelet-driven clot development and strength appear to be diminished during the first six hours post-trauma, as suggested by the MA parameter (**Figure 4-3,E**), typically most

indicative of platelet function [58]. Further, ADP stimulation of heparinized whole blood reveals a distinct platelet aggregation defect on par with the results from calcium mobilization and flow cytometry experiments (**Figure 4-3,F**).

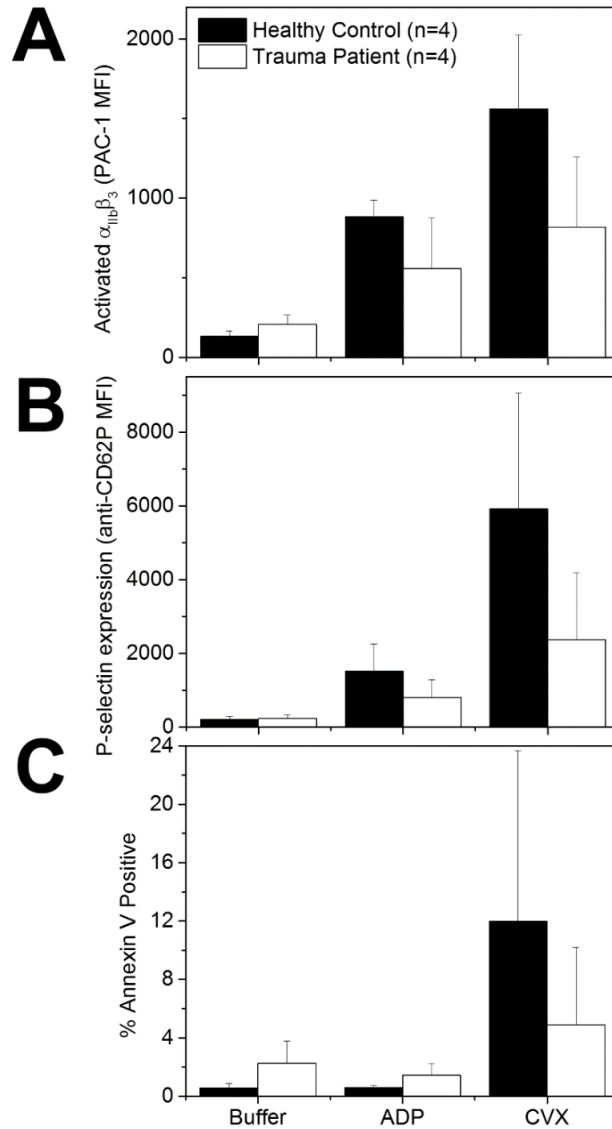


Figure 4-2. Trauma patient samples show impaired integrin $\alpha_{2b}\beta_3$ activation, P-selectin expression, and phosphatidylserine exposure in flow cytometry

Fluorescence-activated cell sorting (FACS) was used to detect platelet activation following stimulation with ADP (2 μ M), convulxin (4 nM), or buffer. Fluorescent antibodies against the activated form of integrin $\alpha_{2b}\beta_3$ (A), P-selectin (B), and exposed phosphatidylserine (C) were incubated with dilute PRP (1% final concentration) prior to agonist stimulation. Conditions were tested in replicate for each donor/patient and mean fluorescent intensities (MFI) of each peak were calculated. For PS exposure, the percentage of positive cells were determined by the relative intensity of the second peak after gating the data.

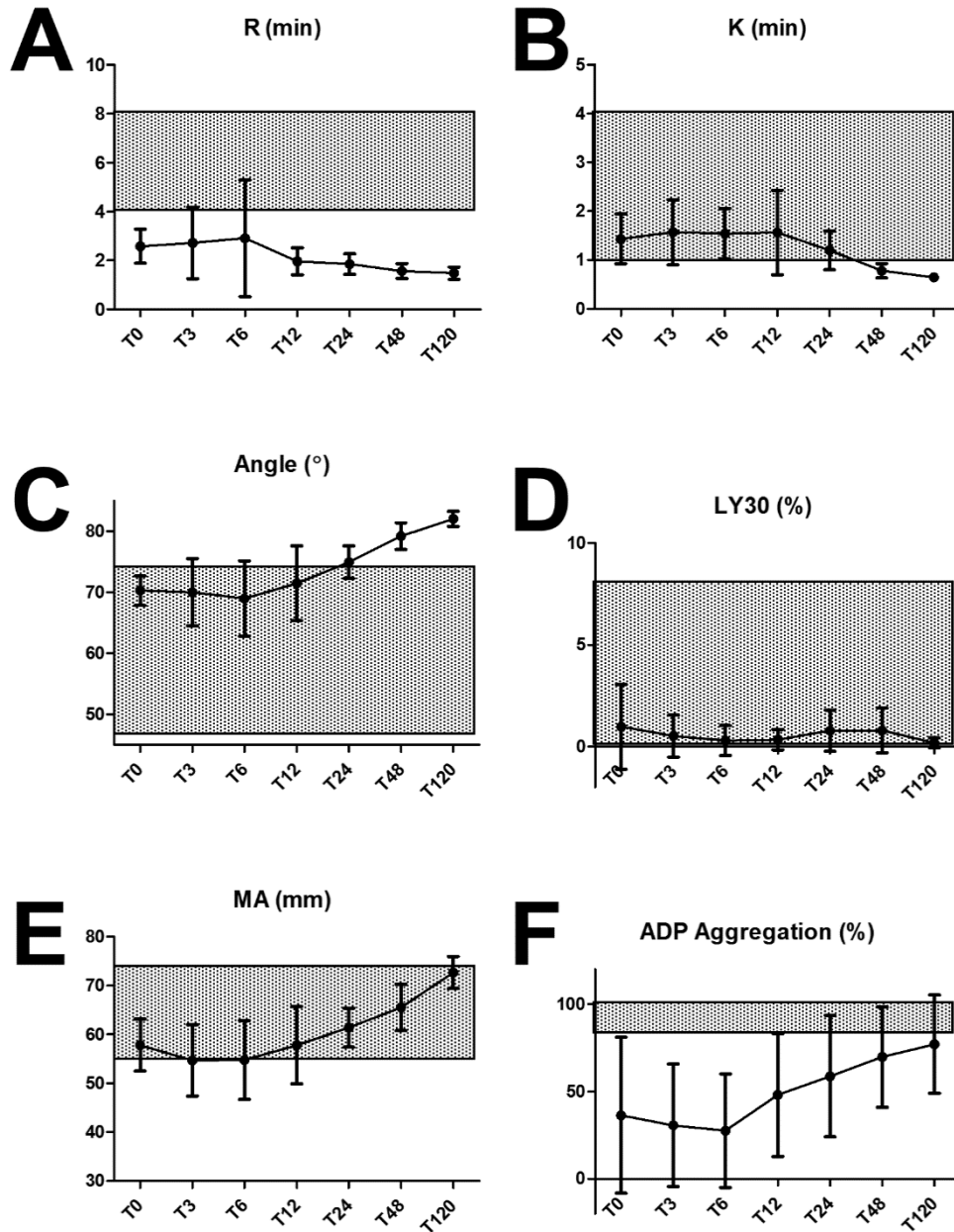


Figure 4-3. Thromboelastography results for patient samples over time

Five important parameters describing clot formation and strength were measured at different timepoints using a TEG[®] 6s Hemostasis System (A-E). Averaged data for trauma patients (n=14) are shown for citrated whole blood treated with RapidTEG[®] reagent (dried kaolin + tissue factor) and CaCl₂ for recalcification. The reported normal ranges (shaded) are: R=4-8 min; K=1-4 min; angle=47-74°; MA/max amplitude=55-73 mm; LY30=0-8%. Additionally, platelet function was measured using the compatible PlateletMapping cartridge. Data was collected using heparinized whole blood and the final metric of platelet activation was calculated as percent aggregation in response to ADP stimulation (F), where the shaded region indicates the reference range (83-100%).

4.3.4 *Healthy human platelets exhibit impaired function in plasma from trauma patients*

Freshly prepared washed platelets reconstituted with plasma (12% v/v plasma, final concentration) were challenged with agonists at high doses ($10 \times EC_{50}$). Responses to convulxin, ADP, U46619, and SFLLRN were significantly reduced when platelets were in the presence of plasma isolated from trauma patient blood samples (**Figure 4-4,A-D**). Specifically, the signals were 54%, 56%, 59%, and 54% lower in terms of area-under-the-curve (AUC) when the system contained patient plasma compared to healthy plasma. These data indicate a clear role for a plasma component on platelet function, perhaps polymerized fibrin or its degradation products as suggested in other work [91,99,101]. ELISA for D-dimer, the smallest fibrin degradation product (FDP) in terms of size, showed ~30-fold increase in D-dimer concentration in trauma patient plasma in comparison to healthy plasma (**Supplemental Figure 14**). The patient and healthy plasma samples used in the experiment shown in **Figure 4-4** contained 21.9 nM and <1 nM D-dimer, respectively.

4.3.5 *Healthy plasma imparts a detectable inhibition of washed platelet activation but patient plasma samples result in more potent effect*

The previous experiment was repeated with a screen of plasma samples from several healthy donors and trauma patients to detect the range of effects of each class of plasma. A control condition (no plasma addition) served as a baseline response to which wells containing healthy or trauma plasma were normalized. High concentrations of convulxin (20 nM) or ADP (10 μ M) were used as challenging stimuli and the calcium mobilization AUC result for each platelet/plasma pair are plotted as percent of the control response (**Figure 4-5,A-B**). In the case of each stimulating agonist, presence of healthy plasma resulted in ~25% reduction of the control response, whereas addition of patient plasma samples further decreased the observed signal to ~50% on average. Each dataset

shows statistical significance from the others, with the difference between the control condition and the trauma plasma samples being the most significant for both agonists.

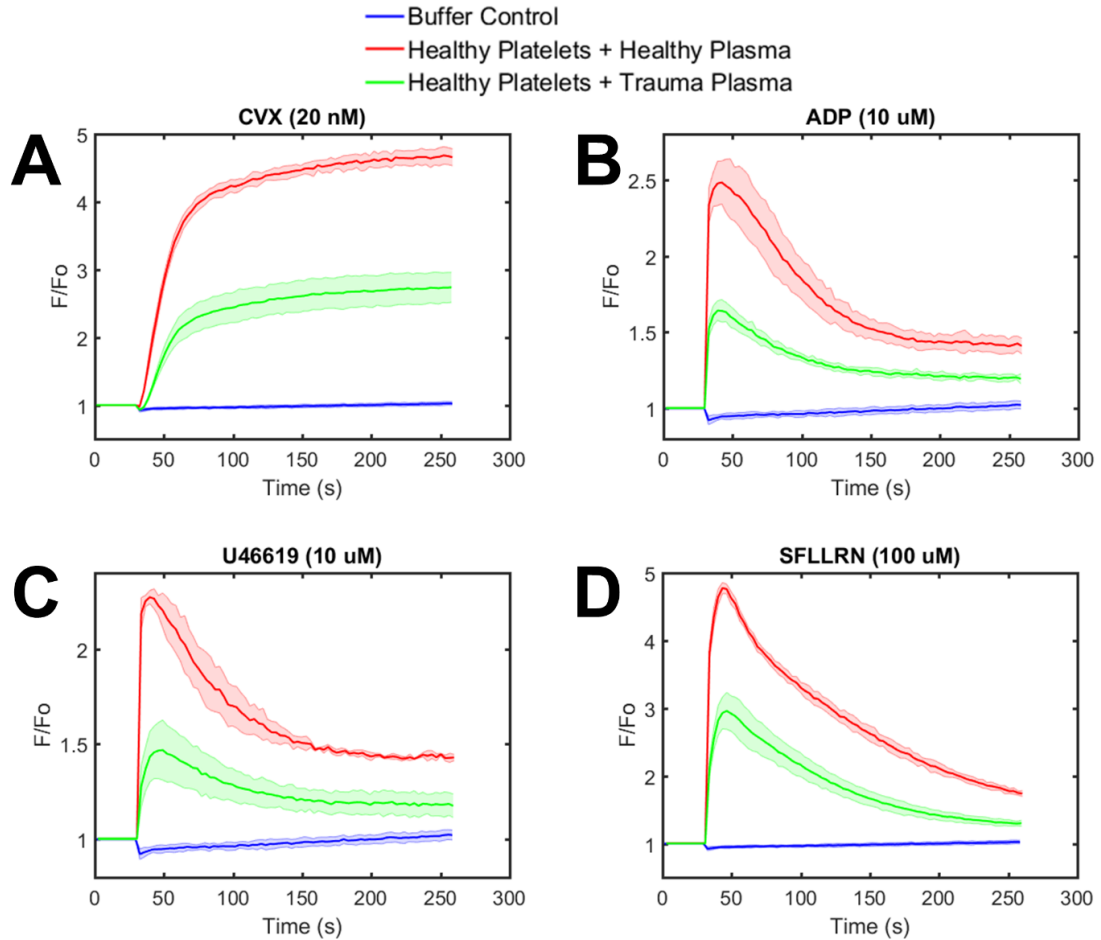


Figure 4-4. Healthy donor platelets lose function when reconstituted in trauma patient-derived plasma

Washed platelets from healthy donors were prepared according to standard protocol and resuspended in platelet-poor plasma (PPP) from healthy donors or trauma patients. The platelet-plasma systems were incubated for about 10 min prior to exposure to various platelet agonists to test cell functionality. The agonists tested were 20 nM convulxin (A), 10 μ M ADP (B), 10 μ M U46619 (C), and 100 μ M SFLLRN (D). In each case, platelets in a trauma plasma setting showed ~50% decrease in calcium mobilization from platelets in a healthy plasma setting.

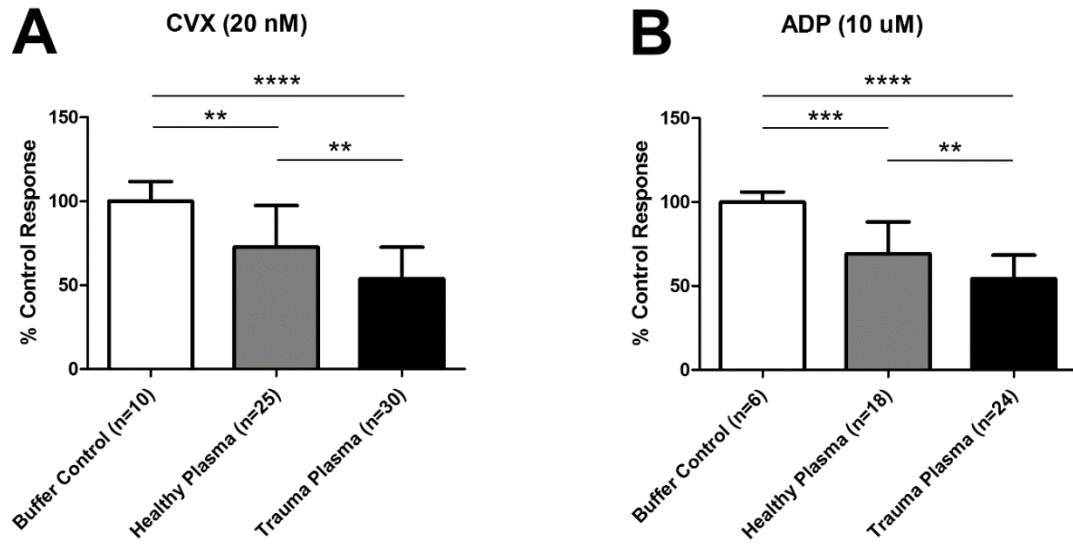


Figure 4-5. Screening several plasma samples reveals a more potent inhibitory effect in trauma samples than healthy samples

Functionality of platelets from healthy donors (n=3-4) was screened in the presence and absence of PPP from several other healthy donors and trauma patients using the same protocol as Fig. 4. Responses to 20 nM convulxin (A) and 10 μM ADP (B) were normalized to the control condition (no plasma). Though healthy plasma showed a down-regulation of platelet function, plasma derived from trauma patients showed a more potent inhibition in both agonist tests. Data are presented as mean ± SEM. (**p<0.01, ***p<0.001, ****p<0.0001).

4.3.6 Plasma concentration is correlated with decreased platelet function

All platelet-plasma combination experiments in previous sections were comprised of 12% plasma and a clear down-regulatory effect was observed. The effect of final plasma content was studied by titrating a range of concentrations (1-30%) and challenging platelet function with 20 nM convulxin, 100 μM SFLLRN, or 10 μM ADP. For each of the agonists, a negatively-sloping dose-response curve was created in which platelets incubated in increasing levels of healthy donor-derived or trauma patient-derived plasma steadily became hypofunctional (**Figure 4-6,A-C**). The negative correlation between platelet calcium mobilization and plasma concentration was evident in both healthy and patient plasma settings, though there was clear parity between the two plasma classes at each concentration to an extent comparable to the results in **Figure 4-4** and **Figure 4-5**.

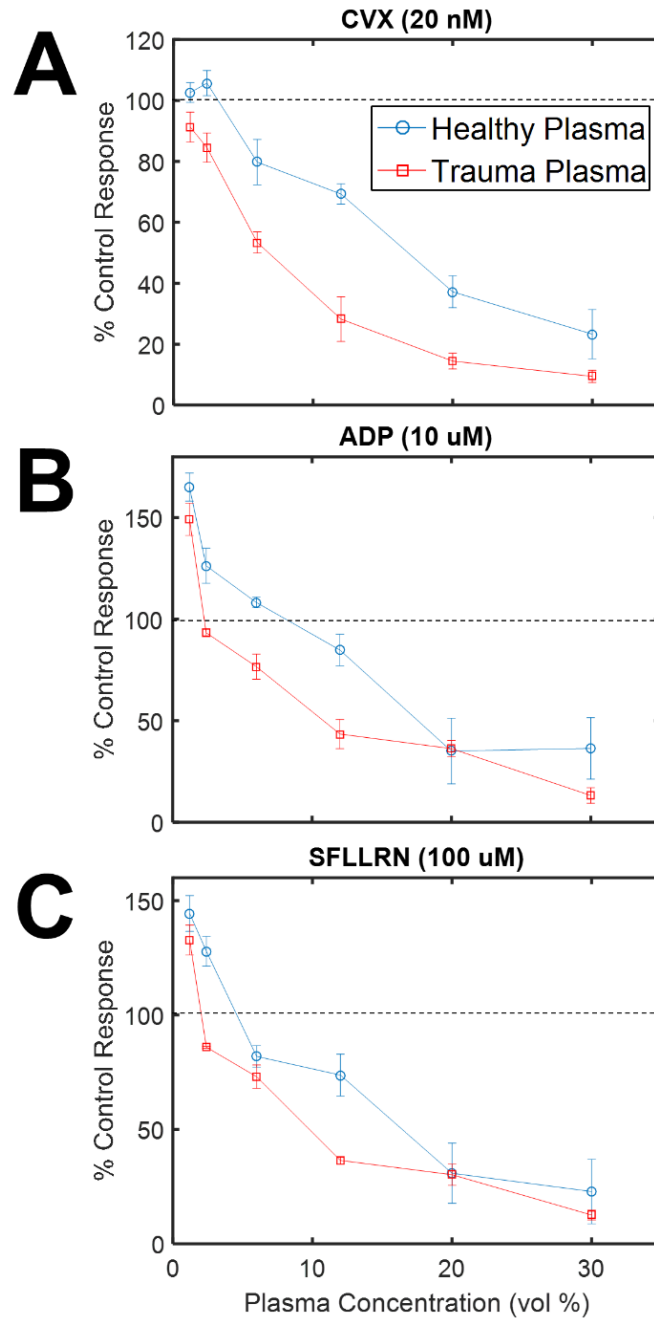


Figure 4-6. Increasing plasma concentrations reduces the calcium fluorescent signal in both healthy and patient plasma settings

Plasma concentration was varied from 1% to 30% and healthy washed platelets were incubated in the presence of healthy (autologous/nonautologous) plasma or trauma plasma. A control response (no plasma) was also prepared for data normalization purposes. All conditions were challenged with a potent dose of convulxin (20 nM) and data were plotted as a dose-response curve showing a negative relationship between plasma concentration and platelet response. Data are presented as mean \pm SD.

4.4 Discussion

In an effort to better understand platelet dysfunction in trauma patients, we present new results confirming the phenotype in several functional assays. Combinatorial agonist stimulation revealed significant depression of platelet calcium mobilization in patient samples compared to healthy controls, though it appeared the two populations show similar sensitivity to strong agonist conditions (e.g. high dose CVX) (**Figure 4-1**). Patient responses varied widely, perhaps due to diverse injury conditions or treatment strategies, and partial recovery of platelet function was observed in one-third of the patients. Trauma patients also showed low $\alpha_{2b}\beta_3$ activation, P-selectin display, and PS exposure following stimulation via flow cytometry (**Figure 4-2**), and thromboelastography (TEG) data showed relatively fast clotting times (R,K) and rates of clot formation (angle), but initially diminished clot development (MA) and platelet aggregation (**Figure 4-3**). The patient sample size in this study (n=16) may prevent the generalizable nature of the results and certainly warrants further investigation, but we have validated the coagulopathic phenotype of platelet dysfunction through the use of several lab and clinical techniques, which has not been reported previously to our knowledge.

A potential link between these results is the injury severity score (ISS), an anatomical quantification system to describe the extremity of a patient's injured state. The ISS accounts for multiple regions of the body, with scores ranging from 0-75 and the threshold for major trauma set at ISS=15 [102,103]. Individual ISS scores for the cohort of 16 trauma patients are listed in **Table 4-1** (median=24.5, IQR=15). This large range led us to hypothesize that the extent of platelet dysfunction may be correlated with the severity of the condition. However, we found no such relationship (**Supplemental Figure 15**), suggesting an added emphasis on the plasma effect observed in **Figure 4-4**, **Figure 4-5**, and **Figure 4-6**. The final ISS assigned to a patient is often determined at some later time

point during or even after the patient's stay and does not account for the patient's previous medical history, which may explain the lack of correlation.

We also show a negative influence of plasma on platelet function. Diluting PRP with PPP to normalize platelet count has previously been shown to impair platelet aggregation [104]. Further, cellular microparticles isolated from traumatic hemothorax blood, and to a lesser extent shed frozen plasma, inhibit platelet response to ADP, arachidonic acid, and collagen [105]. The effect we observed was more potent with trauma patient-derived plasma, implying an amplified role of certain soluble species on cell viability. Other groups have shown elevated levels of soluble FDPs in trauma patient plasma [39,40], which we confirmed via D-dimer ELISA (**Supplemental Figure 14**). The role of circulating fibrin fragments on inherent and transfused platelet function is a subject of continuing study, but initial results show binding sites for fibrin on GPVI [91] and signaling defects following thrombin-mediated platelet activation and fibrin polymerization [99]. At this point it is difficult to elucidate whether these species (e.g. D-dimer) are meant to simply serve as a biomarker or if there exists an important mechanistic explanation linking elevated plasma concentrations and platelet dysfunction. Other possible hypotheses include roles of platelet-silencing species such as cAMP and cGMP, which are reported as elevated in trauma platelets and correlated with injury severity [106].

With the sustained prevalence and diversity of trauma-related injuries and mortalities, understanding the mechanisms of action as well as developing sufficient treatment strategies is becoming increasingly necessary. We highlighted the development of phenotypic profiles of platelet function to be used to guide clinicians in making informed decisions. Additionally, the observation of a plasma-mediated inhibitory effect gives rise to implications of transfusion therapies being ineffective or uninformed. Recent work has debated the appropriate volumes and ratios of blood products to administer to coagulopathic patients [107,108], but perhaps transfusions are not always optimal. In fact,

platelet transfusions in trauma patients have been shown to have little effect on platelet function recovery [47] and resuscitation of hemorrhagic rats via whole blood delivery failed to restore platelet viability [109]. Healthy platelets may inherit the “zombie” nature of the unresponsive but still circulating cells upon exposure to the patient’s plasma, as suggested by the *in vitro* results in this study.

CHAPTER 5: D-DIMER AND FIBRIN DEGRADATION PRODUCTS IMPAIR PLATELET SIGNALING: PLASMA D-DIMER IS A PREDICTOR AND MEDIATOR OF PLATELET DYSFUNCTION DURING TRAUMA

5.1 Introduction

Trauma-induced coagulopathy (TIC) is a relatively common condition observed in patients following severe injuries, and is mainly characterized by an excessive bleeding phenotype attributed to hyperfibrinolysis, coagulation factor deficiency, and platelet dysfunction [10]. Hemorrhagic shock in trauma patients often results in significant thrombin generation and release of tPA, leading to a state of both systemic consumptive coagulation and thrombolysis [36,61]. As a result, fibrin degradation products and D-dimer are produced in large quantities and tend to circulate for extended periods of time [39,40]. Platelet dysfunction in these patients has also been identified as one of the key features of the coagulopathic phenotype. Though endpoint measurements tend to vary amongst studies due to the growing diversity of functional assays, there is general agreement regarding decreased platelet activity in injured patients. Several aspects of the hemostatic response, including aggregation [29,33], calcium mobilization [110], and deposition on prothrombotic surfaces under flow [30], have been shown to be impaired in trauma patient blood. Despite the breadth of literature related to platelet dysfunction following trauma, the underlying mechanisms contributing to the phenotype are not fully understood.

The “exhausted platelet syndrome” has been hypothesized as a potential explanation, in which circulating platelets experience prolonged activation and eventual “tiring” that leads to acquired defects in younger platelets [28,111]. A recent report has suggested potential mechanical damage to platelets during trauma which may impact the cytoskeleton or configuration of integrins on the cell surface [112]. However, on a more biochemical basis, inhibitory effects of factors found in the plasma of traumatized patients

have been reported [110], and the effectiveness of platelet transfusions in restoring in vivo function in hemorrhaging patients is sub-optimal [47]. These latter results have given our group reason to believe certain plasma proteins, specifically fibrin-related species, may carry interfering effects on the ability of platelets to function properly. To our knowledge, there have been no published reports of potential causal relationships between measured D-dimer concentrations and observed platelet dysfunction in trauma, an area we are interested in exploring.

Platelets are dynamic cells that participate in several processes ranging from signaling through a multitude of surface receptors, amplification of the hemostatic response through release of internal granule contents, and interplay with other blood cells and proteins. One of the key interactions that governs platelet aggregation is between the platelet integrin $\alpha_{IIb}\beta_3$ and the plasma protein fibrinogen. Additionally, platelets can interact with several other coagulation enzymes in a protective manner against inhibitors which reduces the risk of conditions like disseminated intravascular coagulation (DIC) [113]. This knowledge, and previous work from our group and others, has led us to conjecture there exists an important physical affinity between platelets and D-dimer or other fibrin-related species. This relationship and its impact on platelet function become especially meaningful in settings of elevated FDP levels. In this work, we attempt to better understand the factors that contribute to platelet dysfunction in trauma by phenocopying patient settings with healthy blood. Further, we investigate the effect of D-dimer on platelet function and propose new findings regarding potential binding events that may guide future therapy strategies.

5.2 Materials and Methods

5.2.1 Reagents

All reagents were used and stored according to manufacturers' instructions. Fluo-4 NW calcium dye and probenecid were obtained from Invitrogen (Carlsbad, CA). Human D-dimer ELISA Kit, native human D-dimer protein, and recombinant human tissue plasminogen activator (tPA) protein were purchased from Abcam (Cambridge, MA). ADP and citrate concentrated solution were from Sigma-Aldrich (St. Louis, MO). Apixaban was obtained from SelleckChem (Houston, TX), thrombin and D-phenylalanyl-prolyl-arginyl chloromethylketone (PPACK) from Haematologic Technologies Inc. (Essex Junction, VT), convulxin from Cayman Chemical (Ann Arbor, MI), PAR-1/4 activating peptides and fibrin polymerization inhibitor GPRP from Bachem (Torrance, CA), $\alpha_{IIb}\beta_3$ antagonist GR144053 from R&D Systems (Minneapolis, MN), Factor XIIIa transglutaminase inhibitor T101, 1,3,4,5-tetramethyl-2-[(2-oxopropyl)thio] imidazolium chloride, from Zedira GmbH (Darmstadt, Germany), type I fibrillar collagen from Chrono-log (Havertown, PA), and APC-conjugated D-dimer antibody from AssayPro (St. Charles, MO). HEPES-buffered saline (HBS) was prepared with 20 mM HEPES and 150 mM NaCl, after which pH was adjusted to 7.4 with 1 N NaOH, all from Fisher Scientific (Fair Lawn, NJ). Tyrode's buffer was prepared with 10 mM HEPES, 127.2 mM NaCl, 11.9 mM NaHCO₃ (Fisher), 5 mM KCl (Fisher), 0.4 mM NaH₂PO₄ (Fisher), 1 mM MgCl₂·6 H₂O (Sigma), and 5 mM D-glucose (Sigma).

Agonist and other reagent concentrations were chosen based on both previous studies and published physiologic ranges. Inhibitor concentrations (GPRP, T101, GR144053) were five to ten-fold greater than the minimum doses required to see anticoagulant or antiplatelet effects, ensuring complete inhibition. Doses of the fibrinolytic agent tPA were supported by published values of plasma levels in trauma patients [47] and purified D-dimer concentrations used in the aggregometry assay were determined by

our D-dimer ELISA results (**Figure 5-3,A**). The antibodies used in the D-dimer ELISA and the flow cytometry assays were able to recognize both D-dimer subunit and D-dimer multimers present in other fibrin degradation products.

5.2.2 *Phlebotomy and patient enrollment*

Whole blood was freshly drawn via venipuncture from volunteer donors following University of Pennsylvania's Institutional Review Board-approved protocols. Syringes were pre-loaded with anticoagulants based on the specific assay being performed: 1.25 μM apixaban to block endogenous thrombin generation through factor Xa activity, 100 μM PPACK to inhibit thrombin activity, or 4% citrate concentrated solution (1 part citrate:9 parts blood) to chelate calcium. Donors self-reported to be free of all medications for seven days and alcohol use for three days leading up to the blood draw and female donors were free of oral contraceptive use.

For patient studies, blood was obtained from a subset of enrolled subjects in the Penn Acute Research Collaboration's Trauma-Induced Coagulopathy and Inflammation study, as documented in previous work [110]. Briefly, patients admitted to the trauma unit who fulfilled enrollment criteria (≥ 18 years old, present as trauma alert, and admitted to Trauma and Surgical Intensive Care Unit) were monitored over the course of 5 days via blood collection at specified timepoints (0, 3, 6, 12, 24, 48, and 120 hr). For this work, blood was drawn into 1.25 μM apixaban and 100 μM PPACK to ensure negligible thrombin generation and activity. General characterizations of trauma patient and healthy control cohorts are provided in **Table 5-1**. All trauma patients and healthy controls were screened for previous medical history prior to inclusion in the study.

	Trauma Patients (n=22)	Healthy Controls (n=7)	P-value
Subject characteristics			
Age, y	39.5 ± 19.0	32.3 ± 8.2	0.34
Male (n, %)	17 (77%)	5 (71%)	
Prev. conditions/meds (n, %)	0 (0%)	0 (0%)	
Mechanism of injury (n, %)			
Gunshot wound	12 (54%)	n/a	
Motor vehicle accident	7 (32%)	n/a	
Fall	3 (14%)	n/a	
ISS	21.4 ± 9.8	n/a	
Laboratory measurements			
Platelet count (x10 ³ /μL)	185.4 ± 44.7	209.3 ± 96.0	0.39
Fibrinogen, mg/dL	425.0 ± 109.5	(150-400)*	
D-dimer, ng/mL DDU	9474 ± 9861	194.6 ± 73.1	0.02
Ca ²⁺ mobilization, AUC	57.9 ± 54.0	238.7 ± 85.6	<0.0001

Values are presented as mean ± SD.

ISS: Injury Severity Score; AUC: area under curve; DDU: D-dimer units

*Typical reference range for fibrinogen in healthy plasma

Table 5-1. Summary of subject characteristics for complete study cohort

Populations of healthy donors (n=7) and trauma patients (n=22) were analyzed in this study. General demographics, clinical presentations for the patient cohort, and lab measurements of common hemostatic variables are summarized in the table. A student's t test was run to compare healthy and patient data for each parameter, and statistical significance is identified by p<0.05. Interestingly, platelet function as measured by calcium mobilization experiments was significantly lower in the patient population, while D-dimer concentrations were significantly higher compared to the healthy control population.

5.2.3 Intracellular calcium mobilization

For calcium mobilization experiments investigating platelet response to combinatorial stimuli in healthy and patient cohorts, platelet-rich plasma (PRP) was isolated from apixaban- and PPACK-treated whole blood via moderate centrifugation (120g, 10min, 20°C), diluted in HEPES-buffered saline (HBS) and incubated with Fluo-4 NW fluorescent dye as described in previous work [99]. Briefly, two independent 384-well plates were prepared: one plate containing dye-loaded PRP and another containing platelet agonists or other reagents. Dynamic data collection was performed with a FlexStation 3 (Molecular Devices, Inc., Sunnyvale, CA), an automated plate reader with liquid handling functions.

In a separate set of experiments designed to mimic coagulant and lytic states during trauma, healthy PRP treated with apixaban only was exposed to a sequential addition of thrombin and tPA, followed by platelet function challenge with glycoprotein VI (GPVI)-activating convulxin. In some experiments, inhibitors of fibrin polymerization and cross-linking (GPRP and T101, respectively) were added to PRP-containing wells 5 min prior to reaction activation (**Supplemental Figure 16,A**). Calcium mobilization traces were all normalized by the initial pre-dispense baseline F_0 .

5.2.4 Platelet aggregometry

Platelet aggregation experiments were performed using a Model 700 Whole Blood/Optical Lumi-Aggregation System (Chrono-log, Havertown, PA). Healthy PRP or washed platelets were prepared as described previously [114] from citrated whole blood followed by recalcification with 2 mM CaCl_2 (Sigma). Platelet-poor plasma (PPP) or Tyrode's buffer were used as respective controls. Platelet agonists were manually dispensed into sample cuvettes at 37°C and aggregation was monitored for 4 min in the presence and absence of purified human D-dimer protein. For study of dense granule function, Chrono-Lume® reagent (Chrono-log) was added to the cuvette and incubated for 5 min prior to beginning the experiment.

5.2.5 ELISA

D-dimer plasma concentrations were measured using the Human D-dimer ELISA Kit from Abcam (PN: ab196269), which recognizes D-dimer and other FDPs containing the D-D epitope. Due to the sandwich nature of the assay with both capture and detector antibodies against D-dimer, we believe that the majority of the signal is indicative of D-dimer presence. Platelet-poor plasma (PPP) samples were prepared via centrifugation of apixaban- and PPACK-treated whole blood (2000g, 10min, 20°C) and diluted adequately

in supplied diluent buffer to ensure the final optical density measurements (450 nm) fell in the pre-determined standard curve range. The assay duration time was about 2 hr from sample preparation to final endpoint read on EnVision 2102 Multilabel Reader (PerkinElmer, Waltham, MA). The ELISA kit was also utilized to measure resulting concentrations in final reaction volumes. Specifically, aliquots from wells described above were analyzed for D-dimer content under differing reaction conditions. Further, reactions of washed platelets and trauma patient plasma samples with elevated D-dimer levels or purified D-dimer were monitored over time to observe the ability of platelets to bind D-dimer (**Supplemental Figure 16,B**). Samples of the reactions were taken at specified time intervals and platelets were removed prior to protein content analysis of the supernatant.

5.2.6 *Flow cytometry*

Surface binding of D-dimer to platelets was measured via fluorescently conjugated anti-D-dimer antibody designed for flow cytometry applications. Dilute (1%) PRP was isolated from apixaban- and PPACK-treated whole blood, prepared in HBS supplemented with 2 mM CaCl₂, and incubated with 10 µL antibody prior to analysis. In some experiments, specified inhibitors were also included to investigate the role of certain surface receptors on D-dimer binding. Samples were analyzed on an Accuri C6 Plus flow cytometer (BD Biosciences, San Jose, CA) for 1 min using the low flow rate setting (14 µL/min, 10 µm core). Data are reported as mean fluorescent intensity (MFI).

5.2.7 *Statistical analysis*

Fluorescence data were analyzed and plotted with MATLAB (MathWorks, Natick, MA). Statistical significance levels between data sets were calculated using a two-tailed unpaired *t* test in Prism version 8.2.1 (GraphPad, San Diego, CA) and set as follows: **p*<0.05, ***p*<0.01, ****p*<0.001. Correlations between data were tested using the curve-

fitting function in OriginPro 9 (OriginLab Corporation, Northampton, MA). Confidence intervals at the 95% confidence level and Pearson's correlation coefficients were reported to indicate the strength of the best-fit line.

5.3 Results

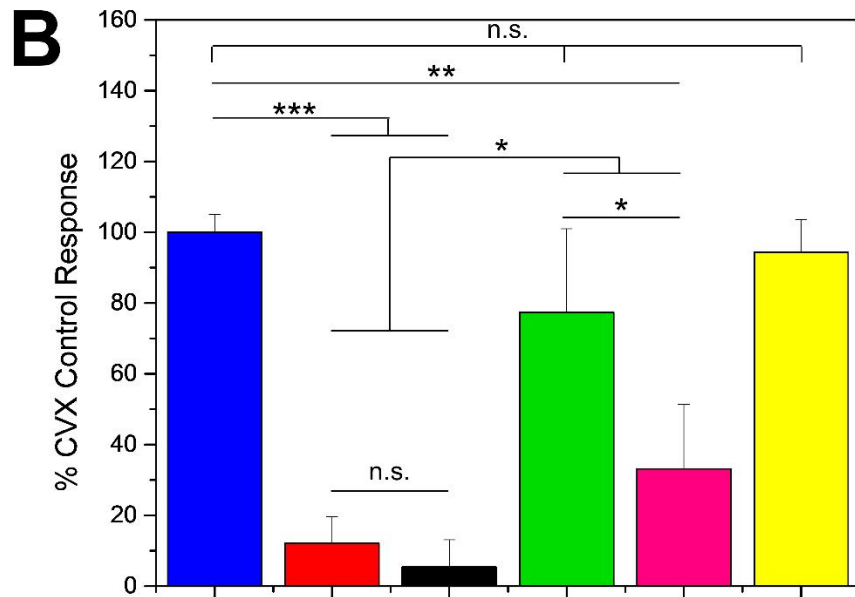
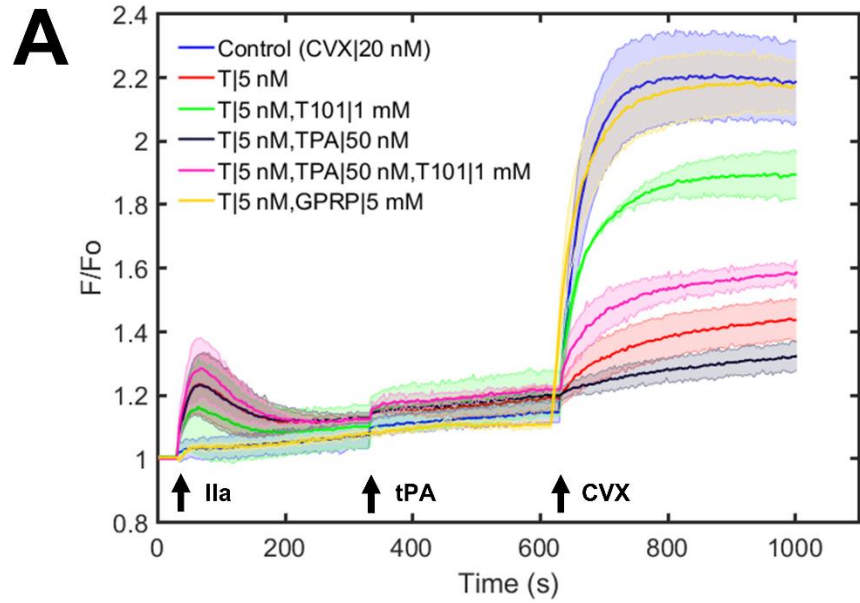
5.3.1 *Factor XIIIa and fibrinolysis contribute to platelet signaling defect*

Treatment of diluted PRP (12 vol%) with thrombin (5 nM) caused a transient increase in intracellular calcium mobilization (**Figure 5-1,A**), consistent with previous results [99]. After 300 s of thrombin activity, tPA (50 nM) was added to certain wells to drive fibrinolysis without eliciting calcium mobilization (**Figure 5-1,A**). Finally, adding convulxin (CVX, 20 nM) to activate GPVI revealed drastically different results depending on the composition of each well, specifically whether tPA or inhibitors of fibrin polymerization (GPRP) or FXIIIa-mediated cross-linking (T101) were included in the pretreatment.

The addition of thrombin alone to generate cross-linked soluble fibrin species caused up to 90% inhibition of platelet GPVI signaling induced by convulxin (red, **Figure 5-1**), consistent with previous results [99]. Incorporating tPA into the system to produce cross-linked FDP further reduced platelet response to CVX (black, **Figure 5-1**). These conditions were repeated in the presence of the FXIIIa inhibitor T101 (1 mM) to investigate the importance of fibrin cross-linking, with and without fibrinolysis. Non-crosslinked soluble fibrin (green, **Figure 5-1**), formed in the presence of thrombin and T101, showed only moderate inhibitory effect on GPVI signaling. Adding tPA to generate non-crosslinked FDP (T101 present) showed substantial inhibition of GPVI signaling (pink, **Figure 5-1**). Full platelet function was recovered when fibrin polymerization was inhibited with 5 mM GPRP (yellow, **Figure 5-1**) as previously observed [99]. The extent of platelet inhibition was quantified by calculating the integrated area under the curve after CVX dispense and

comparing it to the control condition (blue, **Figure 5-1**). Each colored bar in **Figure 5-1,B** corresponds to the signal derived from the colored trace in **Figure 5-1,A**. The relative potency of these species to inhibit convulxin-induced GPVI signaling was: cross-linked FDP (D-dimer) \geq cross-linked soluble fibrin $>$ non-crosslinked FDP \gg non-crosslinked soluble fibrin $\gg\gg$ fibrin monomer. This assumes 50 nM tPA is sufficiently high enough dose to fully dissolve soluble fibrin under the well-mixed conditions of the assay.

To further test that the effect of cross-linked FDP was more inhibitory than cross-linked soluble fibrin (thrombin+tPA vs. thrombin only, respectively), we decreased the thrombin concentration while maintaining the tPA dose. Decreased thrombin concentrations (<5 nM) in control wells showed a dose-dependent restoration of response. The addition of tPA, however, consistently impaired GPVI calcium mobilization (**Supplemental Figure 17,A**). This suggests that, of all fibrin-related species, cross-linked FDP of various sizes (including D-dimer) are the most inhibitory. Generation of the D-dimer epitope in thrombin-treated PRP required tPA and was confirmed by sampling aliquots of the reaction mixtures and measuring plasma concentrations via ELISA (**Supplemental Figure 17,B**).



Thrombin (5 nM)	-	+	+	+	+	+
tPA (50 nM)	-	-	+	-	+	-
T101 (1 mM)	-	-	-	+	+	-
GPRP (5 mM)	-	-	-	-	-	+

Figure 5-1. Effect of cross-linked fibrinolytic products on healthy platelet function

Fibrinolysis was simulated *in vitro* by sequential addition of thrombin and tPA to dilute, calcium dye-loaded PRP isolated from healthy donors. Platelets were then challenged with a potent dose of CVX. Representative calcium mobilization traces for various conditions (A) and quantification of GPVI signaling based on area-under-the-curve following CVX dispense in comparison to a null control condition (B) are shown.

5.3.2 *D-dimer impairs platelet aggregation in response to various agonists*

To further examine the effect of FDP on platelet function, we conducted aggregometry experiments in the presence and absence of purified human D-dimer. Healthy PRP or washed platelets (WP) were incubated with 50 µg/mL D-dimer or HBS and subsequently stimulated with collagen (2 µg/mL), PAR-1 activating SFLLRN (26 µM), or ADP (10 µM). In each condition, platelet aggregation was impaired in the presence of D-dimer, both qualitatively (**Figure 5-2,A-D**) and quantitatively (**Figure 5-2,E**). When washed platelets were isolated and concentrated, creating a fibrinogen-reduced setting, D-dimer strongly inhibited aggregation (**Figure 5-2,A**). In PRP aggregometry, the aggregation was initially identical in the D-dimer and control conditions, but D-dimer soon prevented further aggregation and drove disaggregation (**Figure 5-2,B-D**). This feature is often indicative of defective granule release and is important for secondary aggregation and clot development (confirming data showing dysfunctional ATP release by lumi-aggregometry in **Supplemental Figure 18**) [56]. Recent data has suggested alpha granule release is intact in trauma through the monitoring of P-selectin display [112]. Our data suggest that diminished ATP levels following platelet stimulation in the presence of D-dimer lead to defective dense granule performance.

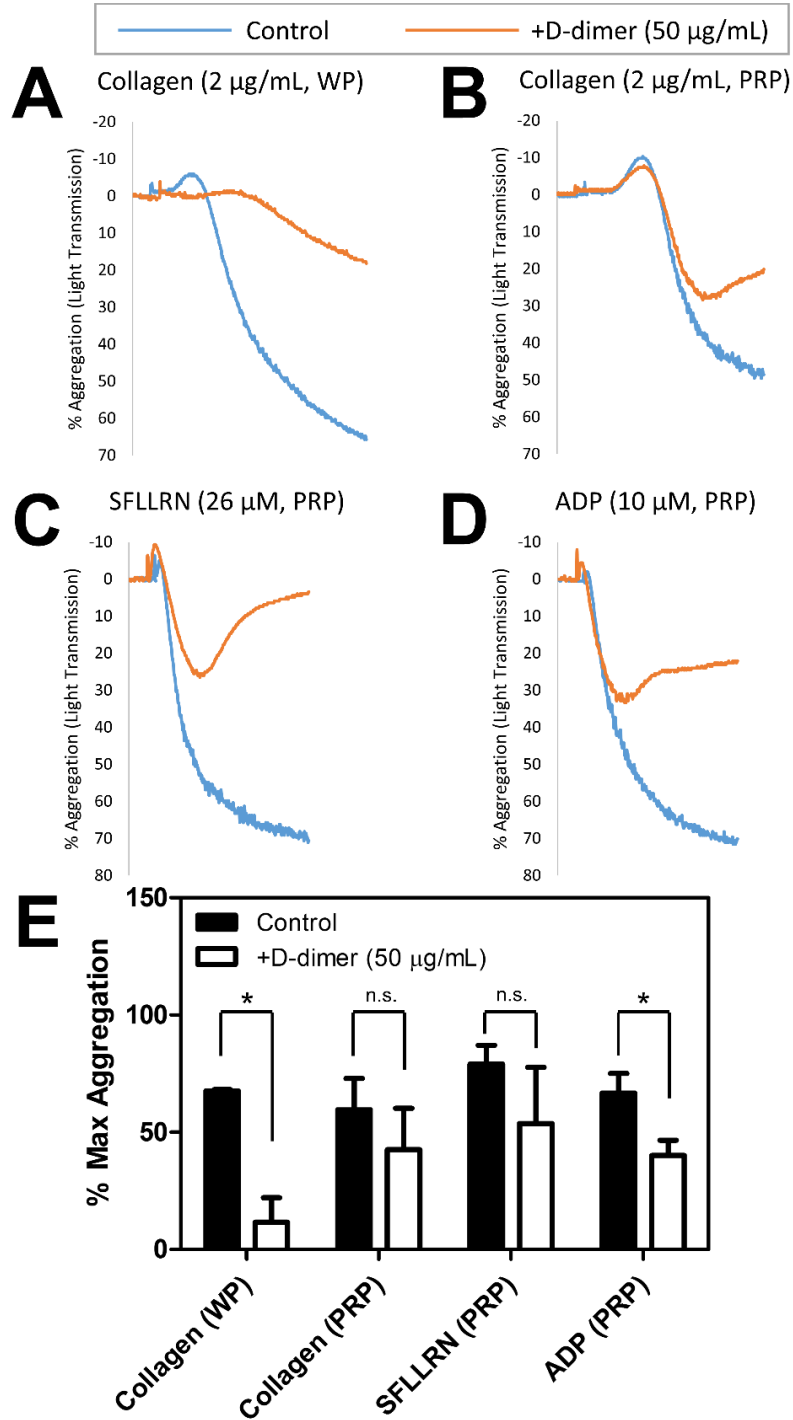


Figure 5-2. Effect of presence of D-dimer on healthy platelet aggregation following agonist stimulation

PRP or washed platelets were prepared from healthy citrated whole blood and incubated with human D-dimer or buffer control. Cells were stimulated with common agonists and aggregation was measured via light transmission. (A-D) Collagen, SFLLRN, and ADP were used as stimuli at the specified concentrations. (E) The experimental data are quantified on the basis of % maximum aggregation.

5.3.3 Plasma D-dimer is a predictor of trauma-induced platelet dysfunction

Using blood from healthy donors and trauma patients, total platelet function in response to an array of stimuli (single and pairwise combinations of six common agonists) was calculated as Total Platelet Calcium Mobilization (TPCM), defined and measured in previous work [110] (see

Supplemental Figure 19 for details). Agonists included ADP, thromboxane A2 analog U46619, convulxin, PAR-1/4 specific peptides SFLLRN and AYPGKF, and IP-receptor activator iloprost and were used at 0.1x, 1x, and 10x EC50, as previously determined [50]. Though TPCM is a quantitative measure of platelet function, it should be interpreted more as a global comparative metric to indicate deviations from normal or healthy behavior, since it is calculated from several independent measurements.

Plasma D-dimer concentrations were measured via ELISA, which provided a metric of D-dimer equivalents for FDP and fully degraded D-dimers in the trauma plasma. Healthy donor blood samples exhibited much higher platelet function and much lower D-dimer concentration than trauma patient-derived samples (**Table 5-1, Figure 5-3**). The D-dimer concentrations of both populations were consistent with previous literature [39,41,115], which increases our confidence in the reliability of the ELISA employed. Analyzing healthy and patient data together showed an inverse correlation between D-dimer concentration and TPCM ($R=0.8236$, Pearson's correlation coefficient), indicating that D-dimer was a predictor of platelet dysfunction within the power of the correlation presented (**Figure 5-3,A**). When the calcium traces were analyzed further by investigating agonist-specific induction (**Supplemental Figure 20**) or patient-specific trends (not shown), D-dimer remained a strong predictor of poor calcium mobilization. Both platelet dysfunction and elevated D-dimer have been reported previously in trauma, but the strong correlation between the two metrics is a novel observation.

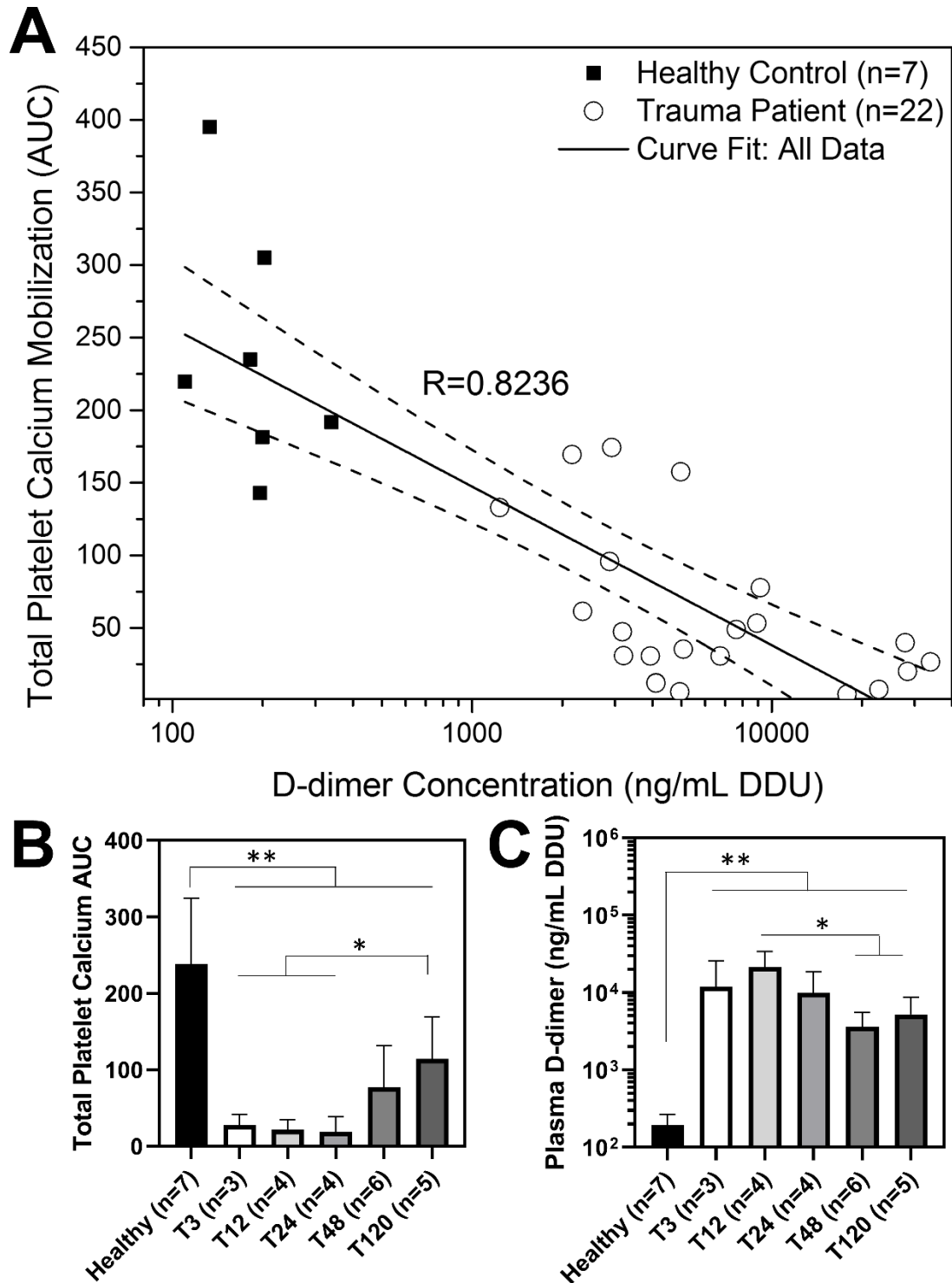


Figure 5-3. Correlation between D-dimer level and total platelet calcium mobilization

TPCM and plasma D-dimer concentrations were calculated for several healthy subjects and trauma patients. (A) The two parameters display a strong negative correlation when plotted against each other. Confidence intervals at 95% confidence level are shown as dotted lines. (B, C) A time dependence of recovery of platelet function and reduction of D-dimer concentration amongst trauma patients is shown. D-dimer concentrations were plotted on a log-scale.

Averaging patient data into bins based on time of sample collection and experimentation revealed statistically significant recovery of platelet function (**Figure 5-3,B**) and declining D-dimer levels (**Figure 5-3,C**). However, full return to healthy baseline was not achieved after several days of hospital treatment, indicating complete restoration of initial hemostatic state in trauma patients is a slow process.

5.3.4 Healthy washed platelets bind D-dimer over time and trauma platelets feature D-dimer on cell surface

We tested the capability of platelets to bind D-dimer by incubating freshly prepared healthy washed platelets with plasma samples from trauma patients. Plasma D-dimer was measured with time of incubation. Compared to control experiments in which no platelets were added to the system and D-dimer levels were constant (data not shown), D-dimer concentrations decreased over the course of 1 hr with platelet incubation (**Figure 5-4,A**). Lower volume fractions of plasma (meaning more platelets present in the system) resulted in a greater decrease in D-dimer concentration; 20 vol% plasma systems achieved ~20% decrease after 60 min, while 10 vol% plasma reactions concluded with ~40% reduction in initial D-dimer level. Additionally, using purified human D-dimer (1.5 $\mu\text{g/mL}$) in place of plasma samples showed a similar kinetic profile (**Figure 5-4,A**). These results indicate that platelets can bind to D-dimer in suspension even in the absence of agonist stimulation.

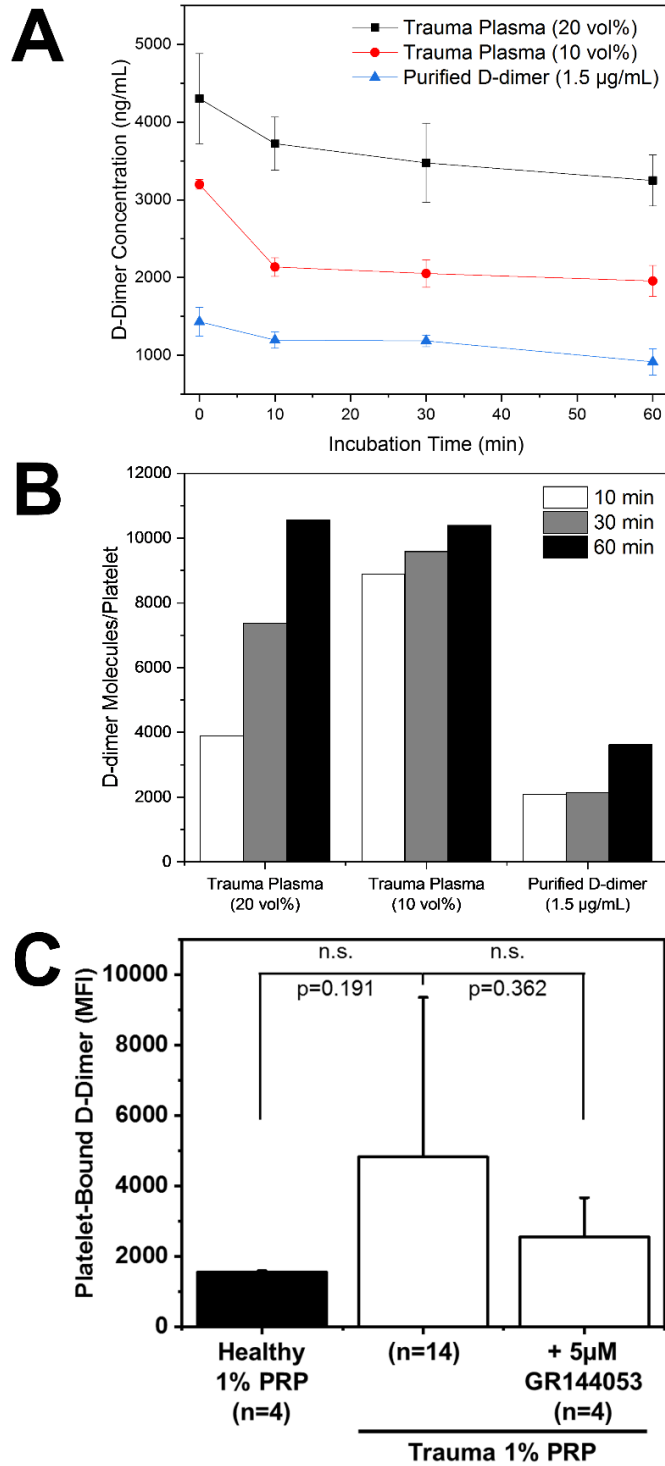


Figure 5-4. Binding of D-dimer by platelets over time

(A) Healthy washed platelets were reconstituted with trauma patient plasma as a D-dimer source or purified human D-dimer. Decreases in protein content over time imply platelet uptake of D-dimer. (B) Calculations of D-dimer occupancy on the platelet surface were performed. (C) Flow cytometry experiments show trauma patient platelets exhibit more D-dimer on the cell surface than healthy donor platelets.

Using the data in **Figure 5-4,A**, we estimated D-dimer occupancy on a normalized per-platelet basis. For ~200,000 platelets/ μL and incubation in 10 vol% and 20 vol% plasma, we calculated approximately 10,000 D-dimer equivalents bound per platelet (**Figure 5-4,B**). In the 20 vol% plasma scenario, cellular uptake was more gradual and constant over time. When more platelets were present (10 vol% plasma system), most of the D-dimer uptake took place in the first 10 min (**Figure 5-4,B**). However, when the calculation was performed on the system in which platelets interacted directly with purified human D-dimer, only 4,000 molecules/platelet were observed after 1 hr. This may be due to the diversity in size and composition of fibrin degradation products in plasma that signal positive for D-dimer in the ELISA being used, which has been discussed as a potential limitation. Certain small oligomers containing the cross-linked D-domain moiety, which may contribute to the total detected protein concentration, may also be able to bind the platelet surface. Considering reported receptor copy numbers in platelets ($\alpha_{\text{IIb}}\beta_3$: 40,000-80,000; GPVI: 4,000) [116,117], we hypothesize that most of the observed uptake of D-dimer involved both $\alpha_{\text{IIb}}\beta_3$ and GPVI.

Trauma patient blood samples also exhibited higher, though not statistically significant, quantities of D-dimer on the platelet surface as quantified by flow cytometry (**Figure 5-4,C**). In contrast to healthy platelets, there was about a 3-fold increase in the mean fluorescent intensity in the patient platelets. In an experiment to explore which platelet receptors were involved in D-dimer binding, we used GR144053 to block integrin $\alpha_{\text{IIb}}\beta_3$ and saw a partial reduction in the bound D-dimer signal. Some of our previous work, as well as that of other groups [91,99,118,119], has implied that GPVI may also be a potential receptor to which D-dimer and other fibrin-derived species can bind.

5.4 Discussion

Fibrinolytic products, like D-dimer, have traditionally been used as biomarkers for deep vein thrombosis (DVT), venous thromboembolism (VTE), and disseminated intravascular coagulation (DIC) [120,121]. For example, Bounameaux et al. first reported elevated levels of D-dimer in subjects with pulmonary embolism in 1991 [122]. Despite the number of papers highlighting D-dimer as a biomarker for thrombosis and elevated D-dimer during trauma, there are few studies investigating the potential mechanistic contributions of these degradation products to dysfunctional hemostasis or platelet activity. In trauma patients whose systemic circulation is exposed to both tissue factor and tPA, elevated levels of soluble fibrin, FDP, D-dimer, F1.2, thrombin-antithrombin complex, and fibrinopeptide A/B are expected [40].

Using a 384-well plate assay, we explored the effect of various fibrin species on platelet function using diluted PRP exposed to the sequential addition of thrombin and tPA. Characterizing the inhibitory effects of various fibrin-related species on downstream platelet signaling through the collagen receptor GPVI led us to develop a hierarchy of GPVI signaling inhibition from the most potent species (D-dimer) to essentially inactive (fibrin monomer) (**Figure 5-1**). As expected, plasma D-dimer concentrations were notably higher in a trauma patient population compared to healthy controls (**Table 5-1**), as measured by sandwich ELISA with specificity for D-dimer and other D-D-containing oligomers. Interestingly, plasma D-dimer was inversely correlated with a metric of platelet function spanning six independent signaling pathways (**Figure 5-3,A**). Addition of pure D-dimer to PRP interfered with platelet aggregation following stimulation with several agonists (**Figure 5-2**). Taken together, these data suggest that D-dimer can both predict and act as a mediator of platelet dysfunction.

Using D-dimer as the primary measure of fibrinolysis, we also report that trauma patient platelets have elevated levels of bound D-dimer and D-dimer in trauma plasma

can be bound by healthy platelets (reaching ~10,000 D-dimer equivalents/platelet), which may have direct implications regarding the functionality of transfused platelets in trauma patients with high D-dimer levels (**Figure 5-4**). These data suggest that platelet transfusions and anti-thrombolytic drugs may not immediately rescue platelet calcium mobilization.

The platelet receptors that bind D-dimer likely include GPVI (**Figure 5-1**) and $\alpha_{IIb}\beta_3$ (**Figure 5-4,C**); our hypotheses and proposed understanding of platelet-fibrin interactions are presented visually in **Figure 5-5**. Due to structural similarities with fibrinogen, fibrin degradation products can also occupy the $\alpha_{IIb}\beta_3$ complex [123]. In continuing studies of the role of different GPVI configurations in D-dimer and fibrin recruitment, one group identified the monomeric form of GPVI as the responsible receptor for fibrin and D-dimer binding [91]. A separate group implicated both $\alpha_{IIb}\beta_3$ and, to a lesser extent, GPVI-dimer as capable of recognizing the D domain of fibrin-related species [118], and an earlier report postulated that fragment D has inhibitory effects on fibrin-dependent platelet activation [124]. In response to the lack of agreement between these groups, a follow-up article considered the role of inconsistent assay procedures and the need for standardization to elucidate the correct biology [119]. Our work does not specifically interrogate preferential activity of monomeric or dimeric GPVI but rather relies on the endogenous platelet repertoire of receptors. While GPVI shedding is highly relevant to pathological states, the conditions of **Figure 5-1** and **Figure 5-2** are far too rapid to include shedding mechanisms. Importantly, the sheddase inhibitor GM6001 was previously shown to have no effect on the GPVI signaling defect caused by soluble fibrin [99].

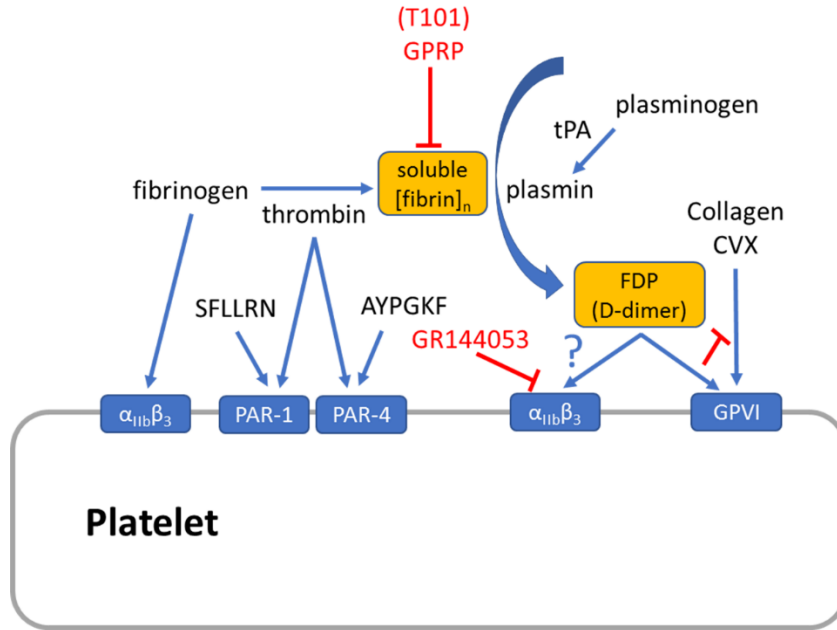


Figure 5-5. Overall summary schematic showing proposed understanding of interactions between platelets and fibrin-related species

Platelet surface receptors are shown with known ligands. Fibrin-related species generated throughout the coagulation process and their respective hypothesized roles in interfering with platelet activation are also shown. Our main focus in this paper is the potent inhibition of D-dimer (and to a lesser extent cross-linked soluble fibrin), as shown by its observed interaction with GPVI and potentially $\alpha_{11b}\beta_3$.

Several different factors during trauma may account for platelet dysfunction. We report in this pilot study that D-dimer is a predictor of this platelet dysfunction and may be a causative agent, along with soluble fibrin and FDP, to interfere with platelet ATP release, aggregation, and signaling. Considering the complex nature of TIC, we are not fully attributing the observed platelet dysfunction phenotype to these fibrinolytic products but rather we are identifying a significant biological role of these species that has not been reported previously. There are likely several other contributing mediators besides D-dimer and FDP and other areas of investigation that need to be considered, but the progress in understanding the multidimensional phenomena that contribute to TIC is encouraging [125]. Further study of platelet structural changes, exposure of surface receptors, and correlation with *in vivo* experiments is certainly warranted to evaluate our observations.

CHAPTER 6: OTHER STUDIES

6.1 Dual antiplatelet and anticoagulant (APAC) heparin proteoglycan mimetic with shear-dependent effects on platelet-collagen binding and thrombin generation

6.1.1 Introduction

Antithrombotic drugs are typically classified into one of three major categories: antiplatelet, anticoagulant, or fibrinolytic agents [126,127]. Common antiplatelet therapeutics include aspirin and clopidogrel which both inhibit secondary platelet agonist generation (thromboxane A₂ and ADP, respectively) [126–128], as well as inhibitors of the integrin $\alpha_{IIb}\beta_3$ [129]. Anticoagulants are responsible for preventing thrombin generation and fibrin polymerization. Warfarin and various heparins have been used as an oral and parental anticoagulant for several decades, but recent advances have focused on specifically targeting coagulation factors, such as thrombin and factor Xa [126]. Finally, fibrinolytic or thrombolytic drugs (most notably tPA: tissue plasminogen activator) promote the generation of plasmin, an enzyme that cleaves fibrin [130].

With increasingly complex cardiovascular disease states comes a need for the administration of multiple antithrombotics with different mechanisms of action. While certain classes of drugs have the potential to function synergistically, there is an associated increased bleeding risk as the number of drugs increases [131,132]. Therefore, identifying a method for combining the antithrombotic functions of antiplatelet and anticoagulant agents into a single therapy can have a potentially great impact on the field, as uncertainty regarding optimal use remains [132].

Heparin (usually referred to as unfractionated heparin; UFH) is yet another common clinically-used antithrombotic agent which carries anticoagulant behavior through its binding and activation of antithrombin. Antithrombin then works to deactivate circulating thrombin and factor Xa to hinder the coagulation process [133]. Heparin can bind directly

to thrombin ($K_d=100$ nM) resulting in anticoagulant behavior [134]. Heparin is derived from mast cells which line the vascular walls usually in the same general location as tissue factor (TF). Upon tissue injury, mast cells are activated and release heparin proteoglycans (HEP-PGs) which are much higher in molecular weight than UFH [135,136]. These structures have been shown to exhibit both anticoagulant features, as does heparin typically [137], as well as specific antiplatelet properties, most notably involving the platelet-collagen interaction and subsequent aggregation and fibrin polymerization [135]. The unconventional ability for a heparin-based entity to impact collagen-dependent platelet activation could be attributed to the fact that type I collagen has binding sites for heparin, in addition to the heparin binding site to von Willebrand Factor (vWF) bridging platelets with collagen, relevant under arterial shear rates [138]. The concept of designing synthetic HEP-PG mimetics, structured with a protein core and conjugated with UFH, has been demonstrated [135,136,139,140].

Despite various results comparing the ability of HEP-PGs and UFH to inhibit collagen-mediated platelet aggregation and serotonin release under flow conditions [135], previous work with dual anticoagulant and antiplatelet (APAC) conjugates has been focused primarily on *in vitro* platelet aggregometry studies and *in vivo* vascular models [136,140]. The importance of understanding the functionality of APACs, as is the case with any novel therapy, in more pathophysiologic scenarios *in vitro* is crucial. Thus, the focus of this work was to compare the results obtained from various *in vitro* experimental techniques to gain a broader understanding for the potential therapeutic effect of synthetic HEP-PG mimetics with varying heparin conjugation levels (CL10, CL18, HICL).

6.1.2 Methods

Reagents were obtained as follows: Anti-human CD61 (BD Biosciences, San Jose, CA), Alexa Fluor® 647 conjugated human fibrinogen (Life Technologies, Waltham, MA),

corn trypsin inhibitor and D-Phe-Pro-Arg-chloromethylketone (CTI and PPACK, respectively; Haematologic Technologies, Essex Junction, VT), Sigmacote® siliconizing reagent (Sigma, St. Louis, MO), Dade® Innovin® PT reagent (Siemens, Malvern, PA), collagen Type I Chrono-Par™ aggregation reagent (Chrono-log, Havertown, PA). Whole blood was drawn via venipuncture from healthy donors following University of Pennsylvania Institutional Review Board approval into a syringe loaded with 100 µM PPACK (to inhibit thrombin activity altogether for the study of platelet deposition on collagen only) or 40 µg/mL CTI (to inhibit contact pathway and measure platelet and fibrin deposition). Prior to each blood draw, donors self-reported to be free of any medications for 7 days and alcohol use for 48 hours. Additionally, female donors self-reported to not using oral contraceptives.

Apixaban (SelleckChem, Houston, TX), HEPES (Fisher Scientific, Hampton, NH), Fluo-4 NW calcium dye and probenecid (Invitrogen, Carlsbad, CA), ADP (Sigma-Aldrich, St. Louis, MO), U46619 (Tocris Bioscience, Bristol, UK), convulxin (Cayman Chemical, Ann Arbor, MI), type I fibrillar collagen (Chrono-log, Havertown, PA), thrombin (Haematologic Technologies Inc., Essex Junction, VT), and SFLLRN and AYPGKF amide (Bachem, Torrance, CA), Protein A Sepharose CL-4B (GE Healthcare, US), vWF (Wilfactin®, 100 IU/mL, LFB Biomedicaments, Les Ulis, FR), rabbit polyclonal anti-vWF (DAKO, Glostrup, DK), enhanced chemiluminescent (ECL) detection reagents (GE Healthcare, US), goat anti-rabbit HRP, (Jackson Immunoresearch, Westgrove, PA, US), streptavidin-ATTO647 (Immune Biosolutions, Sherbrooke, QE, CA) were stored and used according to each manufacturer's instructions. Three different APAC molecules were synthesized (Aplagon, Helsinki, Finland) as previously described [136,140]. In brief, dual antiplatelet and anticoagulant (APAC) conjugate comprises of protein core, where UFH chains are bound by covalent di-sulfide bridges provided by a cross-linker molecule to reach various conjugation levels (CL) of heparin.

Measurements of platelet calcium mobilization were conducted in 384-well plate assay format, as described previously [84]. Briefly, fresh whole blood treated with 250 nM apixaban (a Factor Xa inhibitor used to eliminate endogenous thrombin generation) was centrifuged (120g, 10 min) to isolate platelet-rich plasma (PRP). The PRP was incubated with a vial of Fluo-4 NW calcium dye prepared by reconstitution with sterile 20 mM HEPES-buffered saline (HBS, pH 7.4) and 77 mg/mL probenecid to prevent dye leakage for 30 min. After incubation, two separate 384-well plates were assembled. One plate contained dye-loaded PRP (30 μ L/well) and the other plate contained platelet agonists at previously determined EC50 concentrations [50,84], as well as serial dilutions of three different APAC molecules of varying heparin conjugation levels (CL10, CL18, HICL). The agonist-containing plate was prepared using a JANUS liquid handling system (PerkinElmer, Inc., Waltham, MA) such that all 144 combinations of the six platelet agonists and eight APAC concentrations (0, 1.56, 3.12, 6.25, 12.5, 25, 50, 100 μ g/mL) were prepared in a time-efficient manner with replicates. The two plates were loaded into a FlexStation 3 microplate reader (Molecular Devices, Inc., Sunnyvale, CA) and agonists (20 μ L/well) were dispensed column-wise into PRP. The dynamic fluorescence intensity $F(t)$ was read and normalized by the pre-dispense baseline (F_0) for 4.5 min with readings every 2.5 s (Ex: 485 nm; Em: 525 nm). The final PRP concentration after agonist addition was 12% by volume and previously no evidence of autocrine signaling has been reported in these dilute conditions [84]. Testing of type I fibrillar collagen (20 μ g/mL) in the platelet calcium assay was performed as previously described [99], in which manual pipetting and reading using a Fluoroskan Ascent plate reader was required due to variable delivery of collagen by the FlexStation automated pipetting system.

Platelet aggregation studies were performed using a Chrono-log Model 700 Whole Blood/Optical Lumi-Aggregation System. Whole blood was drawn via venipuncture into a syringe loaded with 250 nM apixaban and 4% (w/v) sodium citrate (Sigma-Aldrich) under

the same IRB approval as above. Citrated whole blood is commonly used to chelate calcium ions and prevent platelet activation, but here we use citrate in conjunction with apixaban to further ensure minimal endogenous thrombin generation. Type I fibrillar collagen (1 μ L) was added to PRP after 10 min incubation of APAC (or buffer as control) and aggregation was measured for 4 min post-dispense.

6.1.3 Results and Discussion

Intracellular calcium mobilization of dilute apixaban-treated PRP in response to several platelet agonists was measured in the presence and absence of three different APAC molecules. Platelet agonists included thrombin (20 nM), convulxin (a potent platelet glycoprotein (GPVI) activator derived from snake venom; 2 nM), ADP (1 μ M), U46619 (a stable thromboxane A2 analog; 1 μ M), fibrillar collagen (20 μ g/mL), and two PAR-specific ligands SFLLRN (PAR-1 agonist; 10 μ M) and AYPGKF (PAR-4 agonist; 300 μ M). All APAC concentrations (1.56-100 μ g/mL) reduced the platelet calcium response to thrombin and collagen at least 50% compared with the negative control condition. Representative results for 12.5 μ g/mL of APAC are shown in **Supplemental Figure 21**.

For each condition, the area under the curve of the resultant calcium fluorescence trace was calculated and converted to a percentage of the control response (**Figure 6-1**). The effect of heparin conjugation level was also identified to impact the extent of inhibition. Incubation of PRP with CL10 resulted in a 76% decrease in thrombin-induced platelet calcium signal and 51% reduction in the collagen response. CL18 showed the highest attenuation of calcium mobilization, yielding an 83% and 95% reduction in response to thrombin and collagen, respectively. However, increasing the conjugation level above 18 (HICL) still exhibited a statistically significant inhibition, but slightly less than that seen with CL18 and closer to that of CL10. For each of the other five agonists tested, virtually no inhibitory effect was observed, as is evident by ~100% calcium mobilization (**Figure 6-1**).

Heparin inhibition of thrombin-mediated platelet calcium mobilization was fully consistent with accelerated thrombin complexation with antithrombin via the heparin functionality of the constructs, while maintaining PAR-1/4 functionality as evidenced by the unchanged responses to SFLLRN and AYPGKF stimuli. In addition to this anticoagulant feature, previous work has shown the APAC conjugates to also display antiplatelet effects [136], however the effects on intracellular calcium mobilization have not been reported. The antiplatelet effects appear to be specific to collagen and thrombin, since all other platelet signaling pathways and receptor agonists (CVX, ADP, U46619, SFLLRN, and AYPGKF for GPVI, P2Y1/12, TP, PAR1, and PAR4, respectively) were active in the presence of APAC. While collagen can bind heparin, convulxin has no known heparin-binding domain, thus likely explaining the striking difference in APAC activity against collagen stimulation of the platelets that remain fully responsive to the GPVI activator, convulxin.

In a similar test as previously reported [136], aggregometry was used to investigate the antiplatelet features of the heparin proteoglycan mimetic APAC. Each individual APAC (100 or 200 µg/mL final concentration) or buffer was added to PRP, and type I fibrillar collagen (2 µg/mL) was used as the stimulus to measure platelet aggregation in citrated PRP with apixaban addition. The negative control condition (buffer treatment) produced 70% aggregation over the course of the experiment (4 min). For each APAC species (CL10, CL18, and HICL), aggregation was impaired in a dose-dependent manner (**Figure 6-2,A-C**). In all cases, the maximal aggregation was lowered, the lag time prior to aggregation was prolonged, and the slope and area under the curve were reduced. The intermediate-chain conjugated species (CL18) was again observed to have the most significant effect, as platelet aggregation was completely abolished at high concentrations (200 µg/mL) (**Figure 6-2,B**). Other platelet agonists were screened in aggregometry and the same observations were made in that APAC conjugates only affect thrombin- and

collagen-mediated platelet aggregation (**Supplemental Figure 22**), confirming the calcium mobilization results.

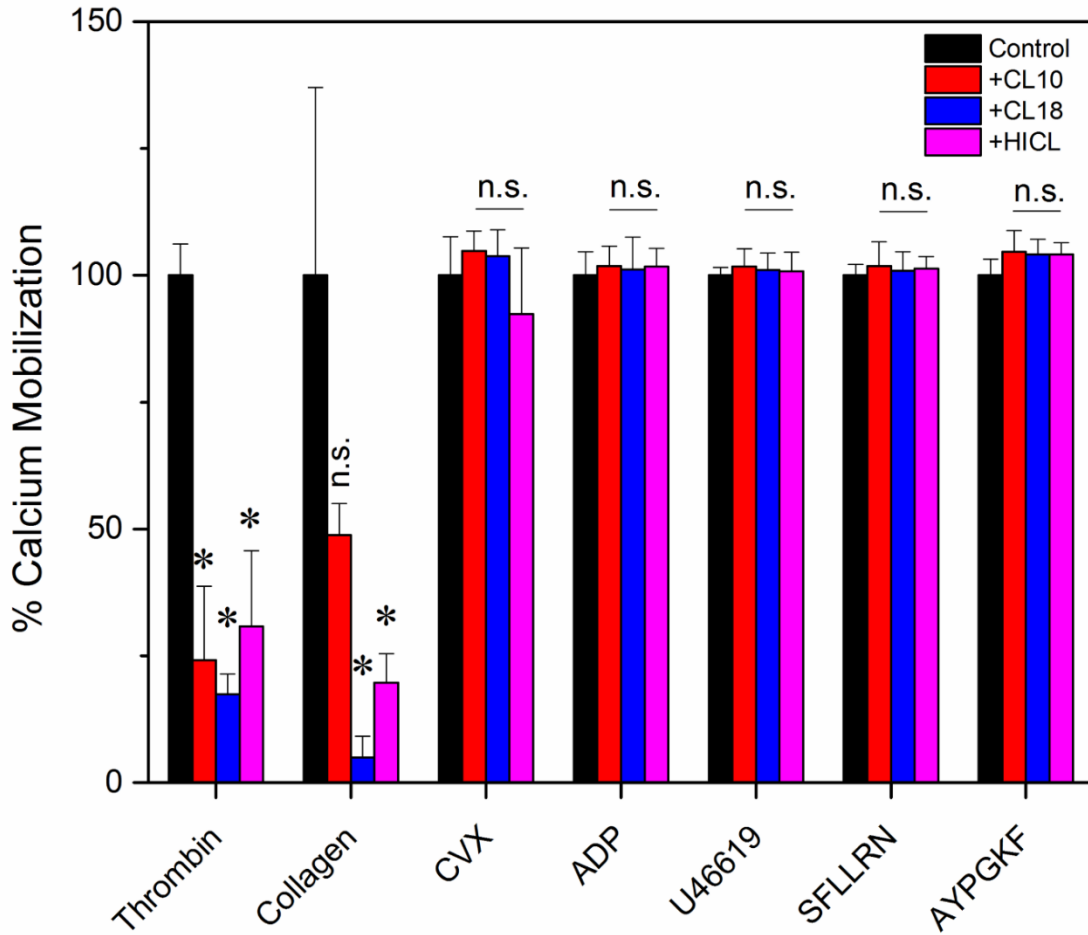


Figure 6-1. Thrombin- and collagen-dependent calcium mobilization is specifically reduced in the presence of APAC

Previously determined EC₅₀ concentrations of several platelet agonists were added to dilute apixaban-treated PRP to stimulate platelet activation. A control condition (absence of APAC) was used as the 100% calcium mobilization baseline to which the effect of three APACs (12.5 µg/mL) was compared. Antiplatelet effects were seen by reduced activation levels in cases where thrombin and fibrillar collagen were used as the stimulus. However, all other platelet agonists were not significantly hindered by APAC. Final agonist concentrations: thrombin, 20 nM; collagen, 20 µg/mL; CVX, 2 nM; ADP, 1 µM; U46619, 1 µM; SFLLRN, 10 µM; AYPGKF, 300 µM. (n=3 donors, * p<0.05, mean ± SD). PRP = platelet-rich plasma.

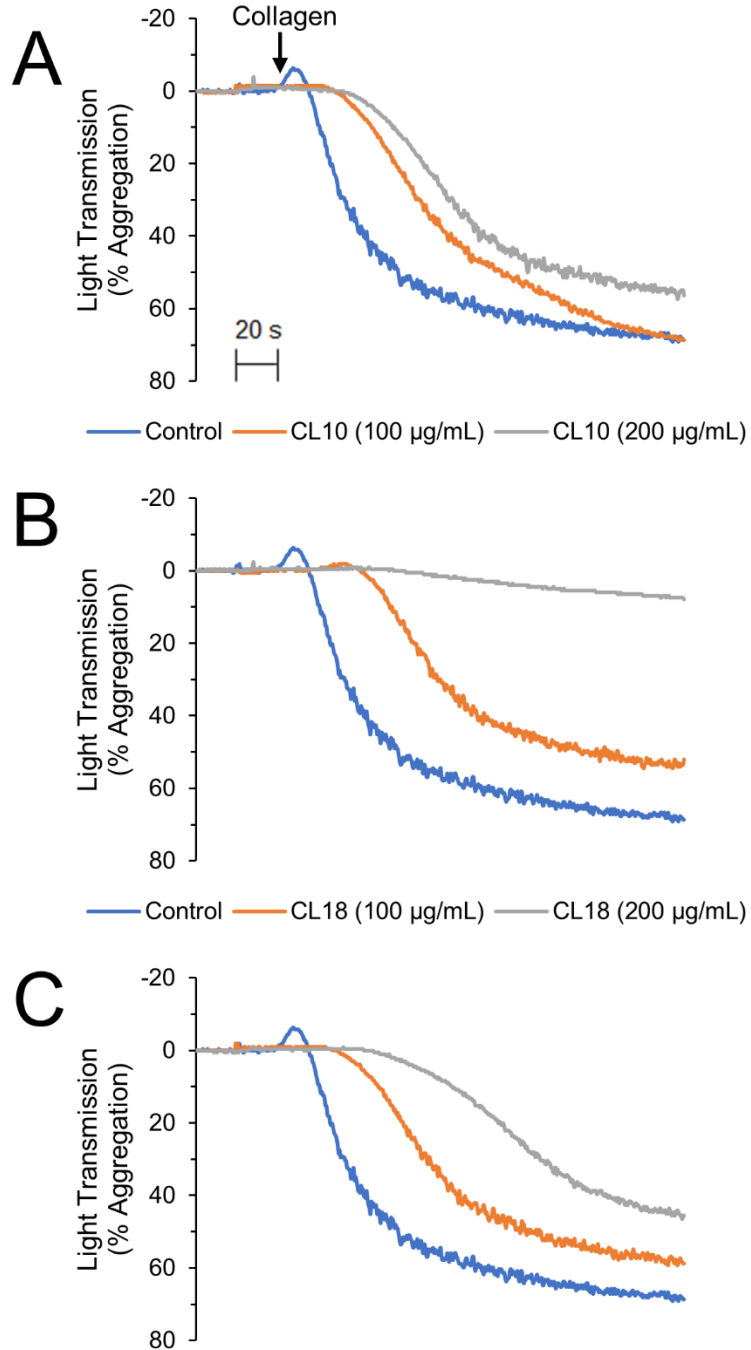


Figure 6-2. Platelet aggregation in PRP is inhibited by APAC

A dose-dependent reduction in collagen-mediated aggregation of apixaban/sodium citrate-treated PRP was observed for each of three APACs (A. CL10; B. CL18; C. HICL). A high dose of CL18 was shown to have the greatest effect as aggregation was almost completely abolished, consistent with the calcium mobilization findings reported in the previous section. PRP = platelet-rich plasma.

Concern of bleeding risks associated with combinations of two or more blood modulating drugs have sparked interest in developing cardiovascular therapies with dual antiplatelet and anticoagulant (APAC) activity. Using naturally-produced HEP-PGs as a framework for synthetic alternatives, protein functionalized with conjugated UFH chains offers a promising route [136,140]. With our 8-channel device, we demonstrated APAC antiplatelet activity with PPACK-treated blood perfused upon collagen. Secondly, we analyzed the ability of APAC to interfere with the thrombus growth when CTI-treated blood was perfused upon a collagen/TF surface. We also provide evidence that APACs can directly interact with collagen to reduce platelet deposition under flow and to decrease collagen-induced calcium mobilization. Additionally, the increased inhibitory activity against platelets under arterial flow conditions suggests that APAC when studied in the absence of any other anticoagulant may also reduce vWF binding to collagen or modulate the VWF-GPIIb/IIIa interaction. APAC interaction with vWF was supported by the immunoprecipitation studies where vWF captured APAC.

To investigate the observed antiplatelet effects of APAC more specifically, we utilized intracellular calcium mobilization as a metric to test the influence of APAC on various platelet signaling pathways. The activation of several platelet receptors leads to distinct signaling cascades that converge on mobilization of calcium ions, so we can infer the level of agonist-induced activation through this reading. A screen of seven common platelet agonists in the presence and absence of three APAC conjugates revealed inhibitory action only towards thrombin and fibrillar collagen (**Figure 6-1, Supplemental Figure 21**). All other agonists (ADP, U46619, convulxin, SFLLRN, and AYPGKF) were sufficiently active with respect to the control buffer condition. Collagen-induced aggregation was also impaired by each APAC molecule (**Figure 6-2**). These results suggest that APAC has specific antiplatelet targets without being a universal inhibitor of platelet activation, leaving the other activation routes intact.

Other than its traditional anticoagulant mechanism, heparin has been implicated to exhibit other antithrombotic effects such as inhibiting endoperoxide metabolites that lead to thromboxane A2 production, suggesting aspirin-like functions [141]. Also, collagen has previously been reported to have unique heparin-binding sites separate from those involved in heparin-triggered thrombin inactivation [138,142,143]. Though the functional significance of heparin-collagen binding is still unclear, it may explain the observed inhibitory phenomenon of heparin proteoglycans and synthetic APAC conjugates on collagen-induced platelet aggregation, especially under blood flow.

Collagen activates platelets primarily through GPVI, a uniquely non-G protein-coupled receptor. GPVI belongs to a class of proteins known as immunoreceptor tyrosine-based activation motifs (ITAM) [13]. The converse to ITAM receptors are immunoreceptor tyrosine-based inhibition motifs (ITIM), which inhibit ITAM signaling in order to suppress platelet activation, a pathway that functions along with the prostacyclin-activated IP receptor [12,144]. Upon first consideration, it would appear, that the APAC conjugates would qualify as ITIM-activating molecules, but the calcium mobilization results showing full GPVI activity via convulxin disproves this hypothesis and points more towards the collagen-heparin interaction. Though certain explanations may be incorrect, and collagen and thrombin appear to be the sole targets, more work should be performed to further refine the specific antiplatelet and platelet anticoagulant mechanisms of APAC.

Currently available treatment by antithrombotics is available only systemically. In our previous publications we have shown that during local application at the injury site, either in vivo (arterial model of crush injury in baboon) or on the collagen coated surface ex vivo (collagen coated chamber - shunt model in baboons) APAC has potency to inhibit platelet thrombosis and reduce platelet accumulation under arterial shear forces [136]. In addition, we have previous data to show by PET scan that APAC (Cu64-APAC) binds at the injury site with extended retention time in respect to UFH (Cu64-UFH) [140]. Our recent

data [145] also shows localization of APAC at the injury site in porcine models of balloon denuded iliac and carotid arteries and at the arteriovenous fistula of femoral artery and vein. Based on the results of the current manuscript showing reduced platelet deposition on the highly thrombogenic collagen/tissue factor surface and the inhibition of collagen-induced platelet aggregation support the suggestion to combine antiplatelet and anticoagulant action in a single antithrombotic, locally acting modality. Importantly, polyvalent APAC constructs may offer PK/PD advantages relative equivalent free drug.

6.2 Testing efficacy, potency, and specificity of platelet inhibitors

6.2.1 Effect of PAR-4 specific antagonist

When developing new antithrombotic drugs, one of the most important considerations for research groups is the potential for bleeding risk in patients. In order to address this concern, receptors with less significant contributions to platelet activation and clot formation are becoming promising targets for drug development. One such receptor of interest lately has been protease-activated receptor 4 (PAR-4) [146,147]. PAR-4 is one of two platelet receptors with affinity towards thrombin, the other being PAR-1. Though both PARs have been studied extensively, there have only been antagonists developed against PAR-1. Vorapaxar is a specific and potent PAR-1 inhibitor approved in 2014, though its benefits are limited due to its requisite administration with other antiplatelet therapies like aspirin. As a result, the bleeding risks associated with vorapaxar treatment are still an ongoing issue [148].

Thrombin is known to activate the two PARs in a concentration-dependent manner. First, at low to moderate thrombin levels, PAR-1 is the primary target for thrombin-mediated platelet activation. As the concentration of thrombin increases to saturating levels, PAR-1 activation is overcome by PAR-4 signaling [149]. Thus, targeting PAR-4 is thought to be a gentler and more controlled manner of platelet inhibition, and the necessity

of high thrombin concentrations ensures that coagulation will also be largely in effect to further prevent excessive bleeding. One of the first and most promising reports of drug screening and development for PAR-4 inhibition was published by Wong and colleagues at Bristol-Myers Squibb [150]. Currently their drug, BMS-986120, is commercially available for lab purposes and has been tested in animal models. In follow-up work, other iterations of this and similar molecules are under investigation to improve the potency of the inhibitor, which had previously been reported to have an IC_{50} of ~ 10 nM [150]. One such variant is known as BMS-986141, and our group was asked to test its activity and potency in some of our assays using human blood.

The first round of experiments we conducted were dose-response experiments against PAR-4 signaling specifically, which was achieved by challenging platelets with the PAR-4 activating peptide AYPGKF. In calcium dye-loaded PRP, we found the inhibitor's potency to be about 10-fold higher than BMS-986120 ($IC_{50} \sim 1.3$ nM) (**Figure 6-3,A-B**). Next, we checked the specificity of BMS-986141 by stimulating platelets with other agonists. No off-target effects were observed, and there was some inhibition against thrombin-mediated platelet signaling which is to be expected (**Figure 6-3,C-H**).

These preliminary data are certainly encouraging and should be validated in other assays. In the future, it would be interesting to study how the inhibitor functions under flow conditions and in living organisms. Our lab is equipped to run *in vitro* microfluidic experiments, but investigating the specificity of this inhibitor against PAR-4 may not be trivial. The microfluidic channels are typically coated with collagen and/or tissue factor to observe both coagulation pathways, so additional inhibitors may have to be included in order to pinpoint effects against the receptor of interest. One initial idea for an experiment may be to include the PAR-1 inhibitor, vorapaxar, at a moderate dose, and high concentrations of tissue factor to ensure a PAR-4 response, followed by dose-response

concentrations of the PAR-4 inhibitor. In this way, we may be able to separate PAR-1 from PAR-4 signaling as was done in the well-plate experiments.

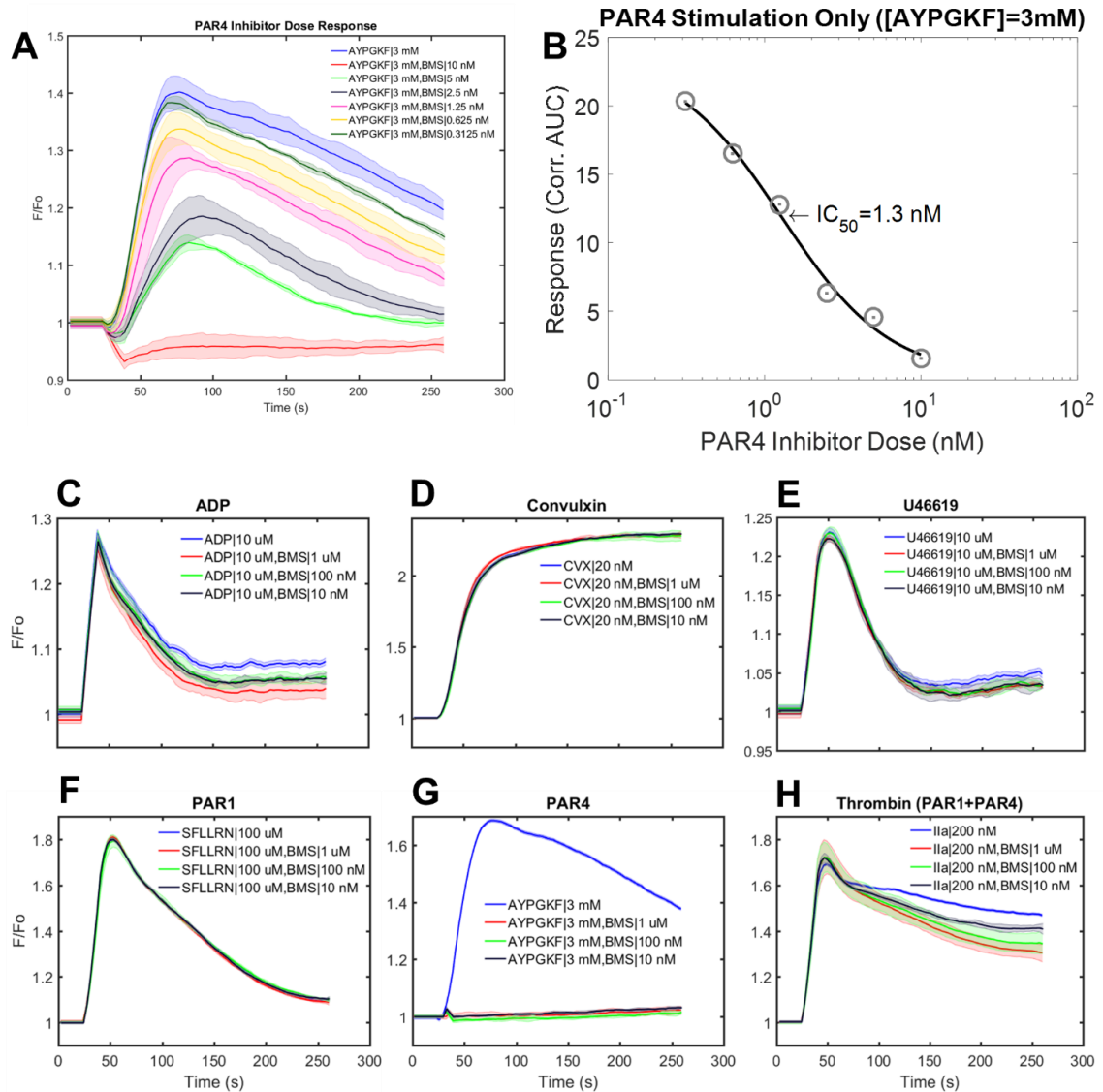


Figure 6-3. Effects of PAR-4 antagonist BMS-986141 on array of platelet agonists

Calcium dye-loaded PRP was incubated with different concentrations of BMS-986141, a specific PAR-4 inhibitor created by Bristol-Myers Squibb. Dose-response experiments of the inhibitor against a strong concentration of PAR-4 activating peptide AYPGKF confirm reported IC_{50} value of ~1 nM (A, B). Target specificity was analyzed by activating platelets with several agonists in the presence and absence of BMS-986141 at potent doses (C-H). Other than AYPGKF and thrombin, which also activates PAR-4 physiologically at high concentrations, no significant inhibitory effects were observed.

6.2.2 *Effect of custom GPVI inhibitor*

Despite the fact much is known about interactions between platelet glycoprotein VI (GPVI) and its primary physiologic ligand collagen, drastically different approaches towards inhibiting the receptor's activity have been reported. Inhibition of GPVI has shown to have clinical benefit other than the expected antithrombotic effects, including protection against myocardial ischemia-reperfusion injury and increased efficacy of cancer treatment by inducing intra-tumor hemorrhage [151,152]. These studies made use of monoclonal antibodies (mAb) directly targeting and blocking the functionality of GPVI. In addition to these mAb strategies, a few small molecules have been developed with affinity for the GPVI receptor. Losartan and honokiol are examples of these small molecules that impart inhibitory effects on platelet aggregation in response to collagen stimulation [153]. Specifically, losartan is hypothesized to block the critical GPVI clustering and dimerization processes, while honokiol has shown direct binding affinity to the receptor though its potency is not very impressive (μM range of concentrations). To this point, it is unclear if either of these small molecules is a reliable method for blocking GPVI activity and likely requires much more work and characterization. Finally, a third class of approaches, which is less direct though seemingly still effective, involves understanding and targeting entities involved in GPVI-mediated intracellular signaling. For example, tyrosine kinase inhibitors like dasatinib, ibrutinib, acalabrutinib, and others prevent platelet activation through the GPVI pathway [99,154]. Phosphorylation of spleen tyrosine kinase (Syk) and Bruton's tyrosine kinase (Btk) are essential for successful platelet activation, so inhibiting these intermediate steps can also be useful techniques.

Considering this project's interest in GPVI signaling and the observed down-regulation in platelet response to convulxin stimulation in the presence of soluble fibrin and FDP, we became interested in using GPVI inhibitors for general mechanistic studies. Many of the function-blocking antibodies used by other groups are custom-made and not

available for purchase, and our attempts towards testing small molecules like honokiol were unsuccessful in calcium mobilization experiments (data not shown). Therefore, we turned our attention to designing a single-chain variable fragment (scFv) using plasmid technology in collaboration with Reaction Biology Corporation. In short, the scFv was Myc-tagged for visualization purposes and subcloned into *E. coli* prior to expression and purification. The first iterations of this production unfortunately yielded low purity (~50%), and relatively high concentrations were required when we tested its capability to inhibit GPVI signaling (**Figure 6-4,A**). A dose-response experiment indicated 100 $\mu\text{g}/\text{mL}$ as the approximate IC_{50} concentration, but when we investigated off-target effects by stimulating platelets with ADP or U46619, we found the scFv also inhibited these modes of platelet signaling (**Figure 6-4,B-C**). Our initial hypothesis is that the low purity of the prepared constructs may be responsible for this lack of specificity and low potency, which should be addressed in future iterations of this custom GPVI inhibitor.

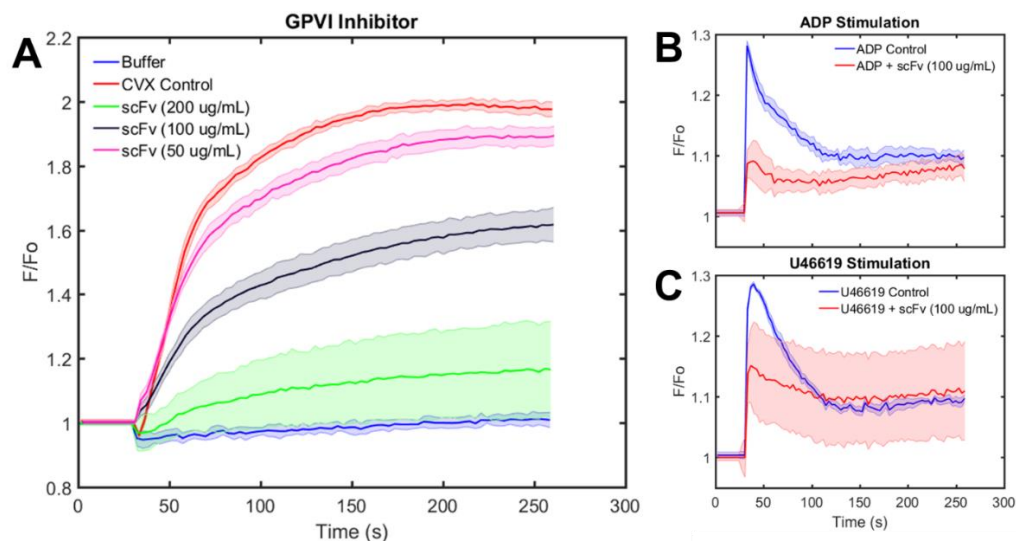


Figure 6-4. Inhibitory effects of custom scFv against GPVI

PRP was loaded with calcium fluorescent dye and incubated with various concentrations of a single-chain variable fragment (scFv) designed in collaboration with Reaction Biology Corporation to target the platelet GPVI receptor. (A) Dose-response effects of the custom inhibitor indicate relatively high concentrations (>100 $\mu\text{g}/\text{mL}$) are required to impart significant inhibition when platelets are stimulated with convulxin. (B, C) Off-target effects are also observed when ADP or U46619 are used to activate platelets, perhaps a result of the low purity of the final formulation.

6.2.3 *Effect of N-acetylcysteine on platelet activation*

N-acetylcysteine (NAC) is a common nutritional supplement that has been shown to have mucolytic properties when used alone or in combination with other medications. Some applications for NAC administration are the neutralization of acetaminophen overdose often observed during pregnancy which may lead to severe liver damage, and the treatment of asthma [155]. Recently, several groups have also implicated efficacy of NAC as a therapy with antithrombotic effects, which may be effective in diabetic patients who tend to have hyperfunctional platelet activity [156,157]. The idea that NAC can be used to inhibit platelet function, however, has been known for several decades now, dating back at least to the work of Stamler et al., which suggested NAC involves endothelium-derived relaxing factor (EDRF) and subsequently enhances the generation of cyclic GMP, a well-understood negative regulator of platelet activation [158]. Other groups have also tried to use knowledge of the chemical structure of NAC to elicit thrombolytic effects through interactions with von Willebrand Factor [159]. However, few if any of these studies investigating the effects of NAC on platelets included complete analysis of platelet signaling pathways, which we have preliminarily designed experiments to address.

To gain an understanding of impacts of NAC on individual platelet receptors, we screened six common ligand-receptor pairs in the presence and absence of NAC, and its amino acid parent, cysteine. The two molecules share much of the same atomic composition, though they differ in the inclusion of an acetyl group one end of the NAC structure. Both compounds exhibit a free thiol group, which has been implicated to be the critical functional group for reducing disulfide bonds that are important for clot strength and integrity [159]. Calcium-dye loaded PRP was incubated with one of the two cysteine derivatives at a potent dose (30 mM), followed by agonist challenge with ADP, U46619, convulxin, SFLLRN (PAR-1 activating peptide), AYPGKF (PAR-4 activating peptide), or thrombin. All agonists were prepared at 10x EC₅₀ concentrations to ensure maximum

dynamic range to observe inhibitory effects. Representative data for these experiments are shown in **Figure 6-5,A-F**, and quantified as a fraction of the control response on the basis of area-under-the-curve (**Figure 6-5,G**).

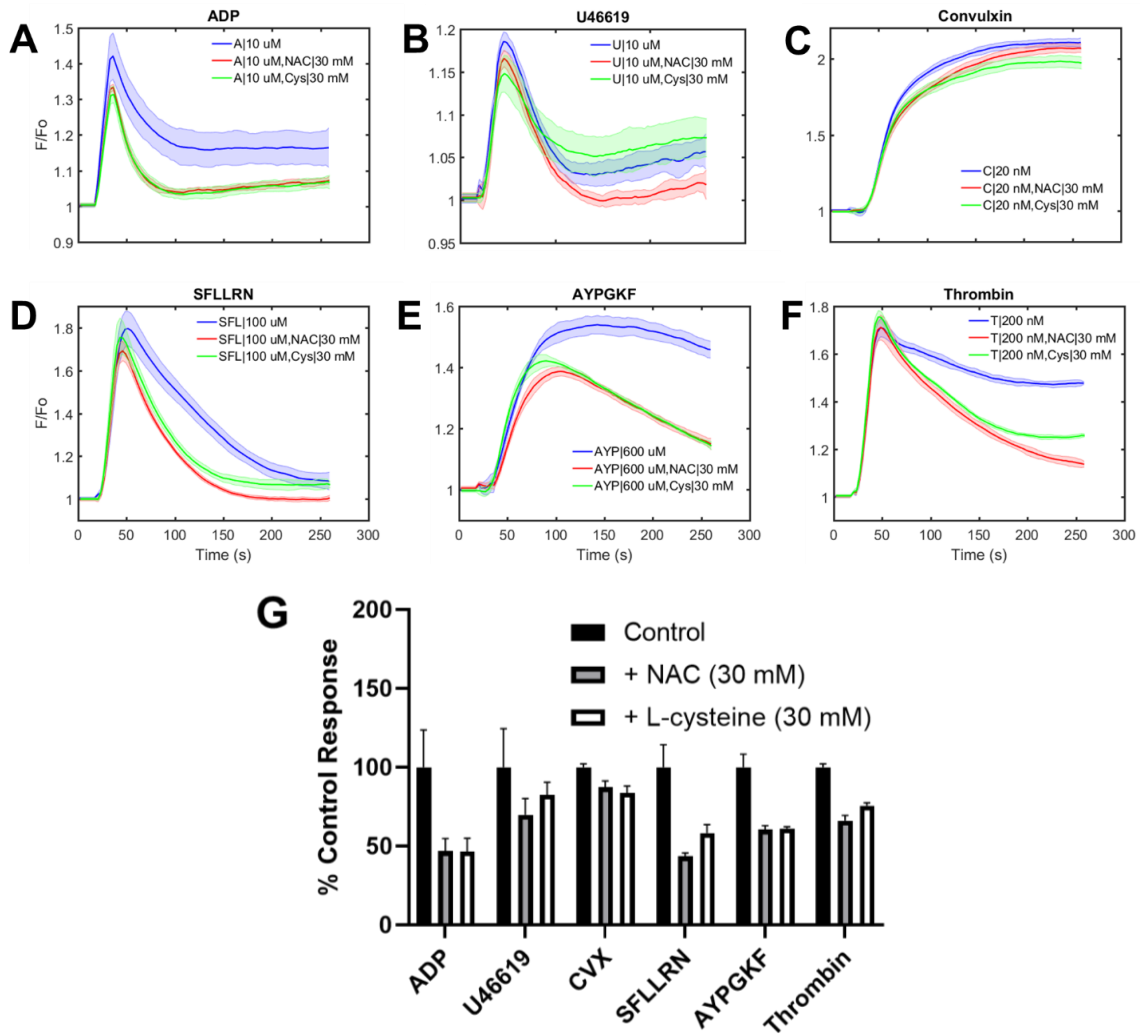


Figure 6-5. Global antiplatelet effects of cysteine derivatives

PRP was loaded with calcium dye and incubated with N-acetylcysteine (NAC, 30 mM) or L-cysteine (30 mM) prior to agonist challenge. ADP, U46619, convulxin, SFLLRN, AYPGKF, and thrombin were added to platelet suspensions and showed varying extents of inhibition when cysteine-derived molecules were present (A-F). The data is quantified as % control response on the basis of area-under-the-curve of the fluorescent time traces for each individual agonist (G).

From these preliminary experiments, it appears both NAC and cysteine impart antiplatelet effects to varying degrees with respect to specific surface receptors. Significant inhibition was observed when challenging with any PAR agonists (SFLLRN, AYPGKF, and thrombin) as well as with ADP, whereas less dramatic effects were observed in the presence of U46619, and challenge with convulxin yielded virtually no separation from the control response. Though these results warrant follow-up experiments, it is interesting that the cysteine derivatives don't affect GPVI signaling, which is the only non-GPCR that was studied in this pilot experiment. The concentration of convulxin may also have been too high, causing any potential inhibitory activity to be overwhelmed by the agonist. Nevertheless, conducting future work in this area would be interesting, especially with regard to the specific significance of the free thiol group present in these compounds. Investigation into other thiol-containing molecules may pave the way towards a better understanding of the biochemical mechanisms of platelet function downregulation in general.

6.3 Computational modeling of the coagulation response during trauma

6.3.1 Introduction

Hemostasis is the body's primary response to vessel injury. During trauma, this pathway may be pushed to its biochemical and physical limits to stop blood loss. Additionally, dramatic changes in inflammation, platelet function, and blood biochemistry set the stage for trauma-induced coagulopathy (TIC). Excessive blood loss (hemorrhagic shock) in combination with tissue trauma, NETosis, endothelial dysfunction, and excess fibrinolysis are evolving components that drive a multi-scale pathogenesis and high dimensional risk for these patients. This section reviews computational modeling efforts to help quantify the interplay of hemodynamics and bleeding. Specifically, simulation tools

(bottom-up and top-down) to describe platelet function and clotting under flow are presented in the context of bleeding.

6.3.2 *Coagulation during bleeding*

Platelets are essential to both hemostasis and thrombosis with extremely complex metabolism driven by receptor signaling. Bottom-up models of platelet signaling have treated calcium regulation by ADP [160,161] or thrombin [162]. Flamm et al. developed a stochastic, patient-specific model of thrombosis under 2D flow over tissue factor surface conditions [100]. The model used the Lattice Kinetic Monte Carlo (LKMC) method to solve for the stochastic platelet motion and binding events, the Finite Element Method (FEM) to solve for the concentration profiles of soluble agonists as a function of time and space, the Lattice Boltzmann (LB) method to solve for the velocity profile over the growing clot, and a neural network (NN) model to predict platelet activation states. The NN was trained via the pairwise agonist scanning (PAS) method (described in more detail later in this chapter), where individual and pairwise combinations of agonists are used to predict a donor's platelet calcium concentration over time [50,84]. Interestingly, the model was highly predictive of microfluidic experiments of whole blood flowing over a collagen patch and predicted a ranked order of sensitivity to drugs such as indomethacin, aspirin, and iloprost. Lu et al. extended the model to include a time-dependent thrombin flux at the TF surface since this is validated by experimental measurements and is more efficient than solving the entire coagulation cascade continuously [163].

While these models of coagulation aid in understanding clot formation on a surface, they primarily relate to thrombosis and are not suitable for simulating bleeding, hemostasis, or TIC. There are several key differences that must be accounted for before they can be used in these cases, however. Blood flowing into a region of vessel damage will exit the vessel as a clot builds up to stop flow. The blood that pools around the wound

extravascularly experiences stasis, has prevailing hematocrit, and will undergo contraction. The clot at the wound wall-blood boundary experiences high shear stresses and is platelet rich with fibrin polymerizing on the wound boundary. A core-shell morphology is typical of these wounds as visualized in animal models [88] or in microfluidics with human blood [164]. These laser-injury models of clot structure, to date, have typically used healthy animals.

During trauma, there are dramatic changes in coagulation proteins and platelet function. Trauma may present as a consumptive coagulopathy with excessive fibrinolysis, endothelial glycocalyx shedding, excessive inflammation, and neutrophil NETosis. Furthermore, some injuries, typically traumatic brain injury (TBI), can lead to defective platelets which is believed to be a key contributor to TIC [32]. In moderate to severe injuries (injury severity score > 15), elevated levels of D-dimer and high prothrombin times have been observed [165]. A model of a severe trauma patient experiencing TIC must account for these differences.

Common platelet activators include collagen (lab analog: convulxin), ADP, thromboxane A2 (lab analog: U46619), and thrombin, the latter of which also plays key enzymatic roles in coagulation (e.g. fibrin polymerization and cross-linking). Following these “outside-in” binding events, cytosolic calcium concentrations rise via two different mechanisms [22,27], which then leads to “inside-out” activation of additional receptors important for platelet aggregation via the plasma protein fibrinogen, among other phenomena [22]. A relatively simplified schematic of external and internal platelet activation with common ligand-receptor interactions is shown in **Figure 1-1**.

6.3.3 *Data-driven development of subject-specific platelet function profiles*

To phenotype platelets, Chatterjee et al. designed a dual experimental-computational technique known as pairwise agonist scanning (PAS) [50]. Essentially,

platelet-rich plasma (PRP) was prepared via centrifugation following collection of whole blood from a consenting donor or patient and incubated with a fluorescent dye that tracks changes in intracellular calcium concentration upon agonist stimulation. In order to generate sufficiently diverse training data for the machine learning algorithm, single and pairwise combinations of six different platelet agonists (or inhibitors) at low, medium, and high concentrations were prepared with liquid handling machines and then dispensed into the cell suspensions for dynamic data collection. In all, the combinatorial space amounted to 154 unique conditions, and the experiment lasted about 2 hr from start to finish. Next, a multi-layer supervised neural network (NN) model could be trained by using the agonist concentrations and corresponding calcium time series as input-output pairs, and then predictions of responses to higher order or more complex stimulation conditions could be generated. Once trained, the NN models serve multiple purposes: (1) phenotypic development of individualized platelet function profiles for each subject included in the study and (2) input into the multiscale models of platelet aggregation discussed previously [100,163]. The general workflow from initial experiments to NN training to multiscale simulation to validation against microfluidic experiments is shown in **Figure 6-6**. There have been other reports of computational simulation of platelet deposition and activation, such as that developed by Sorensen et al. [166,167], but few if any feature capability to predict distributions and effects of multiple stimuli on overall hemostatic state.

Initially, the PAS method was developed using mostly non-physiological activating agents [50], but then was expanded to include the effects of thrombin by Lee et al. for more representative simulation of the hemostatic response [84]. This approach reliably interrogates multiple platelet signaling pathways, and with simple experimental implementation can accurately predict platelet reactivity in the presence of multiple stimuli working in concert. Platelet activation is a highly dynamic process with several contributing factors, which sheds light on the importance of understanding how these factors work

synergistically (or antagonistically) during clot development. Until recently, only healthy human subjects (no previous medical conditions or medications) had been studied with the PAS-NN method.

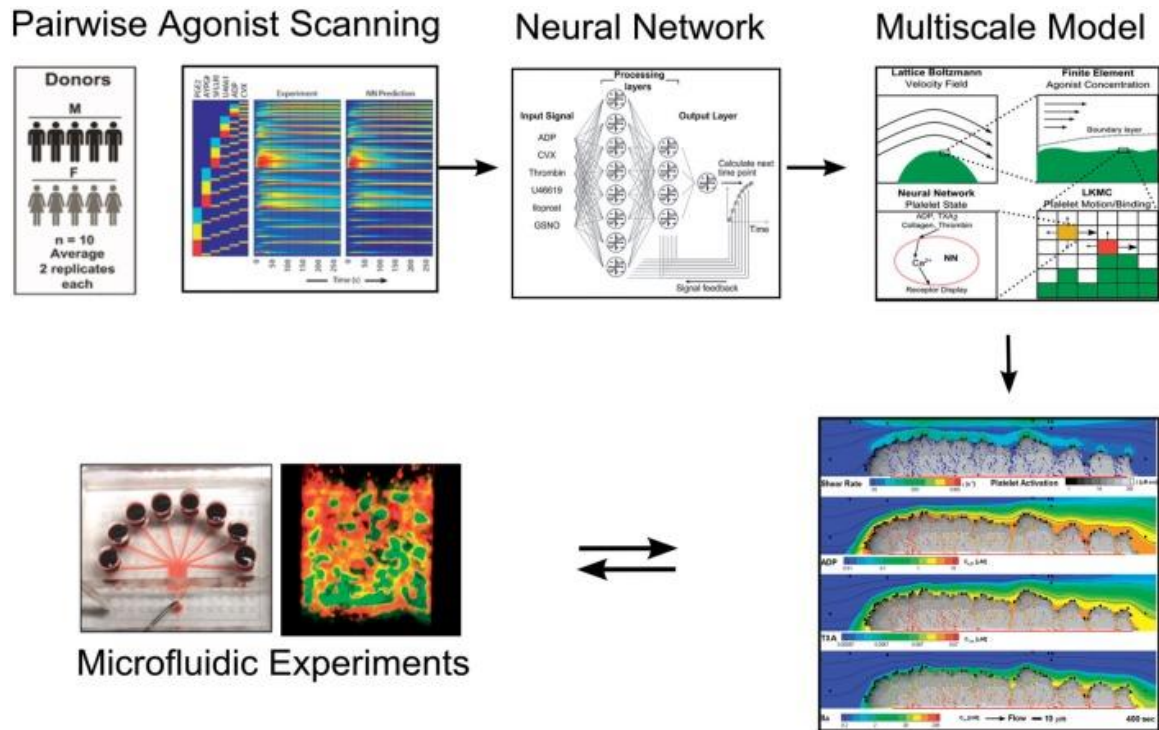


Figure 6-6. Connecting experimental measurements and numerical predictions of platelet activation state

PAS experiments were performed and used to train a NN ensemble to predict calcium response for an average healthy person and was incorporated into the multiscale model to predict platelet activation. An effective boundary flux term was imposed. Thrombus growth dynamics can be predicted by the multiscale model and were compared against microfluidic experiments on healthy human blood conducted under identical conditions. Reprinted with permission from [163].

Verni et al. developed a modified version of PAS with fewer (n=31) agonist conditions, comparing healthy donors with coagulopathic trauma patients [110]. The data indicated a severe level of platelet dysfunction across multiple signaling pathways, as shown in heatmap form in **Figure 4-1**, which was supported by several previous reports [10,29,31]. These other groups typically only characterized platelet function on the basis of single-agonist stimulation or with clinical assays such as thromboelastography (TEG),

which provide useful but limited information. Demonstration of the utility of this high-throughput assay technique in a trauma patient population opens the door for studying countless other patient cohorts.

The principles of PAS can be applied in other assays as well. The original design relied on intracellular calcium mobilization as the primary readout, which is universally recognized to be a correlate of platelet function and activation. However, other markers of activation exist downstream of calcium mobilization and are well-studied among groups in the platelet biology community. For example, upon initial stimulation, the surface integrin $\alpha_{IIb}\beta_3$ converts to an activated state to enable platelet aggregate formation, α granules fuse to the plasma membrane and release contents such as P-selectin, and phosphatidylserine (PS) is exposed on the membrane to provide a charged surface for facilitation of coagulation [23,168].

Observation of multiple biomarkers simultaneously is difficult with traditional well-plate reader technology, but can be achieved by using flow cytometry. Jaeger et al. developed a PAS analog known as pairwise agonist scanning-flow cytometry (PAS-FC) in which each of the activation events discussed above were tracked as a function of combinatorial agonist stimulation [54].

Machine learning provides access to understanding basic biological mechanisms and, perhaps more significantly for the progress of biomedicine, developing diagnostic applications as well. The work by Verni et al. with respect to trauma patients presents a framework to understand platelet dysfunction and potentially influence transfusion strategies employed in the emergency room [110]. Currently, work is being performed to fully simulate a trauma patient's hemostatic state, with the influence of patient-specific NN models and extension to 3D geometries.

Additionally, other machine learning algorithms can be developed that consider relative influences of various clinical variables (e.g. vital signs, demographics, previous

medical history) to make predictions of patient outcomes and inform appropriate treatment regimens. Yoon et al., have published an approach for diagnosing disseminated intravascular coagulation (DIC). DIC is notorious for its lack of accepted biomarkers, so using readily available patient data to train machine learning models, certainly carries significant weight. For example, the DIC diagnostic NN model rank-ordered importance of 32 variables and identified platelet count, D-dimer content, and clinically assigned scoring systems as parameters with most direct implication to development of DIC [169]. Such models, with sufficient learning, have the potential to be used in real-time to obtain a rough understanding of patient prognosis based on previous cases, and perhaps provide hints towards the best method of treatment. Ultimately, all of this work lends itself to the long-term goal of personalized medicine for countless disease states.

6.3.4 Conclusions

The multi-factorial nature and ever increasing complexity of physiological responses to blood vessel injury have been the focus of several efforts of computational modeling. Some groups have chosen to focus on the role and interplay of various coagulation proteins, while others have strived to understand the mechanisms of blood cell (specifically platelet) function and activity. The ultimate goal of simulating hemostasis as completely as possible is becoming more achievable with integration and development of models that span multiple orders of magnitude and combine several individual components together. Applying data-driven modeling approaches that are dependent on bench-scale experimentation and post-simulation verification has proven to be an incredibly valuable method that takes advantage of the power of machine learning technology. Additionally, recent advances have begun to model non-healthy populations (e.g. patient cohorts experiencing coagulopathy and acute inflammation) in an effort to better understand patient prognoses and potentially guide diagnosis and treatment

strategies. Using the examples discussed above as motivation for the future, there should be great optimism for development of similarly structured models for other clinical conditions and diseases.

CHAPTER 7: FUTURE WORK

7.1 Further characterization and study of physiological significance of fibrin species distribution in trauma patient blood

7.1.1 *Using gel electrophoresis and western blot to analyze size and composition of fibrin-related species*

In Chapters 4 and 5, we presented data from enzyme linked immunosorbent assays (ELISA) designed to detect the relative plasma concentrations of D-dimer and other cross-linked fibrin degradation products. Elevated levels were observed in samples obtained from trauma patients and were strongly correlated with a dysfunctional platelet phenotype. Though ELISA is a great method for determining presence or absence of proteins of interest, it lacks the ability to specify other proteins that may also be present in the sample. Due to the heterogeneity of fibrinolytic products in terms of size, composition, and other physical attributes, additional techniques can be applied to learn more about the distribution of fibrin-related species in trauma patient blood.

For example, gel electrophoresis is a commonly used tool to analyze DNA, RNA, or protein content in a given sample on the basis of molecular size. By applying an electric field across a polyacrylamide gel pre-loaded with protein samples in individual lanes, the samples begin to mobilize through the gel and separate as a function of ability to transport. The distance travelled through the gel is inversely proportional to the size of the molecule, meaning smaller molecules will be found towards the end of the gel at the end of the experiment. After this separation step, the gel can be stained through techniques like western blotting which enables visualization of individual protein constructs and relative quantities in the original sample. The gel is transferred to a membrane and is then sandwiched by fiber pads and filter paper to protect the membrane and blot the gel, respectively. Primary and secondary antibodies are used to identify the proteins and a

reference ladder of general molecule sizes is used to determine the size of the protein corresponding to each band [170].

Applying the principles of gel electrophoresis and western blotting can be applied to samples of blood proteins such as the family of fibrin degradation products (FDP) that are produced through the action of plasmin on a fibrin mesh. Analysis of size and composition of FDP has been conducted previously. One study included the design of a system to develop a fibrin-rich clot, perfuse plasmin through the mass, and collecting the effluent material for analysis. Using multi-angle light scattering, size exclusion chromatography, and sodium dodecyl sulfate–polyacrylamide gel electrophoresis (SDS-PAGE), the group identified FDP ranging from 10^5 - 10^7 g/mol [171]. The lower limit was representative of D-dimer, which has been discussed at length in this dissertation as a product with potential clinical significance, and the authors suggested that these smaller FDP can be approximated as rigid rods with little flexibility. Even earlier than this work, another group investigated FDP in acute myocardial infarction (AMI) patients [172]. Blood was collected prior to and after fibrinolytic therapy administration, and serum was isolated for subsequent protein analysis. Specifically, the authors were interested in differentiating between cross-linked fibrin degradation products and fibrinogen degradation products, and gel electrophoresis was used to distinguish the two groups.

Using these success stories as motivation, future work with the trauma patient collaboration should focus on further physical and biochemical characterization of the specific protein complexes that may carry stronger mechanistic implications than others. Plasma samples or serum samples can be prepared following whole blood collection according to the methods outlined in Chapter 4, and separation assays can be run to observe the prevalence of each type of FDP. It is clear that D-dimer and cross-linked fibrin degradation products are present, but to this point the presence of other fibrin-related species specifically in trauma-derived samples is unknown.

7.1.2 *Observing interactions between D-dimer and platelets under flow conditions in microfluidic device*

Virtually all of the experiments discussed in this work have utilized well-plate technology, which enable high-throughput data collection and excellent analysis of cellular signaling processes mediated by ligand-receptor interactions, but typically employ static reaction conditions. Considering the fact that hemostasis is a dynamic process that is highly dependent on the flow properties of blood, recreating these physiologically relevant conditions is crucial for developing a complete understanding of all aspects of the hemostatic response. In light of this, our group and several others have applied principles of biomaterials and soft lithography to fabricate controllable *in vitro* models of blood flow through miniaturized channels. Over the years, members of our lab have designed various microfluidic schemes for simulating a plethora of hemodynamic scenarios [173]. The flagship device design is comprised of eight independent channels, each supplied by its own inlet reservoir and operated by a syringe pump pulling through a single outlet port [85]. Each of the channels includes a region patterned with prothrombotic entities, where fluorescently labeled blood components can be visualized as the hemostatic response is triggered. This setup permits up to 24 test conditions when three devices are run in parallel and is ideal for dose-response characterization of antiplatelet and anticoagulant drugs as well as customized study of specific facets of hemostasis.

To continue the work with trauma patients and assess the validity of the observations regarding the effects of D-dimer and fibrin degradation products on platelet signaling, we plan to employ microfluidic technology to determine how our results compare to those obtained with the incorporation of flow conditions. A previous lab member had also shown similar dysfunctional phenotypes in patients, but did not pursue the underlying mechanisms [30]. Moving forward, it would be interesting to design phenocopying experiments similar to those outlined in **Figure 3-8**, but also with the incorporation of tPA

or plasmin to generate fibrinolytic products or direct addition of purified D-dimer to the initial whole blood sample. In addition to fluorescently labeling platelets and fibrin, it would be important to include a detector of D-dimer and visualize whether or not the platelet and D-dimer signals indicate colocalization. We used a fluorescent anti-D-dimer antibody validated for the flow cytometry experiments in Chapter 5, but other options are available which are more suitable for immunofluorescence applications. A proposed schematic of the experimental design is shown below in **Figure 7-1**. Treatment of apixaban-anticoagulated whole blood with thrombin, tPA/plasmin/D-dimer, and fluorescent antibodies will occur prior to loading into the microfluidic device or a coverslip. After sufficient incubation, both the flow experiment over a collagen patch and the static interaction visualization assay will be conducted. Our hypotheses would include decreased platelet deposition to the collagen surface as well as colocalization of platelets and FDP to further strengthen the notion that the two components contain binding affinity for one another.

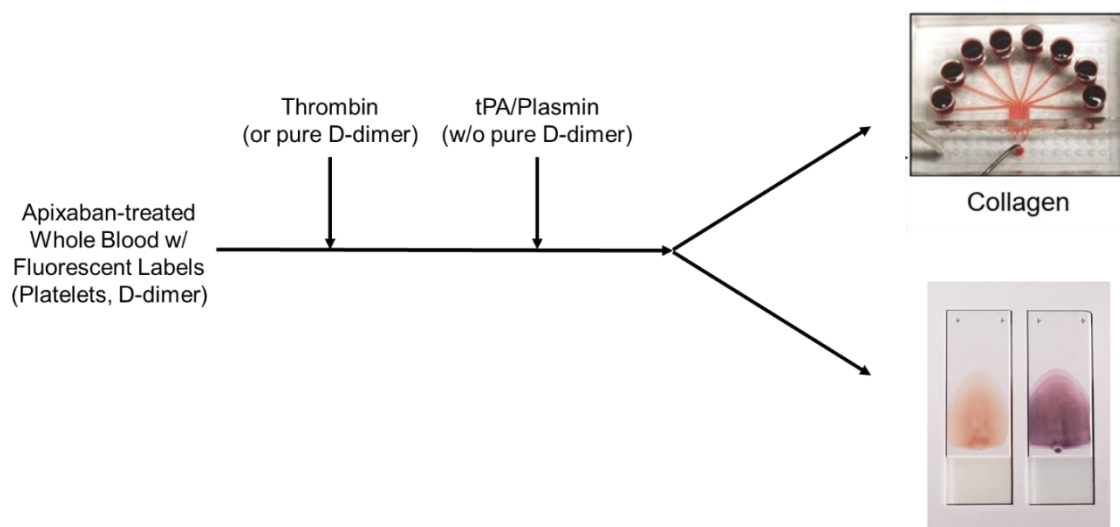


Figure 7-1. Proposed experimental setup for microfluidic investigation of platelet-FDP interactions

Full-scale fibrinolysis will be simulated with thrombin and tPA or plasmin sequential addition prior to microfluidic assay or microscopic visualization of resulting clot components. Parameters such as reagent concentrations and incubation times would require optimization.

7.1.3 *Studying mechanisms of D-dimer binding in mouse knockout cell lines*

A common method for determining specific effects of genes or transcribed proteins on observed phenotypes, or for identification of new functions, is the generation of knockout models with targeted modification of genetic material. These studies are often performed in mice, which have been shown to have relatively high degrees of homology with respect to genetic content compared to humans. Countless knockout mouse models have been developed and studied for all sorts of medical conditions, and this technique can certainly be applied to follow up on the major conclusions made in this work. In Chapters 3 and 5, we showed distinct platelet signaling defects through the GPVI receptor when soluble fibrin and fibrin degradation products were present in solution prior to agonist challenge. Also in Chapter 5, we presented preliminary data using an inhibitor of the integrin $\alpha_{IIb}\beta_3$ to imply decreased interactions between platelets and D-dimer when the receptor was hindered. Though there may be additional surface receptors to consider, we have proposed two candidates to study further. Despite the fact that our lab does not have much expertise in mouse models, we have collaborators in the medical school who could be included to assist in the development of knockout models and cell lines for additional analysis.

Studying functionality of platelet receptors has previously been performed in knockout mice missing key receptors such as GPIIb and GPVI, the PARs, P2Y1 and P2Y12, and integrin $\alpha_{IIb}\beta_3$ [174]. Specifically, one group showed that thrombasthenic mice with knockout of the α_{IIb} gene fail to bind fibrinogen and aggregate adequately, leading to bleeding disorders comparable to those observed in Glanzmann thrombasthenia patients [175]. For the purposes of our interests, we would be interested in a similar model, though ideally a full $\alpha_{IIb}\beta_3$ knockout, to use in D-dimer binding assays utilizing flow cytometry technology or surface plasmon resonance (SPR). Hypothetically, if a myriad of knockout

mouse models would be generated, we could screen several receptors for potential binding interactions to identify targets for future drug development with more confidence.

7.2 Comparison of PAR signaling via activation with thrombin or synthetic peptide combination

7.2.1 Investigating trends in different measures of platelet function

Though thrombin is the physiologic activator of the two protease-activated receptors (PAR) expressed in human platelets, PAR-1 and PAR-4, *ex vivo* studies of individual activation schemes of each receptor are often performed with synthetic peptides. Other published work has investigated functional responses and clinical implications of PAR activation [176,177]. In a study of PAR-1 signaling by agonist peptides and thrombin, different mechanisms of activation were observed and were determined to be dependent on intracellular components [176]. Though this study focused on endothelial cells rather than platelets, which function differently, the relative dose-response results were similar to those observed in platelets. Another group conducted work in extracted cardiovascular tissues from umbilical arteries and similarly investigated effects of PAR-1 activation via thrombin or PAR-1 activating and inhibiting peptides [177]. The conclusions of this study showed similar effects on arterial blood flow when either thrombin or a PAR-1 peptide was utilized, indicating physiological significance of the receptor for cardiovascular applications extending beyond platelet activation. These reports do not consider platelet PAR activity specifically, which presents an opportunity for future directions. It would be interesting to try to determine dosages of various PAR agonists that produce similar platelet responses, and also to extend this notion to multiple metrics of platelet activation to obtain a full understanding of PAR signaling and inform future experiments as to the appropriate peptide concentrations that will mimic a physiologic response in the presence of thrombin.

Preliminary work with respect to this objective has been completed, though there is still ample room for further study. First, calcium mobilization experiments were designed with the goal of producing virtually identical data when platelets were subjected to thrombin stimulation or activation by a combined cocktail of PAR-1 and PAR-4 agonists, SFLLRN and AYPGKF. After several iterations of trial and error, it was determined that high concentrations of thrombin (200 nM) as well as the individual PAR peptides (100 μ M SFLLRN + 300 μ M AYPGKF) generated starkly similar calcium release profiles (**Figure 7-2,A**). This agonist ratio was held constant and other conditions were tested to determine the generalizability of the observations. Using area-under-the-curve (AUC) as a quantitative measure, and plotting the thrombin-mediated results against the peptide-mediated data, a strong linear correlation was observed (**Figure 7-2,B**). Though there may be other agonist concentrations that yield similar results, this initial outcome is encouraging. Similar experiments, in which flow cytometric detection of integrin $\alpha_{IIb}\beta_3$ activation and P-selectin exposure were performed, produced comparable results (**Figure 7-2,C-F**). However, the relative agonist concentration ranges for the calcium and flow cytometry assays were not conserved, probably due to different dose-response relationships for each metric. Standardizing the concentrations in some fashion, perhaps through non-dimensionalization with respect to EC_{50} values, may facilitate the ability to merge the independent observations. Despite this drawback, these preliminary data highlight the potential for developing a data-driven model for mapping platelet responses due to various PAR agonists across multiple common activation methods, which has yet to be successfully done by other groups to our knowledge.

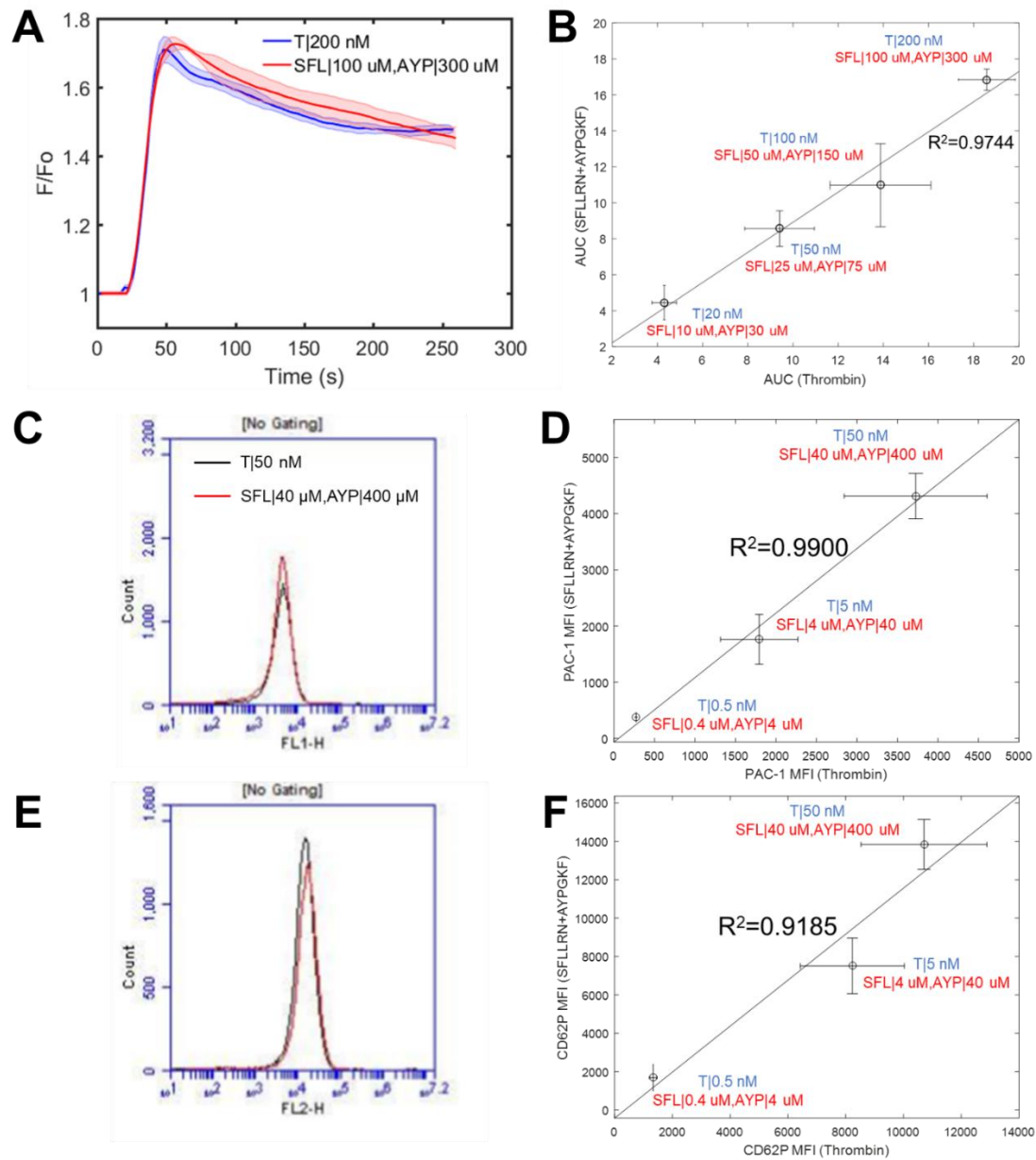


Figure 7-2. Matching of various platelet activation markers for PAR agonists

Platelet stimulation of dilute PRP was performed with either thrombin or a cocktail of SFLLRN and AYPGKF. Characteristic data for specific concentrations of each agonist condition are shown for calcium mobilization (A), GPIIb/IIIa activation measured by PAC1 binding (C), and P-selectin expression detected by anti-CD62P antibody (E). Data from other experiments with fixed agonist ratios are quantified and plotted to show strong correlations between the thrombin concentrations and peptide concentrations that span two orders of magnitude. The basis of quantification was area-under-the-curve for calcium assays (B), or mean fluorescent intensity for measuring PAC1 (D) and P-selectin (F) in flow cytometry.

7.2.2 Training machine learning model to generalize PAR signaling events

Using the pairwise agonist scanning (PAS) method with neural network training as motivation, an area of future interest would be to develop a computational model for describing multiple aspects of PAR signaling. Initial hypotheses present several possible model designs, one of which is shown below in **Figure 7-3**. The models would ideally be trained and validated with data generated in experiments similar to those discussed in the previous section, and then could be used to predict outcomes from diverse scenarios. Though inputs to the model would likely be agonist concentrations and outputs would be traditional metrics of platelet activation, once the model is sufficiently trained it could be used for making other interesting predictions. For example, if the thrombin concentration and corresponding calcium release profile are known and these variables are used as inputs, the model would then be able to generate predictions of the concentration of synthetic peptides required to mimic the calcium response as well as expected levels of PAC1 binding and P-selectin expression. This differs from the traditional PAS method in that the new model doesn't rely on the same inputs and outputs, but rather is versatile depending on the known information.

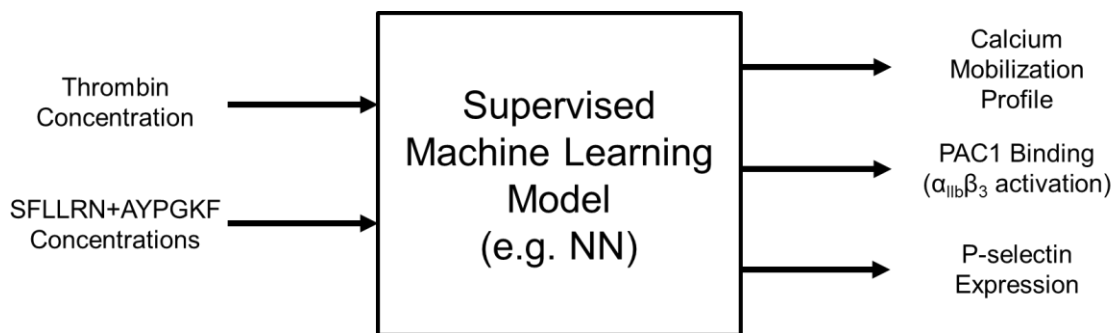


Figure 7-3. Proposed structure of machine learning model for PAR-specific signaling

Data collected from experiments using thrombin and PAR-specific peptides as stimuli to trigger platelet activation events can be used to train computational models as predictive tools for complex scenarios.

Since this model will involve data of different visual contexts (kinetic data traces for calcium experiments vs histogram distributions of cell function in flow cytometry), the model will likely require an image recognition feature in order to reliably learn trends in the data. Though many machine learning models exist and have been developed for various applications, models capable of deep learning, such as convolutional neural networks (CNN), are great for image analysis because of the capability to handle “big data” [178]. As was done for the PAS-NN method described at length throughout this work, optimization of the internal architecture of this model in terms of the number of hidden layers and nodes per layer would have to be performed at length to develop the most efficient and accurate algorithm possible.

7.3 Extension of PAS to studying toll-like receptors

7.3.1 Toll-like receptors (TLR)

Toll-like receptors (TLR) are a class of receptors primarily involved in the innate immune system and inflammatory responses. TLRs are comprised of a family of transmembrane proteins present in a variety of cell types. Immune cells, such as dendritic cells and macrophages, as well as non-immune cells like fibroblasts and epithelial cells, are known to express TLRs [179]. Recognizing a plethora of foreign signals known as pathogen-associated molecular patterns (PAMPs) or danger-associated molecular patterns (DAMPs), TLRs transmit intracellular signals upon activation to induce the expression of genes to initiate host defense. The majority of TLRs signal through proteins like myeloid differentiation primary response gene 88 (MyD88), Toll-interacting protein (TOLLIP), IL-1R-associated kinase (IRAK), and TNF-receptor-associated receptor 6 (TRAF6). These signaling proteins work in concert to elicit downstream activation of nuclear factor kappa-light-chain-enhancer of activated B cells (NF- κ B) and mitogen-activated protein kinase (MAPK) which tend to generate experimentally detectable signals

[179]. Specifically, NF- κ B is a transcription factor for regulation of genes responsible for both innate and adaptive immune response, pro-inflammatory cytokine production, and other cell survival functions.

Though their primary function is not linked directly to the immune system, platelets have also been shown to express the full TLR transcriptome [180,181]. The activation of these receptors in platelets, of which there are known to be at least 10, contributes to both hemostatic and inflammatory responses, though only a subset is known to be involved in platelet function. These include TLRs 1, 2, 3, 4, 6, 7, and 9, and each receptor is uniquely expressed on either the extracellular platelet surface or within the platelet's intracellular endosome compartments (**Table 7-1**). One TLR present on the cell surface is TLR4, which recognizes a variety of PAMPs and DAMPs, the most notable of which being lipopolysaccharide or LPS. Sometimes referred to as endotoxin, LPS is derived from gram-negative bacteria and is typically recognized by CD14 when in the presence of LPS-binding protein (LBP). CD14, which can also exist as a soluble form, then shuttles the bound LPS to TLR4 to trigger the immune response [180].

The other well-characterized TLR present extracellularly is TLR2, but its functional activity requires heterodimer formation with TLR1 (denoted TLR2/1) or TLR6 (TLR2/6) in order to be able to recognize its specific pathogenic ligands. These ligands include gram positive-derived lipoteichoic acid and other bacterial lipoproteins, some of which have been successfully mimicked by synthetically developed molecules. TLR2/1 and TLR2/6 both detect microbial PAMPs, though the former targets triacylated lipoproteins while the later focuses more on diacyl forms [180]. Another difference between these two receptor constructs is their respective effects on platelet function, which will be discussed further in the next section. TLR2/1 activation is often studied through the use of Pam3CSK4, a synthetic triacylated lipoprotein that mirrors the amino terminus of bacterial lipopeptides, which has been shown to positively impact platelet function. Conversely, the diacylated

macrophage activating lipoprotein-2 (MALP-2), agonizes the TLR2/6 complex but exerts inhibitory effects on platelet activation [180].

<i>Receptor</i>	<i>Ligand(s)</i>	<i>Involved in Platelet Function?</i>	<i>Extracellular/Intracellular Platelet Expression?</i>
TLR1	PAM3CSK4	Yes (via heterodimer with TLR2)	Extracellular
TLR2	PAM3CSK4 MALP-2 Zymosan	Yes (via heterodimer with TLR1 or TLR6)	Extracellular
TLR3	Poly (I:C)	Yes	Intracellular (endosomes)
TLR4	LPS HMGB1 Histones (H3, H4)	Yes	Extracellular
TLR5	Flagellin	No	n/a
TLR6	MALP-2	Yes (via heterodimer with TLR2)	Extracellular
TLR7	Imiquimod Imidazoquinoline resiquimod	Yes	Intracellular (endosomes)
TLR8	Imidazoquinoline resiquimod	No	n/a
TLR9	CpG ODN	Yes	Intracellular (endosomes)
TLR10	--	No	n/a

Table 7-1. Expression of toll-like receptors in platelets

Platelets feature all 10 known TLR transcripts, though only a select few are involved in platelet function (shown in bold). The table lists the important receptors with identified ligands, as well as whether the receptor is present on the cell surface (extracellular) or within the cell (intracellular).

The remaining three TLRs that have been implicated to affect platelet function—TLR3, TLR7, and TLR9—are found within the cell and respond to viral PAMPs. Each of these receptors recognizes different forms of genetic material; TLR3 responds to double-stranded RNA (dsRNA) produced during the life cycle of a virus, TLR7 recognizes single-stranded RNA (ssRNA), and TLR9 detects viral DNA containing the unmethylated cytidine-phosphate guanosine (CpG) sequence [180]. Similar to TLR2 and TLR4, these intracellular receptors can also be activated through mimetics of physiologic entities. For example, TLR3 activation can be mediated with polyinosinic:polycytidylic acid, or

Poly(I:C), which serves as an analog for dsRNA replication products, and TLR7-dependent inflammatory signals can be initiated with imiquimod, a prescription drug known to treat genital warts in addition to its capability to boost the immune system.

7.3.2 TLR activation involvement in platelet activation and signaling

As has been discussed, only a selection of the TLR transcripts carry platelet function implications upon activation, and even some of the reported effects are contradictory. **Table 7-2** lists platelet activation signals that have been reported in the literature for each of the functional TLRs. When activated, most of the receptors lead to platelet activation events such as adhesion, aggregation, and intracellular granule release in addition to their usual pro-inflammatory signals through the NF- κ B pathway. Other receptors exhibit antiplatelet activity; the TLR2/6 heterodimer complex competes with TLR2/1 to balance the effects, and TLR7 activation has been shown to induce thrombocytopenia as a result of the formation of platelet-neutrophil aggregates [180]. More interesting and applicable to the work in this dissertation, however, a few TLRs have been reported to elicit increases in calcium mobilization in platelets.

TLRs specifically identified to play a role in platelet calcium signaling are TLR2/1 and TLR3. A few groups have shown positive results for Pam3CSK4 stimulation of platelets through TLR2/1 to elicit rises in calcium concentrations [182,183]. In fact, the calcium mobilization level in response to the TLR2/1 agonist was comparable to that induced by thrombin, and was inhibited if platelets were also stimulated simultaneously with MALP-2 [183]. However, a separate group attempted similar experiments in which platelets were stimulated with Pam3CSK4 or LPS to study calcium signaling in the two known surface TLRs. Their results implied TLR activation fails to effectively mobilize calcium, and have no effects on subsequent challenge with traditional agonists like ADP or platelet-activating factor (PAF) [184]. This lack of agreement may be attributed to the

different calcium detection systems used in the referenced studies, but also provides an opportunity to apply the methods we have developed to further understand the potential physiological significance of TLR signaling in platelets.

TLR	Signals for Platelet Activation
TLR2/1	NF-KB pathway, Syk/Src pathway Increased Ca ²⁺ , TXA ₂ production, p38 phosphorylation, PI3K/AKT activation, PLCγ2 activation Platelet aggregation, adhesion, granule secretion, NET formation
TLR2/6	Anti-platelet activity → inhibitory towards TLR2/1 signaling
TLR3	NF-KB pathway Increased Ca ²⁺ , PI3K/AKT activation, alpha granule secretion, potentiation of activation via other agonists
TLR4	NF-KB pathway, MAPK pathway PI3K/AKT activation, PKG expression through cGMP signaling Platelet aggregation, adhesion, granule secretion, NET formation
TLR7	Granule secretion, platelet-neutrophil aggregation, thrombocytopenia
TLR9	PI3K/AKT activation, Src signaling Alpha granule secretion, integrin activation, aggregation, thrombosis acceleration

Table 7-2. Platelet biochemical signaling mediated by TLR activation

For the specific TLR's involved in platelet activation, some require heterodimer formation (e.g. TLR2/1, TLR2/6), while most lead to activation of the NF-KB pathway. Other receptors are reported to lead directly to rises in calcium mobilization, or other indicators of platelet activity like aggregation, adhesion, or granule release.

7.3.3 Application of PAS to study TLR-mediated platelet function

To this point, our study of platelet function has focused on traditional agonists and receptors whose sole purpose is hemostatic in nature. Several other surface receptors commonly involved in other processes like inflammation, such as toll-like receptors, may also play an important role in platelet activation, as has been described in the previous sections. Our literature review of TLRs has revealed several ligand-receptor interactions to consider in platelets, some of which have already been studied by other groups, and our lab's capability to interrogate countless signaling pathways in a single experiment certainly presents an opportunity for future research.

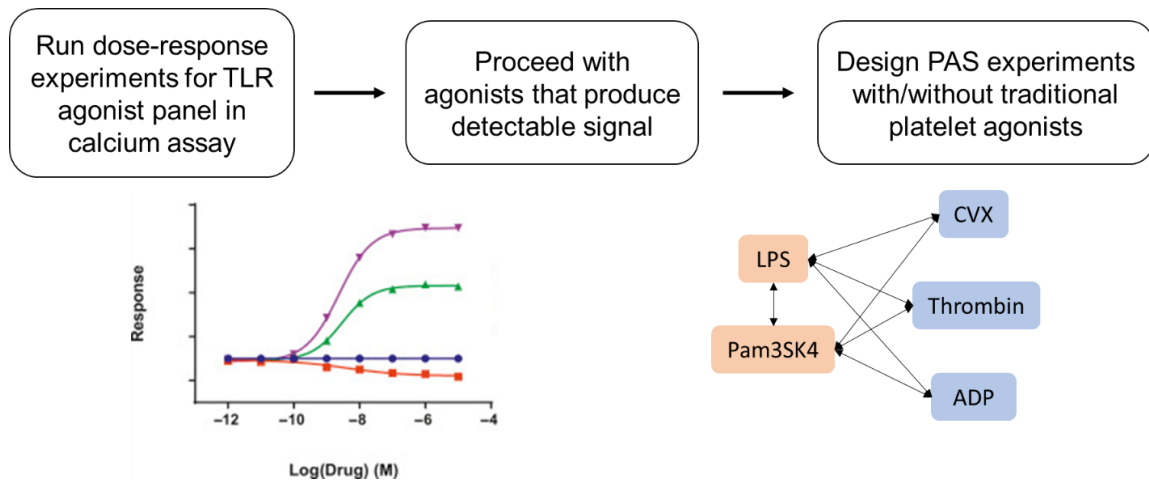


Figure 7-4. Proposed set of experiments for investigating TLR activation in platelets

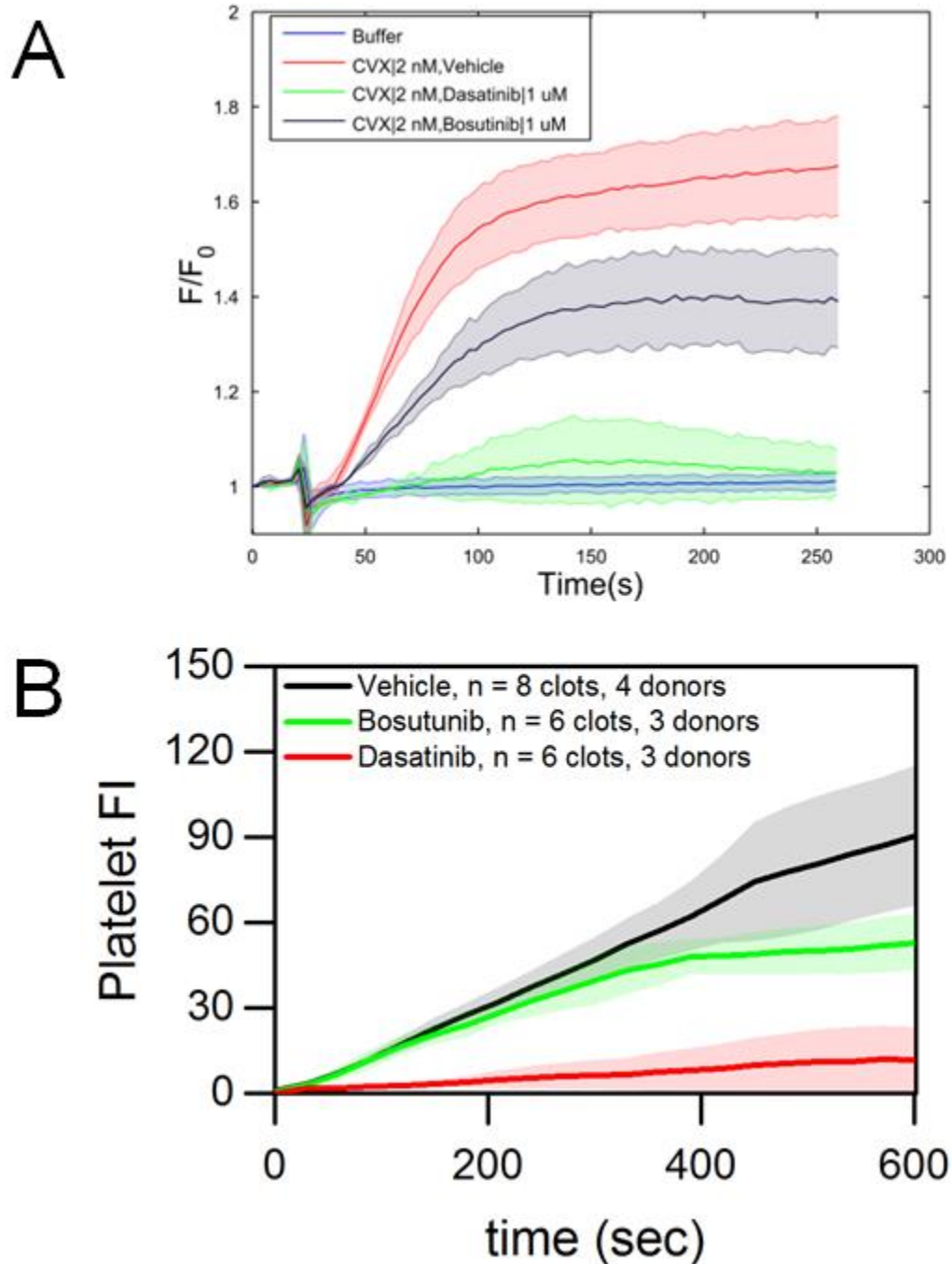
Preliminary studies of TLR-mediated platelet activation will begin with characterization of several of the known agonists listed in Table 7-1, specifically for ability to induce calcium mobilization. If necessary, other platelet function assays can also be incorporated for the most promising agonists. Dose-response experiments will be conducted to determine appropriate concentration ranges to use in future studies, which will include PAS-inspired experiments with multiple TLR ligands (orange boxes) as well as combinations with traditional platelet agonists (blue boxes).

Since this area of research is unfamiliar and relatively poorly understood, several preliminary experiments can be designed to establish how to proceed with future studies. A general outline for the proposed sequence of events in this study is presented in **Figure 7-4**, however this is not an exhaustive list and tangential investigation should certainly be pursued as initial results are obtained. Each of the TLR agonists listed in **Table 7-1** is commercially available and can be purchased for laboratory use. The first step upon acquisition of these reagents, as with most studies in this work, is to characterize their ability to activate platelets. Calcium mobilization experiments in systems of dilute PRP should be conducted in which varying doses of each reagent are used as activating stimuli. Ideally, some of the TLR agonists will yield dose-dependent calcium profiles, and these candidates will progress to the next stage of testing. For those agonists that don't successfully mobilize calcium in platelet suspensions, they should not necessarily be omitted from future work but simply put on the back burner until studies with the more

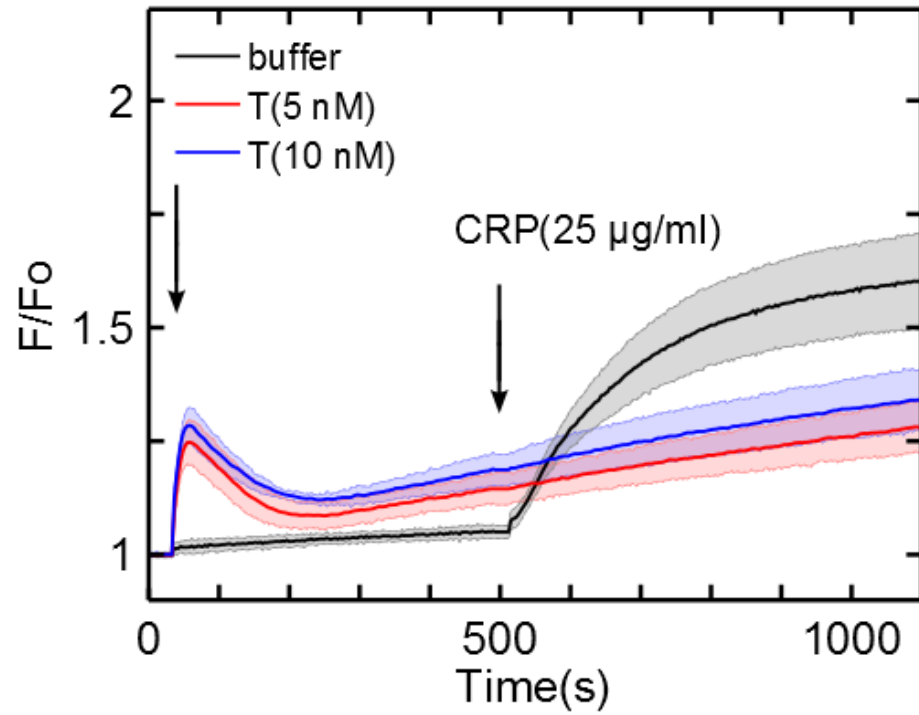
promising reagents are complete. At that point, other assays can be designed (e.g. platelet aggregometry, flow cytometry) to investigate other mechanisms of platelet activation.

After dose-response experiments inform appropriate concentrations to use, PAS studies can be designed to investigate synergies between individual TLR agonists as well as crosstalk between TLRs and traditional platelet receptors. It is difficult to predict the number of TLR agonists that will be used for this second set of tests, so we show a few that should produce some platelet reactivity (LPS and Pam3SK4). Procedures should follow those documented previously [50,84,110], and this pilot study will be novel in that high-throughput experimentation of combined inflammatory and hemostatic receptor activation has not been performed previously to our knowledge.

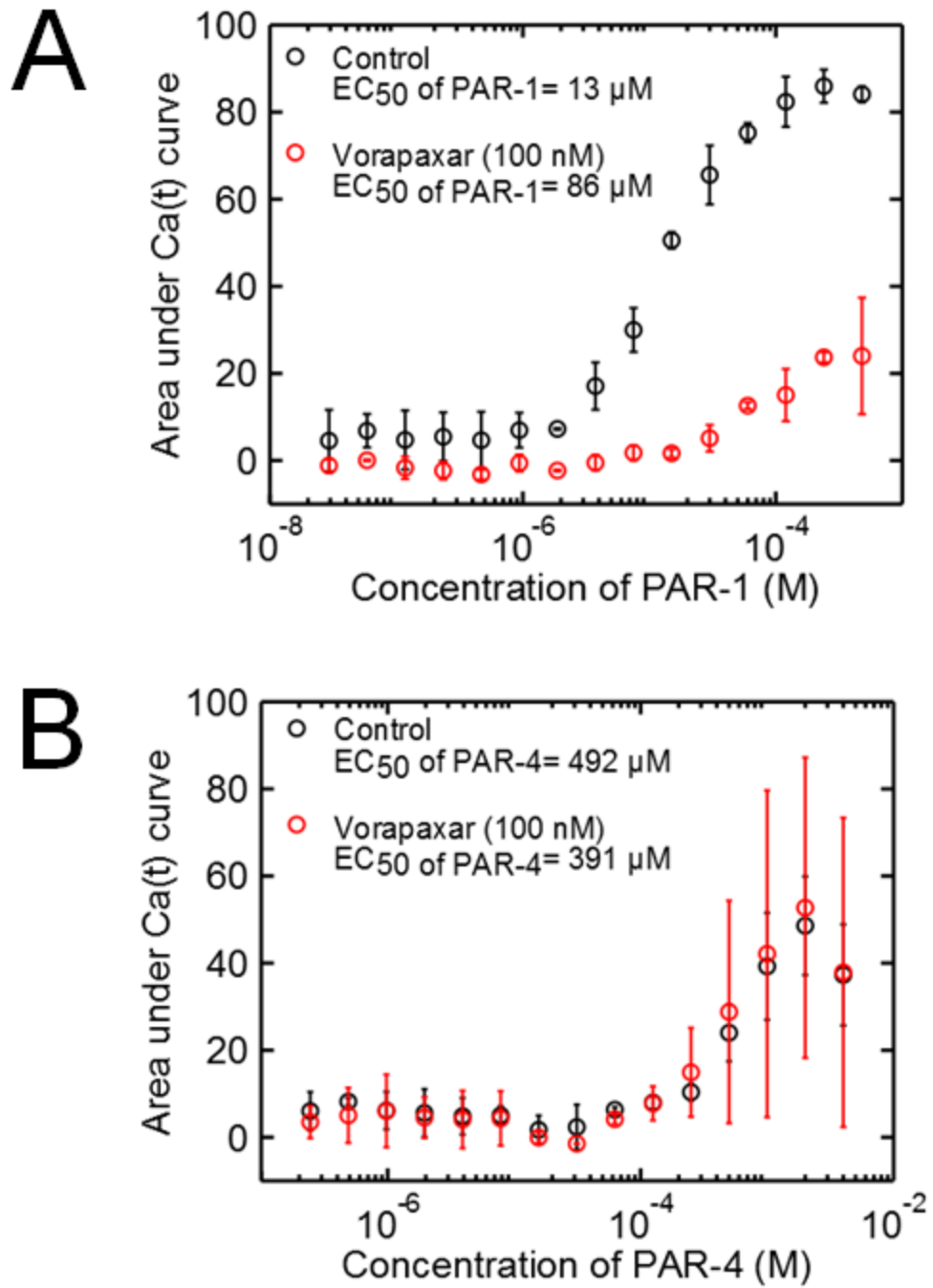
CHAPTER 8: APPENDIX I (SUPPLEMENTAL FIGURES)



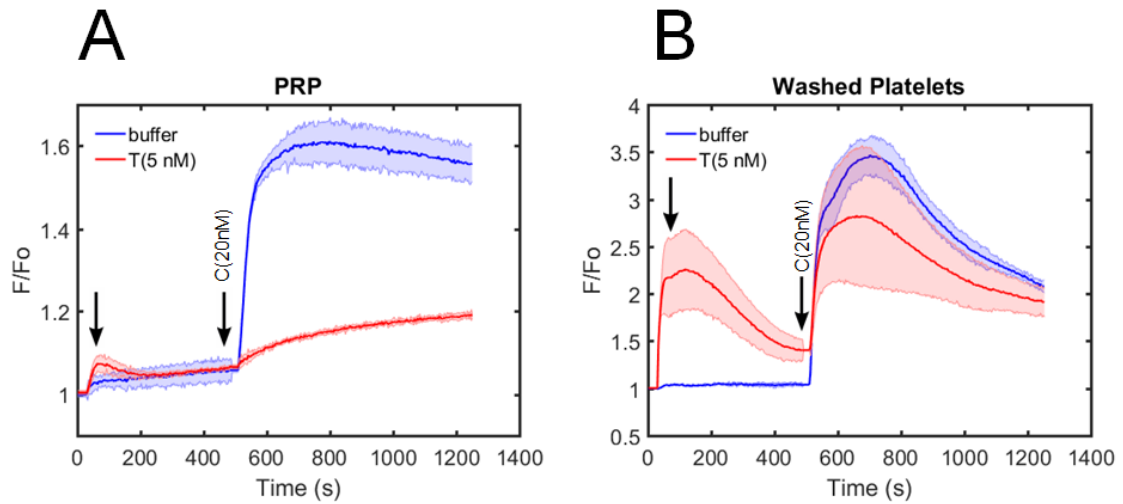
Supplemental Figure 1. Dasatinib, a Syk inhibitor, blocks the GPVI-signaling pathway, confirming that convulxin or collagen activates GPVI with concomitant calcium mobilization and platelet activation dependent on Syk signaling. (A) Stimulation of platelets with convulxin (2 nM) is inhibited by Dasatinib (1 μ M) when measuring calcium mobilization. (B) Platelet deposition on a collagen surface in an 8-channel microfluidic device is abolished when Dasatinib is present.



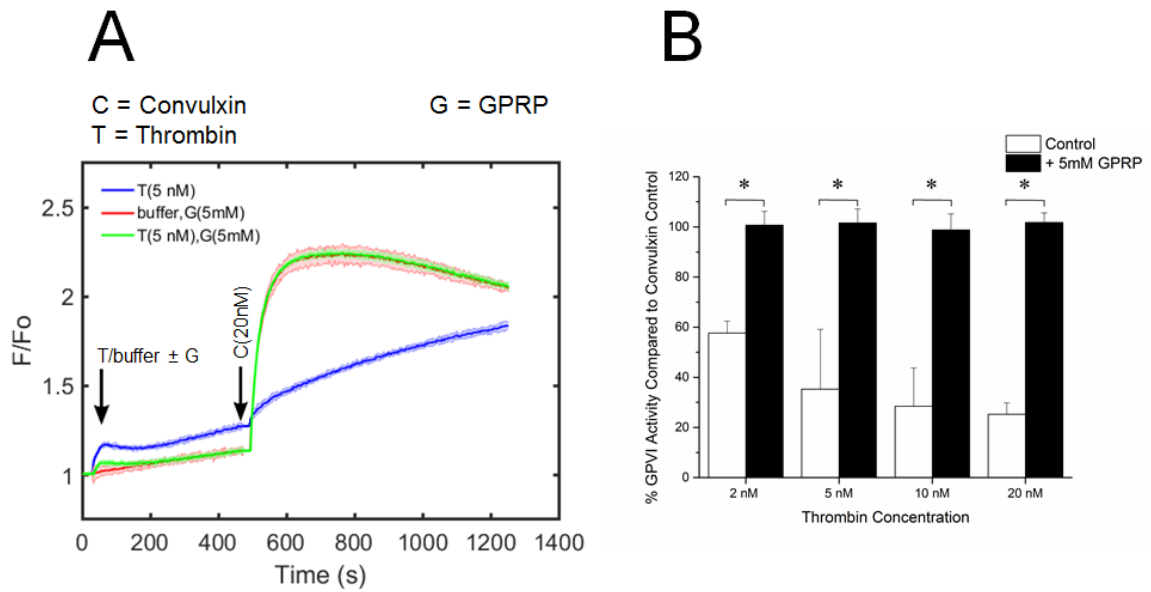
Supplemental Figure 2. Pretreatment of PRP with thrombin blocks subsequent platelet activation by collagen related peptide (CRP).



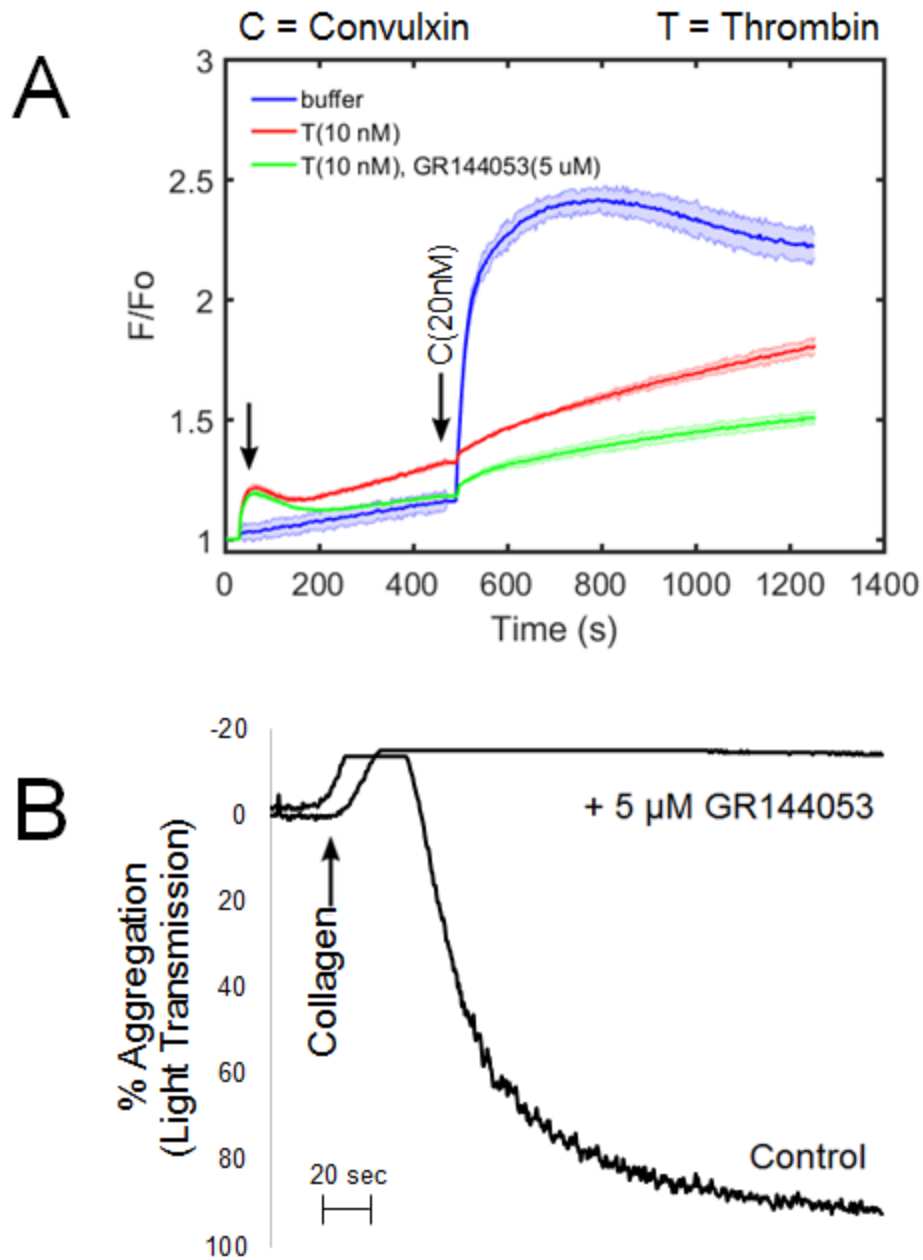
Supplemental Figure 3. Vorapaxar is a specific PAR-1 inhibitor. Vorapaxar (100 nM) reduced PAR-1 agonist peptide induced platelet calcium mobilization in a dose-dependent manner (A), but had no effect on PAR-4 agonist peptide induced calcium mobilization (B).



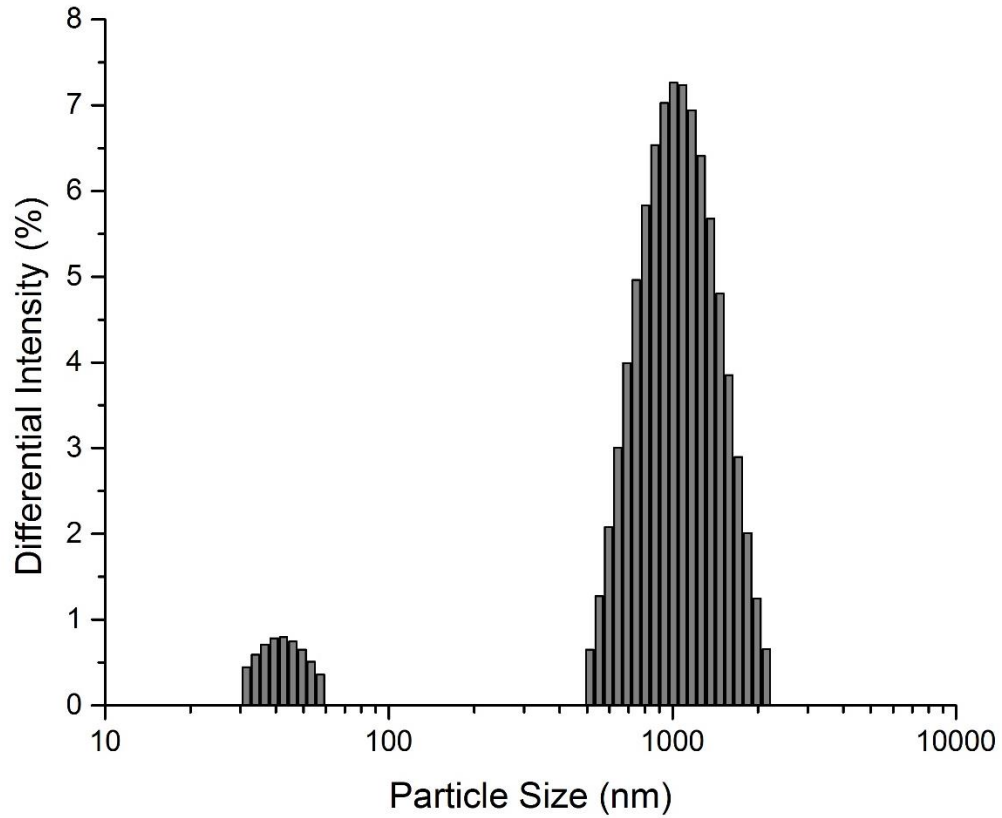
Supplemental Figure 4. Thrombin activation of washed platelets does not exhibit attenuation of GPVI activation as is observed in PRP. (A) Incubation of 12% (v/v) PRP with thrombin (5 nM) results in initial platelet activation and subsequent down-regulation of the GPVI signal when compared to a buffer control. (B) Isolation and preparation of washed platelets (a plasma-free background) shows initial thrombin-induced platelet activation but no significant downstream effect on the functionality of platelet GPVI when exposed to convulxin (20 nM). (C, convulxin; T, thrombin).



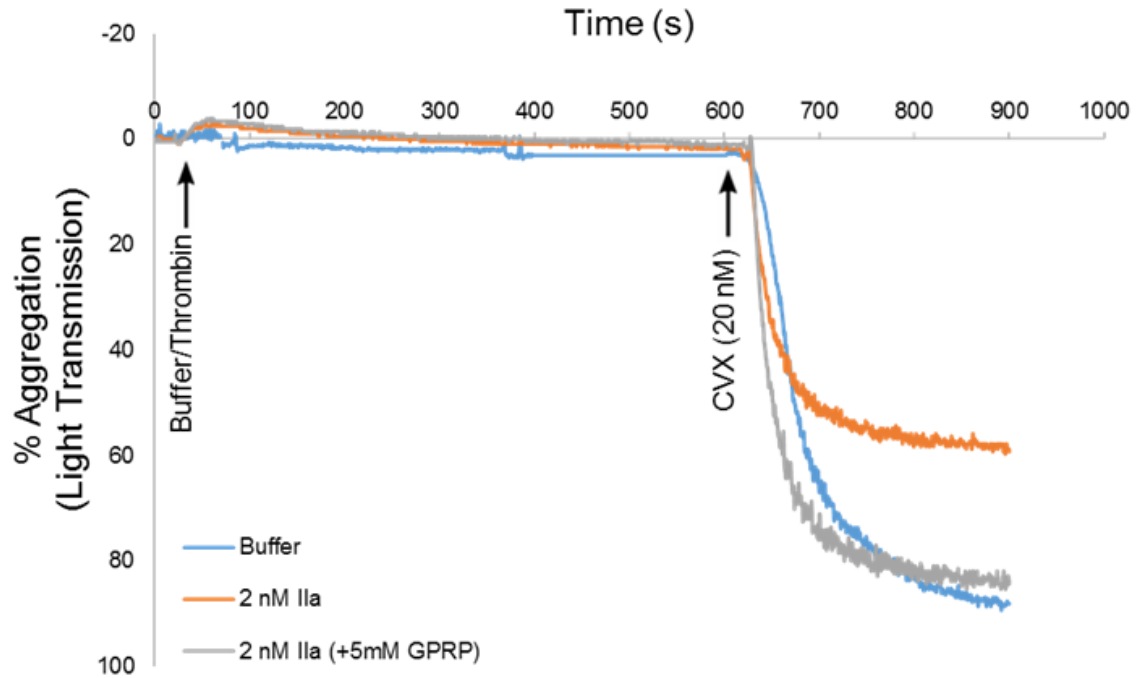
Supplemental Figure 5. Inhibition of fibrin polymerization with GPRP completely eliminates down-regulation of convulxin-induced platelet activation. (A) When GPRP (5 mM) is present in platelets, the attenuation of calcium fluorescence through GPVI signaling is no longer observed after platelets have been activated with thrombin. (B) At several dosage levels of thrombin (2-20 nM) the functionality of platelet GPVI is nearly 100% (n=3 donors, * p<0.05).



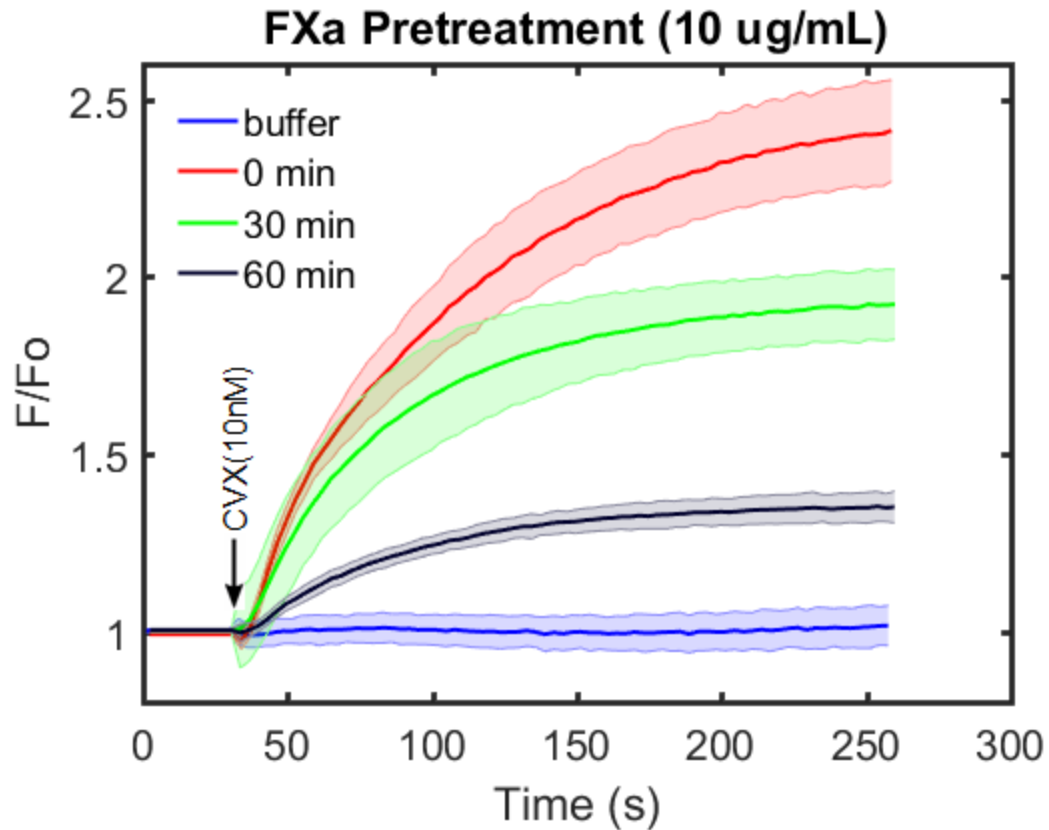
Supplemental Figure 6. Inhibition of glycoprotein IIb/IIIa-mediated platelet aggregation via GR144053 does not prevent GPVI down-regulation after thrombin treatment of PRP. (A) Upon pretreatment with GR144053 (5 μM), platelets exhibit calcium mobilization due to thrombin stimulation but show convulxin-insensitivity similar to that of the negative control (no GR144053 treatment) (n=3 replicates for each condition). (B) Aggregometry shows the effect of GR144053 on collagen-induced platelet aggregation.



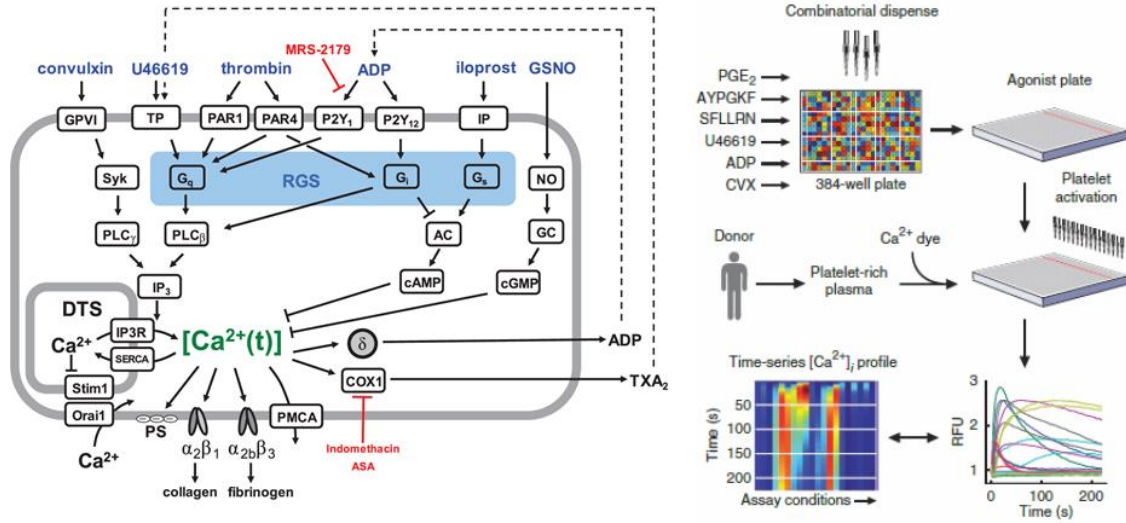
Supplemental Figure 7. Characterization of soluble fibrin via dynamic light scattering. Purified fibrinogen (final concentration = 10 nM) was stimulated with low-dose thrombin (1 nM) for 10 min. The first peak (42.7 ± 7.4 nm) reflects unreacted fibrinogen and the second peak (1095 ± 347.7 nm) indicates soluble fibrin polymerization with an approximate chain length of 25 monomeric units.



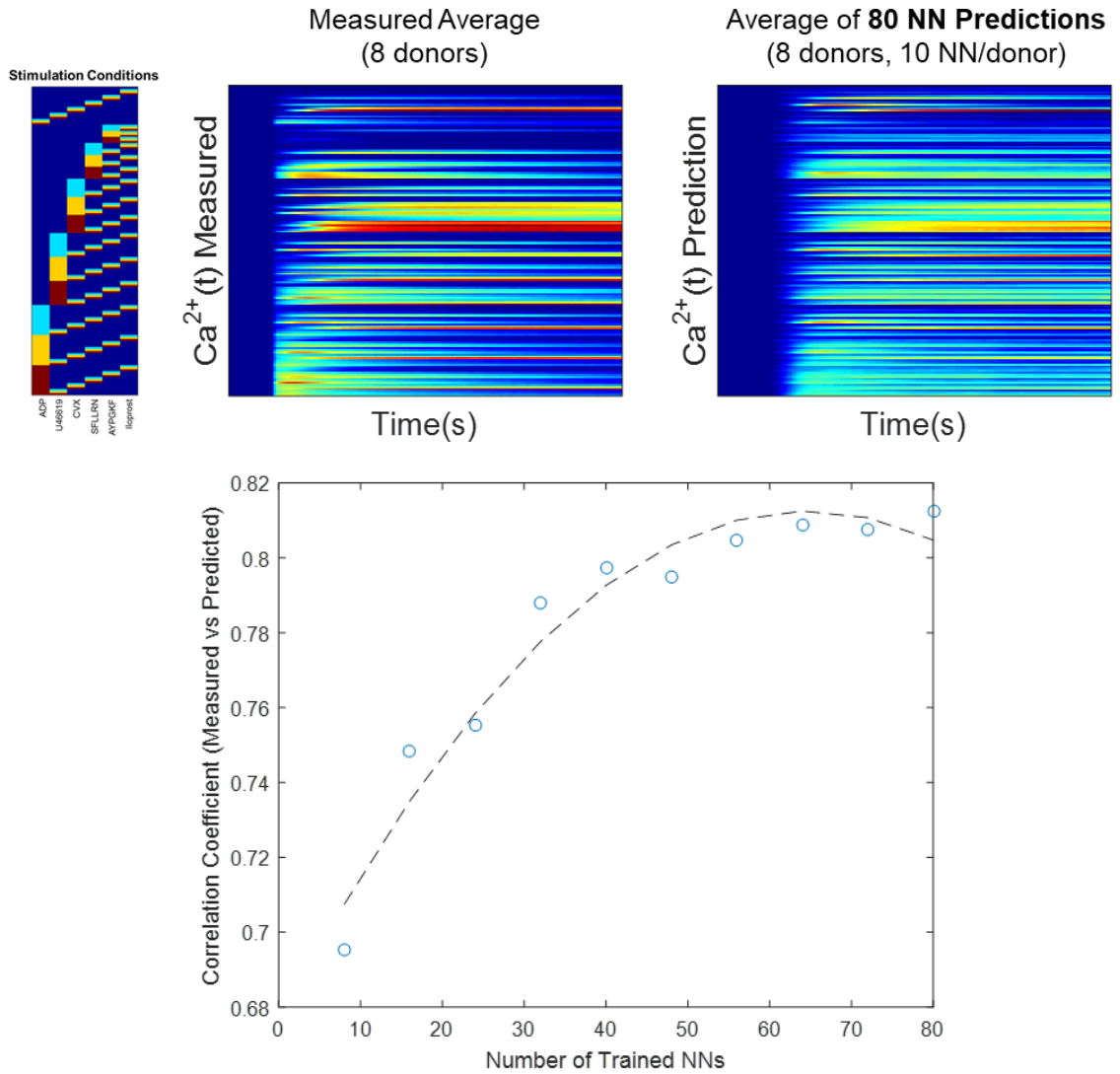
Supplemental Figure 8. Low-dose thrombin treatment (2 nM) of PRP results in ~35% decrease in platelet aggregation in response to convulxin (orange curve). However, full GPVI-mediated platelet aggregation is restored when PRP is incubated with 5 mM GPRP, preventing fibrin polymerization (grey curve). This result is representative of at least three independent experiments and similar results were observed using 1 $\mu\text{g}/\text{mL}$ fibrillar collagen in place of convulxin.



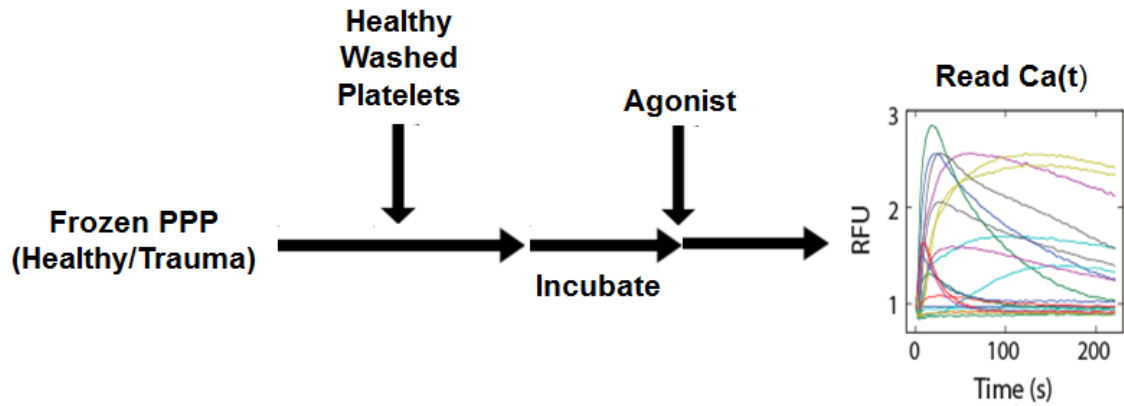
Supplemental Figure 9. Factor Xa is an effective mediator of GPVI shedding, though the process is relatively slow and requires >60 min to exhibit ~80% of the original GPVI signal. Washed platelets were isolated from apixaban-treated whole blood, incubated with calcium dye, and resuspended in HBS buffer, then pretreated with FXa (10 $\mu\text{g}/\text{mL}$) for the times indicated above. Convulxin-induced (10 nM) calcium mobilization was measured at three timepoints (0, 30, 60 min) of FXa incubation to show the time-dependency of FXa-mediated GPVI shedding (n=8 replicates for each timepoint).



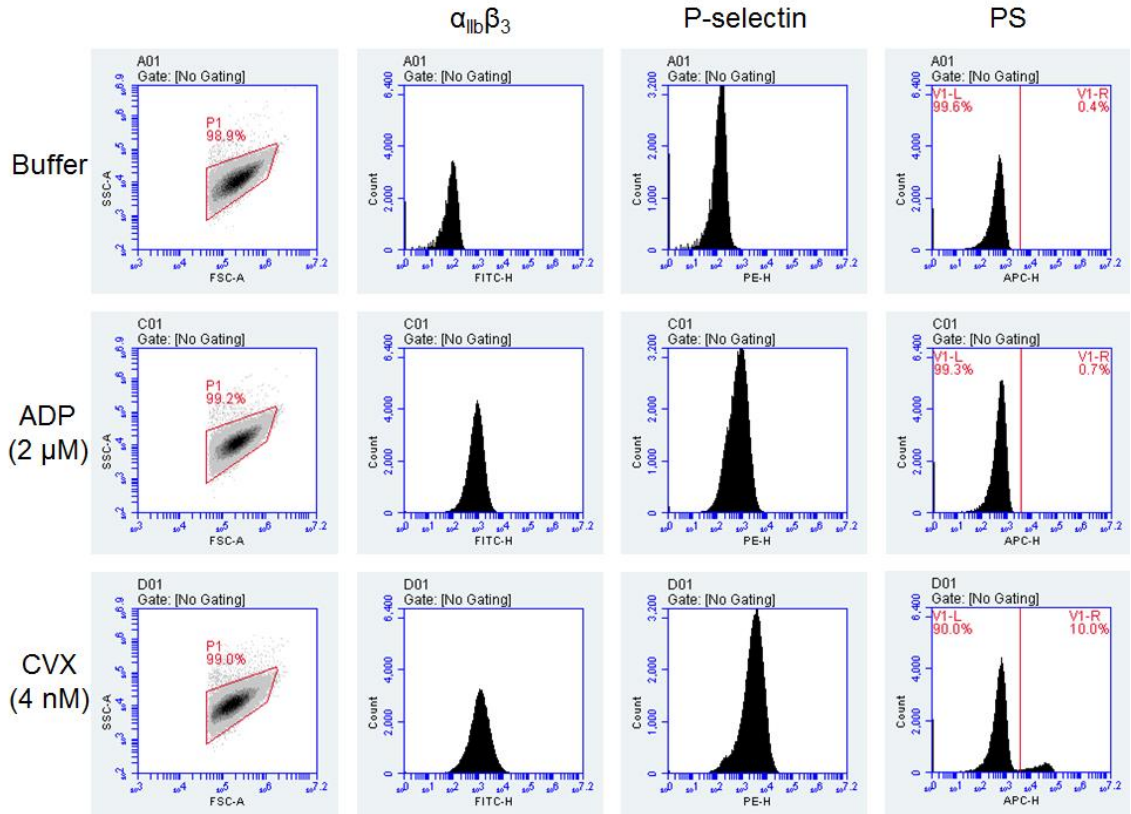
Supplemental Figure 10. Platelet signaling pathways and ligand-receptor binding. Platelet activation is mediated by several surface receptors, each with specific ligands that are either presented to cells upon endothelial disruption or produced following the first stages of the hemostatic response. Major receptors are shown above (GPVI, TP, PAR-1/4, P2Y₁ and P2Y₁₂, and IP) with commonly used activating agents and respective signaling pathways (right), all of which converge upon intracellular calcium mobilization [Ca²⁺(t)]. Dose-response experiments have been conducted previously to determine the EC₅₀ values for each platelet agonist and antagonist listed above and combinations of one or two agonists can be prepared as detailed in the concentration map (left) to build a subject-specific phenotypic profile of platelet activation. This technique is called pairwise agonist scanning (PAS) and has been documented extensively for healthy donors (Chatterjee et al. *Nat Biotechnol*, 2010;**28**:727-32; Lee et al. *PLoS Comput Biol*, 2015;**11**:e1004118).



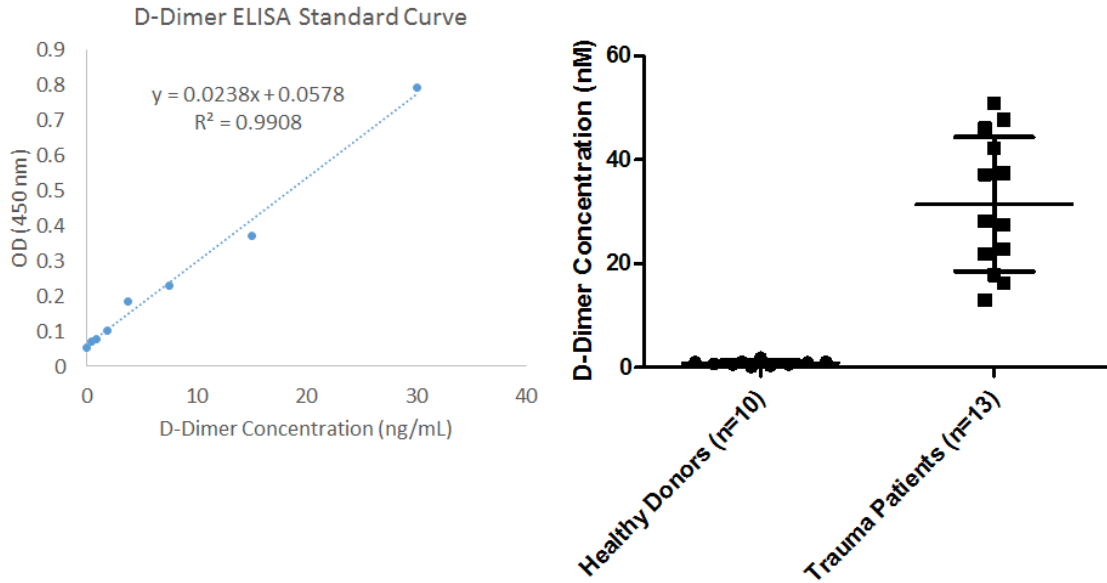
Supplemental Figure 11. Validation of restricted combinatorial space in trauma patient studies of total platelet calcium mobilization. Full ($n=154$ agonist conditions) and restricted ($n=31$) PAS experiments were conducted on healthy donors ($N=8$) and neural network models were trained using data from the restricted space. Up to 10 NNs were trained on each unique donor's data, and the models were averaged together to predict the responses to the full PAS space. The prediction made by an average of 80 NNs yielded high agreement ($R=0.8125$) with the actual measured data.



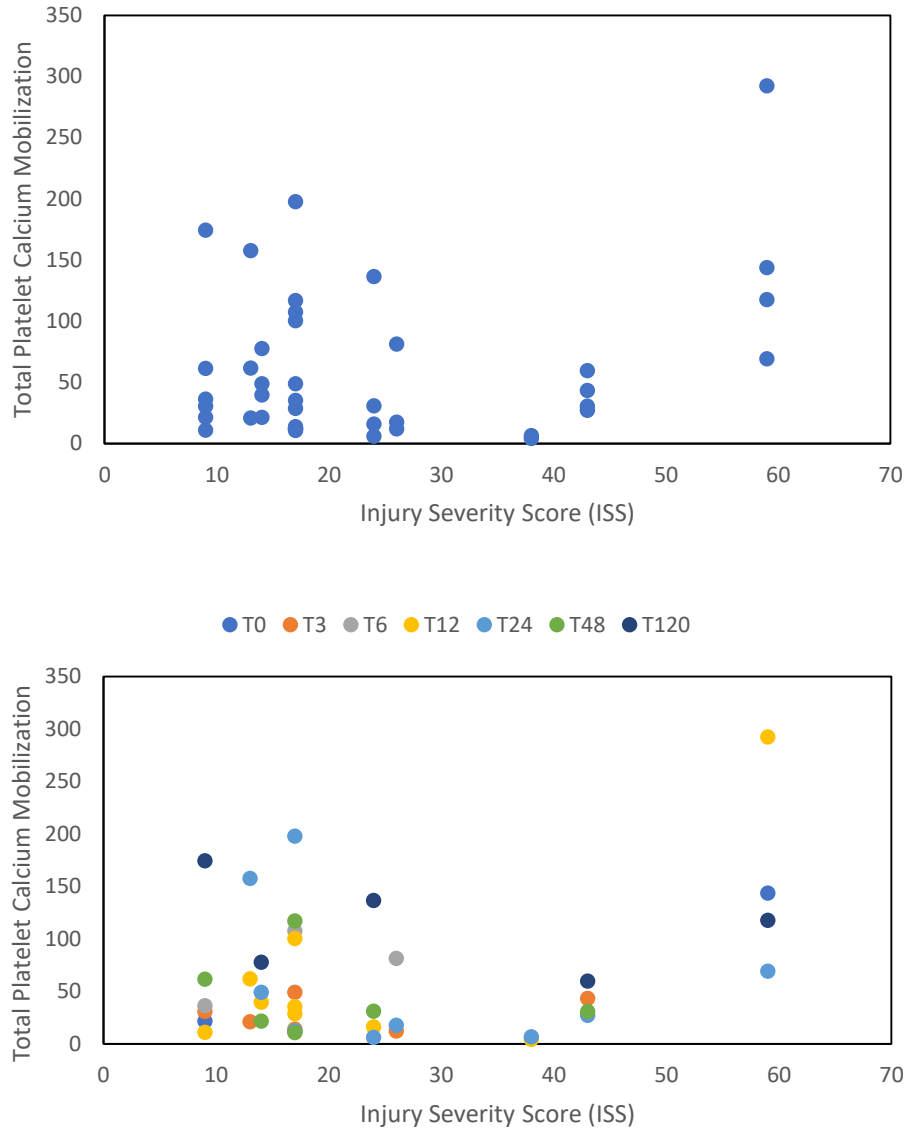
Supplemental Figure 12. Experimental setup for monitoring platelet function following resuspension of washed platelets in platelet-poor plasma (PPP). Anticoagulated whole blood (WB) is centrifuged to isolate platelet-poor plasma (PPP; 2000g, 10min), which can be stored at -80°C for future use, or platelet-rich plasma (PRP; 120g, 10min). PRP can then be incubated with a fluorescent calcium dye, Fluo-4, and centrifuged further to concentrate a platelet pellet which can be washed and resuspended in a medium of choice. Frozen plasma is thawed, reconstituted, and incubated in fresh washed platelets and platelet activity is challenged with various agonists.



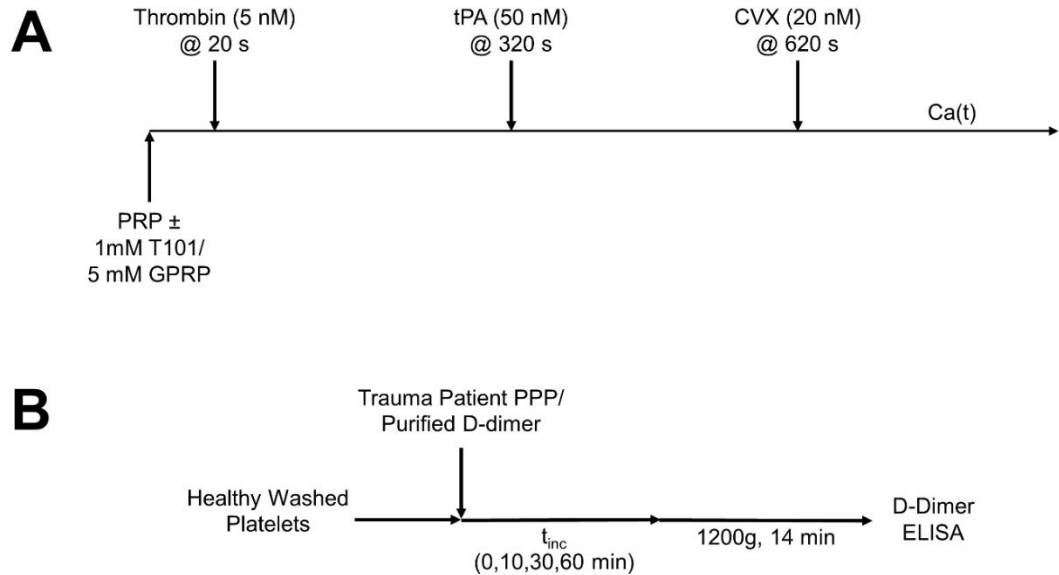
Supplemental Figure 13. Representative flow cytometry results for healthy donor. Platelet function was monitored using antibodies against activated $\alpha_{IIb}\beta_3$, P-selectin, and phosphatidylserine (PS). Results were quantified as mean fluorescent intensity (MFI) or % PS-positive cells as determined by a pre-determined gating function. Dilute PRP (1%) was activated by buffer control, ADP (2 μ M), or CVX (4 nM) and results were compared between trauma patients and healthy donors (Figure 4-2). (Note that the x-axis is in log scale.)



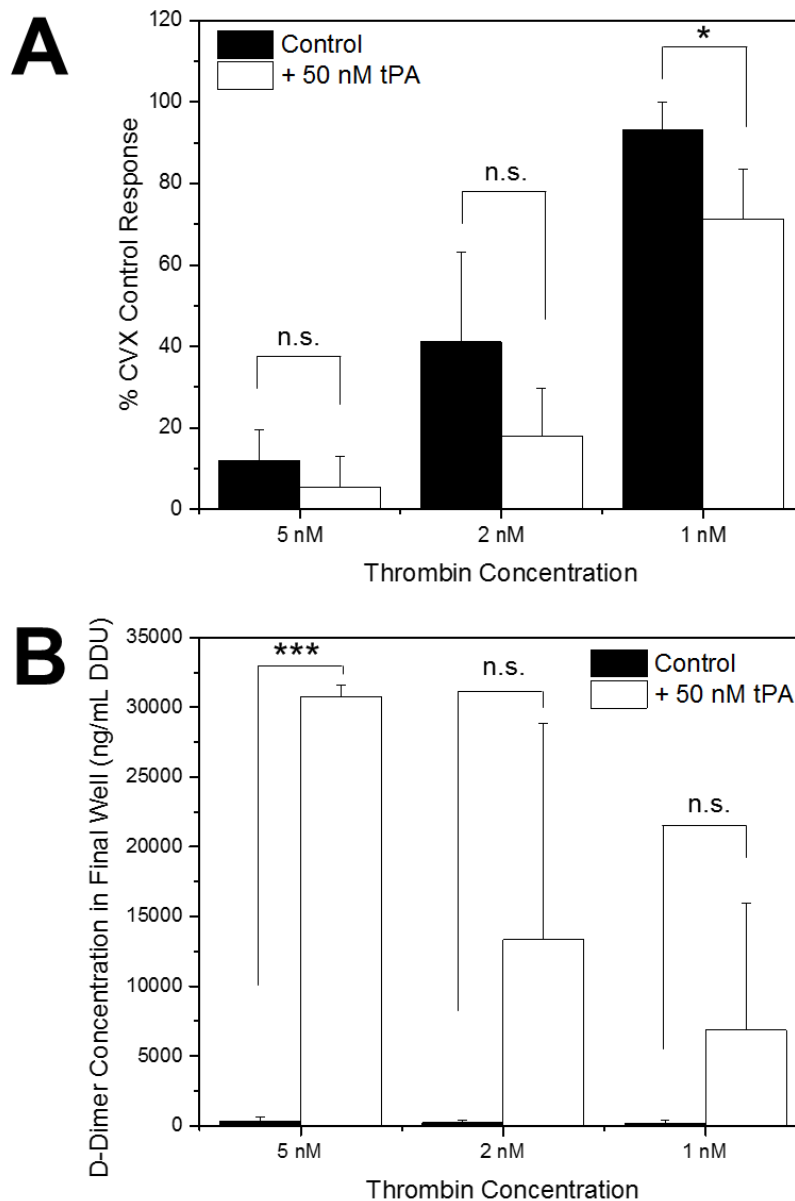
Supplemental Figure 14. D-dimer ELISA results. Plasma concentrations of D-dimer were measured via a Human D-dimer ELISA Kit (Abcam, Cambridge, MA). A standard curve was constructed for a range of D-dimer concentrations (left) and used to determine levels in a cohort of healthy donor and trauma patient plasma samples (right). Trauma patient samples showed ~30-fold increase in D-dimer concentration compared to healthy samples.



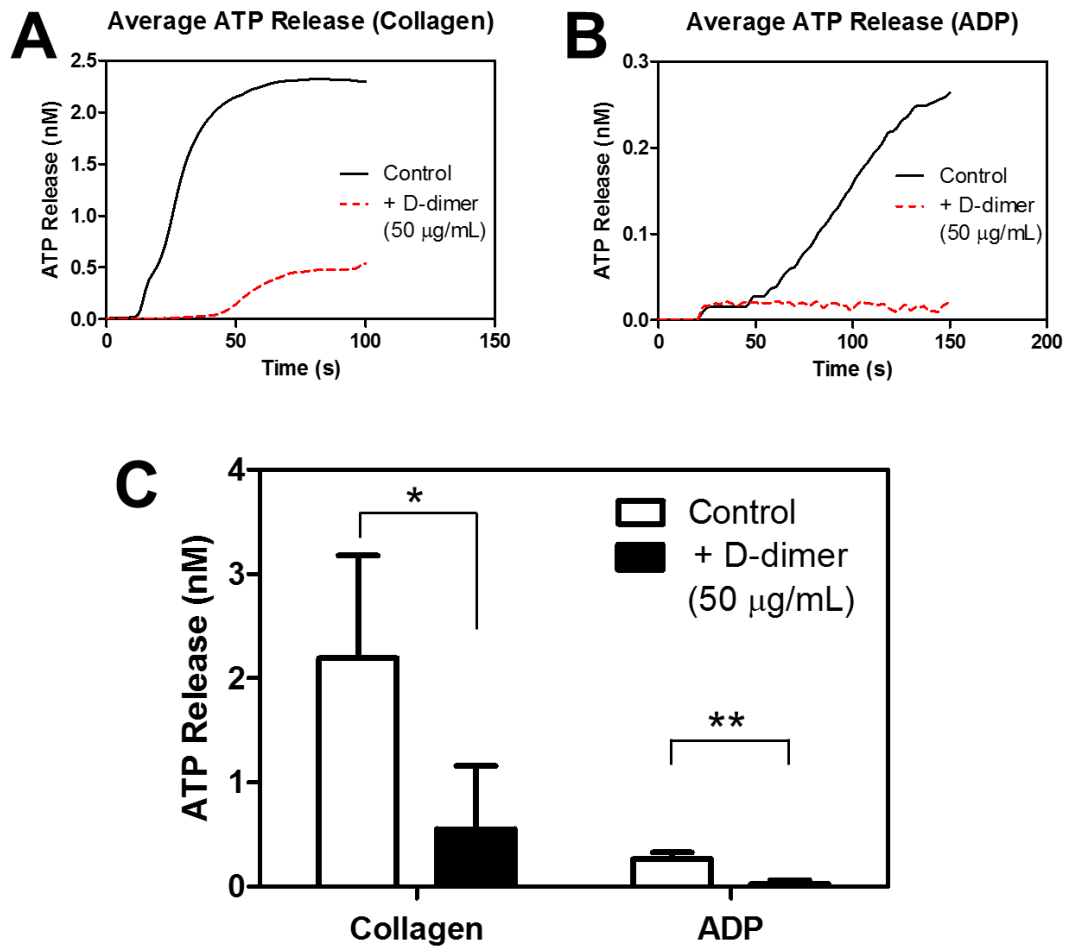
Supplemental Figure 15. Total platelet calcium mobilization as a function of patient injury severity score (ISS). Each enrolled trauma patient was assigned an ISS to denote the seriousness of the presenting conditions. To determine if this unitless parameter was correlated with the level of platelet dysfunction observed in the calcium mobilization assay, the data in Figure 4-1,E was plotted against the ISS for each patient. The top panel includes all collected data, while the bottom panel is the same data labeled with the collection time point. There appears to be no significant relationship between the two variables.



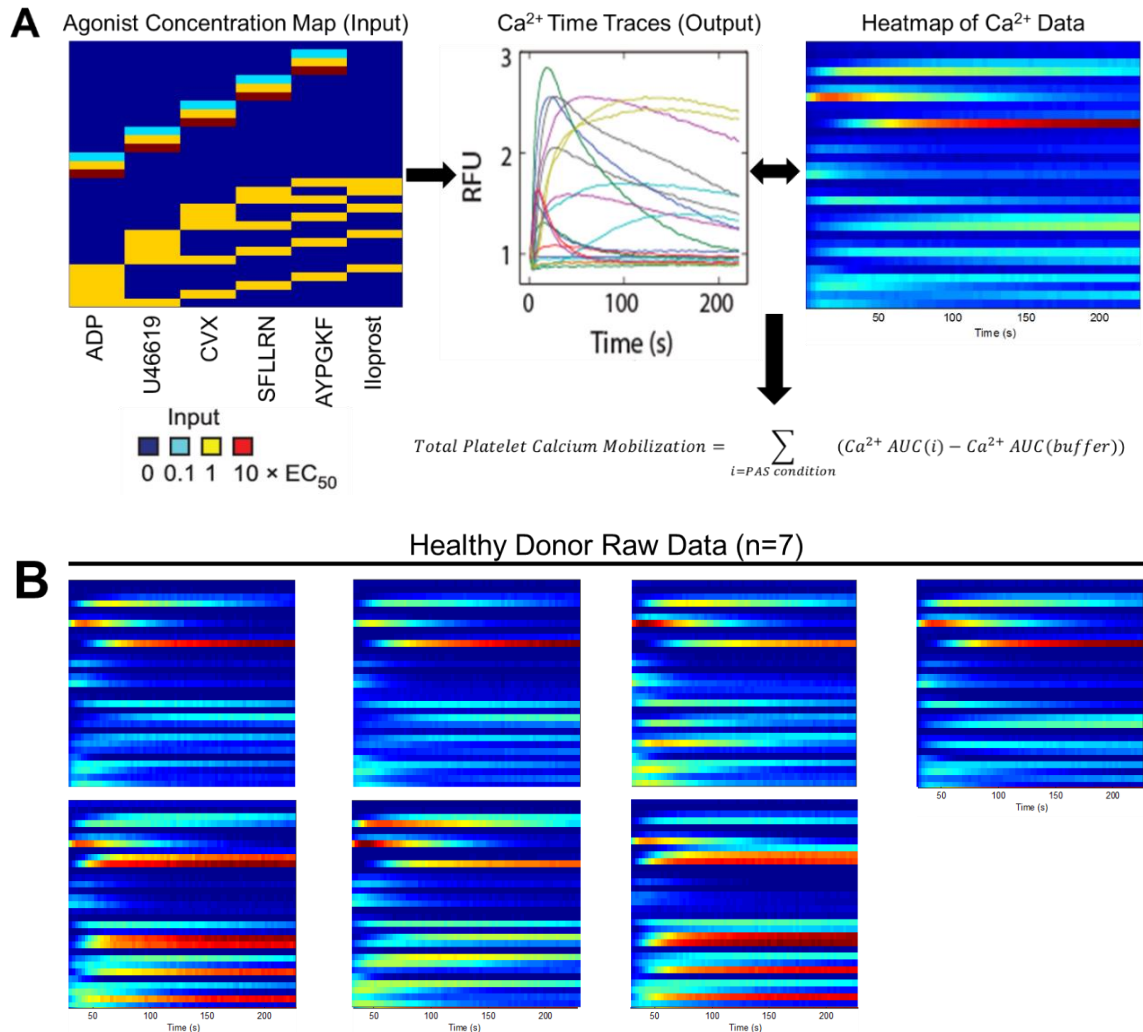
Supplemental Figure 16. (A) Protocol for replication of fibrinolysis in well plate-based calcium mobilization assay. Thrombin is added to fluorescent dye-loaded PRP in the presence and absence of inhibitors, followed by dispenses of tPA and convulxin. (B) Experimental setup for measurement of platelet-mediated consumption of D-dimer. Washed platelets were isolated from healthy whole blood and incubated with sources of D-dimer (trauma patient-derived plasma or pure human D-dimer recombinant protein). Sample supernatants following centrifugation were analyzed for final D-dimer content by ELISA.



Supplemental Figure 17. (A) Addition of tPA to fibrin-containing systems reduces platelet reactivity to CVX stimulation at several low initial thrombin concentrations. (B) D-dimer generation is confirmed at each of the thrombin concentrations tested when tPA is present.



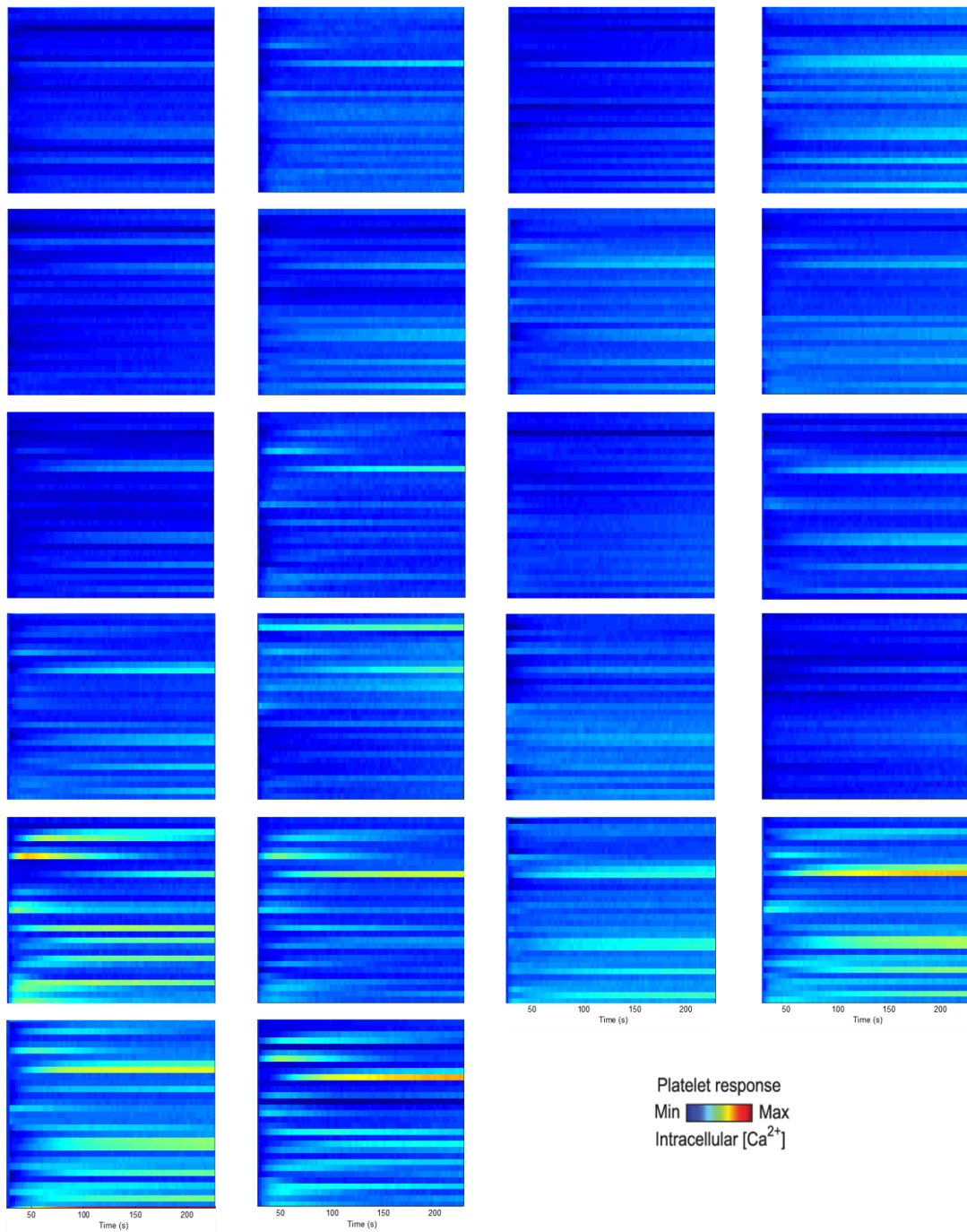
Supplemental Figure 18. Measurements of dense granule activity via ATP release in the presence and absence of D-dimer. When stimulated with 2 µg/mL collagen (A) or 10 µM ADP (B), platelets released less ATP when pre-incubated with D-dimer (50 µg/mL). The traces shown are averages of n=2-3 independent experiments and all data collected are quantified for each condition (C). (*p<0.05, **p<0.01)

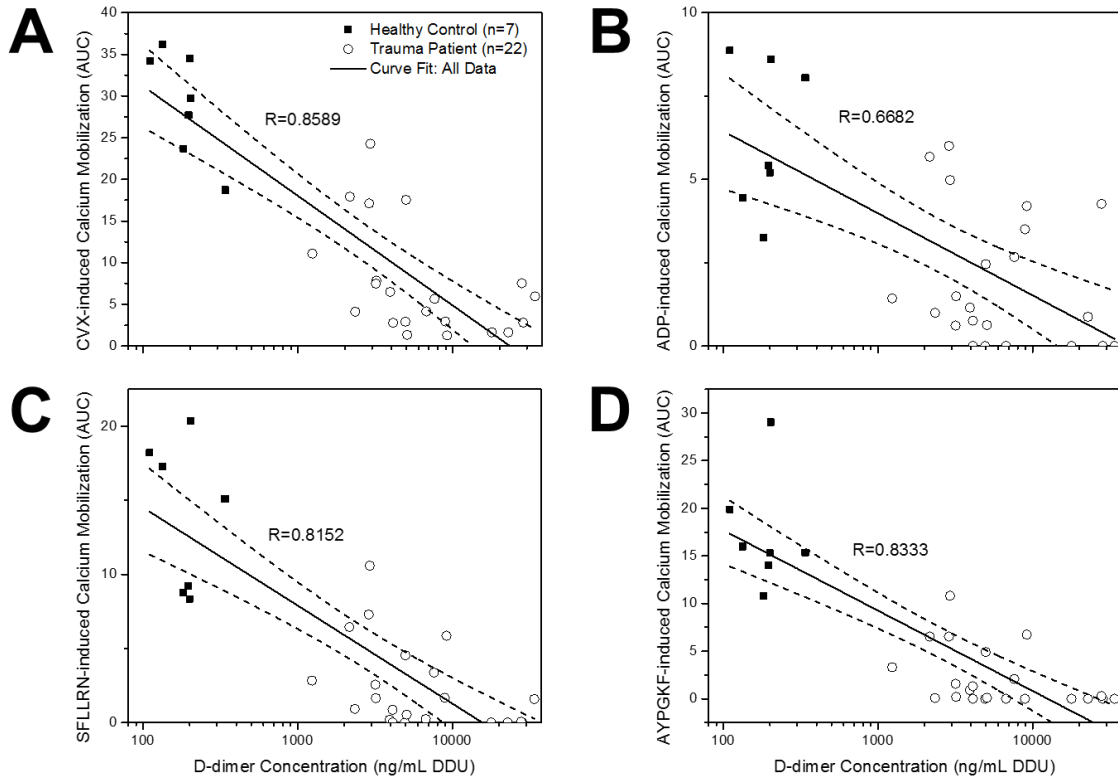


Supplemental Figure 19. Visual representation of data presented in Figure 3 with raw datasets. (A) The calcium experiment begins with the preparation of several (n=31) conditions containing different doses of six common platelet agonists, shown schematically where each condition is represented as a row in the first heatmap (e.g. first condition: buffer control; second condition: low-dose AYPGKF only, etc). After the agonists are dispensed into PRP, each condition generates a calcium time trace, which can also be vectorized and concatenated as a heatmap in the same order as the concentration map. Each of these vectors contributes to the Total Platelet Calcium Mobilization calculation. The datasets obtained from healthy controls (B, above) and trauma patients (C, next page) shows stark differences in platelet response between the two populations as well as intra-group variability.

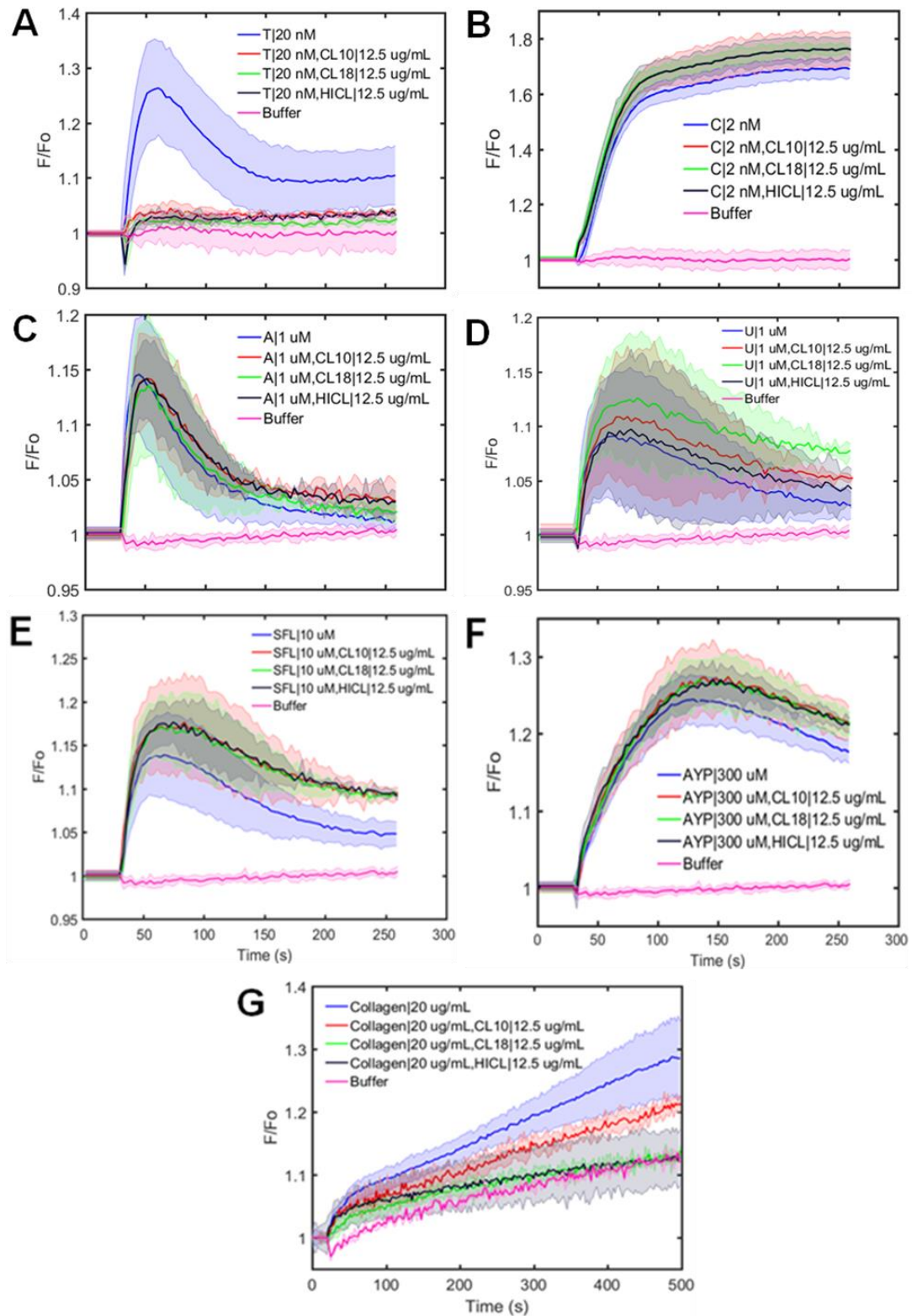
Trauma Patient Raw Data (n=22)

C

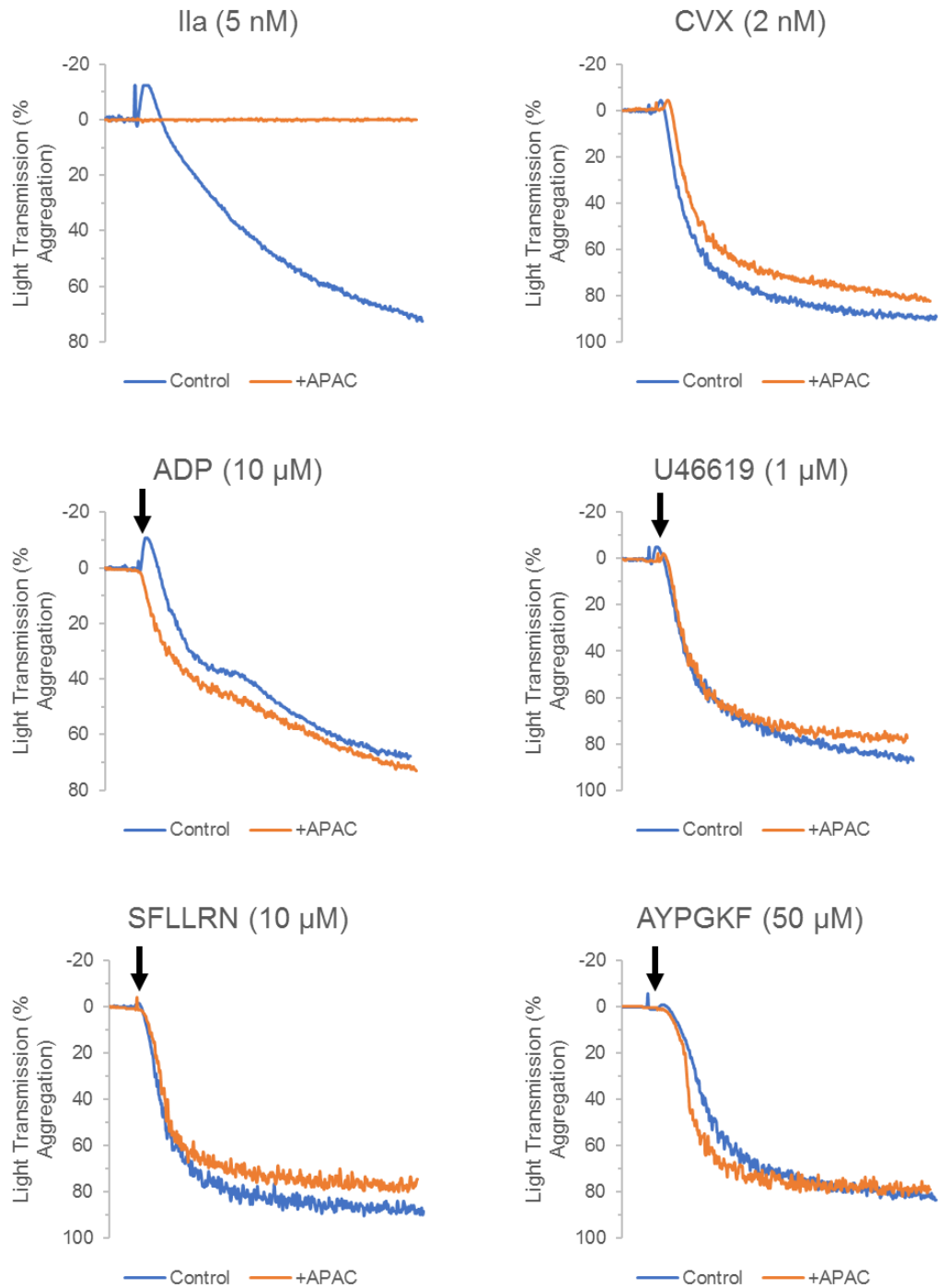




Supplemental Figure 20. Agonist-specific correlations of platelet function and D-dimer concentration. Black solid lines show correlation of all data (healthy/trauma), and dotted line represents 95% confidence interval bounds on the line of best fit. Agonist-receptor pairs include (A) convulxin-GPVI, (B) ADP-P2Y1/P2Y12, (C) SLLRN-PAR1, and (D) AYPGKF-PAR4.



Supplemental Figure 21. Representative calcium traces showing effect of APAC (12.5 µg/mL) on activity of various platelet agonists. (A: T=thrombin, B: C=convulxin, C: A=ADP, D: U=U46619, E: SFL=SFLLRN, F: AYP=AYPGKF, G: type I fibrillar collagen, APAC CL10, APAC CL18, APAC HICL.



Supplemental Figure 22. Platelet aggregation profiles for several platelet agonists in the presence and absence of APAC (200 μg/mL). Taken with Figure 6-2, only thrombin- and collagen-mediated platelet aggregation are inhibited by APAC.

CHAPTER 9: APPENDIX II (DATA ANALYSIS SCRIPTS)

Copies of various MATLAB scripts used for data analysis, figure generation, and machine learning model development are stored in an online Github repository entitled 'Diamond-Lab-MATLAB-Codes'. For more information, please email cverni13@gmail.com.

CHAPTER 10: BIBLIOGRAPHY

- 1 Boon GD. An overview of hemostasis. *Toxicol Pathol* 1993; **21**: 170–9.
- 2 Gale AJ. Current Understanding of Hemostasis. *Toxicol Pathol* 2011; **39**: 273–80.
- 3 Paul BZS, Daniel JL, Kunapuli SP. Platelet shape change is mediated by both calcium-dependent and -independent signaling pathways: Role of p160 Rho-associated coiled-coil-containing protein kinase in platelet shape change. *J Biol Chem* 1999; **274**: 28293–300.
- 4 Golebiewska EM, Poole AW. Platelet secretion: From haemostasis to wound healing and beyond. *Blood Rev* 2015; **29**: 153–62.
- 5 Mackman N. The role of tissue factor and factor VIIa in hemostasis. *Anesth Analg* 2009; **108**: 1447–52.
- 6 Shen L, Lorand L. Contribution of fibrin stabilization to clot strength: Supplementation of factor XIII-deficient plasma with the purified zymogen. *J Clin Invest* 1983; **71**: 1336–41.
- 7 Rosenberg RD, Rosenberg JS. Natural anticoagulant mechanisms. *J Clin Invest* 1984; **74**: 1–6.
- 8 Chapin JC, Hajjar KA. Fibrinolysis and the control of blood coagulation. *Blood Rev* 2015; **29**: 17–24.
- 9 Koupenova M, Kehrel BE, Corkrey HA, Freedman JE. Thrombosis and platelets: an update. *Eur Heart J* 2017; **38**: 785–91.
- 10 Chang R, Cardenas JC, Wade CE, Holcomb JB. Advances in the understanding of trauma-induced coagulopathy. *Blood* 2016; **128**: 1043–9.
- 11 van der Meijden PEJ, Heemskerk JWM. Platelet biology and functions: new concepts and clinical perspectives. *Nat Rev Cardiol* 2019; **16**: 166–79.
- 12 Bye AP, Unsworth AJ, Gibbins JM. Platelet signaling: a complex interplay between inhibitory and activatory networks. *J Thromb Haemost* 2016; **14**: 918–30.
- 13 Estevez B, Du X. New Concepts and Mechanisms of Platelet Activation Signaling. *Physiology* 2017; **32**: 162–77.
- 14 Bergmeier W, Stefanini L. Platelet ITAM signaling. *Curr Opin Hematol* 2013; **20**: 445–50.
- 15 Polgár J, Clemetson JM, Kehrel BE, Wiedemann M, Magnenat EM, Wells TNC, Clemetson KJ. Platelet activation and signal transduction by convulxin, a C-type lectin from *Crotalus durissus terrificus* venom via the p62/GPVI collagen receptor. *J Biol Chem* 1997; **272**: 13576–83.
- 16 Suzuki-Inoue K, Fuller GLJ, Garcia A, Eble JA, Pohlmann S, Inoue O, Gartner TK, Hughan SC, Pearce AC, Laing GD, Theakston RDG, Schweighoffer E, Zitzmann N, Morita T, Tybulewicz VLJ, Ozaki Y, Watson SP. A novel Syk-dependent mechanism of platelet activation by the C-type lectin receptor CLEC-2. *Blood* 2006; **107**: 542–9.

- 17 Faruqi TR, Weiss EJ, Shapiro MJ, Huang W, Coughlin SR. Structure-function analysis of protease-activated receptor 4 tethered ligand peptides: Determinants of specificity and utility in assays of receptor function. *J Biol Chem* 2000; **275**: 19728–34.
- 18 Vu T-KH, Hung DT, Wheaton VI, Coughlin SR. Molecular cloning of a functional thrombin receptor reveals a novel proteolytic mechanism of receptor activation. *Cell* 1991; **64**: 1057–68.
- 19 Daniel TO, Liu H, Morrow JD, Crews BC, Marnett LJ. Thromboxane A2 is a mediator of cyclooxygenase-2-dependent endothelial migration and angiogenesis. *Cancer Res* 1999; **59**: 4574–7.
- 20 Gurbel PA, Kuliopulos A, Tantry US. G-Protein-Coupled receptors signaling pathways in new antiplatelet drug development. *Arterioscler Thromb Vasc Biol* 2015; **35**: 500–12.
- 21 Smolenski A. Novel roles of cAMP/cGMP-dependent signaling in platelets. *J Thromb Haemost* 2012; **10**: 167–76.
- 22 Li Z, Delaney MK, O'Brien KA, Du X. Signaling during platelet adhesion and activation. *Arterioscler Thromb Vasc Biol* 2010; **30**: 2341–9.
- 23 Yun S-H, Sim E-H, Goh R-Y, Park J-I, Han J-Y. Platelet activation: The mechanisms and potential biomarkers. *Biomed Res Int* 2016; **2016**: 9060143.
- 24 Pai M, Wang G, Moffat KA, Liu Y, Seecharan J, Webert K, Heddle N, Hayward C. Diagnostic usefulness of a lumi-aggregometer adenosine triphosphate release assay for the assessment of platelet function disorders. *Am J Clin Pathol* 2011; **136**: 350–8.
- 25 Nagy Jr B, Beke Debreceni I, Kappelmayer J. Flow Cytometric Investigation of Classical and Alternative Platelet Activation Markers. *EJIFCC* 2012; **23**: 124–34.
- 26 Nesbitt WS, Giuliano S, Kulkarni S, Dopheide SM, Harper IS, Jackson SP. Intercellular calcium communication regulates platelet aggregation and thrombus growth. *J Cell Biol* 2003; **160**: 1151–61.
- 27 Varga-Szabo D, Braun A, Nieswandt B. Calcium signaling in platelets. *J Thromb Haemost* 2009; **7**: 1057–66.
- 28 Wohlaer MV, Moore EE, Thomas S, Sauaia A, Evans E, Harr J, Silliman CC, Ploplis V, Castellino FJ, Walsh M. Early platelet dysfunction: An unrecognized role in the acute coagulopathy of trauma. *J Am Coll Surg* 2012; **214**: 739–46.
- 29 Kutcher ME, Redick BJ, McCreery RC, Crane IM, Greenberg MD, Cachola LM, Nelson MF, Cohen MJ. Characterization of platelet dysfunction after trauma. *J Trauma Acute Care Surg* 2012; **73**: 13–9.
- 30 Li R, Elmongy H, Sims C, Diamond SL. Ex vivo recapitulation of trauma-induced coagulopathy and preliminary assessment of trauma patient platelet function under flow using microfluidic technology. *J Trauma Acute Care Surg* 2016; **80**: 440–9.
- 31 Saillant NN, Sims CA. Platelet dysfunction in injured patients. *Mol Cell Ther* 2014; **2**: 37.

- 32 Davis PK, Musunuru H, Walsh M, Cassady R, Yount R, Losiniecki A, Moore EE, Wohlaer MV, Howard J, Ploplis VA, Castellino FJ, Thomas SG. Platelet dysfunction is an early marker for traumatic brain injury-induced coagulopathy. *Neurocrit Care* 2013; **18**: 201–8.
- 33 Ramsey MT, Fabian TC, Shahan CP, Sharpe JP, Mabry SE, Weinberg JA, Croce MA, Jennings LK. A prospective study of platelet function in trauma patients. *J Trauma Acute Care Surg* 2016; **80**: 726–33.
- 34 Bender M, Hofmann S, Stegner D, Chalaris A, Bösl M, Braun A, Scheller J, Rose-John S, Nieswandt B. Differentially regulated GPVI ectodomain shedding by multiple platelet-expressed proteinases. *Blood* 2010; **116**: 3347–55.
- 35 Baaten CCFMJ, Swieringa F, Misztal T, Mastenbroek TG, Feijge MAH, Bock PE, Donners MMPC, Collins PW, Li R, van der Meijden PEJ, Heemskerk JWM. Platelet heterogeneity in activation-induced glycoprotein shedding: functional effects. *Blood Adv* 2018; **2**: 2320–31.
- 36 Dunbar NM, Chandler WL. Thrombin generation in trauma patients. *Transfusion* 2009; **49**: 2652–60.
- 37 Chapman MP, Moore EE, Moore HB, Gonzalez E, Gamboni F, Chandler JG, Mitra S, Ghasabyan A, Chin TL, Sauaia A, Banerjee A, Silliman CC. Overwhelming tPA release, not PAI-1 degradation, is responsible for hyperfibrinolysis in severely injured trauma patients. *J Trauma Acute Care Surg* 2016; **80**: 16–25.
- 38 Yanagida Y, Gando S, Sawamura A, Hayakawa M, Uegaki S, Kubota N, Homma T, Ono Y, Honma Y, Wada T, Jesmin S. Normal prothrombinase activity, increased systemic thrombin activity, and lower antithrombin levels in patients with disseminated intravascular coagulation at an early phase of trauma: Comparison with acute coagulopathy of trauma-shock. *Surgery* 2013; **154**: 48–57.
- 39 Bredbacka S, Edner G. Soluble fibrin and D-dimer as detectors of hypercoagulability in patients with isolated brain trauma. *J Neurosurg Anesthesiol* 1994; **6**: 75–82.
- 40 Wada H, Sase T, Matsumoto T, Kushiya F, Sakakura M, Mori Y, Nishikawa M, Ohnishi K, Nakatani K, Gabazza EC, Shiku H, Nobori T. Increased soluble fibrin in plasma of patients with disseminated intravascular coagulation. *Clin Appl Thromb* 2003; **9**: 233–40.
- 41 Johna S, O'Callaghan T, Cemaj S, Catalano R. Effect of tissue injury on D-Dimer levels: A prospective study in trauma patients. *Med Sci Monit* 2002; **8**: CR5–8.
- 42 Gans H, Lowman JT. The uptake of fibrin and fibrin-degradation products by the isolated perfused rat liver. *Blood* 1967; **29**: 526–39.
- 43 Pizzo S V., Pasqua JJ. The clearance of human fibrinogen fragments D1, D2, D3 and fibrin fragment D1 dimer in mice. *Biochim Biophys Acta* 1982; **718**: 177–84.
- 44 Brommer EJP, Engbers J, v.d. Laarse A, Nieuwenhuizen W. Survival of fibrinogen degradation products in the circulation after thrombolytic therapy for acute myocardial infarction. *Fibrinolysis* 1987; **1**: 149–53.
- 45 Sharma S, Sharma P, Tyler LN. Transfusion of blood and blood products: Indications and complications. *Am Fam Physician* 2011; **83**: 719–24.

- 46 Thorn S, Güting H, Mathes T, Schäfer N, Maegele M. The effect of platelet transfusion in patients with traumatic brain injury and concomitant antiplatelet use: a systematic review and meta-analysis. *Transfusion* 2019; **59**: 3536–44.
- 47 Vulliamy P, Gillespie S, Gall LS, Green L, Brohi K, Davenport RA. Platelet transfusions reduce fibrinolysis but do not restore platelet function during trauma hemorrhage. *J Trauma Acute Care Surg* 2017; **83**: 388–97.
- 48 Paredes RM, Etzler JC, Watts LT, Lechleiter JD. Chemical Calcium Indicators. *Methods* 2008; **46**: 143–51.
- 49 Liu ECK, Abell LM. Development and validation of a platelet calcium flux assay using a fluorescent imaging plate reader. *Anal Biochem* 2006; **357**: 216–24.
- 50 Chatterjee MS, Purvis JE, Brass LF, Diamond SL. Pairwise agonist scanning predicts cellular signaling responses to combinatorial stimuli. *Nat Biotechnol* 2010; **28**: 727–32.
- 51 Adan A, Alizada G, Kiraz Y, Baran Y, Nalbant A. Flow cytometry: basic principles and applications. *Crit Rev Biotechnol* 2017; **37**: 163–76.
- 52 Brown M, Wittwer C. Flow cytometry: Principles and clinical applications in hematology. *Clin Chem* 2000; **46**: 1221–9.
- 53 Shattil SJ, Hoxie JA, Cunningham M, Brass LF. Changes in the platelet membrane glycoprotein IIb/IIIa complex during platelet activation. *J Biol Chem* 1985; **260**: 11107–14.
- 54 Jaeger DTL, Diamond SL. Pairwise agonist scanning-flow cytometry (PAS-FC) measures inside-out signaling and patient-specific response to combinatorial platelet agonists. *Biotechniques* 2013; **54**: 271–7.
- 55 Born GVR. Aggregation of blood platelets by adenosine diphosphate and its reversal. *Nature* 1962; **194**: 927–9.
- 56 Hvas A-M, Favalaro EJ. Platelet Function Analyzed by Light Transmission Aggregometry. In: Favalaro EJ, Lippi G, editors. *Hemostasis and Thrombosis: Methods and Protocols*. New York (NY): Springer New York; 2017. p. 321–31.
- 57 Koltai K, Kesmarky G, Feher G, Tibold A, Toth K. Platelet aggregometry testing: Molecular mechanisms, techniques and clinical implications. *Int J Mol Sci* 2017; **18**: 1803.
- 58 Reikvam H, Steien E, Hauge B, Liseth K, Hagen KG, Størkson R, Hervig T. Thrombelastography. *Transfus Apher Sci* 2009; **40**: 119–23.
- 59 Gill M. The TEG®6s on shaky ground? A novel assessment of the TEG®6s performance under a challenging condition. *J Extra Corpor Technol* 2017; **49**: 26–9.
- 60 Gonzalez E, Moore EE, Moore HB. Management of Trauma Induced Coagulopathy with Thromboelastography. *Crit Care Clin* 2017; **33**: 119–34.
- 61 Hess JR, Brohi K, Dutton RP, Hauser CJ, Holcomb JB, Kluger Y, Mackway-Jones K, Parr MJ, Rizoli SB, Yukioka T, Hoyt DB, Bouillon B. The coagulopathy of trauma: a review of mechanisms. *J Trauma* 2008; **65**: 748–54.

- 62 Ostrowski SR, Johansson PI. Endothelial glycocalyx degradation induces endogenous heparinization in patients with severe injury and early traumatic coagulopathy. *J Trauma Acute Care Surg* 2012; **73**: 60–6.
- 63 Lenz A, Franklin GA, Cheadle WG. Systemic inflammation after trauma. *Injury* 2007; **38**: 1336–45.
- 64 Brohi K, Singh J, Heron M, Coats T. Acute Traumatic Coagulopathy. *J Trauma* 2003; **54**: 1127–30.
- 65 Boldt J, Papsdorf M, Rothe A, Kumle B, Piper S. Changes of the hemostatic network in critically ill patients-Is there a difference between sepsis, trauma, and neurosurgery patients? *Crit Care Med* 2000; **28**: 445–50.
- 66 Conti A, Sanchez-Ruiz Y, Bachi A, Beretta L, Grandi E, Beltramo M, Alessio M. Proteome study of human cerebrospinal fluid following traumatic brain injury indicates fibrin(ogen) degradation products as trauma-associated markers. *J Neurotrauma* 2004; **21**: 854–63.
- 67 Iversen LH, Thorlacius-Ussing O, Okholm M. Soluble fibrin in plasma before and after surgery for benign and malignant colorectal disease. *Thromb Res* 1995; **79**: 471–81.
- 68 Gando S, Nanzaki S, Sasaki S, Kemmotsu O. Significant correlations between tissue factor and thrombin markers in trauma and septic patients with disseminated intravascular coagulation. *Thromb Haemost* 1998; **79**: 1111–5.
- 69 Sakai H, Nishihara H, Kakemizu M, Imai M, Igarashi K, Okazaki A. Discrepancy between soluble fibrin and D-dimer levels among sampling sites in elderly patients with femoral neck fracture. *J Anesth* 2009; **23**: 308–9.
- 70 Toh JMH, Ken-Dror G, Downey C, Abrams ST. The clinical utility of fibrin-related biomarkers in sepsis. *Blood Coagul Fibrinolysis* 2013; **24**: 839–43.
- 71 Giannitsis E, Siemens HJ, Mitusch R, Tettenborn I, Wiegand U, Schmücker G, Sheikhzadeh A, Stierle U. Prothrombin fragments F1+2, thrombin-antithrombin III complexes, fibrin monomers and fibrinogen in patients with coronary atherosclerosis. *Int J Cardiol* 1999; **68**: 269–74.
- 72 Westerlund E, Woodhams BJ, Eintrei J, Söderblom L, Antovic JP. The evaluation of two automated soluble fibrin assays for use in the routine hospital laboratory. *Int J Lab Hematol* 2013; **35**: 666–71.
- 73 Hosaka A, Miyata T, Aramoto H, Shigematsu H, Nakazawa T, Okamoto H, Shigematsu K, Nagawa H. Clinical implication of plasma level of soluble fibrin monomer-fibrinogen complex in patients with abdominal aortic aneurysm. *J Vasc Surg* 2005; **42**: 200–5.
- 74 Hayakawa M, Gando S, Ono Y, Wada T, Yanagida Y, Sawamura A, Ieko M. Noble-Collip Drum Trauma Induces Disseminated Intravascular Coagulation But Not Acute Coagulopathy of Trauma-Shock. *Shock* 2015; **43**: 261–7.
- 75 Alshehri OM, Hughes CE, Montague S, Watson SK, Frampton J, Bender M, Watson SP. Fibrin activates GPVI in human and mouse platelets. *Blood* 2015; **126**: 1601–8.

- 76 Dütting S, Bender M, Nieswandt B. Platelet GPVI: a target for antithrombotic therapy?! *Trends Pharmacol Sci* 2012; **33**: 583–90.
- 77 Bültmann A, Li Z, Wagner S, Peluso M, Schönberger T, Weis C, Konrad I, Stellos K, Massberg S, Nieswandt B, Gawaz M, Ungerer M, Münch G. Impact of glycoprotein VI and platelet adhesion on atherosclerosis-A possible role of fibronectin. *J Mol Cell Cardiol* 2010; **49**: 532–42.
- 78 Schönberger T, Ziegler M, Borst O, Konrad I, Nieswandt B, Massberg S, Ochmann C, Jürgens T, Seizer P, Langer H, Münch G, Ungerer M, Preissner KT, Elvers M, Gawaz M. The dimeric platelet collagen receptor GPVI-Fc reduces platelet adhesion to activated endothelium and preserves myocardial function after transient ischemia in mice. *Am J Physiol Cell Physiol* 2012; **303**: C757–66.
- 79 Inoue O, Suzuki-Inoue K, McCarty OJT, Moroi M, Ruggeri ZM, Kunicki TJ, Ozaki Y, Watson SP. Laminin stimulates spreading of platelets through integrin alpha6beta1-dependent activation of GPVI. *Blood* 2006; **107**: 1405–12.
- 80 Mammadova-Bach E, Ollivier V, Loyau S, Schaff M, Dumont B, Favier R, Freyburger G, Latger-Cannard V, Nieswandt B, Gachet C, Mangin PH, Jandrot-Perrus M. Platelet glycoprotein VI binds to polymerized fibrin and promotes thrombin generation. *Blood* 2015; **126**: 683–91.
- 81 Nieswandt B, Pleines I, Bender M. Platelet adhesion and activation mechanisms in arterial thrombosis and ischaemic stroke. *J Thromb Haemost* 2011; **9**: 92–104.
- 82 Scherer RU, Spangenberg P. Procoagulant activity in patients with isolated severe head trauma. *Crit Care Med* 1998; **26**: 149–56.
- 83 Wada H, Sakuragawa N, Shiku H. Hemostatic Molecular Markers Before Onset of Disseminated Intravascular Coagulation in Leukemic Patients. *Semin Thromb Hemost* 1998; **24**: 293–7.
- 84 Lee MY, Diamond SL. A Human Platelet Calcium Calculator Trained by Pairwise Agonist Scanning. *PLoS Comput Biol* 2015; **11**: e1004118.
- 85 Maloney SF, Brass LF, Diamond SL. P2Y12 or P2Y1 inhibitors reduce platelet deposition in a microfluidic model of thrombosis while apyrase lacks efficacy under flow conditions. *Integr Biol* 2010; **2**: 183–92.
- 86 Arthur JF, Shen Y, Kahn ML, Berndt MC, Andrews RK, Gardiner EE. Ligand binding rapidly induces disulfide-dependent dimerization of glycoprotein VI on the platelet plasma membrane. *J Biol Chem* 2007; **282**: 30434–41.
- 87 Jung SM, Moroi M, Soejima K, Nakagaki T, Miura Y, Berndt MC, Gardiner EE, Howes J-M, Pugh N, Bihan D, Watson SP, Farndale RW. Constitutive dimerization of glycoprotein VI (GPVI) in resting platelets is essential for binding to collagen and activation in flowing blood. *J Biol Chem* 2012; **287**: 30000–13.
- 88 Stalker TJ, Traxler EA, Wu J, Wannemacher KM, Cermignano SL, Voronov R, Diamond SL, Brass LF. Hierarchical organization in the hemostatic response and its relationship to the platelet-signaling network. *Blood* 2013; **121**: 1875–85.
- 89 Arai M, Yamamoto N, Moroi M, Akamatsu N, Fukutake K, Tanoue K. Platelets with 10% of the normal amount of glycoprotein VI have an impaired response to collagen that results in a mild bleeding tendency. *Br J Haematol* 1995; **89**: 124–

- 30.
- 90 Bynagari-Settipalli YS, Cornelissen I, Palmer D, Duong D, Concengco C, Ware J, Coughlin SR. Redundancy and Interaction of Thrombin- and Collagen-Mediated Platelet Activation in Tail Bleeding and Carotid Thrombosis in Mice. *Arterioscler Thromb Vasc Biol* 2014; **34**: 2563–9.
- 91 Onselaer M-B, Hardy AT, Wilson C, Sanchez X, Babar AK, Miller JLC, Watson CN, Watson SK, Bonna A, Philippou H, Herr AB, Mezzano D, Ariëns RAS, Watson SP. Fibrin and D-dimer bind to monomeric GPVI. *Blood Adv* 2017; **1**: 1495–504.
- 92 Qiu Y, Brown AC, Myers DR, Sakurai Y, Mannino RG, Tran R, Ahn B, Hardy ET, Kee MF, Kumar S, Bao G, Barker TH, Lam WA. Platelet mechanosensing of substrate stiffness during clot formation mediates adhesion, spreading, and activation. *Proc Natl Acad Sci* 2014; **111**: 14430–5.
- 93 Al-Tamimi M, Grigoriadis G, Tran H, Paul E, Servadei P, Berndt MC, Gardiner EE, Andrews RK. Coagulation-induced shedding of platelet glycoprotein VI mediated by factor Xa. *Blood* 2011; **117**: 3912–20.
- 94 Gardiner EE, Karunakaran D, Shen Y, Arthur JF, Andrews RK, Berndt MC. Controlled shedding of platelet glycoprotein (GP)VI and GPIb-IX-V by ADAM family metalloproteinases. *J Thromb Haemost* 2007; **5**: 1530–7.
- 95 Bergmeier W, Rabie T, Strehl A, Piffath CL, Prostredna M, Wagner DD, Nieswandt B. GPVI down-regulation in murine platelets through metalloproteinase-dependent shedding. *Thromb Haemost* 2004; **91**: 951–8.
- 96 Stephens G, Yan Y, Jandrot-Perrus M, Villeval J-L, Clemetson KJ, Phillips DR. Platelet activation induces metalloproteinase-dependent GP VI cleavage to down-regulate platelet reactivity to collagen. *Blood* 2005; **105**: 186–91.
- 97 Facey A, Pinar I, Arthur JF, Qiao J, Jing J, Mado B, Carberry J, Andrews RK, Gardiner EE. A-Disintegrin-And-Metalloproteinase (ADAM) 10 Activity on Resting and Activated Platelets. *Biochemistry* 2016; **55**: 1187–94.
- 98 Wu X, Darlington DN, Cap AP. Procoagulant and fibrinolytic activity after polytrauma in rat. *Am J Physiol Regul Integr Comp Physiol* 2016; **310**: R323–9.
- 99 Lee MY, Verni CC, Herbig BA, Diamond SL. Soluble fibrin causes an acquired platelet glycoprotein VI signaling defect: implications for coagulopathy. *J Thromb Haemost* 2017; **15**: 2396–407.
- 100 Flamm MH, Colace T V., Chatterjee MS, Jing H, Zhou S, Jaeger D, Brass LF, Sinno T, Diamond SL. Multiscale prediction of patient-specific platelet function under flow. *Blood* 2012; **120**: 190–8.
- 101 Wilson PA, McNicol G, Douglas A. Effect of fibrinogen degradation products on platelet aggregation. *J Clin Pathol* 1968; **21**: 147–53.
- 102 Baker SP, O'Neill B, Haddon W, Long WB. The Injury Severity Score: A Method for Describing Patients with Multiple Injuries and Evaluating Emergency Care. *J Trauma* 1974; **14**: 187–96.
- 103 Palmer C. Major trauma and the injury severity score--where should we set the

bar? *Annu Proc Assoc Adv Automot Med* 2007; **51**: 13–29.

- 104 Cattaneo M, Lecchi A, Zighetti ML, Lussana F. Platelet aggregation studies: autologous platelet-poor plasma inhibits platelet aggregation when added to platelet-rich plasma to normalize platelet count. *Haematologica* 2007; **92**: 694–7.
- 105 Mitchell TA, Herzig MC, Fedyk CG, Salhanick MA, Henderson AT, Parida BK, Prat NJ, Dent DL, Schwacha MG, Cap AP. Traumatic Hemothorax Blood Contains Elevated Levels of Microparticles that are Prothrombotic but Inhibit Platelet Aggregation. *Shock* 2017; **47**: 680–7.
- 106 Bai X, Wang H, Li Z, Liu K. Correlation between blood cAMP, cGMP levels and traumatic severity in the patients with acute trauma and its clinical significance. *J Huazhong Univ Sci Technol Med Sci* 2004; **24**: 68–70.
- 107 Holcomb JB, Tilley BC, Baraniuk S, Fox EE, Wade CE, Podbielski JM, del Junco DJ, Brasel KJ, Bulger EM, Callcut RA, Cohen MJ, Cotton BA, Fabian TC, Inaba K, Kerby JD, Muskat P, O’Keeffe T, Rizoli S, Robinson BR, Scalea TM, et al. Transfusion of plasma, platelets, and red blood cells in a 1:1:1 vs a 1:1:2 ratio and mortality of patients with severe trauma. *JAMA* 2015; **313**: 471–82.
- 108 Miller TE. New evidence in trauma resuscitation - is 1:1:1 the answer? *Perioper Med* 2013; **2**: 13.
- 109 Chen J, Wu X, Keese J, Liu B, Darlington DN, Cap AP. Limited resuscitation with fresh or stored whole blood corrects cardiovascular and metabolic function in a rat model of polytrauma and hemorrhage. *Shock* 2017; **47**: 208–16.
- 110 Verni CC, Davila A, Balian S, Sims CA, Diamond SL. Platelet dysfunction during trauma involves diverse signaling pathways and an inhibitory activity in patient-derived plasma. *J Trauma Acute Care Surg* 2019; **86**: 250–9.
- 111 Pareti FI, Capitanio A, Mannucci L, Ponticelli C, Mannucci PM. Acquired dysfunction due to the circulation of “exhausted” platelets. *Am J Med* 1980; **69**: 235–40.
- 112 St. John AE, Newton JC, Martin EJ, Mohammed BM, Contaifer D, Saunders JL, Brophy GM, Spiess BD, Ward KR, Brophy DF, López JA, White NJ. Platelets retain inducible alpha granule secretion by P-selectin expression but exhibit mechanical dysfunction during trauma-induced coagulopathy. *J Thromb Haemost* 2019; **17**: 771–81.
- 113 Walsh PN. Platelet Coagulation-Protein Interactions. *Semin Thromb Hemost* 2004; **30**: 461–71.
- 114 Chen J, Verni CC, Jouppila A, Lassila R, Diamond SL. Dual antiplatelet and anticoagulant (APAC) heparin proteoglycan mimetic with shear-dependent effects on platelet-collagen binding and thrombin generation. *Thromb Res* 2018; **169**: 143–51.
- 115 Zhang L, Liu H, Li Y, Ma H, Liu Y, Wang M. Correlation analysis between plasma D-dimer levels and orthopedic trauma severity. *Chin Med J (Engl)* 2012; **125**: 3133–6.
- 116 Wagner CL, Mascelli MA, Neblock DS, Weisman HF, Collier BS, Jordan RE.

- Analysis of GPIIb/IIIa receptor number by quantification of 7E3 binding to human platelets. *Blood* 1996; **88**: 907–14.
- 117 Best D, Senis YA, Jarvis GE, Eagleton HJ, Roberts DJ, Saito T, Jung SM, Moroi M, Harrison P, Green FR, Watson SP. GPVI levels in platelets: relationship to platelet function at high shear. *Blood* 2003; **102**: 2811–8.
- 118 Induruwa I, Moroi M, Bonna A, Malcor J-D, Howes J-M, Warburton EA, Farndale RW, Jung SM. Platelet collagen receptor Glycoprotein VI-dimer recognizes fibrinogen and fibrin through their D-domains, contributing to platelet adhesion and activation during thrombus formation. *J Thromb Haemost* 2018; **16**: 1–16.
- 119 Slater A, Perrella G, Onselaer M-B, Martin EM, Gauer JS, Xu R-G, Heemskerk JW, Ariëns RAS, Watson SP. Does fibrin(ogen) bind to monomeric or dimeric GPVI, or not at all? *Platelets* 2019; **30**: 281–9.
- 120 Refaai MA, Riley P, Mardovina T, Bell PD. The Clinical Significance of Fibrin Monomers. *Thromb Haemost* 2018; **118**: 1856–66.
- 121 Soomro AY, Guerchicoff A, Nichols DJ, Suleman J, Dangas GD. The current role and future prospects of D-dimer biomarker. *Eur Hear J - Cardiovasc Pharmacother* 2016; **2**: 175–84.
- 122 Bounameaux H, Cirafici P, de Moerloose P, Schneider PA, Slosman D, Reber G, Unger PF. Measurement of D-dimer in plasma as diagnostic aid in suspected pulmonary embolism. *Lancet* 1991; **337**: 196–200.
- 123 Podestà MA, Galbusera M, Remuzzi G. Bleeding and Hemostasis in Acute Renal Failure. *Critical Care Nephrology: Third Edition*. Third Edit. 2019. p. 630–5.
- 124 Orloff KG, Michaeli D. Inhibition of fibrin-platelet interactions by fibrinogen-degradation fragment D. *Am J Physiol* 1977; **233**: H305–11.
- 125 Kornblith LZ, Moore HB, Cohen MJ. Trauma-induced coagulopathy: The past, present, and future. *J Thromb Haemost* 2019; **17**: 852–62.
- 126 Sikka P, Bindra VK. Newer antithrombotic drugs. *Indian J Crit Care Med* 2010; **14**: 188–95.
- 127 Watson RDS, Chin BSP, Lip GYH. Antithrombotic therapy in acute coronary syndromes. *BMJ* 2002; **325**: 1348–51.
- 128 Warner TD, Nylander S, Whatling C. Anti-platelet therapy: cyclo-oxygenase inhibition and the use of aspirin with particular regard to dual anti-platelet therapy. *Br J Clin Pharmacol* 2011; **72**: 619–33.
- 129 Stangl PA, Lewis S. Review of currently available GP IIb/IIIa inhibitors and their role in peripheral vascular interventions. *Semin Intervent Radiol* 2010; **27**: 412–21.
- 130 Lijnen HR, Collen D. Fibrinolytic agents: mechanisms of activity and pharmacology. *Thromb Haemost* 1995; **74**: 387–90.
- 131 Holmes DR, Kereiakes DJ, Kleiman NS, Moliterno DJ, Patti G, Grines CL. Combining Antiplatelet and Anticoagulant Therapies. *J Am Coll Cardiol* 2009; **54**: 95–109.

- 132 Lamberts M, Olesen JB, Ruwald MH, Hansen CM, Karasoy D, Kristensen SL, Køber L, Torp-Pedersen C, Gislason GH, Hansen ML. Bleeding after initiation of multiple antithrombotic drugs, including triple therapy, in atrial fibrillation patients following myocardial infarction and coronary intervention: A nationwide cohort study. *Circulation* 2012; **126**: 1185–93.
- 133 Hirsh J, Anand SS, Halperin JL, Fuster V. Mechanism of Action and Pharmacology of Unfractionated Heparin. *Arterioscler Thromb Vasc Biol* 2001; **21**: 1094–6.
- 134 Machovich R. Mechanism of action of heparin through thrombin on blood coagulation. *Biochim Biophys Acta* 1975; **412**: 13–7.
- 135 Lassila R, Lindstedt K, Kovanen PT. Native macromolecular heparin proteoglycans exocytosed from stimulated rat serosal mast cells strongly inhibit platelet-collagen interactions. *Arterioscler Thromb Vasc Biol* 1997; **17**: 3578–87.
- 136 Lassila R, Jouppila A. Mast cell-derived heparin proteoglycans as a model for a local antithrombotic. *Semin Thromb Hemost* 2014; **40**: 837–44.
- 137 Tchougounova E, Pejler G. Regulation of extravascular coagulation and fibrinolysis by heparin-dependent mast cell chymase. *FASEB J* 2001; **15**: 2763–5.
- 138 San Antonio JD, Lander AD, Karnovsky MJ, Slayter HS. Mapping the heparin-binding sites on type I collagen monomers and fibrils. *J Cell Biol* 1994; **125**: 1179–88.
- 139 Kauhanen P, Kovanen PT, Lassila R. Coimmobilized native macromolecular heparin proteoglycans strongly inhibit platelet-collagen interactions in flowing blood. *Arterioscler Thromb Vasc Biol* 2000; **20**: e113–9.
- 140 Tuuminen R, Jouppila A, Salvail D, Laurent C-E, Benoit M-C, Syrjäälä S, Helin H, Lemström K, Lassila R. Dual antiplatelet and anticoagulant APAC prevents experimental ischemia–reperfusion-induced acute kidney injury. *Clin Exp Nephrol* 2017; **21**: 436–45.
- 141 Hwang DH, LeBlanc P. Heparin inhibits the formation of endoperoxide metabolites in rat platelets: aspirin-like activity. *Prostaglandins Med* 1981; **6**: 341–4.
- 142 Sweeney SM, Guy CA, Fields GB, San Antonio JD. Defining the domains of type I collagen involved in heparin- binding and endothelial tube formation. *Proc Natl Acad Sci U S A* 1998; **95**: 7275–80.
- 143 Ricard-Blum S, Beraud M, Raynal N, Farndale RW, Ruggiero F. Structural requirements for heparin/heparan sulfate binding to type V collagen. *J Biol Chem* 2006; **281**: 25195–204.
- 144 Coxon CH, Geer MJ, Senis YA. ITIM receptors: more than just inhibitors of platelet activation. *Blood* 2017; **129**: 3407–18.
- 145 Barreiro KA, Tulamo R, Jouppila A, Albäck A, Lassila R. Novel Locally Acting Dual Antiplatelet and Anticoagulant (APAC) Targets Multiple Sites of Vascular Injury in an Experimental Porcine Model. *Eur J Vasc Endovasc Surg* 2019; **58**: 903–11.
- 146 Rudinga GR, Khan GJ, Kong Y. Protease-activated receptor 4 (PAR4): A promising target for antiplatelet therapy. *Int J Mol Sci* 2018; **19**: 573.

- 147 French SL, Hamilton JR. Drugs targeting protease-activated receptor-4 improve the anti-thrombotic therapeutic window. *Ann Transl Med* 2017; **5**: 464.
- 148 Tricoci P, Huang Z, Held C, Moliterno DJ, Armstrong PW, Van de Werf F, White HD, Aylward PE, Wallentin L, Chen E, Lokhnygina Y, Pei J, Leonardi S, Rorick TL, Kilian AM, Jennings LHK, Ambrosio G, Bode C, Cequier A, Cornel JH, et al. Thrombin-receptor antagonist vorapaxar in acute coronary syndromes. *N Engl J Med* 2012; **366**: 20–33.
- 149 Duvernay MT, Temple KJ, Maeng JG, Blobaum AL, Stauffer SR, Lindsley CW, Hamm HE. Contributions of protease-activated receptors PAR1 and PAR4 to Thrombin-Induced GPIIb/IIIa activation in human platelets. *Mol Pharmacol* 2017; **91**: 39–47.
- 150 Wong PC, Seiffert D, Bird JE, Watson CA, Bostwick JS, Giancarli M, Allegretto N, Hua J, Harden D, Guay J, Callejo M, Miller MM, Lawrence RM, Banville J, Guy J, Maxwell BD, Priestley ES, Marinier A, Wexler RR, Bouvier M, et al. Blockade of protease-activated receptor-4 (PAR4) provides robust antithrombotic activity with low bleeding. *Sci Transl Med* 2017; **9**: eaaf5294.
- 151 Pachel C, Mathes D, Arias-Loza AP, Heitzmann W, Nordbeck P, Deppermann C, Lorenz V, Hofmann U, Nieswandt B, Frantz S. Inhibition of Platelet GPVI Protects Against Myocardial Ischemia-Reperfusion Injury. *Arterioscler Thromb Vasc Biol* 2016; **36**: 629–35.
- 152 Volz J, Mammadova-Bach E, Gil-Pulido J, Nandigama R, Remer K, Sorokin L, Zerneck A, Abrams SI, Ergün S, Henke E, Nieswandt B. Inhibition of platelet GPVI induces intratumor hemorrhage and increases efficacy of chemotherapy in mice. *Blood* 2019; **133**: 2696–706.
- 153 Onselaer M-B, Nagy M, Pallini C, Pike JA, Perrella G, Quintanilla LG, Eble JA, Poulter NS, Heemskerk JWM, Watson SP. Comparison of the GPVI inhibitors losartan and honokiol. *Platelets* 2020; **31**: 187–97.
- 154 Denzinger V, Busygina K, Jamasbi J, Pekrul I, Spannagl M, Weber C, Lorenz R, Siess W. Optimizing Platelet GPVI Inhibition versus Haemostatic Impairment by the Btk Inhibitors Ibrutinib, Acalabrutinib, ONO/GS-4059, BGB-3111 and Evobrutinib. *Thromb Haemost* 2019; **119**: 397–406.
- 155 Mokhtari V, Afsharian P, Shahhoseini M, Kalantar SM, Moini A. A Review on Various Uses of N-Acetyl Cysteine. *Cell J* 2017; **19**: 11–7.
- 156 Gibson KR, Winterburn TJ, Barrett F, Sharma S, MacRury SM, Megson IL. Therapeutic potential of N-acetylcysteine as an antiplatelet agent in patients with type-2 diabetes. *Cardiovasc Diabetol* 2011; **10**: 43.
- 157 Wang B, Aw TY, Stokes KY. N-acetylcysteine attenuates systemic platelet activation and cerebral vessel thrombosis in diabetes. *Redox Biol* 2018; **14**: 218–28.
- 158 Stamler J, Mendelsohn ME, Amarante P, Smick D, Andon N, Davies PF, Cooke JP, Loscalzo J. N-acetylcysteine potentiates platelet inhibition by endothelium-derived relaxing factor. *Circ Res* 1989; **65**: 789–95.
- 159 Martinez De Lizarrondo S, Gakuba C, Herbig BA, Repessé Y, Ali C, Denis CV,

- Lenting PJ, Touzé E, Diamond SL, Vivien D, Gauberti M. Potent thrombolytic effect of N-acetylcysteine on arterial thrombi. *Circulation* 2017; **136**: 646–60.
- 160 Purvis JE, Chatterjee MS, Brass LF, Diamond SL. A molecular signaling model of platelet phosphoinositide and calcium regulation during homeostasis and P2Y1 activation. *Blood* 2008; **112**: 4069–79.
- 161 Dolan AT, Diamond SL. Systems modeling of Ca²⁺ homeostasis and mobilization in platelets mediated by IP₃ and store-operated Ca²⁺ entry. *Biophys J* 2014; **106**: 2049–60.
- 162 Lenoci L, Duvernay M, Satchell S, DiBenedetto E, Hamm HE. Mathematical model of PAR1-mediated activation of human platelets. *Mol Biosyst* 2011; **7**: 1129–37.
- 163 Lu Y, Lee MY, Zhu S, Sinno T, Diamond SL. Multiscale simulation of thrombus growth and vessel occlusion triggered by collagen/tissue factor using a data-driven model of combinatorial platelet signalling. *Math Med Biol* 2017; **34**: 523–46.
- 164 Muthard RW, Welsh JD, Brass LF, Diamond SL. Fibrin, γ' -Fibrinogen, and Transclot Pressure Gradient Control Hemostatic Clot Growth during Human Blood Flow over a Collagen/Tissue Factor Wound. *Arterioscler Thromb Vasc Biol* 2015; **35**: 645–54.
- 165 Oshiro A, Yanagida Y, Gando S, Henzan N, Takahashi I, Makise H. Hemostasis during the early stages of trauma: comparison with disseminated intravascular coagulation. *Crit Care* 2014; **18**: R61.
- 166 Sorensen EN, Burgreen GW, Wagner WR, Antaki JF. Computational Simulation of Platelet Deposition and Activation: I. Model Development and Properties. *Ann Biomed Eng* 1999; **27**: 436–48.
- 167 Sorensen EN, Burgreen GW, Wagner WR, Antaki JF. Computational Simulation of Platelet Deposition and Activation: II. Results for Poiseuille Flow over Collagen. *Ann Biomed Eng* 1999; **27**: 449–58.
- 168 Lentz BR. Exposure of platelet membrane phosphatidylserine regulates blood coagulation. *Prog Lipid Res* 2003; **42**: 423–38.
- 169 Yoon JG, Heo JN, Kim M, Park YJ, Choi MH, Song J, Wyi K, Kim H, Duchenne O, Eom S, Tsoy Y. Machine learning-based diagnosis for disseminated intravascular coagulation (DIC): Development, external validation, and comparison to scoring systems. *PLoS One* 2018; **13**: e0195861.
- 170 Mahmood T, Yang P. Western Blot: Technique, Theory, and Trouble Shooting. *N Am J Med Sci* 2012; **4**: 429–34.
- 171 Walker JB, Nesheim ME. The molecular weights, mass distribution, chain composition, and structure of soluble fibrin degradation products released from a fibrin clot perfused with plasmin. *J Biol Chem* 1999; **274**: 5201–12.
- 172 Francis CW, Connaghan DG, Marder VJ. Assessment of fibrin degradation products during fibrinolytic therapy for acute myocardial infarction. *Circulation* 1986; **74**: 1027–36.
- 173 Zhu S, Herbig BA, Li R, Colace TV, Muthard RW, Neeves KB, Diamond SL. In

- microfluidico: Recreating in vivo hemodynamics using miniaturized devices. *Biorheology* 2015; **52**: 303–18.
- 174 Ware J. Dysfunctional platelet membrane receptors: from humans to mice. *Thromb Haemost* 2004; **92**: 478–85.
- 175 Tronik-Le Roux D, Roullot V, Poujol C, Kortulewski T, Nurden P, Margeurie G. Thrombasthenic mice generated by replacement of the integrin α IIb gene: demonstration that transcriptional activation of this megakaryocytic locus precedes lineage commitment. *Blood* 2000; **96**: 1399–408.
- 176 McLaughlin JN, Shen L, Holinstat M, Brooks JD, DiBenedetto E, Hamm HE. Functional Selectivity of G Protein Signaling by Agonist Peptides and Thrombin for the Protease-activated Receptor-1. *J Biol Chem* 2005; **280**: 25048–59.
- 177 O'Loughlin AJ, O'Sullivan CJ, Ravikumar N, Friel AM, Elliott JT, Morrison JJ. Effects of thrombin, PAR-1 activating peptide and a PAR-1 antagonist on umbilical artery resistance in vitro. *Reprod Biol Endocrinol* 2005; **3**: 8.
- 178 Chen C, Li O, Tao C, Barnett AJ, Su J, Rudin C. This Looks Like That: Deep Learning for Interpretable Image Recognition. *33rd Conference on Neural Information Processing Systems*. Vancouver, Canada; 2019.
- 179 Medzhitov R. Toll-like receptors and innate immunity. *Nat Rev Immunol* 2001; **1**: 135–45.
- 180 D'Atri LP, Schattner M. Platelet toll-like receptors in thromboinflammation. *Front Biosci* 2017; **22**: 1867–83.
- 181 Kapur R, Zufferey A, Boilard E, Semple JW. Nouvelle Cuisine: Platelets Served with Inflammation. *J Immunol* 2015; **194**: 5579–87.
- 182 Fung CYE, Jones S, Ntrakwah A, Naseem KM, Farndale RW, Mahaut-Smith MP. Platelet Ca^{2+} responses coupled to glycoprotein VI and Toll-like receptors persist in the presence of endothelial-derived inhibitors: Roles for secondary activation of P2X1 receptors and release from intracellular Ca^{2+} stores. *Blood* 2012; **119**: 3613–21.
- 183 Kälvegren H, Skoglund C, Helldahl C, Lerm M, Grenegård M, Bengtsson T. Toll-like receptor 2 stimulation of platelets is mediated by purinergic P2X1-dependent Ca^{2+} mobilisation, cyclooxygenase and purinergic P2Y1 and P2Y12 receptor activation. *Thromb Haemost* 2010; **103**: 398–407.
- 184 Ward JR, Bingle L, Judge HM, Brown SB, Storey RF, Whyte MKB, Dower SK, Buttle DJ, Sabroe I. Agonists of toll-like receptor (TLR)2 and TLR4 are unable to modulate platelet activation by adenosine diphosphate and platelet activating factor. *Thromb Haemost* 2005; **94**: 831–8.